Title

THE COORDINATION CHEMISTRY OF DIVALENT BIS(PENTAMETHYLCYCLOPENTADIENYL)LANTHANIDE COMPLEXES WITH NON-CLASSICAL LIGANDS

Author

Burns, C.J.

Publication Date

1987-10-01

LBL-24110

Lawrence Berkeley Laboratory
UNIVERSITY OF CALIFORNIA

Materials & Chemical Sciences Division

The Coordination Chemistry of Divalent Bis(pentamethylcyclopentadienyl)lanthanide Complexes with Non-Classical Ligands

C.J. Burns
(Ph.D. Thesis)

October 1987

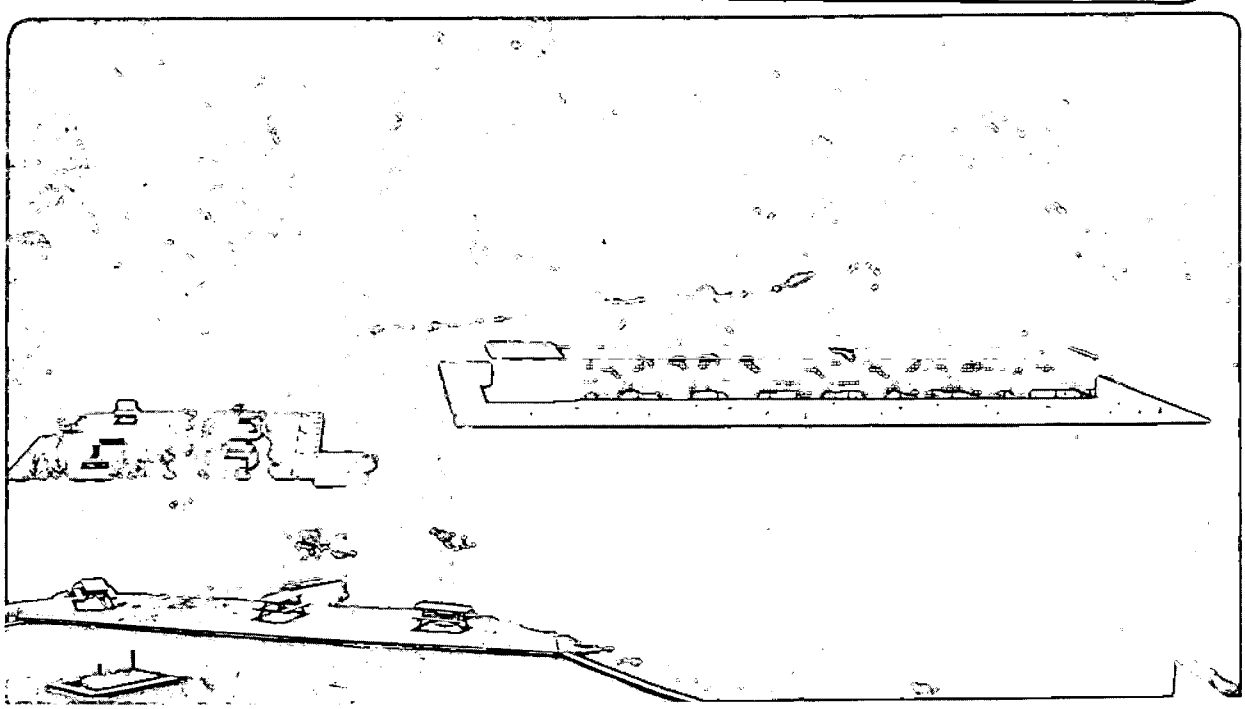

Prepared for the U.S. Department of Energy under Contract DE-AC03-76SF00098

DISCLAIMER

LBL-24110

The Coordination Chemistry of Divalent Bis(pentamethylcyclopentadienyl)lanthanide Complexes with Non-Classical Ligands

Carol Jean Burns

Lawrence Berkeley Laboratory
University of California
Berkeley, California 94720

October 1987

This work was supported by the U.S. Department of Energy under Contract Number DE-AC03-76SF00098.

The Coordination Chemistry of Divalent Bis(pentamethylcyclopentadienyl)lanthanide Complexes with Non-Classical Ligands

Carol Jean Burns

ABSTRACT

Divalent complexes of the formula $(Me_5C_5)_2M$ (M = Eu, Sm, Yb, Ca, Sr, and Ba) have been isolated free of coordinating Lewis bases. X-Ray crystallography and gas-phase electron diffraction reveal that these complexes have a "bent-sandwich" geometry. UV-Photoelectron spectroscopy suggests that the bonding in the compounds is ionic, and a model consistent with this observation is proposed to rationalize the bending of the molecules. Divalent lanthanide and alkaline earth cations of similar ionic radii demonstrate similar coordination chemistry with simple Lewis bases.

Isolation of the base-free species allows the synthesis of coordination compounds of weak bases, such as electron-rich olefins and acetylenes. The complexes $(Me_5C_5)_2Yb(\mu\text{-}C_2H_4)Pt(PPh_3)_2$ and $(Me_5C_5)_2Yb(\eta^2\text{-}MeC{\equiv}CMe)$ have been structurally characterized, and in each case the neutral organic molecule is η^2-coordinated to the lanthanide. Ethylene is rapidly polymerized by $(Me_5C_5)_2Yb$, and methylallene is catalytically isomerized to 2-butyne. Both of these processes are proposed to be involve initial reduction of the organic substrate by the ytterbium. Fluoro-olefins and -arenes undergo reduction followed by fluoride abstraction to give the mixed-valence compound $[(Me_5C_5)_2Yb]_2(\mu\text{-}$

F), which is converted thermally to the tetranuclear species $(Me_5C_5)_6Yb_4(\mu\text{-}F)_4$.

The reaction of $(Me_5C_5)_2Yb$ with polar compounds such as $(Me_5C_5)BeMe$ and $BH_3 \cdot PMe_3$ results in the formation of coordination compounds which may be viewed as models for the coordination of the small molecules CH_4 and BH_3. Zinc alkyl and aryl compounds undergo reduction, yielding zincate complexes of the formula $(Me_5C_5)_2Yb(\mu\text{-}R)_2ZnR$. The trimethylzincate compound displays symmetrically bridging methyl groups, while in the phenyl analog, the bridging geometry is markedly unsymmetric.

Sterically demanding polar molecules such as carboranes react with $(Me_5C_5)_2Yb$ to form inclusion compounds, with no close host-guest contacts in the solid state. First-row transition metal metallocenes, however, form 1:2 adducts with $(Me_5C_5)_2Yb$, in which the ytterbium atoms coordinate to the cyclopentadienyl rings of the metallocene.

Acknowledgements

Many people contributed to the completion of this work. I would first like to thank our collaborators, whose work comprises the bulk of Chapter One: Dr. Arne Haaland, Richard Blom, and Hans Volden (GED); Dr. Jennifer Green, Dr. Notker Rosch, and Detlef Hohl (PES and accompanying calculations).

I am deeply indebted to Dr. Fred Hollander for his patient assistance with the X-ray crystallography described in this thesis. Dave Berg and Phil Matsunaga take all the credit for magnetic susceptibility measurements. I also wish to acknowledge the technical assistance of Tony Stuart, who taught me how to run X-ray powder patterns, Steve Fine, who helped me run NMR spectra on the 500 MHz spectrometer at all sorts of terrible hours, and Roseanne Sension, who patiently looked for the Raman spectrum of the 2-butyne complex. The existence of this dissertation in word-processed form is a tribute to the expert advice of Will Polik and Joanne Stewart.

Financial support for my graduate studies was generously provided by the Fannie and John Hertz Foundation.

Technical assistance was provided in a more intangible form by the helpful discussions of others, particularly the members of the LBL-MCSD Actinide Group, as well as many graduate students in the Department of Chemistry. I won't name them all, because this thesis is long enough already. I will simply say that I am grateful to past and present members of the Huetterties group, Andersen group, and the Dux; you know who you are.

I would like to acknowledge in particular the intellectual and experimental challenge provided by my research director, Dr. Richard Andersen. It has been a privilege to work with him; he truly can make molecules.

The encouragement of my whole family cannot be overestimated. They have put up with a lot of lunacy during my pursuit of an education. I am most grateful to my husband, Michael, whose understanding and support have exceeded any reasonable bounds. The completion of this degree would probably have been impossible without his assistance; it certainly would not have been as meaningful.

Table of Contents

INTRODUCTION

While the earliest synthetic efforts in the field of organometallic lanthanide chemistry dealt almost exclusively with the trivalent cations, the chemistry of divalent lanthanides has received increasing attention in recent years. The +3 oxidation state is the most stable for all of the lanthanide ions, corresponding to ionization of the $6s^2$ and $5d^1$ electrons, which are well shielded from the nuclear charge by the 5s and 5p electron shells[1]. In some cases, however, alternate oxidation states are available when they represent a particularly stable electronic configuration (i.e. close to an empty, half-filled, or filled f-electron shell) such as Ce^{4+} ($4f^0$), Sm^{2+} ($4f^6$), Eu^{2+} ($4f^7$), Tm^{2+} ($4f^{13}$), and Yb^{2+} ($4f^{14}$). A detailed discussion of the trends in the stabilities of lanthanide oxidation states may be found elsewhere[2]. In practice, not all of the elements which can exist as stable divalent binary halides have been successfully employed in synthetic efforts; organometallic compounds have been prepared with Sm^{2+}, Eu^{2+}, and Yb^{2+}, however.

The earliest complexes of this type were $M(C_5H_5)_2L_n$ (M = Eu, Yb; L = NH_3), prepared by the addition of the diene C_5H_6 to solutions of Yb or Eu metal in liquid ammonia[3]. Compounds of the type $(C_8H_8)Ln(L)_n$ (M = Eu, Yb; L = NH_3, dmf, pyridine) have been prepared by a similar liquid ammonia synthesis[4] (there is also a report of the synthesis of (COT)Yb by co-condensation of Yb atoms and cycloocatetraene at -196°C[5]). Reductive methods were also employed in the early synthesis of cyclopentadienyl compounds of divalent lanthanides. The reduction of

$Yb(C_5H_5)_2Cl$ with either sodium or ytterbium metal in thf was used to prepare $Yb(C_5H_5)_2(thf)$[3d], and the analogous samarium compound was prepared by the reduction of $Sm(C_5H_5)_3$ by potassium naphthalide[6]. Milder conditions were adequate in effecting the reduction of $[(MeC_5H_4)_2YbMe]_2$ to produce the complex $(MeC_5H_4)_2Yb(thf)$[7]:

$$[(MeC_5H_4)_2YbMe]_2 \xrightarrow{h\nu} (MeC_5H_4)_2Yb + thf \longrightarrow (MeC_5H_4)_2Yb(thf) \quad (1)$$

$$[(MeC_5H_4)_2YbMe]_2 \xrightarrow{80\,^\circ C} (MeC_5H_4)_2Yb + thf \longrightarrow (MeC_5H_4)_2Yb(thf) \quad (2)$$

Another common method of preparing cyclopentadienyl compounds of divalent lanthanides has been metathetical exchange with the metal dihalides[10]:

$$MX_2 + 2\ M'(C_5Me_5) \xrightarrow{L} M(C_5Me_5)_2(L)_n + 2\ M'X \quad (M' = Li, Na, K;\ X = Cl, Br, I) \quad (3)$$

A large number of compounds of the type $Cp_2M(L)_n$ have been prepared to date, with a variety of Cp ligands: C_5H_5[3,6,8], MeC_5H_4[7], $(Me_3Si)C_5H_4$[9], C_5Me_5[10,11], and C_5Me_4Et[12,13].

There are few reported examples of organometallic compounds of divalent lanthanides which do not contain either the Cp or the COT ligand. Reactions of Eu or Yb metal with terminal alkynes in liquid ammonia are reported to yield compounds of the type $M(C{\equiv}CR)_2$[14]. Another successful synthetic strategy has been transmetalation; the reaction of Yb metal with HgR_2 (R = C≡CPh, C_6F_5) precipitates Hg(0) to yield the corresponding dialkyl ytterbium species[15] (the pentafluorophenyl complex was isolated as a base adduct with thf). Several recent reviews of

organometallic lanthanide chemistry have been published[16]; these contain sections on low-valent complexes.

Interest in the chemistry and reaction patterns of organolanthanide complexes has turned to an examination of the divalent species, owing to their ability to act as electron transfer reagents towards organic[17] and inorganic[18] substrates. The oxidation potentials in aqueous solution for the divalent cations are as follows[16a]: Sm^{2+}, +1.55 V; Eu^{2+}, +0.43V; and Yb^{2+}, +1.15V (vs. NHE). The species $(Me_5C_5)_2Sm$ has been used to reduce molecules such as CO[17a], PhC≡CPh[17b], and PhN=NPh[17c], while the compound $(Me_5C_5)_2Yb(OEt_2)$ has been shown to reduce a large number of nitrogen-containing heterocycles[13,19]. The latter species has also been used to reduce a variety of metal carbonyl complexes[18], often inducing interesting structural rearrangements. Divalent lanthanides complexes have found utility in organic synthesis other than as electron-transfer reagents[20]. Species formulated as RMI (R = alkyl, aryl; M = Eu, Yb), synthesized by the reaction of the bulk metals with alkyl or aryl iodides in thf, have been used as Grignard-type reagents in alkylation reactions[21]. The divalent reagents gave higher yields of the alkylated product than trivalent species formed from the use of Sm or Ce. The diodides of Sm and Yb have also been extensively inves-tigated as organic reagents for hydrogenation, alkylation, and coupling[22].

In the development of the chemistry of divalent lanthanide species, two major problems were encountered. The first of these was the insolubility of most of the cyclopentadienyl compounds in hydrocarbon solvents; the loss of coordinated base often lead to the formation of insoluble coordination polymers. This problem has been solved by the

use of the peralkylsubstituted ring $C_5Me_5^-$. As has been shown in early transition metal[23] and actinide[24] systems, the use of the pentamethylcyclopentadienyl group can increase the crystallinity and hydrocarbon solubility of complexes by filling the coordination environment of the metal ion, preventing polymerization. The use of this electron-rich ligand also increases the reducing power of the divalent lanthanide; the measured reduction potentials (with respect to the Cp_2Fe/Cp_2Fe^+ couple) for $(Me_5C_5)_2M$ complexes in acetronitrile are: Sm^{2+}, -2.4V; Eu^{2+}; -1.22V; Yb^{2+}, -1.78V[25].

The second problem has not been as easy to overcome. The synthesis and isolation of lanthanide complexes often necessitates the use of Lewis bases such as ethers or amines, and these species coordinate very strongly to hard Lewis acids such as lanthanides. A qualitative series of ligand affinities has been established for $(Me_5C_5)_2Yb$: pyridine $\gg$ thf $>$ $Et_2O \cong$ dmpm[10e]. Any examination of the coordination chemistry of these species is limited to bases which are more strongly coordinating than ethers. The only way to extend this series would be to start with a base-free species. Complexes of the type $M(C_5H_5)_2$ (M = Yb, Eu) have been prepared by the sublimation of base adducts[3b], but these species suffer from insolubility in non-coordinating solvents. Recently, methods have been developed for synthesizing $M(C_5Me_5)_2$ (M = Eu, Sm)[26] by metal vapor synthesis or by sublimation of base adducts, and for $Yb(C_5Me_5)_2$ by the removal of $HN(SiMe_3)_2$ from a base adduct[13]. None of these methods can be generalized to all three metals, however, and the procedures are often involved. In order to extend the chemistry of

these species, it is necessary to develop a high-yield, general method for preparing the base-free compounds.

The affinity of lanthanides for hard Lewis bases is related to the nature of the bonding in these complexes. The valence orbitals in the lanthanide series are the 4f orbitals, which are of limited radial extent when compared to 3d orbitals. They are also well shielded by the 5s and 5p shell, so that orbital overlap with ligand-based orbitals is minimal. The result of this is that the bonding in all lanthanide complexes has generally been believed to be predominantly ionic. Thus, the metals prefer to coordinate polar nolecules, such as those with highly directional lone pairs.

Many spectroscopic observations exist which confirm the assertion of ionic bonding. The optical spectra of lanthanide complexes show weak bands due to f-f transitions; these are narrow due to a lack of ligand field splitting. The positions of these bands are largely insensitive to the coordination of the netal, but the small perturbations visible have been correlated with the extent of covalency for a series of trivalent compounds[27]. The estimated covalent contributions range from 0-2.5%, with the organometallic conplexes lying in the higher end of the range. Examination of the photoelectron spectra of a series of Gd compounds has shown that the relative intensities of the "shake-up" satellite peaks of the $3d_{5/2}$ photopeak, related to the degree of metal-ligand orbital overlap, remain almost constant upon changing a ligand from Cl to C_5H_5, He, or C≡CPh, given similar molecular geometries[28]. ^{151}Eu Mossbauer neasurements have suggested that $Eu(C_5H_5)_2$ has approximately the same degree of covalency as $EuCl_2$[29].

Structural evidence also supports this bonding model. For ionic complexes, changes in the M-C bond distance across the series for a given coordination environment should be readily predictable given the ionic radii of the metals. This seems to be the trend in organometallic lanthanide species, unless the coordination sphere is excessively crowded[30].

Recently, however, data and calculations have been presented which would suggest a higher degree of covalent bonding in some lanthanide compounds[31], particulary those with the C_5Me_5 and COT ligands. It is of interest to study the structure and spectroscopy of bis(pentamethylcyclopentadienyl)lanthanide complexes, with the aim of elucidating the bonding in such species. The ionic radii of the lanthanide ions are large relative to those of the first-row transition metal ions, and coordination numbers as high as twelve are observed[32]. At that point, the molecular geometry can be dictated by intraligand electronic and steric repulsions, rather than by bonding preferences. For this reason, it is preferable to examine the molecular structures of coordinatively unsaturated molecules such as the base-free species $M(C_5Me_5)_2$ when discussing the nature of bonding in organolanthanide complexes.

One type of acid-base interaction one would like to explore would be that implied by the stoichiometric and catalytic reations of lanthanide complexes with organic molecules. Lanthanide metal vapors react with olefins, dienes, and terminal and internal alkynes[33] to give a variety of products in which the metal is considered to be in an oxidation state less than three. The reactions of dienes and internal alkynes give products formulated as $M(L)_{1-3}$, depending on the substrate

used. These species show weak catalytic hydrogenation activity. Hydrolysis or thermal decomposition of the materials gives rise to hydrogenated hydrocarbons. Olefins and terminal alkynes show evidence of C-H and C-C bond cleavage, oligomerization, and dehydrogenation.

The most commonly studied reaction of homogeneous lanthanide complexes with unsaturated molecules is the polymerization/oligomerization of olefins by trivalent bis(cyclopentadienyl)lanthanide alkyls and hydrides[34]. The $(Me_5C_5)_2Lu(R)(OEt_2)$ system has been particularly well studied, and a mechanism has been proposed based on the sequential (but reversible) concerted insertion of ethylene units[35]. The similarity of this type of process to Ziegler-Natta polymerization has prompted a great deal of research on the tacticity and stereoregularity of polymers produced by homogeneous trivalent lanthanide systems from a wide variety of unsaturated substrates[16a,36].

Perhaps the most interesting reaction exhibited by a trivalent homogeneous lanthanide species is the facile activation of all manner of C-H bonds by $(Me_5C_5)_2LuR$ (R = He, H)[35c,37]. These complexes reportedly metallate benzene, pyridine, and tetramethylsilane, eliminating RH and forming the Lu alkyl or aryl species. The hydride undergoes H-D exchanges with D_2, and Et_2O reacts to give the Lu ethoxide and ethane. The methyl compound even activates methane, as evidenced by labeling experinents:

$$(Me_5C_5)_2LuCH_3 + {}^{13}CH_4 \longrightarrow (Me_5C_5)_2Lu^{13}CH_3 + CH_4 \qquad (4)$$

All of these reactions, as well as the samarium reductions discussed previously, intimate that the substrate molecules may first coordinate as σ-bases to the acidic lanthanides prior to further

reaction. No direct evidence has ever been seen for this intermediate, however. If such an interaction is to be studied, coordination compounds of lanthanides with olefins, alkynes, and alkanes (or analogs of these molecules) must be synthesized. Because the substrate molecules react with trivalent species and strongly reducing divalent complexes, the most likely systems for study would be the base-free divalent bis(pentamethylcyclopentadienyl)ytterbium or europium compounds.

The purpose of this research has been to address some of these questions and needs. The first chapter describes a general synthetic route to produce base-free bis(pentamethylcyclopentadienyl)lanthanide complexes, and examines their spectroscopy and simple coordination chemistry in order to gain insight into the bonding in these species. The second chapter deals with the interaction of the divalent compounds with unsaturated molecules, and addresses some aspects of transformations of these molecules catalyzed by Yb(II). Finally, the coordination chemistry of $(Me_5C_5)_2Yb$ with analogs of saturated hydrocarbons is explored, along with the question of what constitutes a basic ligand.

References:

1.) Cotton, F. A.; Wilkinson, G., "Advanced Inorganic Chemistry," 4th ed., Wiley-Interscience, New York, 1980, pp. 981-996.

2.) Johnson, D. A., "Some Thermodynamic Aspects of Inorganic Chemistry," 2nd ed., Cambridge University Press, Cambridge, 1982, pp. 158-168.

3.) a) Fischer, E. O.; Fischer, H., Angew. Chem., 1964, 76, 52. b) Fischer, E. O.; Fischer, H., J. Organomet. Chem., 1965, 3, 181.

c) Hayes, R. G.; Thomas, J. L., Inorg. Chem., 1969, 3, 2421. d) Calderazzo, F.; Pappalardo, R.; Losi, S., J. Inorg. Nucl. Chem., 1966, 28, 987.

4.) a) Hayes, R. G.; Thomas, J. L., J. Am. Chem. Soc., 1969, 91, 6876. b) Wayda, A. L.; Mukerji, I.; Dye, J. L.; Rogers, R. D., Organometallics, 1987, 6, 1328.

5.) DeKock, C. W.; Ely, S. R.; Hopkins, T. E.; Brault, M. A., Inorg. Chem., 1978, 17, 625.

6.) Watt, G. W.; Gillow, E. W., J. Am. Chem. Soc., 1969, 91, 775.

7.) Zinnen, H. A.; Pluth, J. J.; Evans, W. J., J. Chem. Soc. Chem. Comm., 1980, 810.

8.) Deacon, G. B.; MacKinnon, P. J.; Hambly, T. W.; Taylor, J. C., J. Organometallic Chem., 1983, 259, 91.

9.) Lappert, M. F.; Yarrow, P. I.; Atwood, J. L.; Shakir, R.; Holton, J., J. Chem. Soc. Chem. Comm., 1980, 987.

10.) a) Watson, P. L., J. Chem. Soc. Chem. Comm., 1980, 652. b) Tilley, T. D.; Andersen, R. A.; Spencer, B.; Ruben, H.; Zalkin, A.; Templeton, D. H., Inorg. Chem., 1980, 19, 2999. c) Tilley, T. D.; Andersen, R. A.; Spencer, B.; Zalkin, A., Inorg. Chem., 1982, 21, 2647. d) Tilley, T. D.; Andersen, R. A.; Zalkin, A., Inorg. Chem., 1983, 22, 856. e) Tilley, T. D.; Ph.D. Thesis, University of California, Berkeley, California, U.S.A., 1982.

11.) a) Evans, W. J.; Bloom, I.; Hunter, W. E.; Atwood, J. L., J. Am. Chem. Soc., 1981, 103, 6507. b) Evans, W. J.; Grate, J. W.; Choi, H. W.; Bloom, I.; Hunter, W. E.; Atwood, J. L., J. Am. Chem. Soc., 1985, 107, 941.

12.) Evans, W. J.; Bloom, I.; Hunter, W. E.; Atwood, J. L., Organometallics, 1985, 4, 112.

13.) Boncella, J. M., Ph.D. Thesis, University of California, Berkeley, California, U.S.A., 1984.

14.) Murphy, E.; Toogood, G. E., Inorg. Nucl. Chem. Lett., 1971, 7, 755.

15.) a) Deacon, G. B.; Koplick, A. J., J. Organomet. Chem., 1978, 146, C43. b) Deacon, G. B.; Koplick, A. J.; Raverty, W. D.; Vince, D. G., J. Organomet. Chem., 1979, 182, 121. c) Deacon, G. B.; Vince, D. G., J. Organomet. Chem., 1976, 112, C1.

16.) a) Marks, T. J.; Ernst, R. D., "Comprehensive Organometallic Chemistry" (G. Wilkinson, F. G. A. Stone, and E. W. Abel, eds.), Chap. 21, Pergamon Press, Oxford, 1982. b) Evans, W. J., Advances

in Organometallic Chemistry, 1985, 24, 131. c) Marks, T. J., Prog. Inorg. Chem., 1978, 24, 51.

17.) a) Evans, W. J.; Grate, J. W.; Hughes, L. A.; Zhang, H.; Atwood, J. L., J. Am. Chem. Soc., 1985, 107, 3728. b) Evans, W. J.; Hughes, L. A.; Drummond, D. K.; Zhang, H.; Atwood, J. L., J. Am. Chem. Soc., 1986, 108, 1722. c) Evans, W. J.; Drummond, D. K.; Bott, S. G.; Atwood, J. L., Organometallics, 1986, 5, 2389.

18.) a) Tilley, T. D.; Andersen, R. A., J. Chem. Soc. Chem. Comm., 1981, 985. b) Tilley, T. D.; Andersen, R. A., J. Am. Chem. Soc., 1982, 104, 1772. c) Boncella, J. M.; Andersen, R. A., Inorg. Chem., 1984, 23, 432.

19.) Berg, D. J., Ph.D. Thesis, University of California, Berkeley, California, U.S.A., 1987.

20.) Kagan, H. B.; Namy, J. L., Tetrahedron, 1986, 42, 6572.

21.) Evans, D. F.; Fazakerly, G. V.; Phillips, R. F., J. Chem. Soc. (A), 1971, 1931.

22.) a) Namy, J. L.; Girard, P.; Kagan, H. B., Nouv. J. Chem., 1977, 1, 5. b) Girard, P.; Namy, J. L.; Kagan, H. B., J. Am. Chem. Soc., 1980, 102, 2693.

23.) Wolczanski, P. T.; Bercaw, J. E., Acc. Chem. Res., 1980, 13, 121.

24.) Marks, T. J., Science, 1982, 217, 989.

25.) Finke, R. G.; Keenan, S. R.; Schiraldi, D. A.; Watson, P. L., Organometallics, 1986, 5, 598; Footnote 5.

26.) Evans, W. J.; Hughes, L. A.; Hanusa, T. P., Organometallics, 1986, 5, 1285.

27.) a) Jørgensen, C. K., "Oxidation Numbers and Oxidation States" Chap. 5, Springer-Verlag, Heidelberg, 1969. b) Jørgensen, C. K. "Modern Aspects of Ligand Field Theory", North-Holland, Amsterdam, 1971. c) Nugent, L. J.; Lauberau, P. G.; Werner, G. K.; van der Sluis, K. L., J. Organomet. Chem., 1971, 27, 365.

28.) Dubois, R.; Carver, J.; Tsutsui, M., J. Coord. Chem., 1977, 7, 31.

29.) a) Hufner, S.; Kienle, P.; Quitmann, D.; Brix, P., Z. Physik, 1965, 187, 67. b) Gibb, T. C., "Principles of Mossbauer Spectroscopy" Chap. 5.6, Chapman and Hall, London, 1976.

30.) Raymond, K. N.; Eigenbrot, C. W., Jr., Acc. Chem. Res., 1980, 13, 276.

31.) a) Streitwieser, A., Jr.; Kinsley, S. A.; Rigsbee, J. T.; Fragala, I. L.; Ciliberto, E.; Rosch, N., J. Am. Chem. Soc., 1985, 107, 7786. b) Hazin, P. N.; Bruno, J. W.; Brittain, H. G., Organometallics, 1987, 6, 913.

32.) a) Clearfield, A.; Gopal, R.; Olsen, R. W., Inorg. Chem., 1977, 16, 911. b) Sinha, S. P., Struct. Bonding, 1976, 25, 69.

33.) a) Evans, W. J.; Coleson, K. M.; Engerer, S. C., Inorg. Chem., 1981, 20, 4320. b) Evans, W. J.; Engerer, S, C.; Neville, A. C., J. Am. Chem. Soc., 1978, 100, 331. c) Evans, W. J.; Engerer, S. C.; Coleson, K. M., J. Am. Chem. Soc., 1981, 103, 6672. d) Evans, W. J.; Engerer, S. C.; Piliero, P. A.; Wayda, A. L., J. Chem. Soc. Chem. Comm., 1979, 1007.

34.) a) Ballard, D. G. H.; Courtis, A.; Holton, J.; McMeeking, J.; Pearce, J., J. Chem. Soc. Chem. Comm., 1978, 994. b) Jeske, G.; Lauke, H.; Mauermann, H.; Swepston, P. N.; Schumann, H.; Marks, T. J., J. Am. Chem. Soc., 1985, 107, 8091.

35.) a) Watson, P. L., J. Am. Chem. Soc., 1982, 104, 337. b) Watson, P. L.; Roe, D. C., J. Am. Chem. Soc., 1982, 104, 6471. c) Watson, P. L.; Parshall, G. W., Acc. Chem. Res., 1985, 18, 51. d) Watson, P. L.; Herskovitz, T., "Initiation of Polymerization" (F. E. Bailey, ed.), A.C.S. Symposium Series, 1983, 212.

36.) Bruzzone, M.; Carbonaro, A., "Fundamental and Technological Aspects of Organo-f-Element Chemistry" (T. J. Marks and I. L. Fragala, eds.), D. Reidel, Dordrecht, 1985, and references therein.

37.) a) Watson, P. L., J. Am. Chem. Soc., 1983, 105, 6491. b) Watson, P. L., J. Chem. Soc. Chem. Comm., 1983, 276.

CHAPTER ONE: The Synthesis of Bis(pentamethylcyclopentadienyl)-Lanthanide and -Alkaline Earth Complexes

Synthesis

The methods first employed to successfully synthesize the base-free compounds $(Me_5C_5)_2M$ (M = Sm, Eu, and Yb) involved the removal of a volatile, labile ligand under reduced pressure[1,2]:

$$(Me_5C_5)_2M(L) \rightleftharpoons (Me_5C_5)_2M + L \uparrow \qquad (1)$$

Perturbation of such a coordinative equilibrium could lead to a general method for the synthesis of the divalent lanthanide species, given the proper choice of ligand. The base adduct chosen for investigation, $(Me_5C_5)_2M(OEt_2)$, can be synthesized in a one-step procedure (eq. 2), and yet has a ligand which has been demonstrated to be relatively weakly

$$MI_2 + 2\ NaC_5Me_5 \xrightarrow{OEt_2} (Me_5C_5)_2M(OEt_2) + 2\ NaI \qquad (2)$$

coordinating[3]. While the diethyl ether complexes of ytterbium and europium have been prepared previously[3], the samarium analog had not been reported. The most convenient synthesis of samarium(II) iodide yields $SmI_2(thf)_n$, which results in the formation of a thf adduct in the metathetical preparation of the (Me_5C_5) complex, even from diethyl ether solution[4]. Heating the diiodide under vacuum, however, will remove the thf, and the diethyl ether adduct of $(Me_5C_5)_2Sm$ can be isolated from the reaction shown in equation 2 (M = Sm).

If a toluene solution of $(Me_5C_5)_2Yb(OEt_2)$ is heated to 100°C, then exposed slowly to dynamic vacuum so that the solvent is removed over a period of several hours, the coordinated diethylether is removed

quantitatively, resulting in a high yield of bis(pentamethylcyclopentadienyl)ytterbium. This desolvation process can be extended to the earlier divalent lanthanides.

It is of interest in the study of the bonding and chemistry of these species to examine the analogous bis(pentamethylcyclopentadienyl) alkaline earth complexes (M = Ca, Sr, Ba). The ionic radii of the alkaline earth cations are similar to those of the divalent lanthanide cations in similar coordination environments[5] (see Table I); if ionic

Table I Ionic Radii (Å) of Lanthanide and Alkaline Earth Dications

(C.N. = Coordination Number)

M	C.N.	Ionic Radius	M	C.N.	Ionic Radius
Yb	6	1.02	Ca	6	1.00
Yb	7	1.08	Ca	7	1.06
Yb	8	1.14	Ca	8	1.12
Eu	6	1.17			
Eu	7	1.20			
Eu	8	1.25	Sr	6	1.18
			Sr	7	1.21
Sm	6	-	Sr	8	1.26
Sm	7	1.22			
Sm	8	1.27			
			Ba	6	1.35
			Ba	7	1.38
			Ba	8	1.42

bonding is strictly followed, the chemistry of the ytterbium and calcium analogs should be nearly identical, while the chemistry of the europium and samarium compounds should resemble that of the strontium compound most closely. The alkaline earth ether adducts (M = Ca, Sr, Ba) can be prepared by the method of Equation (2). The calcium and strontium

reactions are carried out in diethylether, as in the case of the lanthanides, but there is no reaction between BaI_2 and NaC_5Me_5 in this solvent, presumably due to the insolubility of the barium salt. If the reaction is instead conducted in tetrahydrofuran solution, the isolated product is $(Me_5C_5)_2Ba(thf)_2$. All three of these ether adducts may be desolvated by the same "toluene reflux" method to give the compounds $(Me_5C_5)_2M$ (M = Ca, Sr, Ba). Some physical characteristics of the base-free complexes are given in Table II.

Table II Physical Characteristics of $(Me_5C_5)_2M$

M	Color	M.P.	^{1}H NMR	^{13}C NMR
Sm	Green	214-217°C	δ 1.16 ($\nu_{1/2}$ = 25Hz)	δ -98.2 ($\underline{C}_5Me_5$), δ 99.0 ($C_5\underline{Me}_5$) (ref 6)
Eu	Red	219-222°C	not visible	not visible
Yb	Brown	189-191°C (red>130°C)	δ 1.92 (s)	δ 113.4 ($\underline{C}_5Me_5$), δ 10.61 ($C_5\underline{Me}_5$)
Ca	White	207-210°C	δ 1.90 (s)	δ 114.3 ($\underline{C}_5Me_5$), δ 10.27 ($C_5\underline{Me}_5$)
Sr	White	216-218°C	δ 1.95 (s)	δ 113.6 ($\underline{C}_5Me_5$), δ 10.83 ($C_5\underline{Me}_5$)
Ba	White	265-268°C	δ 1.97 (s)	δ 114.0 ($\underline{C}_5Me_5$), δ 11.10 ($C_5\underline{Me}_5$)

The colors of the base-free complexes are the same as those of their ether adducts with the exception of the ytterbium compound, whose diethyl etherate is green. The ytterbium species displays a variety of colors, depending on the physical form of the compound. Samples crystallized from hydrocarbon solvent can display two different crystalline forms: a dark brown-black form, and a dark green form which

loses occluded solvent under reduced pressure to give light brown, opaque crystals. Freshly sublimed samples appear brown-green. The compound is also thermochroic in all forms, reversibly turning orange-red above ca. 130°C. This will be discussed in more detail in Chapter Three.

All of the compounds are thermally stable; they melt without decomposition and sublime readily. Electron impact mass spectra show strong molecular ions. Where multiple isotopes of the metal occur naturally, these molecular ions display isotopic envelopes which can be simulated (see Experimental Section). In the case of $(Me_5C_5)_2Sm$, higher molecular weight clusters are observed in the gas phase, corresponding to $(Me_5C_5)_2Sm_2$ and $(Me_5C_5)_3Sm_2$; these clusters can also be simulated (Fig. 1).

Figure (1) Isotopic Clusters for $(Me_5C_5)_3Sm_2$

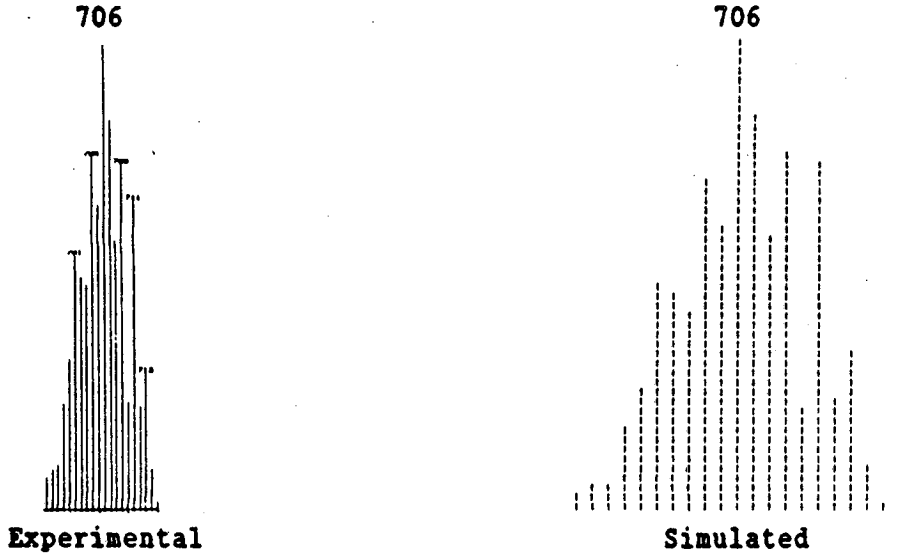

Two of the divalent lanthanide complexes, $(Me_5C_5)_2Eu$ and $(Me_5C_5)_2Sm$, are paramagnetic, and the temperature dependence of their

solid-state magnetic susceptibility has been examined. The plots of $1/\chi_M$ vs. T can be seen in Figures (2) and (3), respectively. As mentioned in the Introduction, the partially filled 4f orbitals in lanthanides are well shielded from interaction with ligand-based orbitals, resulting in very small crystal field splittings ($\leq$ 300 cm^{-1}, on the order of kT at room temperature). Therefore, unlike first-row transition metal ions, the magnitude of the crystal field splitting is smaller than both electron-electron repulsion and spin-orbit coupling, and the spectroscopic states of the lanthanides can be predicted by the Russell-Saunders coupling scheme. For most lanthanide electron configurations, the value of the spin-orbit coupling is of a sufficient magnitude that any excited states are much higher in energy than the ground state configuration. The magnetic moment can then be calculated from equation (3), where g_J is the Lande splitting factor (equation (4)). The magnetic behavior of $(He_5C_5)_2Eu$ (Eu^{2+}, $4f^7$, ^8S) is an example

$$\mu_{eff} = g_J [J(J+1)]^{1/2} \qquad (3)$$

$$g_J = 1 + \frac{S(S+1) + J(J+1) - L(L+1)}{2J(J+1)} \qquad (4)$$

of this case. The plot (Figure 4) shows essentially Curie behavior in the range 5-280 K with θ very close to 0 K and μ = 7.70 and 7.84 B.M. at 5 and 40 kG, respectively.

In $(He_5C_5)_2Sm$ (Sn^{2+}, $4f^6$, $^7F_0$), however, the J = 0 and J = 1 states in the free ion are separated by only ca. 300 cm^{-1}, and the J = 2 state lies only ca. 200 cm^{-1} above the J = 1 state. Both of these first two excited states are thermally accessible, and contributions due to these in proportion to their thermal populations must be taken into account in

Figure (2) Plot of $1/\chi_M$ vs. T for $(Me_5C_5)_2Eu$

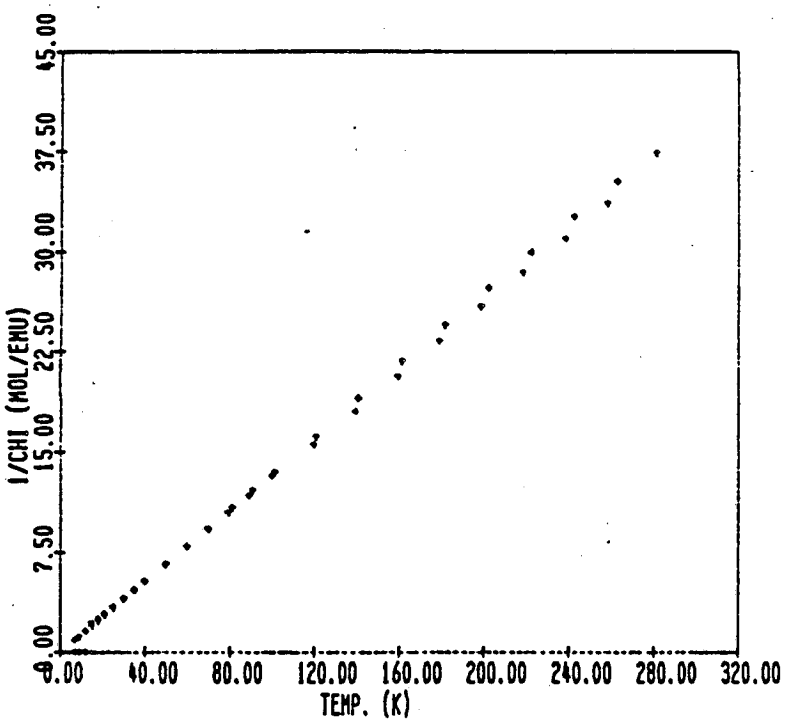

Figure (3) Plot of $1/\chi_M$ vs. T for $(Me_5C_5)_2Sm$ (40 kG)

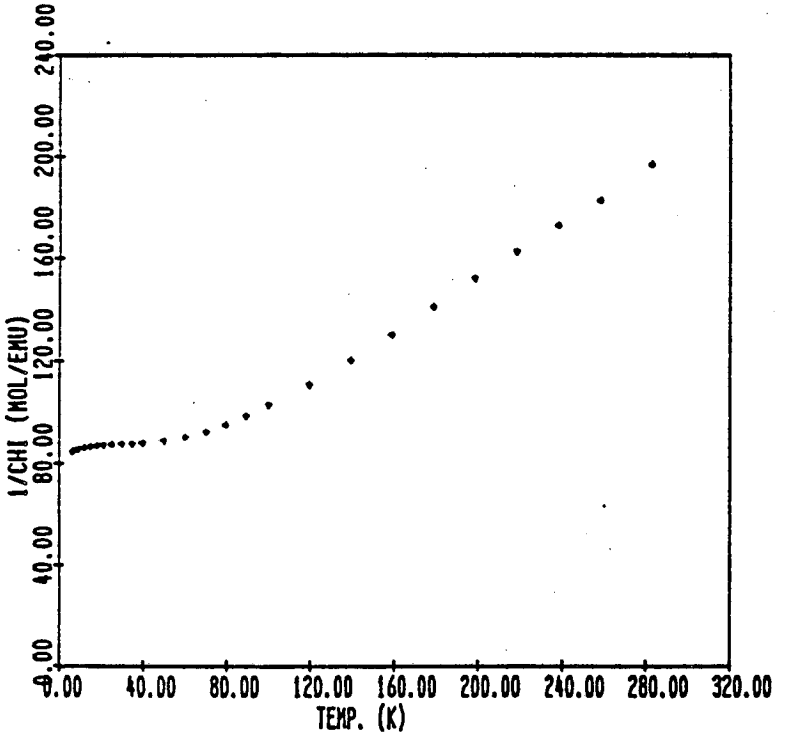

a calculation of the moment. Ions with a $4f^6$ configuration should display temperature independant paramagnetism at low temperatures (when there is little thermal population of excited states). The molar susceptibility then rises with temperature as the J = 1 and 2 states become populated; the value of μ at 300 K is predicted[7] to be 3.4-3.5 B.M. The plot of $1/\chi_M$ vs. T for $(Me_5C_5)_2Sm$ clearly demonstrates this behavior: at 5 kG $\chi_M(corr) = 5.016 \times 10^{-3}$ emu/mol and μ = 3.36 B.M. (281.7 K), while at 40 kG $\chi_M(corr) = 5.032 \times 10^{-3}$ emu/mol and μ = 3.37 B.M. (282.7 K). A solution measurement has previously reported that μ(297 K) = 3.7 B.M.[6].

It is noteworthy that the plots for these compounds closely resemble those of the free M^{2+} ions, as well as those of inorganic salts of Sm(II) and Eu(II)[7]. This indicates that the crystal field splitting induced by the pentamethylcyclopentadienyl ligand in these compounds is not significantly larger than that induced by simple halide and pseudo-halide ligands. The extent of metal-ligand orbital interaction is small, and therefore the compounds are best considered to be ionic.

Structure

Bis(cyclopentadienyl) compounds have been shown to adopt a bewildering variety of structures, depending on the central element, M. Where M is a d-transition element, the structure is generally a D_{5h} or D_{5d} parallel-ring "sandwich"[8], as is that of $Mg(C_5H_5)$[9]. Bis(cyclopenta-dienyl)beryllium, however, exhibits a ring slip structure described alternately as η^2-η^5 or η^3-η^5 [10]. The compound $Ca(C_5H_5)_2$ has been found to have a complicated solid state structure in which each calcium has in

its coordination sphere two η^5-rings, one η^3-ring, and one η^1-ring[11]. Most compounds of the Group 14 elements have been shown generally to adopt a C_{2v} "bent sandwich" structure both in the solid[12] and gas phases[13], except when prevented by interligand repulsions[14] (one interesting exception to this is $(Me_5C_5)_2Si$, which has bent and parallel sandwich molecules in the same asymmetric unit[15]). The Group 12 compounds can also display a range of structures. The compound $Zn(C_5H_5)_2$ is a linear polymer[16], while $Zn(C_5Me_5)_2$ and $Zn(C_5H_4SiMe_3)_2$ have been shown to have "slip-sandwich"[17] structures in the gas phase.

The solid-state structures of $(Me_5C_5)_2Sm$ and $(Me_5C_5)_2Eu$ have been determined by single crystal X-ray crystallography[2]. As expected, the steric requirements of the pentamethylcyclopentadienyl ligand prevent coordination polymerization. The molecules have a bent sandwich geometry in the solid state. The space group and unit cell constants of the brown-green crystalline form of $(Me_5C_5)_2Yb$ derived from sublimation were determined by precession photography, and it was found to be isomorphous with the samarium and europium structures (Table III).

Table III Unit Cell Constants for $(Me_5C_5)_2M$

M	Space Group	a(Å)	b(Å)	c(Å)	β	Ref.
Sm	$P2_1/n$	9.815(3)	13.436(9)	14.163(8)	94.98(4)	2
Eu	$P2_1/n$	9.838(4)	13.443(4)	14.174(3)	95.03(2)	2
Yb[a]	$P2_1/n$	9.8	12.4	14.9	95.	this work
Yb[b]	$P2_1/n$	31.013(3)	12.466(2)	9.836(1)	95.960(9)	this work

[a] brown-green form, from precession photographs. [b] brown-black form.

The dark brown-black form obtained from aliphatic hydrocarbon solvent had one doubled cell constant, however, indicating that this form was

not strictly isomorphous with the previously determined structure. The crystal structure of this modification was determined by X-ray diffraction.

The structure of this form also consists of individual molecules of a bent sandwich geometry, but there are two crystallographically unique molecules in the asymmetric unit. Figure (4) shows an ORTEP drawing of the molecules, while Table IV contains relevant bond distances. Comparison of the individual $(Me_5C_5)_2M$ units in the Sm, Eu, and Yb structures reveals that they are qualitatively quite similar (Table V). In all three cases, the metal aton is η^5-coordinated to two non-parallel

Table IV Bond Distances for $(Me_5C_5)_2Yb$ (Å)

Yb1-C1	2.670(4)	Yb2-C21	2.684(3)
Yb1-C2	2.651(3)	Yb2-C22	2.690(3)
Yb1-C3	2.646(3)	Yb2-C23	2.656(3)
Yb1-C4	2.641(3)	Yb2-C24	2.636(3)
Yb1-C5	2.656(3)	Yb2-C25	2.640(3)
Yb1-C11	2.672(3)	Yb2-C31	2.671(3)
Yb1-C12	2.667(3)	Yb2-C32	2.665(3)
Yb1-C13	2.673(3)	Yb2-C33	2.662(4)
Yb1-C14	2.664(3)	Yb2-C34	2.676(4)
Yb1-C15	2.682(3)	Yb2-C35	2.690(3)
Yb1-Cp1	2.366	Yb2-Cp3	2.377
Yb1-Cp2	2.386	Yb2-Cp4	2.390

Cp1 through Cp4 are the ring centroids for the rings composed of C1-C5, C11-C15, C21-C25, and C31-C35, respectively.

Table V Molecular Geometries of $(Me_5C_5)_2M$ Compounds

	Sm	Eu	Yb (two molecules)
M-C (ring, avg)	2.79(1) Å	2.79(1) Å	2.662(3) Å, 2.667(3) Å
M-Cp (avg)	2.53 Å	2.53 Å	2.376 Å, 2.384 Å
∠Cp-M-Cp	140.1°	140.3°	145.7°, 145.0°

Figure (4) ORTEP Labeling Diagram of $(Me_5C_5)_2Yb$ (Two Unique Molecules)

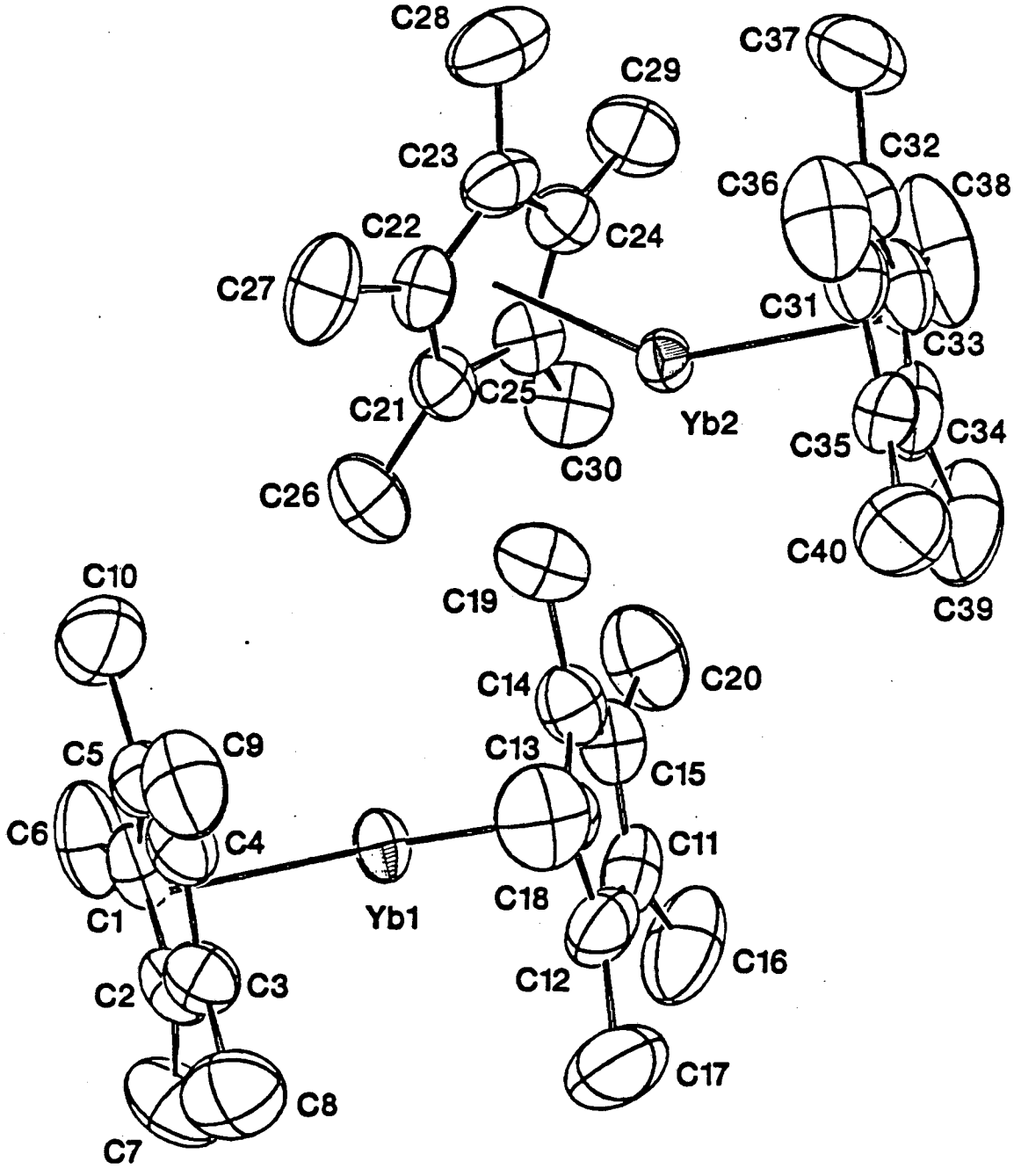

pentamethylcyclopentadienyl rings, with the rings staggered with respect to one another.

The molecular geometry of the ytterbium compound is typical of Yb(II)bis(pentamethylcyclopentadienyl) complexes. The averaged M-C (ring) distance, 2.665(3) Å, is similar to that found in the complexes $(Me_5C_5)_2Yb(OEt_2)$ [2.69(2) Å][3] and $(Me_5C_5)_2Yb(thf)\cdot 1/2$ PhMe [2.66(2) Å][18]. The ring centroid-metal-ring centroid angle is slightly larger than that found in base adducts [140.6° for $(Me_5C_5)_2Yb(OEt_2)$, 143.5 for $(Me_5C_5)_2Yb(thf)$]; in the adducts, steric repulsions between the rings and the coordinated base cause the ring-metal-ring angle to be compressed. The greatest deviation from planarity for a carbon atom in any of the rings is 0.010(4) Å. In the two unique molecules, the rings are twisted with respect to one another by 21.5(3)° and 25.3(4)° (this angle is reported as 19° in $(Me_5C_5)_2Sm$[2]). The nethyl groups on the cyclopentadienyl rings are bent out of the plane of the rings away from the ytterbium atoms by an average of 0.131(5) Å and 0.150(5) Å in the two unique molecules (0.13 Å for Sm and Eu); this structural feature has been noted in other lanthanide complexes[19].

The differences in the M-C bond lengths and the ring-metal-ring angles for the three lanthanides are readily explainable in terms of the size of the metal radii. As the size of the divalent ion decreases in the series Sm > Eu > Yb, the metal to carbon bond length decreases by a commensurate amount (see Table I). In the structure of $(Me_5C_5)_2Yb$, the closest non-bonding contacts between the two rings on one metal atom are 3.494(6) Å and 3.680(7) Å for the independant molecules. The corresponding values in the Sm and Eu structures are 3.56(1) Å and

3.55(2) Å, respectively. As the size of the metal ion increases, the effective distance between the ligands increases, and a smaller ring-metal-ring can be tolerated before this non-bonding limit is reached.

The difference in the structures of $(Me_5C_5)_2M$ (M = Sm, Eu) and the structure of $(Me_5C_5)_2Yb$ determined in this study lies in the nature of the intermolecular interactions. In the structures of the samarium and europium compounds (and presumably the brown-green form of the ytterbium compound, given the similarity of the unit cell parameters), each molecule has one close metal to methyl carbon intermolecular contact with a molecule related by a crystallographic center of inversion. In $(Me_5C_5)_2Sm$, this contact is 3.22(1) Å, while in $(Me_5C_5)_2Eu$ it is 3.19(2) Å. There are no other intermolecular contacts closer than 3.7 Å. This close contact has the effect of creating a "coordination dimer" (Figure 5).

Figure (5) Intermolecular Contacts in $(Me_5C_5)_2Sm$

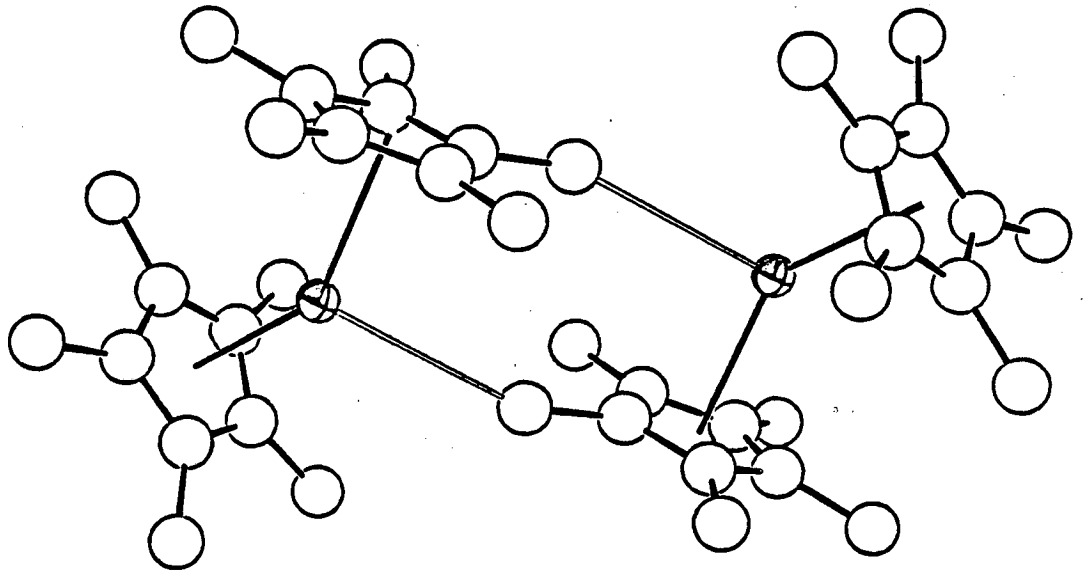

In the brown-black form of $(Me_5C_5)_2Yb$, the analogous molecules are no longer related by an inversion center; one unit twists with respect to the other, so that it forms close contacts with a molecule in an adjoining asymmetric unit. Yb(2) now has two close contacts with methyl groups on a ring bonded to Yb(1): Yb2···C19 = 3.078(4) Å and Yb2···C20 = 3.305(5) Å. The Yb(1) in turn has one close contact (Yb1···C36 = 2.944(4) Å) to a methyl group on a ring associated with a Yb(2) in an asymmetric unit related by a unit translation along the c axis. The result of these contacts is a "linear coordination polymer" (Figure 6). The strength of these interactions is obviously weak; they must be on

Figure (6) Intermolecular Contacts in $(Me_5C_5)_2Yb$

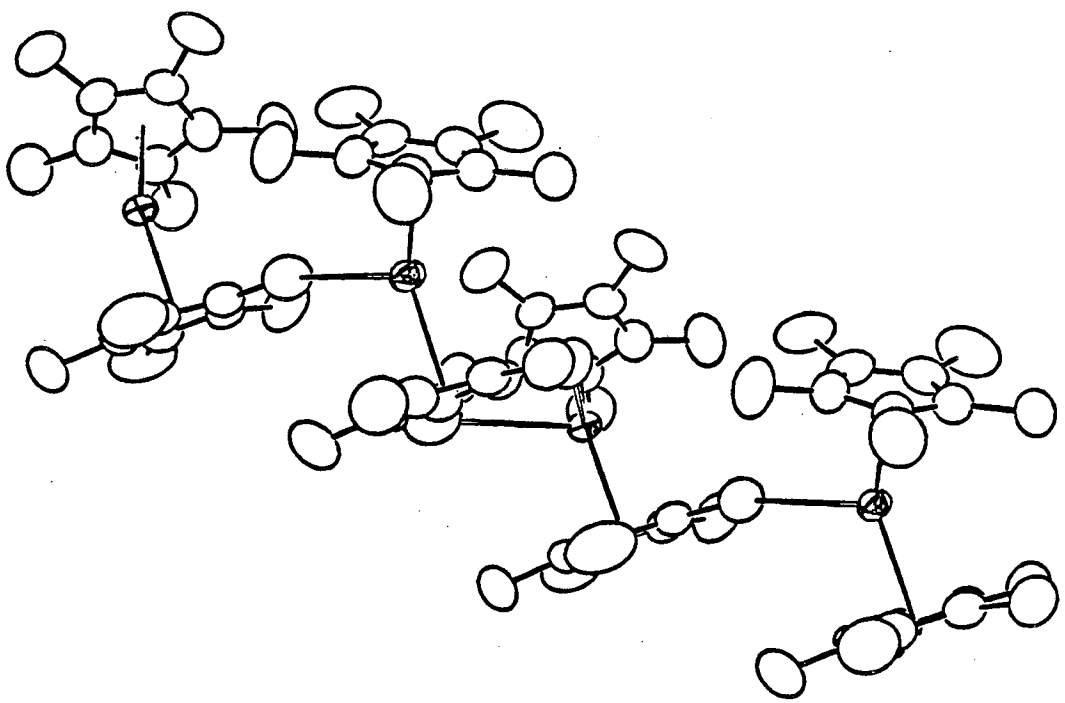

the order of solvation energies, since the compounds are all hydrocarbon soluble. The IR spectra of the different crystal morphologies are superimposible. It is unknown whether the structure distorts to allow these acid-base interactions to occur in the solid state, or whether they exist incidentally simply because of crystal packing forces. This topic will be discussed further in Chapter Three.

Whatever their origin, these intermolecular interactions may have the effect of compressing the ring-centroid-ring centroid angle in the solid state, in the same way that the angle is compressed in base adducts. In order to study the structure of these molecules in the absence of such perturbations, electron diffraction experiments have recently been carried out in the gas phase on $(Me_5C_5)_2M$ (M = Yb, Mg, Ca, Sr, and Ba)[19]. The results of these investigations can be found in Table VI.

The gas phase results indicate that the compounds (except for Mg)

Table VI Geometrical Paramaters for $(Me_5C_5)_2M$

M	M-C/Å (mean)	l/Å[e]	M-Cp/Å	α/°[a]	θ/°[b]	$\angle C_5,C_5$/°[c]
Yb	2.622(6)	9.4(5)	2.326(5)	158(4)	-1(2)	20(3)
Mg	2.341(6)	11.9(13)	2.101(8)	0[d]	0[d]	0[d]
Ca	2.609(6)	9.9(11)	2.312(6)	154(3)	-3(1)	20(2)
Sr	2.750(8)	10.5(7)	2.469(6)	149(3)	-3(2)	25(3)
Ba	2.898(17)	14.8(16)	1.631(6)	148(6)	-3(3)	26(6)

[a]The ring centroid-metal-ring centroid angle. [b]The tilt angle of the ring away from a perpendicular to the metal-centroid axis. [c]The angle between the ring planes. [d]Fixed value. [e]l = r.m.s. amplitude of vibration

have a bent-sandwich geometry. The best fit to the experimental data was obtained when the rings in the refinement model had a staggered geometry. Within experimental error, the differences in the metal-carbon bond lengths are exactly as one would expect given the differences in metal ion radii (see Table I). The Yb-C bond length is slightly smaller than the value found in the solid state; this may indicate that the intermolecular contacts in the solid state may effectively increase the coordination number of the metal, thereby increasing its ionic radius.

Refinement of α and θ clearly shows that the non-parallel ring geometry is due to a bending of the molecule, rather than to tilting of the rings. The bend angle in the case of Yb is not statistically larger than the value in the solid state; the smallest intramolecular Me-Me distance in the gas phase is 4.15(10) Å. The bend angles decrease with increasing metal radius. It must be cautioned that the structures correspond to thermal average values; the data are not corrected for shrinkage effects[21], and a regular sandwich can not be ruled out as the equilibrium structure. A regular sandwich structure is considered unlikely, however, based on a comparison of the r.m.s. amplitudes of vibration for the M-C bond lengths with the values for other decamethylmetallocenes[22]. If the equilibrium geometry is regular, the energy required to bend the molecule 20° must be less than ca. 1.9 kJ/mol.

Bonding

Any explanation for the unusual bent geometry of the bis(penta-

methylcyclopentadienyl)lanthanides and alkaline earths must rely on an assumption for the bonding model to be employed. Information about the nature of the bonding in these complexes has been derived from the results of recent UV photoelectron spectroscopy (PES) experiments[23]. In UV PES studies, electrons are ionized from valence molecular orbitals, and so information may be obtained as to the extent of stabilization of the ligand orbitals through covalent interaction with metal-based orbitals. This is illustrated in Figure 7. In the familiar molecular orbital diagram for a metallocene in D_{5d} symmetry, it can be seen that the most easily ionized electrons are those in the a_{1g} and e_{2g} orbitals, primarily metal-based orbitals. The next highest occupied molecular orbitals are those principally involved in metal-ligand bonding: the e_{1g} and e_{1u} orbitals. These orbitals are derived from the occupied cyclopentadienyl π-bonding orbitals, stabilized through interaction with

Figure (7) Molecular Orbital Diagram for D_{5d} $M(C_5H_5)_2$

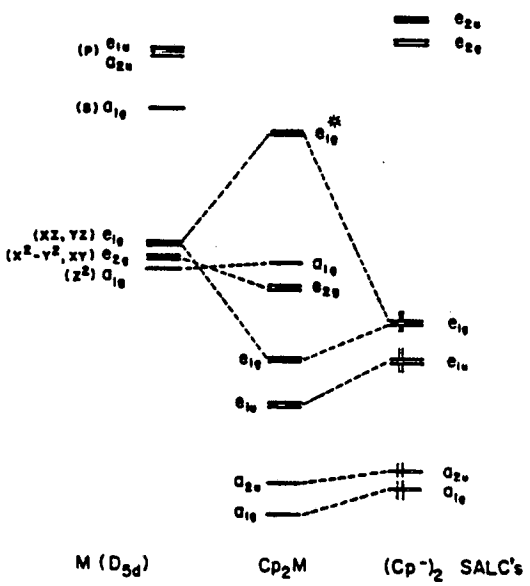

metal-based orbitals. The more covalent the interaction, the more these orbitals are stabilized, and the higher the energy required to ionize the electrons. The splitting between the e_{1g} and e_{1u} bands can also be indicative of the degree of covalent interaction. The e_{1g} set interacts with metal nd_{xz} and nd_{yz} orbitals, while the e_{1u} set must interact with the higher-lying $(n + 1)p_x,p_y$ pair. As the covalent interaction increases, the e_{1g} orbitals are stabilized to the point where they move below the e_{1u} in energy in the d-transition metal series (these may be distinguished by their differing He(I)/He(II) intensity ratios). The larger the splitting, the more covalent the interaction. In Table VII, the PES data is presented for the lanthanide[23] and alkaline earth[24]

Table VII Vertical Ionization Energy (eV) Data for $(Me_5C_5)_2M$

M	Adiabatic Edge of e_1 band	e_1u	e_{1g}	Splitting	Other
Mg	6.90	7.75	7.05	0.70	-
Ca	6.46	6.99		-	-
Sr	6.30	6.98		-	-
Ba	6.13	6.75		-	-
Sm	6.30	7.05		-	5.37, 5.57[a]
Eu	6.30	6.93		-	6.26[a]
Yb	6.50	7.11		-	6.11[a]
V	7.00	7.27	7.69	0.42	5.87[b]
Cr	7.10	7.27	7.89	0.62	4.93, 6.18, 6.34, 6.69[b]
Mn	7.10	7.26	7.95	0.69	5.33, 5.72, 6.37, 6.50, 6.72[b]
Fe	7.30	7.31	8.08	0.77	5.88, 6.28[b]

[a] 4f ionizations. [b] 3d ionizations from e_{2g} and a_{1g} orbitals; for detailed discussion, see reference 25a.

compounds, as well as the assignments for some first row decamethylmetallocenes[25] for comparison. The primary feature to note is the position of the ring ionizations. For the first row metallocenes, the e_1 ionizations are higher in energy, indicating stabilization of the ring π-orbitals interaction with metal-based orbitals: covalent bonding. For the lanthanide and alkaline earth complexes, the e_1 ionizations are much lower in energy, corresponding to a greater localization of charge density on the rings, or ionic bonding. It should also be noted that there is no separation of the e_{1g} and e_{1u} bands in these latter species. This is taken primarily as a further indication of ionic bonding, but there may be another factor involved in decreasing the resolution. In a reduction symmetry from D_{5d} to C_{2v}, the e_{1g} and e_{1u} degenerate orbital pairs are reduced in symmetry to $a_2 + b_2$ and $a_1 + b_1$, respectively. This closely spaced manifold of 4 orbitals may not be resolved, but appear as a single broad band. For the ionic D_{5d} metallocene $(Me_5C_5)_2Hg$, the degenerate levels will still be resolvable.

Quasi-relativistic Xα-SW molecular orbital calculations[23] have confirmed the essential results of the PES study. Covalent contributions to the bonding of the bis(pentamethylcyclopentadienyl)-lanthanides are small, as indicated by the localization of charge on the ligands, and by the very small ligand field splitting of the 4f orbitals (0.07 eV). Molecular orbital calculations could not establish a reason for the bending of the molecules, however.

The explanation for the trends in the geometries of these species may be similar to that used to explain the bending in alkaline earth dihalides. Experiments using the electric quadrupole deflection of

molecular beams[26] have established that for a given halide, the molecular geometry of its alkaline earth compound becomes progressively more bent as one progresses down the group:

Table VIII Geometries of Alkaline Earth Dihalides

∠ X-M-X	F	Cl	Br	I
Be	180°	180°	180°	180°
Mg	≈ 160°	180°	180°	180°
Ca	140°	180°	180°	180°
Sr	108°	118-130°	180°	180°
Ba	≈ 100°	≈ 120°	"bent"	"bent"

Two models have been employed to explain these structural trends. An orbital hybridization model has been proposed[27] in which a linear geometry for a triatomic molcule is considered to be the result of an s-p hybridization of the central metal, while a bent structure is the result of s-d hybridization. The factor which determines what geometry a molecule will adopt is the energy of rehybridization. Descending Group 2, the ns → (n - 1)d electron promotional energy decreases with respect to that for ns → np, so that the heavier alkaline earths are more likely to exhibit a bent geometry. With decreasing halide size, the electronegativiy of the halide increases, leading to increased cationic character for the central metal. This is proposed to lower the sd "valence state" with respect to the sp valence, giving rise to an increased bending angle. What this model fails to take into account, however, is cation polarizability. The error of this assumption is apparent when one considers that some estimates place the polarizability of Ba^{2+} above that of F^- [30].

Considering the preponderance of evidence suggesting ionic bonding for the lanthanide and alkaline earth compounds studied here, it is

desirable to invoke a model which relies only on electrostatic considerations to explain the geometry. The polarizable-ion model, first applied to a calculation of the binding energies and dipole moments of alkali halide molecules[28], has subsequently been used successfully to calculate not only thermochemical properties[29], but also equilibrium geometries of alkaline earth dihalides[30].

The model is empirical, requiring the knowledge of certain parameters such as internuclear distances, vibrational force constants, and ion polarizabilities, but these values can then be used to derive binding energies, dipole moments, and bending angles. The basis of the model as applied to metal dihalides is a calculation of U_T, the total heat of formation of MX_2 from the free ions (see Figure 8):

$$U_T = U_e + U_r + U_{vw} \qquad (5)$$

U_e = electrostatic binding energy
U_r = repulsive energy
U_{vw} = van der Waals attractive energy

This formula neglects zero point and thermal energies. The term U_r accounts for the repulsion between ions when the outer electron shells begin to overlap. It is usually calculated by a formula similar to equation (6), summed over all ion pairs. The term U_{vw} describes the instantaneous dipole attractions between the ions, and is of the form of equation (7).

$$U_r = \sum_{ij} A_{ij}\exp(-r_{ij}/\rho_{ij}) \ , \ \rho = \text{large} \qquad (6)$$

$$U_{vw} = - \sum C_{ij}/(r_{ij})^6 \qquad (7)$$

Both of these terms operate only at very short range, and do not make significant contributions to the total energy for values of θ greater

Figure (8) Electrostatic Parameters for a Triatomic Molecule

$$U_{tot} = U_e + U_{vw} + U_r$$

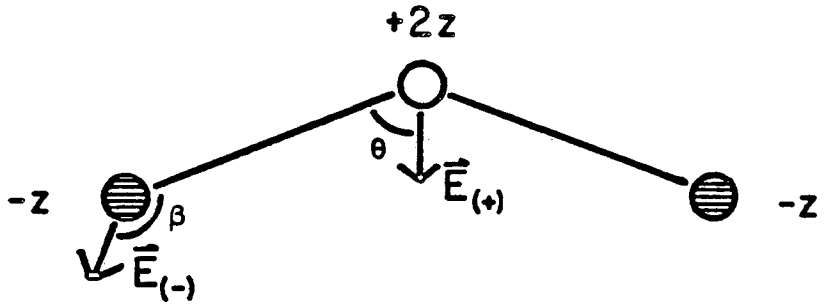

$$\text{dipole moment } \mu_i = \alpha_i E_i$$

α_i = static ion polarizability

than ca. 30°. They must be included in any energy calculations, but can be neglected when calculating the geometry of the molecule. The final term, U_e, is the sum of all the electrostatic forces in the molecule:

$$U_e = U_{cc} + U_{cd} + U_{dd} + U_{fd} \qquad (8)$$

U_{cc} = charge-charge interactions
U_{cd} = charge-dipole interactions
U_{dd} = dipole-dipole interactions
U_{fd} = work of inducing dipoles

Assuming values for r_1 and z, E+ and E- can be calculated. Then by assuming values for the static ion polarizabilities, the induced dipole moments can be calculated as functions of θ. This allows the terms in equation (8) to be evaluated. A detailed treatment may be found in reference 30. If the molecule consists of a large, polarizable cation and small, relatively non-polarizable anions, bending the molecule increases the magnitude of the electrostatic field (and hence the dipole moment) at the cation more than at the anions. This in turn increases

favorable negative charge-positive dipole and negative dipole-positive dipole attractions. For large values of θ, this increase more than offsets the increase in repulsion between the anions, and bending is favored.

This model can be successfully applied to lanthanides, and has been used not only to predict trends in structures and vibrational frequencies for halides[31], but also to calculate dissociation energies both for halides[32] and for mono-oxides[33] in the gas phase. The question of the applicability of this model to bis(cyclopentadienyl) lanthanides then lies in the assumption that $C_5Me_5^-$ is a relatively non-polarizable anion. The polarizabilities of ions are sometimes approximated by an equation of the form:

$$\alpha \propto C\ r^2/IP \qquad (9)$$

where r^2 is the average value of the square of the radius of the valence electron orbit, and IP is the ionization potential of the ion[34]. The component of the polarizability of interest is that perpendicular to the plane of the ring, since when θ is large, so is β. The radial extent of the valence orbitals in this direction is that of the C 2p orbitals, i.e. the polarizability in the direction of the cation is not expected to be large.

Coordination Chemistry

The postulate that similar ionic radii for lanthanides and alkaline earth bis(pentamethylcyclopentadienyl) compounds should lead to similar coordination behavior seems to be verified by the coordination chemistry with ethers. Metals of the same approximate size, such as Yb and Ca, will form the same adduct (e.g. a mono-diethylether adduct), whereas a

larger metal, such as Ba, will not form the analogous compound. On the other hand, the largest members of each series, Sm and Ba, both form 1:2 adducts with thf[35], whereas the Yb compound only forms a 1:1 adduct[18]. In an attempt to extend the comparison, a series of compounds has been prepared using three ligands of varying base strengths: bipyridine, 2,6-dimethylphenylisocyanide, and triethylphosphine. All of the adducts can be made in the same stoichiometry for each metal, however, and so no additional information can be gained about relative ligand affinities for metals of different sizes.

All of the coordination compounds are synthesized by reaction of the base-free metal complex with the appropriate number of equivalents of ligand in hydrocarbon solvent, followed by crystallization, although for the stronger ligands bipyridine and isocyanide, the ytterbium complexes have been synthesized from the diethylether adduct[18,36].

Bipyridine

The products of the reaction of $(Me_5C_5)_2Eu$ and $(Me_5C_5)_2Yb$ with bipyridine have been previously characterized[3,18]. The Eu complex forms a simple 1:1 adduct, but the Yb species reduces the heterocyclic ligand to form a radical anion-Yb(III) complex. The Yb product was therefore not used for comparison. Some physical characteristics of these compounds can be found in Table IV. The most important feature of the coordination compounds is their insolubility in hydrocarbon solvents; the complexes must be recrystallized from hot toluene. Because of this insolubility, the complexes could not be characterized by solution methods, and evaluation of the stoichiometry was based on analytical

Table IV Data for $(Me_5C_5)_2M(bipy)$

M	Color	MP	Anal.
Eu	Brown	>300°C	C 62.3, H 6.62, N 4.84 Found: C 60.9, H 6.67, N 4.75
Ca	Red	>330°C	C 77.2, H 8.21, N 6.00 Found: C 76.9, H 8.27, N 5.82
Sr	Red	>330°C	C 70.0, H 7.46, N 5.45 Found: C 69.4, H 7.51, N 5.38
Ba	Red	317-319°C	C 63.9, H 6.80, N 4.97 Found: C 63.0, H 6.92, N 4.96

data. Of all of the base adducts of the alkaline earth compounds, the bipyridine complexes are the most stable towards hydrolysis. The alkaline earth species are very sensitive to hydrolysis, seemingly more so than the lanthanides; this is a feature of their chemistry which is not well understood. The hydrolytic sensitivity increases in proportion to the metal ionic radius. Because of this, analytical data are generally poor.

The most startling feature of the alkaline earth complexes is their bright color; although the coordination of heterocyclic bases was observed to induce color changes in $Ca(C_5H_5)_2$[37], the colors produced were much paler. Other main group complexes of bipyridine have been shown to exhibit bright colors, however[38].

Triethylphosphine

The phosphine was the most weakly coordinating base to be studied in this series, as evidenced by the colors of the alkaline earth species. While phosphine complexes of $(Me_5C_5)_2Yb$ have been synthesized

previously[39], phosphine complexes of Group 2 elements have not been reported. Reaction of the base-free species with any number of equivalents of phosphine produced only the 1:1 adduct. Some physical characteristics of these species are given in Table X. These

Table X Data for $(Me_5C_5)_2M(PEt_3)$

M	Color	MP	^{1}HNMR	^{31}PNMR
Yb	Green	128-132°C	δ 2.05 (30H) δ 1.24 (9H), δ 0.93 (6H)	δ -20.1 (s)
Ca	White	111-113°C	δ 1.98 (30H) δ 1.21 (9H), δ 0.87 (6H)	δ -20.3 (s)
Sr	White	140-142°C	δ 2.03 (30H) δ 1.21 (9H), δ 0.85 (6H)	δ -20.1 (s)
Ba	White	250-255°C	δ 1.96 (30H) δ 1.17 (9H), δ 0.89 (6H)	δ -20.3 (s)

species were studied by $^{31}P\{^1H\}$NMR spectroscopy in an attempt to discern any solution perturbation of the phosphorus chemical shift. The values for all of the complexes were the same, at approximately the free value of PEt_3. This indicated the possibility of a dissociative equilibrium in solution. Variable temperature studies were then carried out, with the goal of freezing out this equilibrium. These experiments were not successful. While in the case of the heavier alkaline earth compounds (Sr, Ba) the phosphorus resonance was observed to move upfield slightly upon cooling to -80°C, the signal had not broadened significantly ($\nu_{1/2}$ = 4 Hz), indicating that the equilibrium was not being slowed substantially.

2,6-Dimethylphenylisocyanide

The isocyanide ligand forms a 2:1 adduct with all of the alkaline earth complexes, as well as with $(Me_5C_5)_2Eu$ and $(Me_5C_5)_2Yb$. It is

reduced by the samarium complex to give an uncharacterized mixture of products. Some physical characteristics of the coordination compounds are given in Table XI. The position of the νCN band in the IR spectra

Table XI Data for $(Me_5C_5)_2M(CNR)_2$ (R = 2,6-dimethylphenyl)

M	Color	MP	ν CN (cm^{-1})
Eu	brown	229-231°C	2144s, 2115w
Yb	green-brown	199-202°C	2131s, 2116sh, 2095m
Ca	yellow	213-215°C (dec)	2145s, 2115m
Sr	yellow	230-233°C (dec)	2150s, 2115m
Ba	yellow	211-212°C (dec)	2138s, 2115m

of the compounds can be indicative of the nature of the metal ligand interaction. If the isocyanide is acting simply as a σ-donor, the CN stretching frequency will increase upon complexation, whereas if the ligand is acting as a π-acceptor, the stretching frequency will be reduced[40]. For example, νCN for free cyclohexylisocyanide is 2135 cm^{-1}. This value is raised to 2215 cm^{-1} in the coordination compound with $AlPh_3$[41], and to 2160 in the complex with $U(C_5H_5)_3$[42]. The values of νCN for the complexes considered in Table XI are all raised from that of the free ligand, 2115 cm^{-1}. In addition, a band is seen in all the spectra at the position of the free ligand, indicating either hydrolysis, or dissociation of the isocyanide in the Nujol mull.

While the ^{1}HNMR spectra of the alkaline earth adducts all showed normal diamagnetic shifts, the spectrum of the Yb species showed broadened resonances at room temperature. Solid state magnetic susceptibility measurements indicated that the compound was diamagnetic, however, indicating that the broadened signals were probably due to

chemical exchange. Variable temperature NMR experiments were carried out on the Ca, Sr, Ba, and Yb compounds with added excess isocyanide. In the case of the alkaline earth compounds, there was one sharp signal for the ortho-methyl groups at room temperature, indicating rapid exchange of free and coordinated ligand. Upon cooling to -80°C, the methyl resonance of the ligand had begun to broaden ($\nu_{1/2}$ = 10 Hz), but exchange had not been stopped. In the case of the Yb compound, adding excess ligand caused the room temperature spectrum to broaden further; the isocyanide methyl resonance appeared as a broad singlet at δ 2.89 ($\nu_{1/2}$ = 35 Hz), and the C_5Me_5 protons appeared at δ 2.34 ($\nu_{1/2}$ = 12 Hz). Warming this sample to +70°C caused the resonances to sharpen as the fast exchange limit was approached. When the sample was cooled, the resonances remained unchanged until -50°C; at this point, a multiplet was observed in the aryl region at δ 6.76, and two other signals were visible at δ 2.72 ($\nu_{1/2}$ = 28 Hz) and δ 2.46 ($\nu_{1/2}$ = 4 Hz), corresponding to isocyanide methyl and C_5Me_5 resonances. The resonances then became sharper down to -70°C, when resolution was lost.

The differences in the solution behavior of the complexes $(Me_5C_5)_2M(CNR)_2$ (M = Yb, Ca) is significant in that it represents the only evidence in the study of the coordination chemistry of these species that the lanthanide and alkaline earth complexes may display different bonding properties. While the origin of this difference is not understood (the similarity of the IR stretching frequencies argues against any substantial degree of π back-bonding), it would appear that the barrier to dissociation of the isocyanide is higher for the Yb complex than for its calcium analog.

References

1.) Boncella, J. M., Ph.D. Thesis, University of California, Berkeley, California, U.S.A., 1984.

2.) Evans, W. J.; Hughes, L. A.; Hanusa, T. P., Organometallics, 1986, 5, 1285.

3.) Tilley, T. D., Ph.D. Thesis, University of California, Berkeley, California, U.S.A., 1982.

4.) Berg, D. J., Ph.D. Thesis, University of California, Berkeley, California, U.S.A., 1987.

5.) Shannon, R. D., Acta Cryst., 1976, 32A, 751.

6.) Evans, W. J.; Hughes, L. A.; Hanusa, T. P., J. Am. Chem. Soc., 1984, 106, 4270.

7.) a) Van Vleck, J. H., "The Theory of Electronic and Magnetic Susceptibilities", Clarendon Press, Oxford, 1932. b) Edelstein, N. M., in "Organometallics of the f-Elements" (T. J. Marks and R. D. Fischer, eds.), D. Reidel, Dordrecht, 1979, p. 37.

8.) a) Robbins, J. L., Ph.D. Thesis, University of California, Berkelely, California, U.S.A., 1981, and references therein.

9.) a) Bunder, W.; Weiss, E., J. Organomet. Chem., 1975, 92, 1. b) Haaland, A.; Lusztyk, J.; Brunvoll, J.; Starowieyski, K. B., J. Organomet. Chem., 1975, 85, 279.

10.) a) Nugent, K. W.; Beattie, J. K.; Hambley T. W.; Snow, M. R., Austr. J. Chem., 1984, 37, 1601. b) Almenningen, A.; Haaland, A.; Lusztyk, J., J Organomet. Chem., 1979, 170, 271.

11.) Zerger, R.; Stucky, G., J. Organomet. Chem., 1974, 80, 7.

12.) a) Jutzi, P.; Kohl, F.; Hofmann, P.; Kruger, C.; Tsay, Y.-H., Chem. Ber., 1980, 113, 757. b) Grenz, M.; Hahn, E.; du Mont W.-W.; Pickardt, J., Angew. Chem., 1984, 96, 69. c) Atwood, J. L.; Hunter, W. E.; Cowley, A. H.; Jones, R. A.; Stewart, C. A., J. Chem. Soc. Chem. Comm., 1981, 925.

13.) a) Almenningen, A.; Haaland, A.; Motzfeldt, T., J. Organomet. Chem., 1967, 7, 97. b) Fernholt, L.; Haaland, A.; Jutzi, P.; Kohl, F. X.; Seip, R., Acta Chem. Scand., 1984, A38, 211. c) Almlof, J.; Fernholt, L.; Faegri, K., Jr.; Haaland, A.; Schilling, B. E. R.; Seip, R.; Taugbol, K., Acta Chem. Scand., 1983, A37, 131.

14.) Heeg, M. J.; Janiak, C.; Zuckerman, J. J., J. Am. Chem. Soc., 1984, 106, 4259.

15.) Jutzi, P.; Kanne, D.; Kruger, C., Angew. Chem. Int. Ed. Engl., 1986, 25, 164.

16.) Budzelaar, P. H. M..; Boersma, J.; v.d. Ker, G. J. M.; Spek, A. L.; Duisenber, A. J. M., J. Organometal. Chem., 1985, 281, 123.

17.) Blom, R.; Boersma, J.; Budzelaar, P. H. M.; Fischer, B.; Haaland, A.; Volden H. V.; Weidlein, J., Acta Chem. Scand., 1986, A40, 113.

18.) Tilley, T. D.; Andersen, R. A.; Spencer, B.; Ruben, H.; Zalkin A.; Templeton, D. H., Inorg. Chem., 1980, 19, 2999.

19.) Gong, L.; Streitwieser, A., Jr.; Zalkin, A., J. Chem. Soc. Chem. Comm., 1987, 460.

20.) a) Andersen, R. A.; Boncella, J. M.; Burns, C. J.; Blom, R.; Haaland, A.; Volden H. V., J. Organomet. Chem., 1986, 312, C49. b) Andersen, R. A.; Blom R.; Boncella, J. M.; Burns, C. J.; Volden H. V., Acta Chem. Scand., 1987, A41, 24. c) Andersen, R. A.; Blom, R.; Burns, C. J.; Volden H. V., J. Chem. Soc. Chem. Comm., in press.

21.) a) Almenningen, A.; Bastiansen, O.; Traetteberg, M., Acta Chem. Scand., 1961, 15, 1557. b) Morino, Y., Acta Cryst., 1960, 13, 1107. c) Cyvin, S. J., "Molecular Vibrations and Mean Square Amplitudes", Universitetsforlaget, Oslo, and Elsevier, Amsterdam, 1968.

22.) Almenningen, A.; Haaland, A.; Samdal S.; Brunvoll, J.; Robbins, J. L.; Smart, J. C., J. Organomet. Chem., 1979, 173, 293.

23.) a) Andersen, R. A.; Boncella, J. M.; Burns, C. J.; Green, J. C.; Hohl, D.; Rosch, N., J. Chem. Soc. Chem. Comm., 1986, 405. b) Green, J. C.; Hohl, D.; Rosch, N., Organometallics, 1987, 6, 712.

24.) Green, J. C., personal commumication.

25.) a) Cauletti, C.; Green, J. C.; Kelly, M. R.; Powell, P.; van Tilborg, J.; Robbins, J.; Smart, J., J. Electr. Spectr., 1980, 19, 327. b) Green, J. C., Struct. Bonding, 1981, 43, 37.

26.) a) Wharton, L; Berg, R. A.; Klemperer, W., J. Chem. Phys., 1963, 39, 2023. b) Buchler, A.; Stauffer, J. L.; Klemperer, W.; Wharton, L., J. Chem. Phys., 1963, 39, 2299. c) Buchler, A.; Stauffer, J. L.; Klemperer, W., J. Am. Chem. Soc., 1964, 86, 4544.

27.) a) Hayes, E. F., J. Phys. Chem., 1966, 70, 3740. b) Coulson, C. A., Isr. J. Chem., 1973, 11, 683.

28.) Rittner, E. S., J. Chem. Phys., 1951, 19, 1030.

29.) a) Brackett, T. E.; Brackett, E. B., J. Phys. Chem., 1962, 66, 1542. b) Buchler, A.; Klemperer, W.; Emslie, A. G., J. Chem. Phys., 1962, 36, 2499. c) Eliezer, I.; Reger, A., Theor. Chim. Acta, 1972, 26, 283.

30.) Guido, M.; Gigli, G., J. Chem. Phys., 1976, 65, 1397.

31.) Drake, M. C.; Rosenblatt, G. M., J. Electrochem. Soc., 1979, 126, 1387.

32.) Hildenbrand, D. L., J. Electrochem. Soc., 1979, 126, 1396.

33.) Guido, M.; Gigli, G., J. Chem. Phys., 1974, 61, 4138.

34.) a) Hildenbrand, D. L. J. Chem. Phys., 1968, 48, 3657. b) Blue, G. D.; Green, J. W.; Ehlert, T. C.; Margrave, J. L., Nature, 1963, 199, 804.

35.) Evans, W. J.; Bloom, I.; Hunter, W. E.; Atwood J. L., J. Am. Chem. Soc., 1981, 103, 6507.

36.) Henley, T., unpublished results.

37.) Allan, K. A.; Gowenlock, B. G.; Lindsell, W. E., J. Organomet. Chem., 1973, 55, 229.

38.) Arnold, J.; Tilley, T. D.; Rheingold; A. L.; Geib, S. J., Inorg. Chem., 1987, 26, 2106.

39.) Tilley, T. D.; Andersen, R. A.; Zalkin, A., Inorg. Chem., 1983, 22, 856.

40.) a) Sarapu, A. C.; Fenske, R. F., Inorg. Chem., 1975, 14, 247. b) Cotton, F. A.; Zingales, F., J. Am. Chem. Soc., 1961, 83, 351.

41.) Hesse, G.; Witte, H.; Mischke, P., Angew. Chem., 1965, 77, 380.

42.) Kanellakopulos, B.; Fischer, E. O.; Dornberger, E.; Baumgartner, F., J. Organomet. Chem., 1970, 24, 507.

CHAPTER TWO: Coordination Chemistry with Unsaturated Ligands

Coordination Compounds

Coordination compounds of d-block transition metals with olefins and acetylenes[1] have been studied extensively. The bonding in such complexes is described as consisting of two components[2]; the filled π-bonding orbitals of the unsaturated molecules act as σ-donor electron pairs to the metal, while the empty π-antibonding orbitals are available to accept electron density from occupied metal π-symmetry orbitals. Coordination of potential π-accepting ligands to lanthanides has also been implied to exist in a number of reduction[3] and insertion[4] reactions, and a complex of Sm(III) with a neutral arene ((Me_6C_6)-$Sm(AlCl_4)_3$) has been isolated[5]. In spite of this, no coordination compound of a lanthanide with a neutral olefin or acetylene has previously been characterized.

The base-free bis(pentamethylcyclopentadienyl)lanthanide compounds are ideal starting materials for the synthesis of such species. Most homoleptic cyclopentadienyl compounds are coordinatively saturated by the presence of three cyclopentadienyl groups or strong auxiliary Lewis bases. The compounds $(Me_5C_5)_2M$, however, are coordinatively unsaturated, and the ytterbium and europium complexes are stable with respect to oxidation, minimizing the likelihood of subsequent reaction. The ytterbium compound is particularly well suited because it is diamagnetic, allowing the use of NMR spectroscopy as a diagnostic tool.

The structure of $(Me_6C_6)Sm(AlCl_4)_3$ reveals that the arene is η^6-bound to the lanthanide[5], and it is suggested that the electron rich π-

system of the aromatic ring is forming a dative bond to the lanthanide. While lanthanides are fully capable of participating in such an acid-base interaction, the only occupied metal valence orbitals of the proper symmetry to interact in a π fashion with a donor ligand are the f orbitals, which are too shielded to overlap appreciably with empty π^* orbitals on an unsaturated molecule. Thus, the lanthanides are not capable of engaging in back-bonding.

In d-transition metal chemistry, the importance of back-bonding is manifested in the preference of the later transition metals for olefins and acetylenes with electron-withdrawing substituents[1c,6]; the inductive effect of the substituents increases the metal to ligand back-donation, increasing the M-L bond strength. If ligand to metal σ-donation is the only component to the bonding, however, the strongest interaction will be created by increasing the effective electron density in the π system of the unsaturated molecule.

One way of achieving this is to coordinate an olefin to an electron-rich, low-valent metal, such as a member of the nickel triad. The π-donation of electrons from the metal to the olefin should create a partial negative charge at the olefin carbons. Addition of a solution of $(PPh_3)_2Pt(C_2H_4)$ to $(Me_5C_5)_2Yb$ results in the isolation of a red crystalline 1:1 adduct, $(Me_5C_5)_2Yb(\mu\text{-}C_2H_4)Pt(PPh_3)_2$. The analogous nickel complex can be prepared, and is isolated as green crystals. The IR spectra of these compounds resemble a superposition of the spectra of the component molecules, indicating little or no structural perturbation has taken place on complexation.

In an attempt to evaluate the strength of such an interaction,

variable temperature NMR studies have been carried out on the Pt complex. The phosphorus chemical shift is very close to that of the free platinum olefin complex, although the Pt-P coupling constant is slightly higher. Neither the chemical shift nor the linewidth change appreciably, however, upon cooling the sample to -70°C.

The behavior of the ^{1}HNMR spectrum with temperature, however, gives a clear indication that this is a chemically exchanging system (the exchange observed is presumed to be between free and coordinated $(C_2H_4)Pt(PPh_3)_2$ (eqn. 1)). In d^6-benzene, the resonance due to the

$$(Me_5C_5)_2Yb + (C_2H_4)Pt(PPh_3)_2 \rightleftharpoons (Me_5C_5)_2Yb(\mu\text{-}C_2H_4)Pt(PPh_3)_2 \quad (1)$$

ethylene protons is visible at 90 MHz (30°C) as a broadened triplet at δ 2.18 (shifted somewhat upfield from the free complex). At 500 MHz, however, this signal is not visible at room temperature, and only begins to reappear in the spectrum at δ 2.23 upon warming the solution to 50°C. The fast exchange limit is not reached by 90°C on this NMR time scale. In d^8-toluene, the averaged signal due to the ethylene protons is visible at room temperature at 500 MHz at δ 2.06. Cooling this solution causes the ethylene signal to broaden and disappear. At -70°C, the signal due to the C_5Me_5 ligand is also broad, indicating that a region of intermediate exchange has been reached. The rate of exchange is evidently faster in d^8-toluene than in d^6-benzene, as indicated by the regions of intermediate exchange (-70°C and 30°C, respectively). It is possible that the aromatic solvents themselves can act as bases towards the ytterbium complex through polarization of the π-electrons, in a manner analogous to an olefin. In that case, the electron-donating effect of the methyl group on toluene should improve the "basicity" of

the molecule. The more strongly coordinating solvent could be expected to enhance the rate of dissociation of the Pt complex by competing for the Yb coordination site. Further evidence of coordinating effects of aromatic solvents will be discussed later in this chapter.

Although the NMR studies indicated that the ethylene unit was perturbed more by coordination to Yb than the phosphines, the inability to stop chemical exchange rendered the choice of a coordination site ambiguous. In order to establish the nature of the interaction, the structure of the compound has been determined by X-ray crystallography. Figure (1) is an ORTEP diagram of the complex, and pertinent bond distances and angles can be found in Tables I and II.

The molecule has approximately C_s symmetry, with the pseudo-mirror plane passing through both Yb, Pt, and the midpoint of the ethylene unit. The rings on the Yb are staggered, with a torsional angle of 30.6°. The structure of the $(C_2H_4)Pt(PPh_3)_2$ unit in the coordination

Table I Bond Distances for $(Me_5C_5)_2Yb(\mu\text{-}C_2H_4)Pt(PPh_3)_2$ (Å)

Pt-C1	2.084(3)	Pt-P1	2.284(1)	Yb-C11	2.693(3)
Pt-C2	2.085(3)	Pt-P2	2.266(1)	Yb-C12	2.675(3)
Yb-C1	2.770(3)			Yb-C13	2.672(3)
Yb-C2	2.792(3)	P1-C111	1.833(3)	Yb-C14	2.681(3)
		P1-C121	1.834(3)	Yb-C15	2.690(3)
C1-C2	1.436(5)	P1-C131	1.833(3)	Yb-C21	2.660(3)
C1-H1	0.85(5)	P2-C211	1.823(3)	Yb-C22	2.650(3)
C1-H2	1.07(4)	P2-C221	1.825(3)	Yb-C23	2.634(3)
C2-H3	0.93(3)	P2-C231	1.822(3)	Yb-C24	2.679(3)
C2-H4	0.97(4)			Yb-C25	2.694(3)
				Yb-Cp1	2.398
				Yb-Cp2	2.378

Cp1 and Cp2 are the centroids of the rings comprised of C11-C15 and C21-C25, respectively.

compound remains essentially unchanged from the structure of the free compound[7a], and the structure of the $(Me_5C_5)_2Yb$ unit does not differ

Figure (1) ORTEP Labeling Diagram of $(Me_5C_5)_2(\mu\text{-}C_2H_4)Pt(PPh_3)_2$

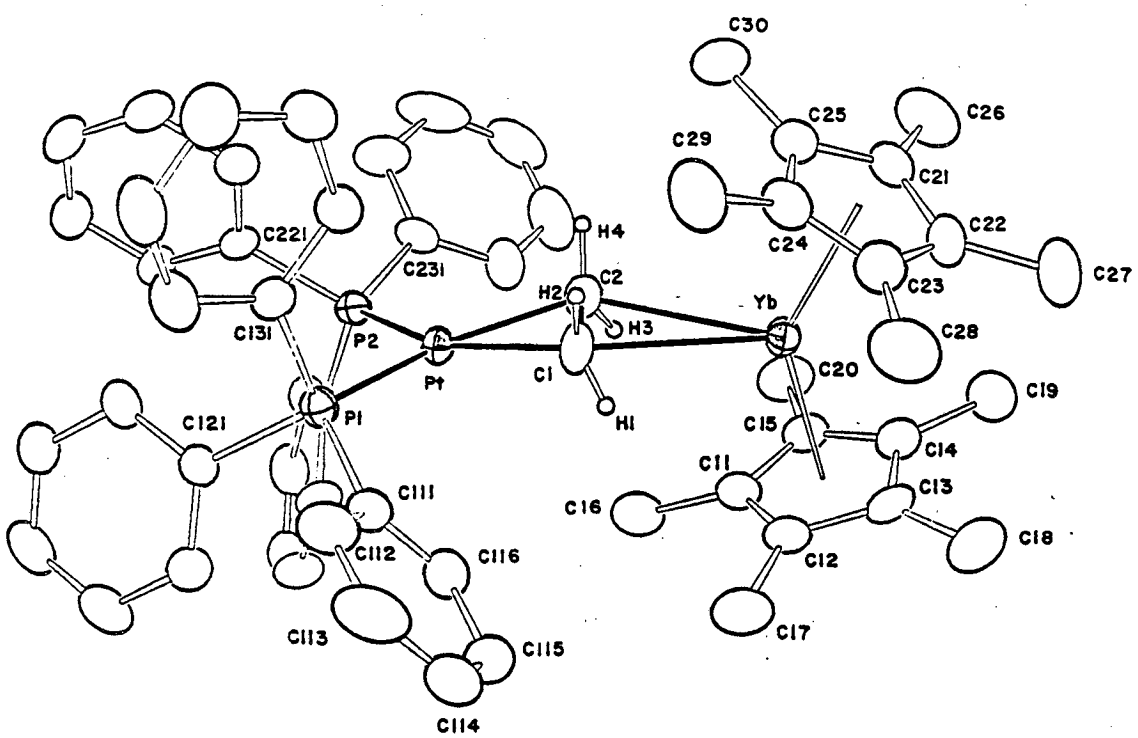

Table II Intramolecular Angles for $(Me_5C_5)_2Yb(\mu\text{-}C_2H_4)Pt(PPh_3)_2$ (°)

C1-Yb-C2	29.9(1)	Yb-C1-Pt	142.7(2)
Cp1-Yb-C1	108.7	Yb-C2-Pt	141.1(2)
Cp2-Yb-C1	106.8	Yb-C1-C2	75.9(2)
Cp1-Yb-C2	105.5	Yb-C2-C1	74.2(2)
Cp2-Yb-C2	111.6	Pt-C1-C2	69.9(2)
Cp1-Yb-Cp2	142.3	Pt-C2-C1	69.8(2)
C1-Pt-C2	40.3(1)	H1-C1-H2	117(4)
P1-Pt-C1	104.7(1)	H1-C1-C2	121(3)
P2-Pt-C1	148.9(1)	H2-C1-C2	113(2)
P1-Pt-C2	144.2(1)	H3-C2-H4	118(3)
P2-Pt-C2	108.7(1)	H3-C2-C1	117(2)
P1-Pt-P2	106.31(3)	H4-C2-C1	120(2)
H1-C1-Yb	68(3)	Pt-P1-C111	114.3(1)
H2-C1-Yb	97(2)	Pt-P1-C121	121.5(1)
H3-C2-Yb	71(2)	Pt-P1-C131	109.1(1)
H4-C2-Yb	103(2)	Pt-P2-C211	115.5(1)
H1-C1-Pt	118(3)	Pt-P2-C221	115.3(1)
H2-C1-Pt	110(2)	Pt-P2-C231	115.2(1)
H3-C2-Pt	113(2)		
H4-C2-Pt	108(2)		

substantially from the observed structure of the ytterbium complex determined in Chapter One. Some comparisons are given in Table III.

Table III Comparisons of Free and Coordinated Molecules

$(C_2H_4)Pt(PPh_3)_2$

	Bond Lengths (Å)			Bond Angles (°)		Ref.
	C-C	M-C	M-P	CMC	PMP	
Free	1.43(1)	2.106(8) 2.116(9)	2.265(2) 2.270(2)	39.7(4)	111.6(1)	7a
Coordinated	1.436(5)	2.084(3) 2.085(3)	2.284(1) 2.266(1)	40.3(1)	106.31(3)	this work
$(C_2H_4)NiP_2$	1.43(1)	1.98(1) 2.00(1)	2.147(4) 2.157(4)	42.1(5)	110.5(2)	7b

$(Me_5C_5)_2Yb$

	Bond Lengths (avg, Å)		Bond Angles (°)	Ref.
	Yb-C	Yb-Cp	Cp-Yb-Cp	
Free	2.665(3)	2.380	145.4	Chap. 1
Coordinated	2.673(3)	2.388	142.3	this work
$(Me_5C_5)_2Yb(thf)$	2.66(1)	2.37	143.5	8

The hydrogen atoms positions in free $(C_2H_4)Pt(PPh_3)_2$ were not determined, and so no comparison of the geometry of the ethylene unit is available. One parameter often used to describe the geometry of coordinated olefins is α, defined as the angle between the normals to the planes containing the olefinic C atoms and their substituents[9]. This angle is proposed to increase as the amount of π-back bonding increases. For $Pt(C_2H_4)_3$, the value has been determined by neutron diffraction[10] to be 31.4°, while in $Pt(C_2H_4)_2(C_2F_4)$, the values for the ethylene and tetrafluoroethylene units are 32° and 70.4°, respectively. The value of α in the structure of the Yb coordination complex is 52.7°.

The ytterbium atom does form the closest contact with the ethylene unit of the platinum compound, as indicated by the NMR data. The values of the Yb-C (olefin) bond distances are 2.770(3) Å and 2.792(3) Å. In the complex $(Me_5C_5)_2Lu(\mu\text{-}Me)Lu(Me)(Me_5C_5)_2$[11], the dative C(Me)-Lu contact distance is 2.756(9) Å; when this number is corrected for the larger effective ionic radius of Yb(II) relative to Lu(III) in the same coordination number (0.16 Å)[12], the value of a Yb-C dative bond length would be expected to lie in the range 2.85-2.9 Å.

The ytterbium-olefin interaction in this molecule is similar to alkali metal cation-olefin interactions seen in the solid state structures of salts of d-transition metal olefin anionic complexes such as $K[Co(C_2H_4)(PMe_3)_3]_2$[14a] and $\{LiCo(C_2H_4)(PMe_3)_3\}_3$[14b], and $[(NaC_6H_5)_2(thf)_2]NiC_2H_4$[14c]. In these compounds, the alkali metals are η^2-coordinated to ethylene units, with an average M-C distance of 3.12 Å in the potassium compound, 2.71 Å in the sodium compound, and M-C distances ranging from 2.21-2.61 Å in the lithium compound.

The planes defined by Pt-C1-C2 and Yb-C1-C2 meet in a dihedral angle of 15.1°. While the origin of this tilt is not known (it may simply be due to intermolecular packing forces), it brings two of the ethylene hydrogen atoms to within ca. 2.6 Å of the Yb atom: Yb-H1 = 2.58(5) Å, Yb-H3 = 2.64(3) Å (the other Yb-H distances are substantially longer: Yb-H2 = 3.09(4) Å, Yb-H4 = 3.15(3) Å). These distances are similar to non-bonding Yb-H distances of 2.53, 2.63, and 2.72 Å in $Yb[N(SiMe_3)_2]_2(Me_3Al)_2$[13a], and 2.77 and 2.86 Å in $Yb[N(SiMe_3)_2]_2(dmpe)$[13b]. This tilt is eventually stopped by the close approach of methyl carbons to the ethylene unit (C2···C16 = 3.406(5) Å).

Acetylenes should also provide electron-rich π systems available for coordination to acidic lanthanides. The presence of two orthogonal π-bonding orbitals enhances the basicity of these molecules. One way to infer the relative basicities of weak bases is to examine the changes that they produce in the infrared stretching frequencies of the O-H bond of phenol. Based on tabulated information, the the order of basicity of unsaturated hydrocarbons is alkynes > alkenes > 1,3-dienes $\simeq$ allenes[15]. This data reveals also that internal acetylenes are significantly more basic than their terminal counterparts (terminal acetylenes are sufficiently acidic to cause ring protonation[16], and therefore they are unsuitable for coordination studies). In agreement with this qualitative ordering, simple acetylene coordination compounds of ytterbium can be isolated.

Reaction of a variety of substituted acetylenes with $(Me_5C_5)_2Yb$ results in the formation of 1:1 coordination compounds:

$$(Me_5C_5)_2Yb + RC{\equiv}CR' \rightarrow (Me_5C_5)_2Yb(RC{\equiv}CR') \qquad (2)$$

(R= R'= Me; R = R'= Ph; R = Ph, R'= Me; R = t-Bu, R'= Me)

The 2-butyne adduct is red; all others are dark brown or black. No band attributable to $\nu C{\equiv}C$ is visible in the IR spectra of these compounds, indicating that the symmetry of the acetylene is not reduced appreciably upon coordination to the metal center. All of the spectra show a band at ca. 275 cm^{-1}. This band has been attributed to a M-ring stretching mode, and its position is often found to correlate with the oxidation state of the lanthanide; in divalent ytterbium complexes, the band appears below 300 cm^{-1}, while in trivalent species, it appears at or above 300 cm^{-1}. Attempts have been made to examine the Raman spectrum

of the 2-butyne adduct with a red dye laser, but these have not been successful. Any number of factors may be contributing to the failure of the measurements: the sensitivity of the samples, ytterbium fluorescence, scattering, concentration effects, etc.

The NMR spectroscopy of the compounds also shows little perturbation of the coordinated ligand. In the $^{13}C\{^{1}H\}$ spectra, the quarternary carbons are generally deshielded slightly with respect to the free ligands. In the ^{1}H spectra of the complexes, the most noticeable difference exists in the case where R or R' is Me; these resonances are shifted upfield by 0.1-0.25 ppm. For example, the spectrum of free 2-butyne in d^{6}-benzene shows a singlet at δ 1.52, whereas the resonance in the ytterbium adduct appears at δ 1.27. The complexes are undergoing rapid exchange of free and coordinated alkyne in solution; NMR samples with excess alkyne show a single set of averaged resonances for the ligand. Variable temperature NMR studies have been carried out on the 2-butyne adduct. Keeping in mind the solvent dependence of the exchange rate in the platinum complex, the experiments were conducted in methylcyclohexane, a saturated solvent. A sample prepared with a 10-fold molar excess of 2-butyne showed a single resonance for the ligand at δ 1.63 (the free ligand appears in C_7D_{14} at δ 1.64). Cooling the sample to -70°C did not cause this resonance to broaden, although it moved downfield to δ 1.73. Evidently the exchange is still quite rapid at this temperature.

The mode of coordination of the acetylenes in the solid state has been verified by determining the molecular structure of $(Me_5C_5)_2Yb(\eta^2$-

MeC≡CMe). An ORTEP diagram of the complex is shown in Figure 2, and bond distances and angles can be found in Tables IV and V.

Table IV Bond Distances for $(Me_5C_5)_2Yb(\eta^2MeC{\equiv}CMe)$ (Å)

Yb-C1	2.829(5)	Yb-C11	2.674(5)	Yb-C21	2.660(4)
Yb-C2	2.871(5)	Yb-C12	2.671(4)	Yb-C22	2.641(5)
		Yb-C13	2.678(4)	Yb-C23	2.652(5)
C1-C2	1.154(6)	Yb-C14	2.659(4)	Yb-C24	2.651(5)
C1-C3	1.477(9)	Yb-C15	2.654(4)	Yb-C25	2.651(4)
C2-C4	1.458(8)	Yb-Cp1	2.384	Yb-Cp2	2.370
C3-H31	1.02(8)	C4-H41	0.98(5)		
C3-H32	0.95(8)	C4-H42	0.90(7)		
C3-H33	0.82(9)	C4-H43	1.04(6)		

Cp1 and Cp2 are the centroids of the rings comprised of C11-C15 and C21-C25, respectively.

Table V Intramolecular Angles for $(Me_5C_5)_2Yb(\eta^2MeC{\equiv}CMe)$ (°)

C1-Yb-C2	23.4(1)	C1-C3-H31	116(4)
Cp1-Yb-C1	107.8	C1-C3-H32	120(4)
Cp2-Yb-C1	107.7	C1-C3-H33	102(6)
Cp1-Yb-C2	108.8	H31-C3-H32	95(6)
Cp2-Yb-C2	107.5	H31-C3-H33	106(7)
Cp1-Yb-Cp2	143.3	H32-C3-H33	118(7)
C2-C1-C3	178.9(6)	C2-C4-H41	118(3)
C1-C2-C4	175.8(6)	C2-C4-H42	113(4)
Yb-C1-C2	80.4(4)	C2-C4-H43	115(3)
Yb-C2-C1	76.3(3)	H41-C4-H42	104(5)
Yb-C1-C3	99.4(4)	H41-C4-H43	112(4)
Yb-C2-C4	107.9(4)	H42-C4-H43	93(5)

The molecule has pseudo-C_{2v} symmetry, with the dihedral angle between the plane of the 2-butyne and the Cp1-M-Cp2 plane equal to 91.5°. The geometry of the $(Me_5C_5)_2Yb$ unit is again typical of divalent ytterbium coordination compounds; the average Yb-C (ring) distance is 2.659(5) Å, and the average Yb-ring centroid distance is 2.377 Å. The centroid-Yb-centroid angle is 143.3°. The rings are staggered, with the torsion angle equal to 35.2°.

The C≡C and average C-C(Me) bond distances in the complex are

1.154(6) Å and 1.468(9) Å, respectively. These values are identical within statistical errors to the values determined at -50°C in the crystal structure of 2-butyne[17] of 1.21(2) Å and 1.46(1) Å. The terminal methyl groups are staggered; the torsion angle is 55°. Although the hydrogen atom positions are not well determined, there appears to be no Yb-H contacts closer than 3.1 Å.

The average Yb-C(acetylene) bond distance is 2.850(5) Å,

Figure (2) ORTEP Labeling Diagram of $(Me_5C_5)_2Yb(\eta^2\text{-}MeC{\equiv}CMe)$

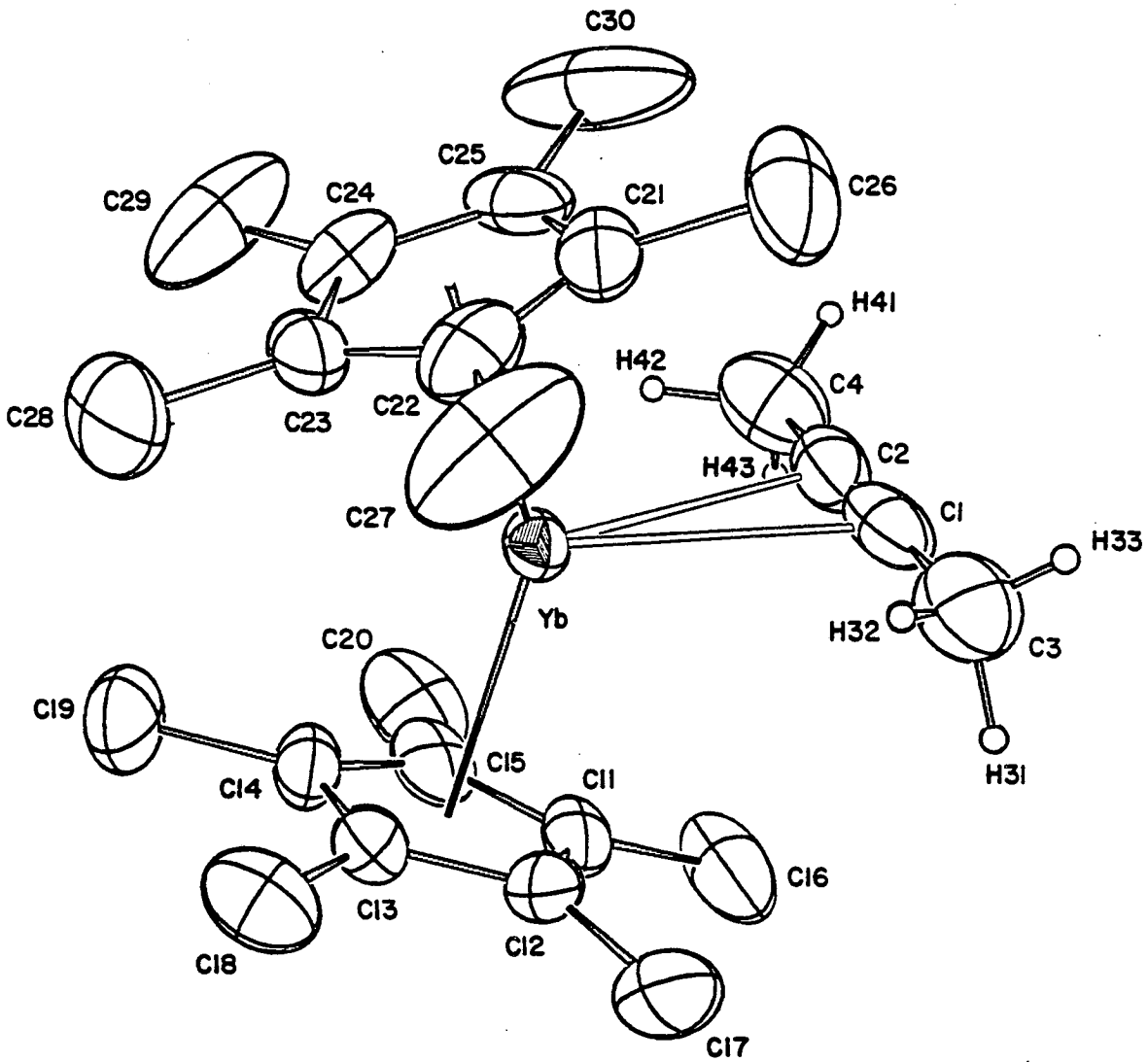

approximately the same as was found in the platinum olefin complex. In d-transition metal acetylene complexes, the most important structural parameter in estimating the degree of metal to ligand back bonding is the angle about the acetylenic carbon atoms. The smaller the angle (i.e. the more "bent back" the substituents), the greater the component of M→L π-donation. This angle tends to be smaller in low valent electron-rich complexes (142(2)° in $(PPh_3)_2Pt(PhC{\equiv}CMe)$ for the methyl substituent[18]), and tends to be larger in compounds with the metal in a higher formal oxidation state, due to the reduced metal d-electron density available for back bonding (168(2)° in trans-$[MePt(PMe_2Ph)_2(\eta^2$-$MeC{\equiv}CMe)]PF_6$[19]). In the 2-butyne adduct of the ytterbium complex, however, the ligand shows virtually no deviation from linearity (the average angle about the acetylenic carbon is 177.4(6)°), indicating that there is no component of Yb 4f to π^* back donation in the bonding. Additional evidence for the lack of this type of bonding lies in the fact that the analogous 2-butyne coordination compound can be isolated with $(Me_5C_5)_2Ca$, which lacks valence electrons in any orbitals which would be suited by symmetry for π-back-bonding.

If both platinum-olefin complexes and acetylenes have sufficiently electron-rich π-systems to coordinate to ytterbium, it might be reasoned that platinum-acetylene complexes would be even more activated to serve as bases for the lanthanide. Reaction of $(Me_5C_5)_2Yb$ with $(PPh_3)_2Pt(\eta^2$-$MeC{\equiv}CMe)$ fails to produce a coordination compound, however, and the starting materials are reisolated. The reason for this probably lies in the structure of the platinum complex. While the solid state structure of $(PPh_3)_2Pt(\eta^2$-$MeC{\equiv}CMe)$ has not been determined, it is probable that

the angles about the acetylenic carbons are similar to those found in the PhC≡CMe complex, ca. 140°. Therefore, the ytterbium can not approach the C-C triple bond for coordination without encountering unfavorable steric repulsions due to the methyl groups, which are bent back. This serves as a reminder that while Yb(II) may be acidic enough to readily coordinate to a number of ligands, the steric requirements created by the $C_5Me_5^-$ ligands are quite demanding, and may have a large effect on the chemistry of the molecule.

Ethylene Polymerization

The reaction of $(Me_5C_5)_2Yb$ with ethylene does not produce a simple coordination compound; the solution changes color from orange to green, and the ethylene is rapidly polymerized. Homogenous ethylene polymerization by lanthanide catalysts is well documented[4], but in all reported cases the catalyst is a trivalent lanthanide alkyl or hydride complex. The proposed mechanism for these polymerization reactions is comprised of three basic steps. The initiation step involves the concerted insertion of an ethylene unit into the metal-carbon or metal-hydride bond. The propogation of the chain occurs by repeated insertions into the bond between the lanthanide and the growing polymer. The termination step is proposed to be β-H (or in the case of substituted ethylenes even β-alkyl) transfer; this regenerates the lanthanide hydride catalyst.

In the absence of a metal-carbon or metal-hydride σ-bond, however, the key insertion step cannot occur. It is likely, therefore, that in the polymerization of ethylene by divalent bis(pentamethylcyclopenta-

dienyl)lanthanide complexes, the active catalyst is a trivalent species. This idea is supported by the observation that only those complexes which are capable of exhibiting the trivalent oxidation state, Yb and Sm, show catalytic activity; ethylene is not polymerized by the Ca or Eu compounds. The concentration of catalyst in solution must be small, however; in the case of ytterbium no bulk change in the oxidation state of the species is observed. The samarium-containing solutions eventually undergo an color change from green to yellow. This could be due either to irreversible oxidation to a trivalent species, or to decomposition of the $(Me_5C_5)_2Sm$ by impurities in the ethylene employed. It has previously been reported[4e] that $(Me_5C_5)_2Sm(OEt_2)$ will polymerize ethylene without undergoing a bulk change in the oxidation state of the solution species.

Given the sensitivity of the lanthanide complexes to air oxidation, it seems possible that products of such oxidation could be present in small concentrations even in carefully prepared solutions. It is first necessary to rule such species out as possible polymerization catalysts. The compound $[(Me_5C_5)_2Sm]_2(\mu\text{-}O)$ has previously been prepared by the reaction of $(Me_5C_5)_2Sm(thf)_2$ with such chemical oxidants as nitric oxide, pyridine N-oxide, and 1,2-epoxybutane[20]. An improved yield of the material can be obtained by reaction of the base free complex $(Me_5C_5)_2Sm$ with nitrous oxide in hydrocarbon solution. The ytterbium analog has also been prepared in this manner. Although the bridging oxide compounds can be prepared from the diethyl ether adducts of the respective metals, the yield is reduced, particularly in the case of ytterbium. Some physical characteristics of these species are given in

Table VI.

Table VI Physical Data for $[(Me_5C_5)_2M]_2(\mu\text{-}O)$

M	Color	MP	^{1}HNMR
Sm	Yellow	265°C (dec)	δ 0.06 ($\nu_{1/2}$ = 9.5 Hz)
Yb	Orange	334-337°C	δ 24.4 ($\nu_{1/2}$ = 980 Hz)

In the published solid state structure of $[(Me_5C_5)_2Sm]_2(\mu\text{-}O)$, the Sm-O-Sm angle is crystallographically required to be 180°, and the Sm-O distance is described as being short for an oxide-bridged system. It is suggested that these factors are "consistent with a bridging oxygen ligand which has perpendicular π-interactions with both $(Me_5C_5)_2Sm$ units." The X-ray powder pattern of the ytterbium complex reveals it to be isomorphous with the published Sm structure. In light of the interesting structural features, the solid state magnetic susceptibility was studies as a function of temperature to determine if the two metal centers were behaving as independent paramagnets, or if any magnetic exchange was occurring. The plots of $1/\chi_m$ vs. T for the Sm and Yb compounds are shown in Figures (3) and (4), respectively.

In the free Sm(III) ion ($4f^5$, ^6H), the J = 5/2 ground state is predicted[21] to lie only about 900 cm^{-1} below the J = 7/2 state, so that the latter is significantly thermally populated at higher temperatures. The result is that the ion exhibits temperature independent paramagnetism at higher temperatures. The moment is predicted to rise to a value of 1.55 to 1.65 B.M. at 300K. The plot in Figure (3) demonstrates this behavior; the calculated moment at 300K is 1.53 B.M. per Sm(III), close not only to the free ion value, but also to the value of 1.8 B.M. measured in solution[20].

Figure (3) Plot of $1/\chi_M$ vs. T for $[(Me_5C_5)_2Sm]_2(\mu\text{-}O)$ (40 kG)

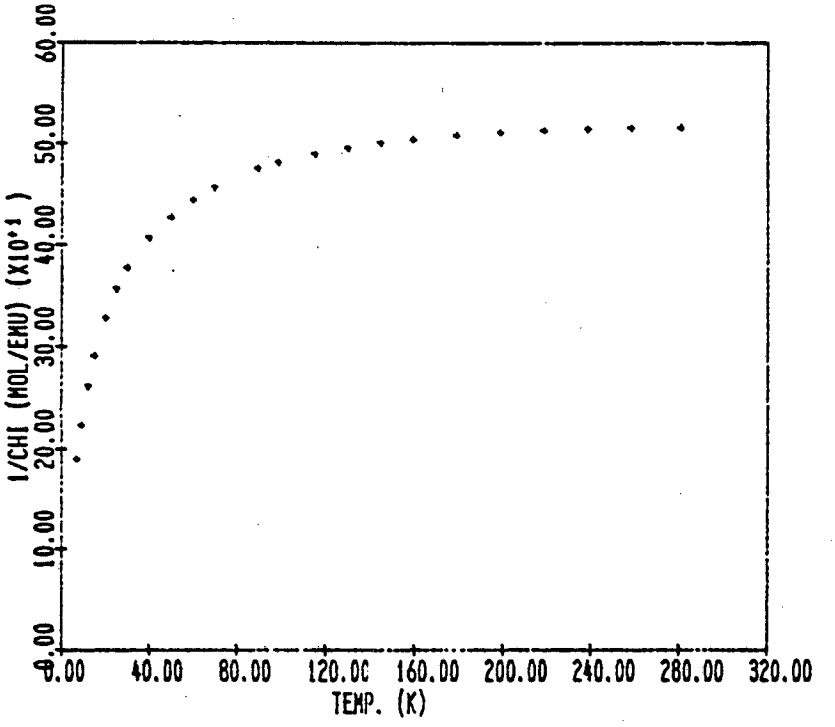

Figure (4) Plot of $1/\chi_M$ vs. T for $[(Me_5C_5)_2Yb]_2(\mu\text{-}O)$ (5 kG)

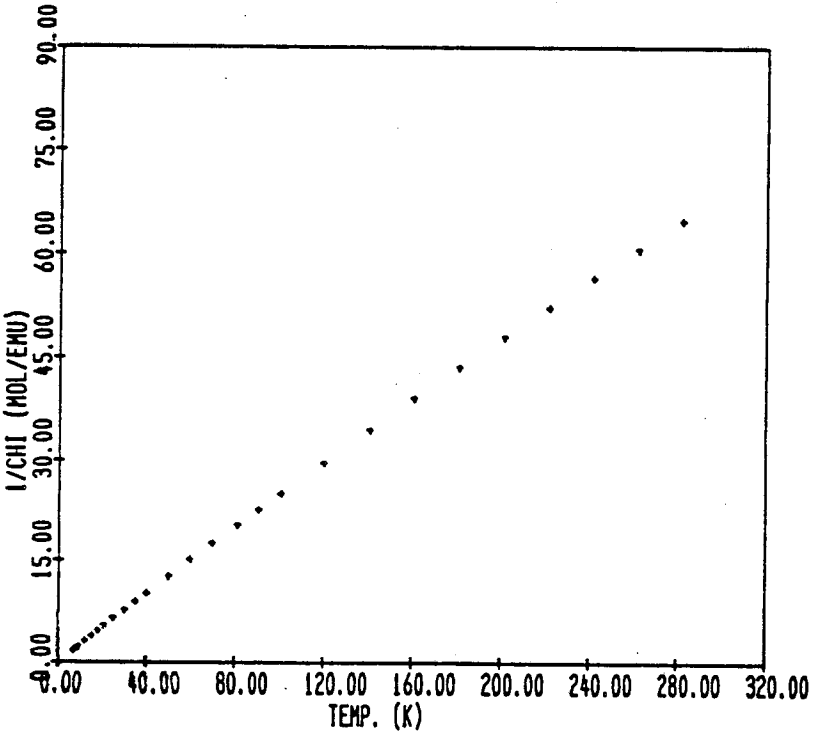

For $[(Me_5C_5)_2Yb]_2(\mu\text{-}O)$, two separate regions of Curie-Weiss behavior are observed. The degeneracy of the $^2F_{7/2}$ ground state is removed by crystal field splitting (although small, this splitting is on the order of kT), so that the slope of $1/\chi_M$ vs. T changes above ca. 100K as the population of the crystal field levels changes. From 6-35K, the magnetic moment is calculated to be 4.07 B.M. per Yb(III), with θ = -2K. From 100K-280K μ = 4.31 B.M. per Yb(III), with θ = -14K. The predicted value for the free ion at 300K is 4.50 B.M.[21]. Both of these complexes behave in a manner consistent with the postulate that the paramagnetic centers are magnetically isolated.

Reaction of the bridging oxide complexes with ethylene produces no significant amount of polymer over a 24 hour period. Evidently, these compounds are not acting as the catalytically active species in solution. The proposed trivalent catalyst must be formed in solution by reaction of the $(Me_5C_5)_2M$ compounds with ethylene. Several such reactions can be envisioned:

1.) The ethylene unit may be transferring a proton to one of the cyclopentadienyl rings, creating a vinyl complex of the lanthanide, which can then undergo ethylene insertion into the metal-carbon bond.

$$(Me_5C_5)_2M + H_2C{=}CH_2 \rightarrow C_5Me_5H + (Me_5C_5)M\text{-}CH{=}CH_2 \qquad (3)$$

This reaction is judged unlikely based on a comparison of the relative pK_a values for C_5Me_5H (27.5[22]) and ethylene (44[23]). In addition to this, any of the cyclopentadienyl complexes should be able to undergo such a reaction, not just the Sm and Yb species.

2.) In metal vapor reactions of Yb, Sm, and Er, the activation of the C-H bonds of unsaturated hydrocarbons to form lanthanide hydrides has

been proposed[24]. The analogous solution process would be the homolytic cleavage of a C-H bond in ethylene to give a lanthanide hydride and butadiene (or a lanthanide vinyl complex):

$$(Me_5C_5)_2M + H_2C{=}CH_2 \rightarrow (Me_5C_5)_2MH + H_2C{=}CH{-}CH{=}CH_2 \quad (4)$$
$$(\text{or } (Me_5C_5)_2M{-}CH{=}CH_2)$$

This process is also considered unlikely, at least in the case where M = Yb. Attempts to synthesize bis(pentamethylcyclopentadienyl)ytterbium-hydride suggest that it is thermodynamically unstable (vide infra); its formation could not provide the driving force necessary to break the strong olefinic C-H bond.

3.) The probable initiation step in the polymerization step is the direct electron-transfer reduction of ethylene by Yb(II) or Sm(II):

$$2\ (Me_5C_5)_2M + H_2C{=}CH_2 \rightarrow (Me_5C_5)_2MCH_2CH_2M(C_5Me_5) \quad (5)$$

There is no electrochemical information available on the reduction of ethylene to support this hypothesis, but this process is not without precedent. In the presence of naphthalene, lithium will reduce ethylene to produce 1,4-dilithiobutane[25]. It is postulated that the species initially formed is $LiCH_2CH_2Li$, which subsequently inserts ethylene to produce the butane derivative, inducing a greater charge separation. It is notable in this respect that propylene is neither polymerized nor oligomerized by the divalent ytterbium complex (no propylene is consumed over several days' time), although it does produce a change in the solution color to green. Trivalent lanthanide species have been observed to oligomerize propylene[4]; no kinetic barrier to insertion is indicated. If a trivalent catalyst were formed by a process other than direct reduction, propylene should be oligomerized. This failure to

react can be ascribed to the increased reduction potential of propylene (due to the inductive effect of the methyl group). Additional evidence for the direct reduction of unsaturated hydrocarbons by ytterbium (II) will be discussed later in this chapter.

Once a trivalent complex has been formed which contains a metal-carbon σ-bond, an additional molecule of ethylene can then coordinate to the metal center, and be inserted into the M-C bond to propogate the polymer chain. It has been demonstrated that olefins have the ability to coordinate to lanthanides; it can also be shown that olefin coordination is necessary to the polymerization process. The presence of a coordinating base is sufficient to suppress olefin polymerization, as indicated by the report[4e] that the diethyl ether adduct of $(Me_5C_5)_2Yb$ shows low polymerization activity (the greater activity of the Sm complex may be ascribed to the increased lability of the larger ion).

Much weaker bases are also effective in suppressing polymerization. Experiments have been conducted in which a variety of gases have been reacted with $(Me_5C_5)_2Yb$ in pentane solution. When an orange solution of $(Me_5C_5)_2Yb$ is exposed to low pressures of CO (i.e. 2-3 atm.), the solution color rapidly changes to dark green, indicating the formation of a coordinative interaction. The color change reverses when the pressure is released, but IR spectra taken immediately of the solutions show an intense band at 2117 cm^{-1}. Gaseous CO by itself is insufficiently soluble in hydrocarbon solvents at room temperature to give a spectrum (this in itself indicates that the coordinative equilibrium is sufficient to "solubilize" the gas), but values have been reported for νCO at 12K in CH_4 matrix[26a] (2137 cm^{-1}), Nujol mull[26b]

(2130 cm^{-1}), and perfluorokerosene mull[26b] (2134 cm^{-1}). The small perturbation detected in the stretching frequency of CO (even smaller than that caused by coordination to $(Me_3SiC_5H_4)_3U$, where νCO = 1976 cm^{-1} [27]) attests to the weakness of the interaction. If ethylene is added to a solution already pressurized with CO, no polymer is formed.

The addition of CH_4 or Xe does not produce a color change in solution, but polymerization is similarly inhibited. Polymerization termination experiments were also conducted in which the gases were added to solutions in which polymerization had already commenced; it was observed that polymerization was halted in all cases. It is possible that these gases are acting as very weak bases towards ytterbium, and are either preventing the coordination of the olefin, or at least limiting the lifetime of the Yb-C_2H_4 complex to such an extent that the electron-transfer step never occurs.

The basicity of the neutral gas molecules is related to the extent to which they can be polarized by the Yb, and as mentioned in Chapter One, the polarizability of a species is inversely proportional to its first ionization potential (Chapter One, eqn. 9). Table VII lists the first I.E.'s for some small molecules:

Table VII First Ionization Energies[28] (eV)

Gas	NH_3	Xe	H_2	CO	CH_4	N_2	C_2H_4
IE	≃ 11	12.1	13.6	14.0	≃ 14	15.6	10.5

There is a solvent dependence of the rate of ethylene polymerization. Reactions carried out in toluene proceed at a slower rate

than those in aliphatic hydrocarbons (for the same amount of catalyst, approximately equal amounts of polymer were formed in toluene in 6 h, and in hexane in 1.25 h). This rate retardation is reminiscent of the enhancement of the rate of dissociative exchange of the platinum olefin complex. In both cases, the aromatic hydrocarbon is evidently acting as a base, competing with the olefin for the coordination site at Yb.

Addition of H_2 (10 atm.) to a solution of $(Me_5C_5)_2M$ (M = Sm, Yb) causes no color change, and reaction of D_2 with the ytterbium complex over a period of weeks does not bring about any deuterium encorporation into the methyl groups of the rings (as indicated by the lack of νC-D bands in the IR spectrum). If ethylene is added to a solution of $(Me_5C_5)_2Yb$ already pressurized with H_2, no polymer is formed, but the solution color changes to bright green, indicating that the hydrogen does not prevent ethylene from coordinating to the metal center. It must therefore prevent polymerization in some other manner. One likely possiblilty is that the trivalent catalyst is hydrogenolized as soon as it forms, producing $(Me_5C_5)_2YbH$ and ethane. Insertion of another molecule of ethylene into the Yb-H bond, followed by further reaction with H_2, could lead to a catalytic olefin hydrogenation system. Experiments are planned to attempt to detect ethane in the gases over the reaction mixture. The question remains how the ytterbium regains the divalent oxidation state.

This question relates also to the third step in the overall polymerization process: the termination step. The most commonly proposed[4] chain termination step in the polymerization of ethylene by trivalent lanthanides is β-hydride abstraction from the polymer chain by

the lanthanide metal to give a lanthanide hydride and a terminal alkene:

$$(Me_5C_5)_2MCH_2CH_2-(CH_2)_nCH_3 \rightarrow (Me_5C_5)_2M-H + H_2C=CH-(CH_2)_nCH_3 \qquad (6)$$

There is little or no information in the literature on organometallic ytterbium hydrides, however. There is a report that the hydrogenolysis of $[(MeC_5H_4)_2YbMe]_2$ results in a green precipitate which, when dissolved in thf, yields the divalent complex $(MeC_5H_4)_2Yb(thf)$[29]. It appears that trivalent ytterbium hydrides are thermodynamically unstable with respect to reduction and loss of H_2. In order to examine the stability of the hydride in the presence of the C_5Me_5 ligand, an attempt has been made to prepare a trivalent Yb hydride by a route which has been successful in the synthesis of hydrides of La, Nd, Sm, and Lu[4c].

Reaction of $(Me_5C_5)_2Yb(\mu\text{-}Cl)_2Li(OEt_2)_2$[16a,30] with $LiCH(SiMe_3)_2$ in toluene results in the formation of a purple crystalline solid identified by its IR spectrum, NMR spectrum, mass spectrometry, and elemental analysis to be $(Me_5C_5)_2Yb[CH(SiMe_3)_2]$. Lanthanide alkyls generally cannot be isolated free of coordinating solvents or halide directly from metathetical routes, but these reactions have been successful when the alkyl group is sterically bulky.

Stirring a hexane solution of the ytterbium alkyl under 10 atm. of H_2 or D_2 results in the gradual lightening of the solution from purple to red, accompanied by the formation of a purple precipitate (a second, red product may be isolated from the supernatent in low yield; the nature of this product is still under investigation). All attempts to recrystallize or otherwise purify this precipitate result in its decomposition. The IR spectrum reveals that the $SiMe_3$ groups are no

longer present, but fails to show any distinct band which can be identified as a metal-hydride stretch; it is apparent, though, that the spectra of the H_2 and D_2 products are not identical (see Experimental Section). The material is only slightly soluble in aromatic hydrocarbons, but a dilute NMR sample can prepared in d^6-benzene. The complex initially appears as a single broad resonance at δ 7.80 ($\nu_{1/2}$ = 98 Hz). When the powder is hydrolyzed with H_2O in C_6D_6, only C_5Me_5H is visible in the ^{1}HNMR spectrum of the hydrolysate. On this basis, the species is formulated as a paramagnetic hydride.

Solid state variable temperature magnetic susceptibility studies reveal that the compound is a mixed valence Yb(II)/Yb(III) species; the moment calculated on the basis of the formula $[(Me_5C_5)_2Yb]_2(\mu\text{-}H)$ has a value of 4.03 B.M. in the range 25-45 K (θ = -2 K), and a value of 4.25 B.M. in the range 100-280 K (θ = -30 K). Although mixed-valence complexes of this type are not common, at least one other example of the class has been structurally characterized (vide infra). It is worth noting that in the investigation of the green precipitate formed from the hydrogenolysis of bis(methylcyclopentadienyl)(methyl)ytterbium (presumed to be the hydride), it is reported that the reaction with CH_3I, only 40-50% of the CH_4 is produced that would be expected if the complex were $(MeC_5H_4)YbH$[29]. This suggests that this green material may also be a mixed-valence hydride.

The question of the stability of the hydride has been examined by monitoring the time evolution of the ^{1}HNMR spectrum for a solution of the complex warmed to 70°C (Figure 5). The paramagnetic resonance at δ 7.80 gradually broadens and shifts upfield. After 3 days, the resonance

Figure (5) Pyrolysis of $[(Me_5C_5)_2Yb]_2(\mu\text{-H})$ in C_6D_6

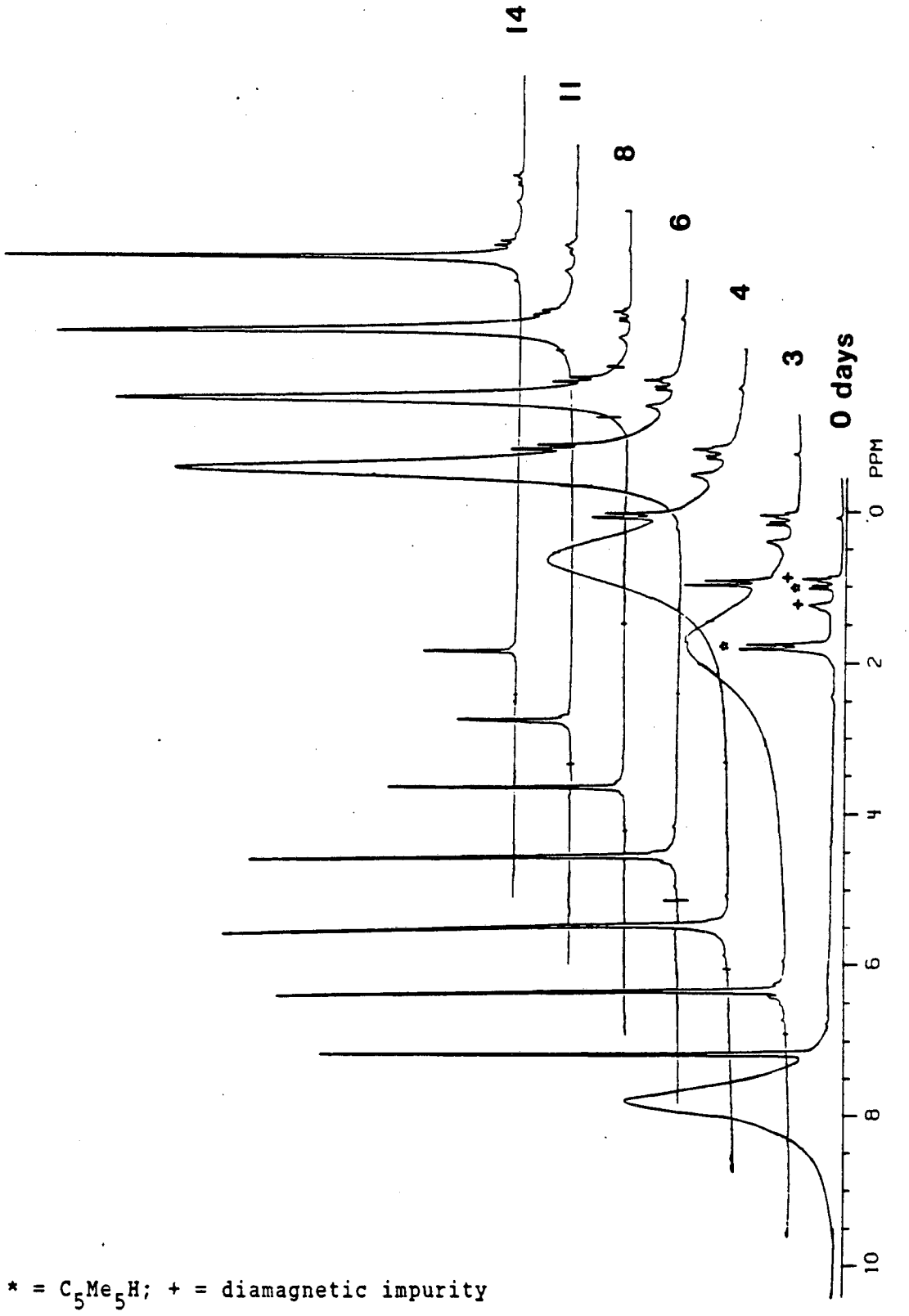

* = C_5Me_5H; + = diamagnetic impurity

appears at δ 2.57 ($\nu_{1/2}$ = 230 Hz). As the heating is continued, the resonance continues to move slowly upfield, but begins to sharpen again, so that after 14 days, the resonance appears at δ 1.97 ($\nu_{1/2}$ = 6.5 Hz), very close to the diamagnetic value of $(Me_5C_5)_2Yb$. In the complex $[(Me_5C_5)_2Yb]_2(\mu\text{-}H)$, only one paramagnetic signal is visible; either the divalent and trivalent ytterbium sites are undergoing a rapid exchange (ring exchange or electron transfer), or the ring protons on the trivalent ytterbium unit are too broad to be detected. As the hydride decomposes with time, the divalent ytterbium unit exchanges with the free $(Me_5C_5)_2Yb$, and an averaged signal is observed. This signal moves upfield, approaching the diamagnetic value as all of the bridging hydride is converted to $(Me_5C_5)_2Yb$. At no point during the reaction is H_2 visible in solution (δ 5.2).

There is also no evidence of the formation of trivalent species arising from solvent activation. This is surprising in light of the reported reaction patterns of other lanthanide and early transition metal hydrides. Both $(Me_5C_5)_2LuH$[31] and $(Me_5C_5)_2ScH$[32] have been demonstrated to activate C-H bonds in a variety of molecules. The reaction of the lutetium hydride with benzene initially yields dihydrogen and a lutetium phenyl complex; longer reaction times result in the formation of a 1,4-dimetallated arene. In the case of scandium, the hydride and benzene are in very rapid equilibrium with the phenyl complex and dihydrogen in solution.

The slow rate with which hydrogen loss proceeds in a sealed NMR tube can be accelerated considerably if the pyrolysis is carried out in an open system. Bulk scale pyrolyses are carried out by heating the

powder in toluene, and removing the solvent under dynamic vacuum. The divalent complex $(Me_5C_5)_2Yb$ can be isolated in good yield from these reactions. The presence of bases capable of coordinating to the free divalent lanthanide apparently also enhance the rate of hydrogen loss. The coordination of $(Me_5C_5)_2Yb$ to the trivalent hydride seems to confer some measure of kinetic stability to the species; breaking up this interaction destabilizes the hydride with respect to hydrogen loss.

This "decomposition" reaction closes the loop of the hypothetical catalytic cycle. The catalyst, $(Me_5C_5)_2Yb$, can be regenerated from the product of the chain termination step. The complete postulated mechanism for ethylene polymerization is shown in Figure (6).

A number of other olefins have been studied, in hopes that the catalytic activity can be extended, but the results have been disappointing. In many cases it is evident (as in the case of propylene) that the olefin cannot undergo the necessary reduction for catalyst formation. Other olefins would appear to be activated for reduction (e.g. styrene and vinyltrimethylsilane), and yet polymerization does not occur. The chemistry of ytterbium with unsaturated hydrocarbons appears to be delicately balanced between the need for an electron-rich π-system for coordination, and the requirement of a moderate reduction potential. The demanding steric environment of the metal center is undoubtedly an additional complication in this system.

Allene Isomerization

In some cases, sequential insertion may not be the lowest energy

Figure (6) Mechanism of Ethylene Polymerization

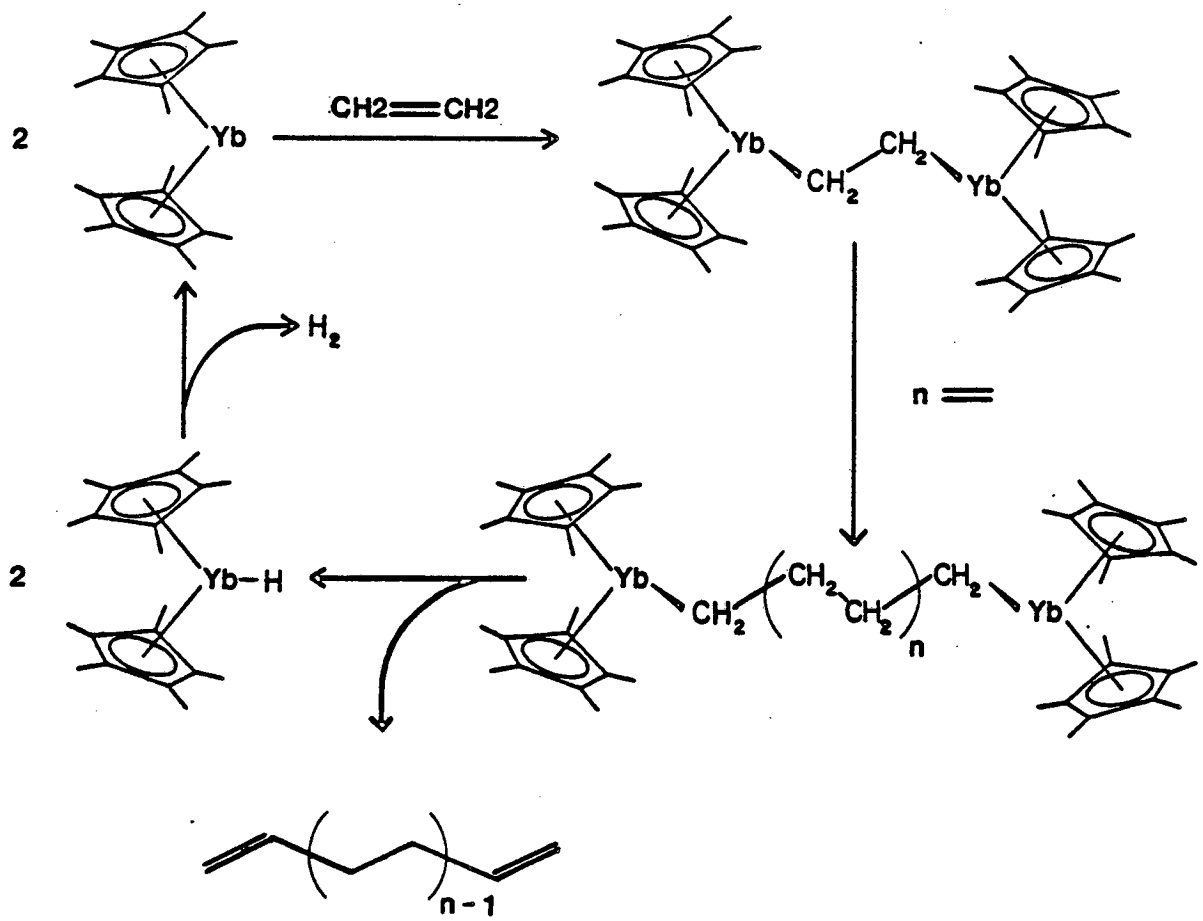

reaction pathway for the reduced substrate. This appears to be true in the reaction of Yb(II) with 1,2-dienes. When 1,2-propadiene (allene) is added to solution of $(Me_5C_5)_2Yb$, the initial dark green-brown color of the mixture gradually changes to red, and a red-brown paramagnetic powder is isolated from solution. This compound has eluded identification, but the IR spectrum shows a distinctive band at 2168 cm^{-1}, indicative of a carbon-carbon triple bond stretch. The allene has apparently been isomerized to an acetylene during the course of the

reduction by Yb(II).

This proposal is supported by the results of the reaction with 1,2-butadiene. The addition of methylallene to $(Me_5C_5)_2Yb$ again results in a dark-colored solution, which turns deep red after ca. 1 h. Red crystals isolated in high yield from this solution can be identified by ^1H and ^{13}CNMR spectra as the previously characterized diamagnetic complex $(Me_5C_5)_2Yb(\eta^2\text{-MeC}\equiv\text{CMe})$. Methylallene is isomerized to 2-butyne:

$$(Me_5C_5)_2Yb + MeHC{=}C{=}CH_2 \rightarrow (Me_5C_5)_2Yb(\eta^2\text{-MeC}\equiv\text{CMe}) \qquad (7)$$

It cannot be determined from the bulk scale reaction if the isomerization process is stoichiometric or catalytic, and so the reaction of the ytterbium complex in the presence of an excess of methylallene has been monitored by ^1HNMR spectroscopy in both d^{12}-cyclohexane and d^6-benzene. In both cases, the resonances due to the 1,2-butadiene disappear, as the methyl resonance attributable to 2-butyne grows into the spectrum. The process is catalytic, with the C_5Me_5 of the ytterbium complex remaining unchanges in integration with respect to the signal due to the residual protons in the solvent. Figure (7) shows the time evolution of the reaction in d^6-benzene. The methyl signal of 2-butyne appears initially at the value of the coordination complex; as more alkyne forms, the coordinated and free ligand exchange, and the methyl resonance moves downfield to the averaged value of the chemical shift.

Plots of ln[methylallene] vs. time show that the reactions are first order in allene over approximately three half-lives (Figures 8 and 9). In d^{12}-cyclohexane (20°C, $[(Me_5C_5)_2Yb] = 0.16$ M, $[methallene]_0 = 2.6$ M), $k = 6.4 \times 10^{-6}$ sec^{-1}, which corresponds to a half-life of $t_{1/2} =$

Figure (7) Reaction of $(Me_5C_5)_2Yb$ with 1,2-butadiene in C_6D_6

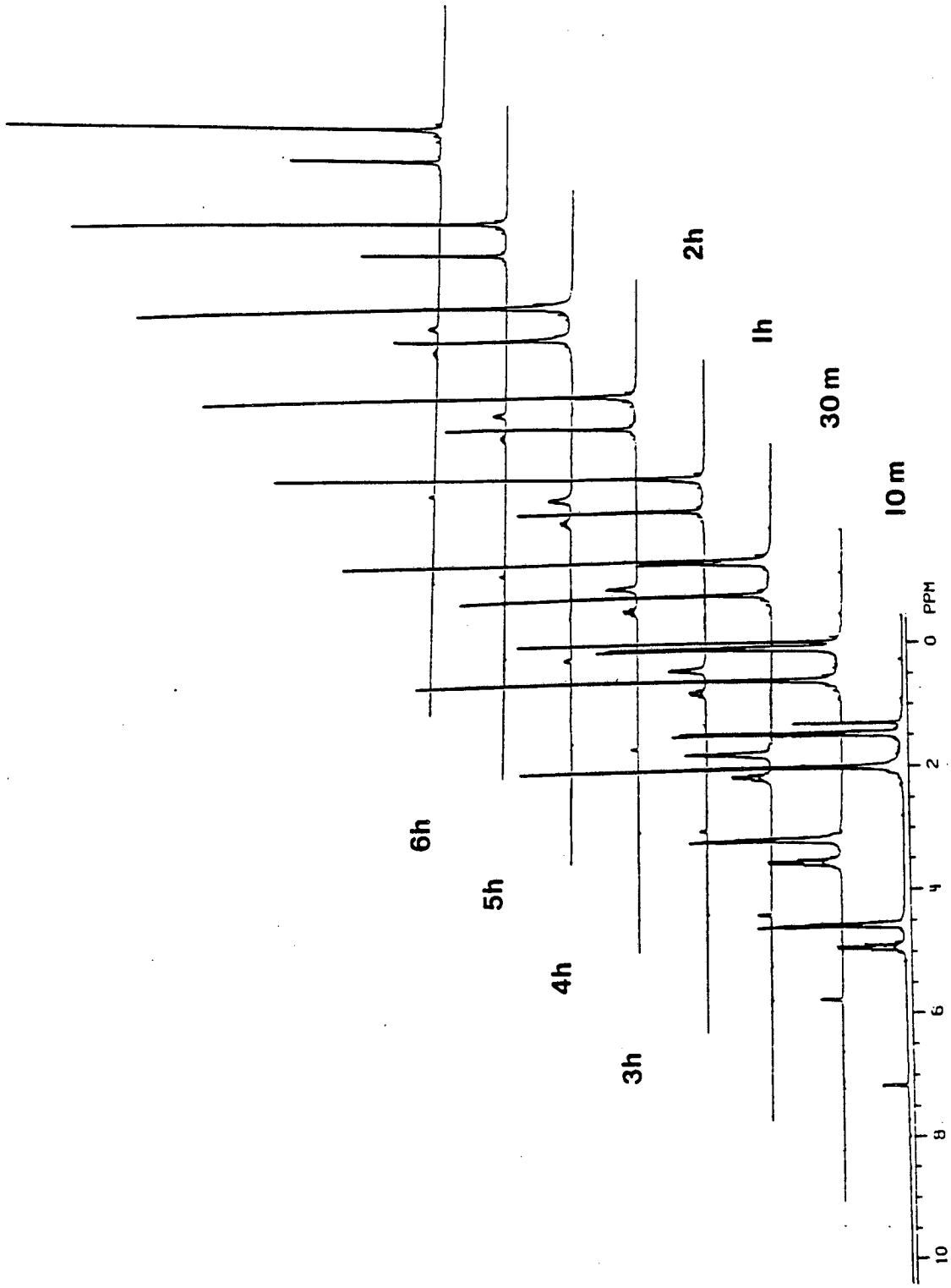

Figure (8) Plot of ln[methylallene] vs. t in d^{12}-cyclohexane

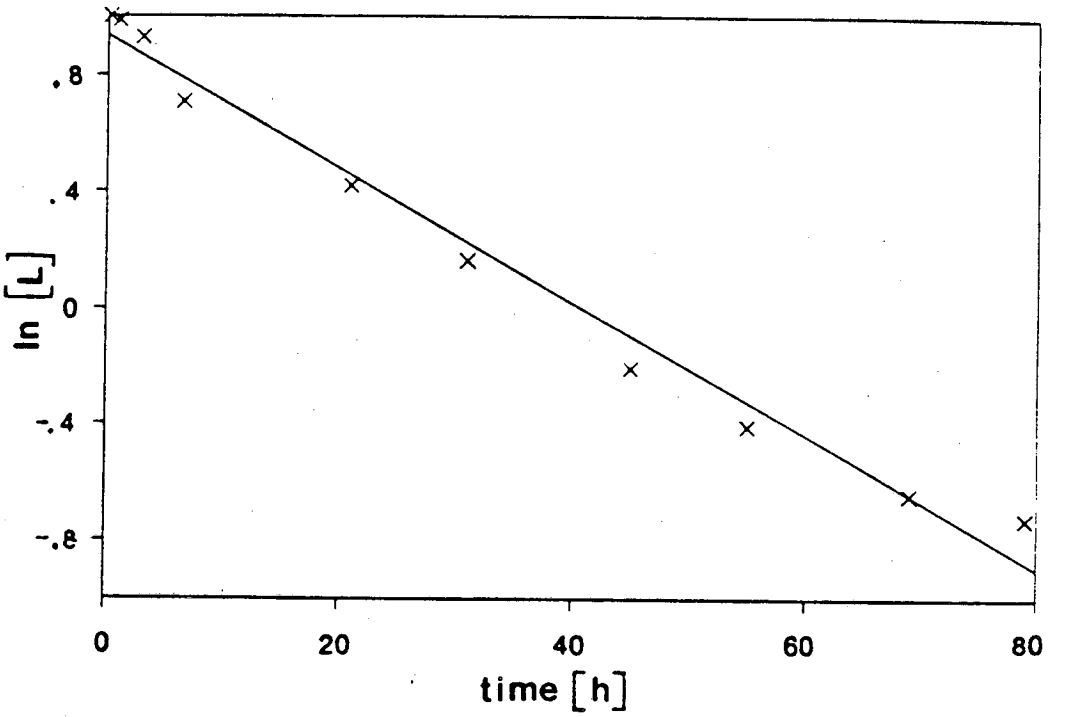

Figure (9) Plot of ln[methylallene] vs. t in d^{6}-benzene

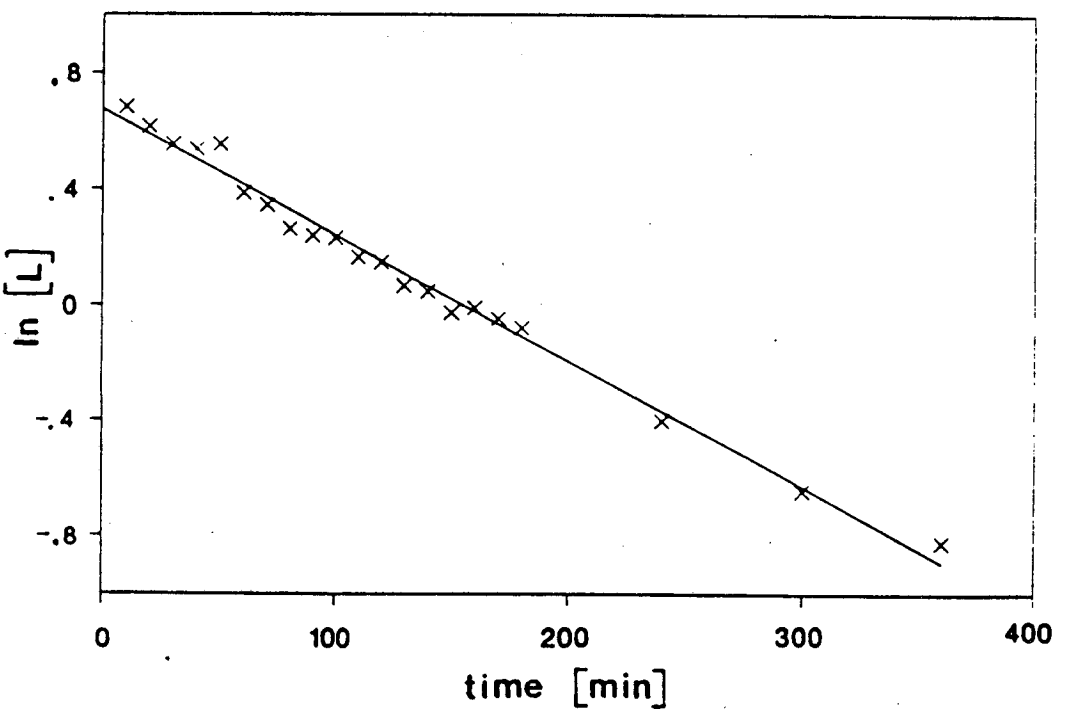

30 h. In d^6-benzene (20°C, $[(Me_5C_5)_2Yb] = 0.19$ M, $[methylallene]_0 = 2.0$ M), $k = 7.4 \times 10^{-5}$ sec^{-1}, corresponding to a half-life of $t_{1/2} = 160$ min. The detailed kinetic expression cannot be derived due to the complication that both the starting material and the product are in rapid equilibrium with free $(Me_5C_5)_2Yb$. In order to simplify the expression, assumptions would have to be made about the relative rates of the equilibria and the magnitudes of the equilibrium constants, for which no information is available.

The interconversion of allenes and alkynes has been effected in organic synthesis by a variety of reagents[33]. The most commonly employed reagents are strong bases such as metal alkoxides or metal amides, either in protic or non-protic solvents. The proposed mechanism is the abstraction of a allenic proton, followed by rearrangement of the carbanion intermediate, and subsequent reprotonation (this is often referred to as a prototropic rearrangement). Such a process usually occurs intermolecularly, but the use of some bases in non-protic solvents can lead to an intramolecular pathway, in which the proton, athough formally attached to the base, is still hydrogen-bonded to the carbanion and a suprafacial 1,3-migration, normally symmetry-forbidden, occurs[34]. Other methods employed in isomerization reactions include acid catalyzed prototropic rearrangements, anionotropic rearrangements involving halide solvolysis, and photolytically-initiated free radical halogenations.

A common feature in all of these mechanisms is the intermediacy of an organic species (either anion, cation, or radical) which is described as a resonance hybrid of the allenic and acetylenic forms:

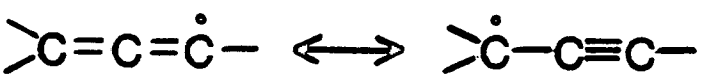

The distribution of the products in a given reaction depends in part on their relative thermodynamic stabilities. In general, increased stability results from alkyl substitution of sp- or sp^2-hybridized carbon atoms. The order of stability for C_4H_6 isomers based on the free energies of formation at 298K shows that 2-butyne is 3.0 kcal/mol more stable than 1,2-butadiene, while 1,3-butadiene is 8.4 kcal/mol more stable than the internal acetylene. In agreement with this, the principal product of isomerization of 1,2-butadiene by $KOBu^t$ in Bu^tOH is 2-butyne. The importance of kinetic control, however, is emphasized by the fact that little 1,3-butadiene is formed in the reaction. Kinetic factors (dependant on solvent, catalyst, etc.) can often overcome unfavorable energies of interconversion, resulting in systems where substantial amounts of 2-butyne to 1,2-butadiene isomerization are observed[35].

In the isomerization of methylallene by $(Me_5C_5)_2Yb$, as in the polymerization of ethylene, it appears that the rate of isomerization is related to the accesibility of the trivalent oxidation state. In a control experiment, $(Me_5C_5)_2Ca$ was reacted with a 2-fold excess of methylallene in d^{12}-cyclohexane. While a very slow isomerization of the allene to acetylene did occur (perhaps catalyzed by $Ca(OH)_2$ impurities), the rate was very much slower than that of Yb ($t_{1/2}$ > 100h). This suggests that the process involves direct reduction of the substrate, perhaps followed by hydride migration in a "pseudo-anionotropic"

rearrangement (Figure 10).

Figure (10) Isomerization of 1,2-Butadiene

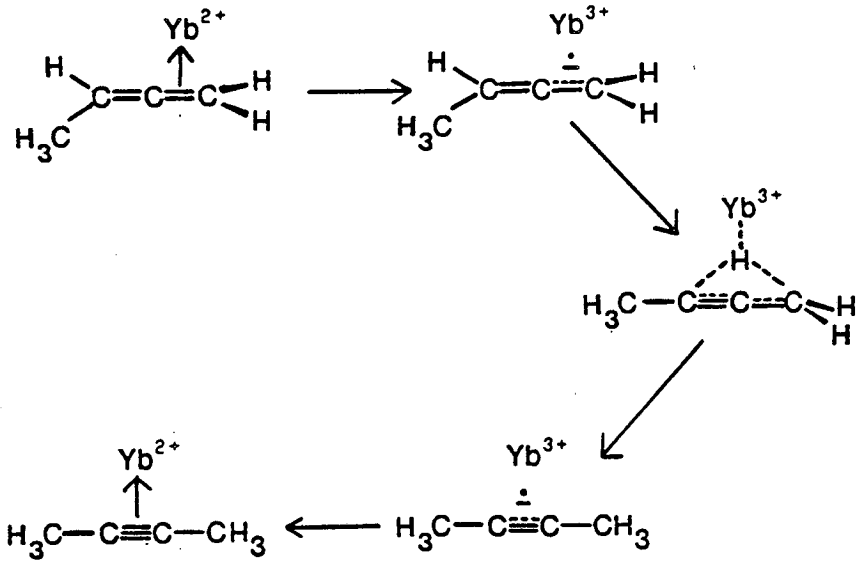

While no information is available on the electrochemical reduction of alkylallenes, the similarity of the second reduction potentials of haloallenes and -alkynes has been interpreted in terms of a common reduction product for the two species[36].

The re-reduction of the lanthanide center or the reversible electron transfer may be compensated for energetically not only by the increased thermodynamic stability of the 2-butyne isomer, but also by the increased strength of the metal-alkyne interaction relative to that with the allene. This is demonstrated by the solvent dependance of the isomerization reaction rate. In the absence of a "coordinating" solvent, the 2-butyne preferentially binds to the ytterbium, suppressing the rate of catalysis. In benzene, however (as in the case of the platinum-olefin complex), the rate of dissociative exchange of the

alkyne is enhanced, effectively freeing the catalytic center for reaction with methylallene. The preference of the ytterbium complex for alkynes is also indicated in the bulk scale reactions, where after relatively short reaction times (ca. 2 h), when the methylallene should remain largely unconverted (judging by the established rate in cyclohexane), only the 2-butyne adduct of ytterbium is isolated.

Fluoride Abstraction

While studying the effect of electron-withdrawing substituents on olefin polymerization, it was observed that fluoro-ethylenes react with $(Me_5C_5)_2Yb$ to form metal fluorides. If a hexane solution of $(Me_5C_5)_2Yb$ is pressurized with $HFC{=}CH_2$, $H_2C{=}CF_2$, or $F_2C{=}CF_2$, an insoluble brown precipitate forms. This is merely the kinetic product, however. Attempts to recrystallize this material from hot toluene result in its partial conversion to another product, and the crystalline solid isolated is a mixture of two species: green-brown blocks and red needles. Both compounds are insoluble in aliphatic and cold aromatic solvents, and so cannot be characterized by solution means. The IR spectra of the complexes are not revealing, except for the presence of a strong band at 434 cm^{-1} in the brown product, and at 449 cm^{-1} in the red product; these has been attributed to νYb-F. These two products can be synthesized independently from the reaction of $(Me_5C_5)_2Yb$ with silver fluoride.

The stoichiometries of the respective complexes were determined from single crystal X-ray diffraction studies. The green-brown product is found to have the formula $[(Me_5C_5)_2Yb]_2(\mu\text{-}F)$. An ORTEP diagram is

presented in Figure (11), and intramolecular bond distances and angles can be found in Tables VIII and IV, respectively.

Table VIII Bond Distances for $[(Me_5C_5)_2Yb]_2(\mu\text{-}F)$ (Å)

Yb1-F	2.317(2)	Yb1-C1	2.676(3)	Yb2-C11	2.577(3)
Yb2-F	2.084(2)	Yb1-C2	2.676(3)	Yb2-C12	2.569(3)
		Yb1-C3	2.706(3)	Yb2-C13	2.559(3)
Yb1-Cp1	2.407	Yb1-C4	2.707(3)	Yb2-C14	2.604(3)
Yb2-Cp2	2.290	Yb1-C5	2.673(3)	Yb2-C15	2.609(3)

Cp1 and Cp2 are the centroids of the rings corresponding to C1-C5 and C11-C15, respectively.

Table IV Intramolecular Angles for $[(Me_5C_5)_2Yb]_2(\mu\text{-}F)$ (°)

Cp1-Yb1-F	110.1	Cp2-Yb2-F	110.7
Cp1-Yb1-Cp1'	139.9	Cp2-Yb2-Cp2'	138.6
Yb1-F-Yb2	180.0		

The complex consists of a divalent $(Me_5C_5)_2Yb$ unit coordinated in a linear fashion to a trivalent $(Me_5C_5)_2YbF$ unit. The planes formed by the metal atoms and ring centroids for each ytterbium are perpendicular to one another. The molecule lies on a crystallographic two-fold axis of symmetry, and so the Yb1-F-Yb2 angle is constrained to be linear. The average metal-carbon bond lengths (Yb1-C = 2.688(3) Å, Yb2-C = 2.584(3) Å) clearly shows Yb2 to be the trivalent metal center. The difference in the average metal-carbon length, 0.10 Å, is close to the value of 0.15 Å predicted by Shannon[12] to be the difference between Yb(II) and Yb(III) in 7-coordination. The Yb-F bond lengths differ by 0.23 Å, consistent with the notion that the Yb(II) to F distance reflects a dative interaction, not a single ionic bond.

Although a linear M-F-M bridge is normally associated with the

Figure (11) ORTEP Labeling Diagram of $[(Me_5C_5)_2Yb]_2(\mu\text{-}F)$

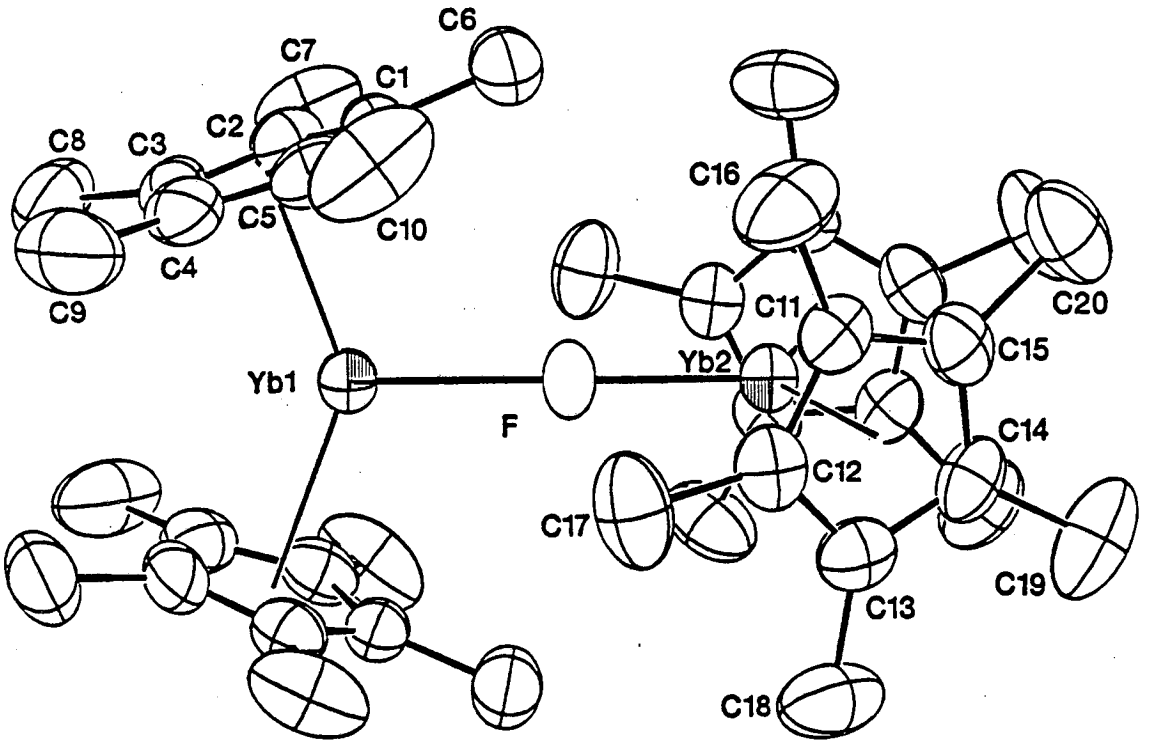

presence of a F 2p → M d orbital component in the bonding, the linear geometry in this molecule is necessitated by the severe steric repulsions between the Me_5C_5 rings. The two ytterbium units approach each other closely enough that the closest contact distances between methyl groups on Cp1 and Cp2 are 3.6-3.7 Å. These steric repulsions manifest themselves in many ways. The Yb2-F distance 2.084(2) Å, is longer than the Yb-F distance of 2.026 Å found in the complex $(Me_5C_5)_2YbF(thf)$[37]; the distance should be shorter for the metal in a lower coordination number. The rings on each ytterbium are in an eclipsed geometry (torsion angles of 16.0(3)° and 16.6(4)° for Cp1 and

Cp2, respectively. This structural feature has also been observed in the structure of $[(Me_5C_5)_2Sm]_2(\mu\text{-}O)$[20], and is due to the fact that further twisting of the rings would bring the methyl groups of C6 and C17 into even closer contact with the rings on the adjacent metal. A combination of this and the small ring centroid-Yb-ring centroid angles (139.9° and 138.6°) decreases the closest contacts between methyl groups on rings on the same metal atom; the C19-C20' distance is 3.419(6) Å. Furthermore, the methyl groups engaged in these close contacts (C8, C9, C19, and C20) are bent back out of the plane of the cyclopentadienyl rings by as much as 0.25 Å.

The red product, formed by heating the dinuclear species in toluene, is a tetranuclear complex of the formula $(Me_5C_5)_6Yb_4(\mu\text{-}F)_4$. This complex crystallizes as a di-toluene solvate. An ORTEP labeling diagram of the complex can be found in Figure (12), while Figure (13) shows the eight-membered ring which forms the core of the molecule. Some bond distances and intramolecular angles are presented in Tables X and XI, respectively.

Table X Bond Distances for $(Me_5C_5)_6Yb_4(\mu\text{-}F)_4$ (Å)

Yb1-F1	2.221(3)	Yb1-C1	2.684(10)	Yb2-C11	2.630(6)
Yb1-F2	2.219(3)	Yb1-C2	2.637(9)	Yb2-C12	2.629(6)
		Yb1-C3	2.653(7)	Yb2-C13	2.631(6)
Yb2-F1	2.132(3)	Yb1-C4	2.631(7)	Yb2-C14	2.639(6)
Yb2-F2	2.126(3)	Yb1-C5	2.667(8)	Yb2-C15	2.669(6)
Yb1-Cp1	2.386	Yb2-C21	2.580(7)	Yb2-C24	2.611(7)
Yb2-Cp2	2.357	Yb2-C22	2.570(7)	Yb2-C25	2.612(6)
Yb2-Cp3	2.311	Yb2-C23	2.601(7)		

Cp1, Cp2, and Cp3 are the centroids of the rings comprised of C1-C5, C11-C15, and C21-C25, respectively.

Figure (12) ORTEP Labeling Diagram for $(Me_5C_5)_6Yb_4(\mu\text{-}F)_4$

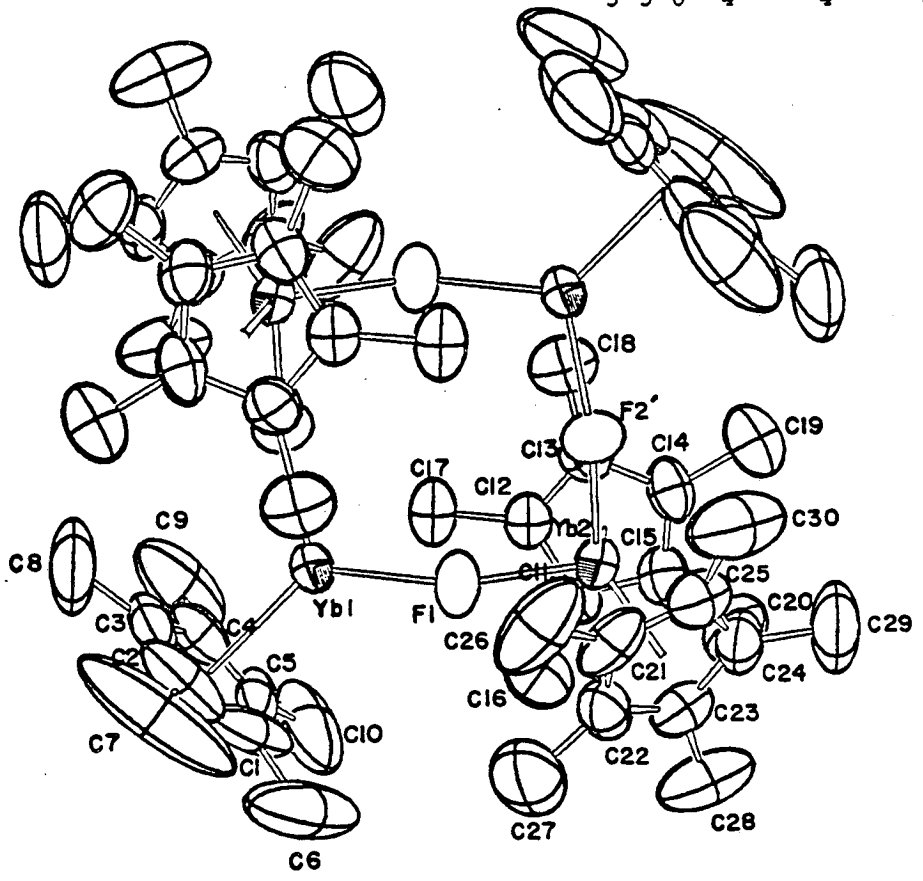

Figure (13) Core Unit of $(Me_5C_5)_6Yb_4(\mu\text{-}F)_4$

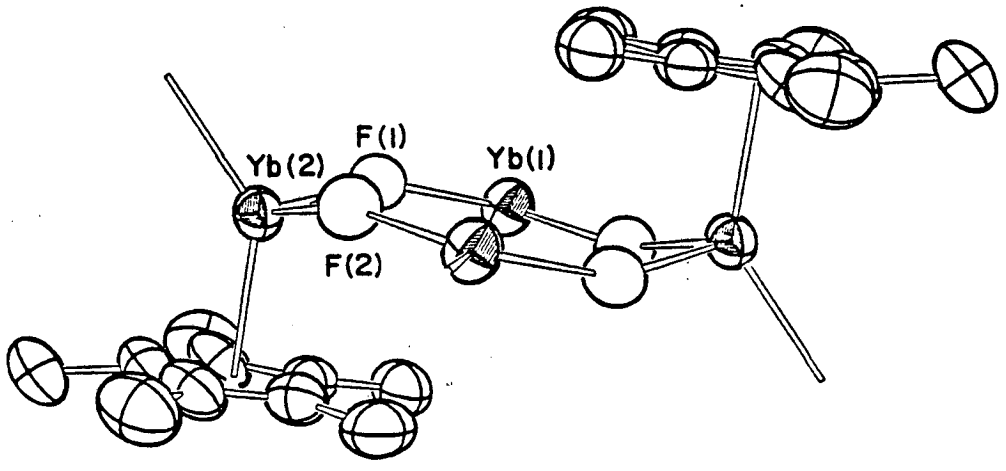

Table XI Intramolecular Angles for $(Me_5C_5)_6Yb_4(\mu\text{-}F)_4$ (°)

F1-Yb1-F2	106.0(1)	F1-Yb2-F2	91.9(1)
F1-Yb1-Cp1	129.2	F1-Yb2-Cp2	103.7
F2-Yb1-Cp1	124.9	F1-Yb2-Cp3	104.0
		F2-Yb2-Cp2	104.0
Yb1-F1-Yb2	157.3(2)	F2-Yb2-Cp3	105.4
Yb1-F2-Yb2	160.0(2)	Cp2-Yb2-Cp3	138.4

The complex consists of two independent types of ytterbium fragments: a trivalent $(Me_5C_5)_2YbF$ unit and a divalent $(Me_5C_5)YbF$ unit. These units are connected by fluoride bridges to each other and to units related by a crystallographic center of inversion to form the tetranuclear cluster. The oxidation states of the metals can be distinguished by the metal-fluoride bond distances. The average Yb1-F bond length (2.220(3) Å) is approximately the same within statistical errors as the average Yb2-F bond length (2.129(3) Å), and the average Yb1-C distance (2.654(8) Å) is the same as the average Yb2-C distance (2.617(7) Å). Yb2 is in a higher coordination number, however, and so should have a larger effective ionic radius. This implies that Yb(2) is trivalent.

The geometry about Yb2 is pseudo-tetrahedral, with distorted angles of F1-Yb2-F2 = 91.9(1)° and Cp2-Yb2-Cp3 = 138.4°. The average Cp-Yb2-F angle is 104.3°. The average metal-carbon length is in the range found for other Yb(III) complexes in eight-coordination[13,16]. The coordination environment of Yb1 is pseudo-trigonal, with a F1-Yb1-F2 angle of 106.0(1)°, and an average Cp1-Yb1-F angle of 127.1°. The angles about the bridging fluorides are near linear: Yb1-F1-Yb2 = 157.3(2)°, and Yb1-F2-Yb2 = 160.0(2).

One curious feature of the structure is the Yb-F bond lengths. It

was observed in the structure of the dinuclear fluoride that a distinction could be made between a single ionic bond and a dative bond based on bond length. In the tetranuclear complex, each ytterbium should be singly bonded to one fluoride and form a dative interaction with the other. The two Yb-F bond lengths about each ytterbium are identical, however. This implies that the structure is a mixture of two resonance forms, so that each Yb-F bond is part ionic and part dative. This type of resonance has been observed in many main-group oligomers where the bridging group is a halide[38], alkoxide[39], or amide[40].

The overall eight-membered Yb_4F_4 ring is not completely planar. The plane defined by Yb2-F1-F2' is bent away from the plane formed by the four fluorine atoms by 26.1°, so that Yb2 is 0.65 Å out of the latter plane. This bending decreases the angles about the bridging fluorides. It also brings C17 and C18 into close contact with Yb1 and Yb1', respectively: Yb1···C17 = 3.124(7) Å and Yb···C18 = 3.232(7) Å. This effectively increases the coordination number of the divalent ytterbium. Repulsions develop, however, between the ring carbons of Cp2 and the bridging fluorides, causing this ring to be pushed away from Yb2 slightly. The average Yb-C bond length for C11-C15 (2.640(6) Å) is significantly longer than that for C21-C25 (2.595(7) Å).

There are relatively few structurally characterized organometallic fluorides of the d- or f-transition metal elements[41], and only one which contains M-F-M bridging interactions. The compound $(H_5C_5)_2ScF$[41a] is a cyclic trimer in the solid state. All of the Sc-F distances are the same within error limits, with an average value of 2.046(8) Å, and the average F-Sc-F and Sc-F-Sc angles are 86.5(3)° and 153.4(4)°,

respectively. Oligomers with linear or near linear fluoride bridges are common in main group organometallic chemistry, however[38,42]. In the gas phase structure of the complex $[Me_2AlF]_4$, the model which refines the best is one in which all of the Al-F bond distances are the same (1.810(3) Å), and in which the eight-membered ring is puckered. The refined values of the F-Al-F and F-Al-F angles are 92(1)° and 146(3)°, respectively.

Attempts have been made to synthesize all-trivalent ytterbium fluorides free of coordinating bases for structural comparison with these compounds. It was hoped that solvent removal from $(Me_5C_5)_2YbF(L)$ (L = thf, acetonitrile, Et_2O) by the "toluene-reflux" method could lead to complexes of the formula $[(Me_5C_5)_2YbF]_x$. The complex $(Me_5C_5)_2YbF$-(thf) is successfully synthesized by reaction of the divalent ytterbium thf adduct with AgF. The analogous reaction with $(Me_5C_5)_2Yb(NCMe)_2$ gives a mixture of products, however, probably due to fluorination of the unsaturated ligand. Diethyl ether proves to be too weak as a base, and the products isolated from silver oxidation are the dinuclear and tetranuclear complexes already characterized. The hot solvent method ultimately proved unsuccessful; heating $(Me_5C_5)_2YbF(thf)$ in toluene merely resulted in its decomposition.

The near linear M-F-M angles and the "resonance" of the M-F bond lengths suggested that it might be interesting to study the magnetic behavior of the complexes, in order to determine if there is any interaction between the paramagnetic centers. Variable temperature magnetic susceptibility measurements show that both the dinuclear and tetranuclear compounds display behavior which is consistant with

isolated Yb(III) paramagnets, however. The plots of $1/\chi_M$ vs. T (Figures 14 and 15) show that powdered samples of both species follow Curie-Weiss behavior, with the bend expected for Yb(III). At 5 kG, the values of the moment for $[(Me_5C_5)_2Yb]_2(\mu\text{-}F)$ are μ = 4.11 B.M. (θ = 0 K) in the range 7-35 K, and μ = 4.69 B.M. (θ = -25 K) in the range 100-280 K. For the tetranuclear compound, μ = 3.67 B.M. (θ = -3 K) in the range 7-35 K, and μ = 4.95 B.M. (θ = -37 K) in the range 80-280 K.

If magnetic susceptibility measurements are conducted on crystalline samples, the measured moments are much higher in the high temperature region: μ = 6.07 B.M. with θ = 1 K for the dinuclear comound, and μ = 6.06 B.M. with θ = -64 K for the tetranuclear complex at 5 kG. This effect is commonly observed in lanthanide complexes. The fact that the crystal field splitting is small in comparison with the spin-orbit coupling means that the orbital angular momentum is largely unquenched. This can lead to an anisotropic value of g, the Lande splitting factor[43]. In a measurement of the magnetic susceptibility of a bulk crystalline sample, the individual crystals have the ability to orient themselves in the sample container along the preferred direction of magnetization. This results in an anomalously high measured value of μ.

The thermal conversion of the dinuclear species to the tetranuclear compound is an indication of the thermodynamic strength of the Yb-F bond. The energy gained by formation of a second Yb-F dative interaction is apparently sufficient to induce ring loss. The relatively low yield of the interconversion suggests that another ytterbium-containing product is present in the reaction solution.

Figure (14) Plot of $1/\chi_M$ vs. T for $[(Me_5C_5)_2Yb]_2(\mu\text{-}F)$ (5 kG)

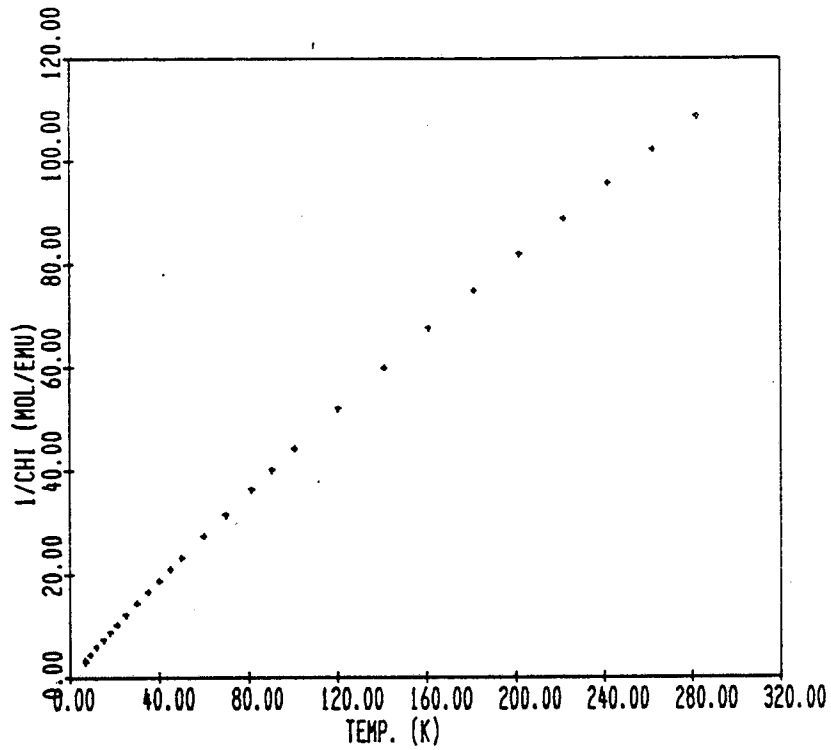

Figure (15) Plot of $1/\chi_M$ vs. T for $(Me_5C_5)_2Yb_4(\mu\text{-}F)_4 \cdot 2PhMe$ (5 kG)

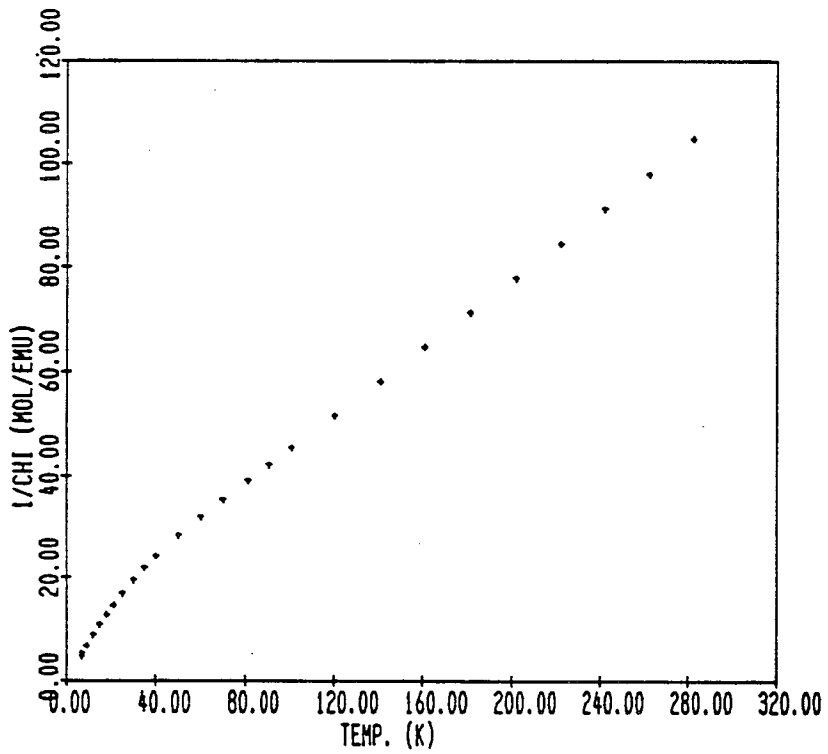

Removal of the solvent from the mother liquors results in the isolation of a small amount of $(Me_5C_5)_2Yb$, although in insufficient yield to be quantified. One possible balanced equation for the reaction is given in equation (8).

$$4\ [(Me_5C_5)_2Yb](\mu\text{-}F) \rightarrow (Me_5C_5)_6Yb_4(\mu\text{-}F)_4 + 4\ (Me_5C_5)_2Yb + "(Me_5C_5)_2" \qquad (8)$$

The results of the reactions of $(Me_5C_5)_2Yb$ with fluoroolefins appear to suggest that the initiation step in the polymerization of ethylene is homolytic C-H bond cleavage. In order to explore this possiblity further, the reaction of the ytterbium compound with a series of fluoroarenes has been studied.

An enormous difference is observed in the relative rates of reaction in aliphatic hydrocarbon solvent. The reaction of $(Me_5C_5)_2Yb$ with C_6F_6 is complete in a matter of minutes, while the reaction with $C_6H_5CF_3$ takes place over a period of 12-14 h. The slowest member of the series is C_6H_5F; this reaction has an estimated half-life of 7-10 days. The ytterbium-containing products formed depend upon the rate of the reaction. The faster reactions precipitate only $[(Me_5C_5)_2Yb]_2(\mu\text{-}F)$ as a powder, while the reaction with fluorobenzene slowly precipitates a crystalline mixture of the dinuclear and tetranuclear fluorides over a period of two weeks. The kinetic product dominates the product mixture during the first week, while the tetranuclear species makes up the bulk of the solid precipitated thereafter.

If the reaction of ytterbium with fluorocarbons involved simple homolytic C-F bond cleavage, then the rates of reaction should correlate

with the thermodynamic C-F bond strengths for a series of related molecules. The C-F bond dissociation energy of hexafluorobenzene, though, is more than 30 kcal/mol higher than that of fluorobenzene[44], implying that the latter should react more quickly. It is obvious that this mechanism does not explain the experimental observations.

If the mechanism of fluoride abstraction involves prior reduction of the substrate, the rate of reaction might then be expected to follow the relative reduction potentials of the organic species, with the more reducible molecules reacting faster. Information is not available on the electron affinities of all of these molecules, but the E.A. of C_6F_6 has been measured[44], and is found to have a minimum value of 1.8 ± 0.3 eV. The ease of oxidation and reduction of a molecule can often be related to its susceptibility to electrophilic and nucleophilic attack. Compared with aromatic hydrocarbons, fluoroarenes are relatively resistant to electrophilic attack, and yet nucleophilic attack is one of the most commonly observed reactions of the latter[45]. Furthermore, the rate of nucleophilic attack by anions or radicals is found to increase with increasing fluorine substitution[45,46].

It may be postulated from these trends that the initial step in the fluoride abstraction reaction is the reduction of the fluorocarbon, followed by C-F bond cleavage. This contention is further supported by the observation that $(Me_5C_5)_2Yb$ does not activate saturated fluorocarbons, even those possessing a permanent dipole moment (e.g. CH_3CF_3). This lack of reactivity of alkyl fluorides towards Yb(II) has also been reported by others (ref. 47c, supplementary material).

A comparison may now be made between the reactions of ytterbium

with fluoroolefins and ethylene. The initial step in both reactions is coordination of the unsaturated substrate to the metal, followed by reduction. The reactions merely take different paths subsequent to this step. Sequential ethylene insertion results in polymerization in one case, while the strength of the Yb-F bond drives the abstraction process in the other.

Several studies have been reported on halide abstraction by organometallic complexes of actinides and lanthanides[47]. These reactions are proposed to occur by way of an inner-sphere, single-electron transfer pathway, and give rise to multiple metal-containing products. In the case of the lanthanides, the formation of one ring products such as $(Me_5C_5)YbCl_2$ or $[(Me_5C_5)_2SmCl\cdot(Me_5C_5)SmCl_2]_z$ has been attributed to "Grignard-like" reactions of $(Me_5C_5)_2MX$ with excess RX to produce $(Me_5C_5)MX_2$ and Me_5C_5R. Mechanistic schemes have been presented which propose the formation of Me_5C_5R, RR, RH, and R - H to account for the organic radical produced by the initial abstraction.

Although it has been demonstrated that the formation of one-ring fluorides can take place even in the absence of an excess of the fluoride source (the dinuclear compound can be converted to the tetranuclear), it is of interest to study the fate of the organic radical in the fluoride abstractions. The reaction solutions remaining after deposition of the ytterbium fluorides are light-colored in the case of $C_6H_5CF_3$ and C_6H_5F. Hydrolysis of these solutions, followed by extraction with diethyl ether and removal of the solvent results in the isolation of colorless to pale yellow oils. ^{1}HNMR and mass spectral analysis of these oils indicates that they contain C_5Me_5H and C_5Me_5R.

No trace of dimerized products is visible in the mixture, although these species may be formed in insufficient yield for isolation.

In the case of C_6F_6, however, the reaction solution is bright purple, and a further Yb-containing species can be isolated in low yield. The IR, ^1H and ^{19}FNMR spectra of the compound indicates that it contains both C_5Me_5 and C_6F_5 groups, and the presence of a Yb-F bond is suggested in the IR spectrum by a strong band at 445 cm^{-1}. The highest molecular weight fragments in the EI mass spectrum correspond to $(Me_5C_5)YbF(C_6F_5)$ and $(Me_5C_5)_2YbF$ units. The analytical data do not conclusively support any one formulation, but the closest calculated percentages are for the formula $[(Me_5C_5)_2YbF\cdot(Me_5C_5)YbF(C_6F_5)]$ (C, 45.2; H, 4.75). Unfortunately, X-ray quality crystals could not be obtained of the compound.

The similarity of this formula to the product mixtures obtained from chloride abstraction prompted a study of the reaction of $(Me_5C_5)_2Yb$ with simple chloride salts, in hopes that these reactions might produce the same complexes as halide abstraction reactions, as is observed in the case of AgF. The reactions of AgCl and $HgCl_2$ with the divalent ytterbium compound produce the same light blue paramagnetic product which shows a strong band in the IR spectrum at 326 cm^{-1}. Three resonances are visible in the ^1HNMR spectrum in a 1:1:1 integration. This spectrum resembles that reported for $[(Me_5C_5)_3Sm_2Cl_3]$, indicating that the blue compound may also be a mixed one-ring/two-ring species, but to date, all attempts to further characterize this material have failed.

References

1.) a) Green, M. L. H., "Organometallic Compounds", Vol. 2, Chapman and Hall, London, 1968. b) Herberhold, M., "Metal π-Complexes", Elsevier, Amsterdam, 1974. c) Ittel, S. D.; Ibers, J. A., Adv. Organomet. Chem., 1976, 14, 33. d) Otsuka, S.; Nakamura, A., Adv. Organomet. Chem., 1976, 14, 245.

2.) a) Chatt, J., J. Chem. Soc., 1949, 3340. b) Dewar, M. J. S., Bull. Soc. Chim. Fr., 1951, 18, 79. c) Chatt, J.; Duncanson, L. A., J. Chem. Soc., 1953, 2939. d) Rosch, N.; Hoffmann, R., Inorg. Chem., 1974, 13, 2656. e) Pitzer, R. M.; Schaefer, H. F., J. Am. Chem. Soc., 1979, 101, 7176. f) Dewar, M. J. S.; Ford, G. P., J. Am. Chem. Soc., 1979, 101, 783.

3.) Evans, W. J.; Hughes, L. A.; Drummond, D. K.; Zhang, H.; Atwood, J. L., J. Am. Chem. Soc., 1986, 108, 1722.

4.) a) Watson, P. L., J. Am. Chem. Soc., 1982, 104, 337. b) Watson, P. L.; Row, D. C., J. Am. Chem. Soc., 1982, 104, 6471. c) Jeske, G.; Lauke, H.; Mauermann, H.; Swepston, P. N.; Schumann, H.; Marks, T. J., J. Am. Chem. Soc., 1985, 107, 8091. d) Jeske, G.; Lauke, H.; Mauermann, H.; Schumann, H.; Marks, T. J., J. Am. Chem. Soc., 1985, 107, 8111. e) Watson, P. L.; Herskovitz, T., in "Initiation of Polymerization", F. E. Bailey, ed., ACS Symposium Series, 1983, 212, 459.

5.) a) Cotton, F. A.; Schwotzer, W., J. Am. Chem. Soc., 1986, 108, 4657. b) Cotton, F. A.; Schwotzer, W., Organometallics, 1987, 6, 1275.

6.) Cramer, R., J. Am. Chem. Soc., 1967, 89, 4621.

7.) a) Cheng, P.-T.; Nyburg, S. C., Can. J. Chem., 1972, 50, 912. b) Cheng, P.-T.; Cook, C. D.; Koo, C. H.; Nyburg, S. C.; Shiomi, M. T., Acta Cryst., 1971, B27, 1904.

8.) Tilley, T. D.; Andersen, R. A.; Spencer, B.; Ruben, H.; Zalkin, A.; Templeton, D. H., Inorg. Chem., 1980, 19, 2999.

9.) Stalick, J. K.; Ibers, J. A., J. Am. Chem. Soc., 1970, 92, 5333.

10.) Howard, J. A. K.; Spencer, J. L.; Mason, S. A., Proc. R. Soc. Lond., 1983, A386, 145.

11.) Watson, P. L.; Parshall, G. W., Acc. Chem. Res., 1985, 18, 51.

12.) Shannon, R. D., Acta Cryst., 1976, 32A, 751.

13.) a) Boncella, J. M.; Andersen, R. A., Organometallics, 1985, 4, 205. b) Tilley, T. D.; Andersen, R. A.; Zalkin, A., J. Am. Chem. Soc., 1982, 104, 3725.

14.) a) Klein, H. F.; Gross, J.; Bassett, J.-M.; Schubert, U., Z. Naturforsch., Teil. B, 1980, 35, 614. b) Klein, H. F.; Witty, H.; Schubert, U., J. Chem. Soc. Chem. Comm., 1983, 231. c) Jonas, K.; Kruger, C., Angew. Chem. Int. Ed. Engl., 1980, 19, 520.

15.) Hopkinson, A. C., in "The Chemistry of the Carbon-Carbon Triple Bond", S. Patai, ed., J. Wiley and Sons, New York, 1978, and references therein.

16.) a) Tilley, T. D., Ph.D. Thesis, University of California, Berkeley, California, U.S.A., 1982. b) Boncella, J. M., Ph.D. Thesis, University of California, Berkeley, California, U.S.A., 1984.

17.) Pignataro, E.; Post, B., Acta Cryst., 1955, 8, 672.

18.) Davies, B. W.; Payne, N. C., J. Organomet. Chem., 1975, 99, 315.

19.) Davies, B. W.; Payne, N. C., Can. J. Chem., 1973, 151, 3477.

20.) Evans, W. J.; Grate, J. W.; Bloom I.; Hunter, W. E.; Atwood, J. L., J. Am. Chem. Soc., 1985, 107, 405.

21.) Van Vleck, J. H., "The Theory of Electronic and Magnetic Susceptibilities", Clarendon Press, Oxford, 1932.

22.) Bordwell, F. G.; Baisch, M. J., J. Am. Chem. Soc., 1983, 105, 6188.

23.) Mascornick, M. J.; Streitwieser, A., Jr., Tet. Lett., 1972, 1625.

24.) Evans, W. J.; Coleson, K. M.; Engerer, S. C., Inorg. Chem., 1981, 20, 4320.

25.) Rautenstrauch, V., Angew. Chem. Int. Ed. Engl., 1975, 14, 259.

26.) a) Rest, A. J.; Whitwell, W. A.; Graham, W. A. G.; Hoyano, J. K.; McMaster, A. D., J. Chem. Soc. Chem. Comm., 1984, 624. b) Mascetti, J.; Rest, A. J., J. Chem. Soc. Chem. Comm., 1987, 221.

27.) Brennan, J. G., Ph.D. Thesis, University of California, Berkeley, California, U.S.A., 1985.

28.) DeKock, R. L.; Gray, H. B., "Chemical Structure and Bonding", Benjamin/Cummings Publishing, Co., Menlo Park, 1980.

29.) Zinnen, H. A.; Pluth, J. J.; Evans, W. J., J. Chem. Soc. Chem. Comm., 1980, 810.

30.) Watson, P. L.; Whitney, J. F.; Harlow, R. L., Inorg. Chem., 1981, 20, 3271.

31.) Watson, P. L., J. Chem. Soc. Chem. Comm., 1983, 276.

32.) Thompson, M. E.; Baxter, S. M.; Bulls, A. R.; Burger, B. J.; Nolan, M. C.; Santarsiero, B. D.; Schaefer, W. P.; Bercaw, J. E., J. Am. Chem. Soc., 1987, 109, 203.

33.) a) Rutledge, T. F., "Acetylenes and Allenes", Reinhold, New York, 1969. b) Bushby, R. J., Quart. Rev., 1970, 24, 585. c) Huntsman, W. D., in "The Chemistry of Ketenes, Allenes, and Related Compounds", S. Patai, ed., J. Wiley and Sons, New York, 1980, and references therein.

34.) Cram, D. J.; Willey, F.; Fischer, H. P.; Relles, H. M.; Scott, D. A., J. Am. Chem.Soc., 1966, 88, 2759.

35.) Kay, E. L.; Roberts, D. T., Jr.; Calihan, L. E.; Wakefield, L. B., U.S Patent No. 3,751,511; Chem. Abstr. 1973, 79, 93213.

36.) a) Jones, E. R. H.; Leeming, P. R.; Remers, W. A., J. Chem. Soc., 1960, 2257. b) Bew, R. E.; Chapman, J. R.; Jones, E. R. H.; Lowe, B. E.; Lowe, G., J. Chem. Soc. (C), 1966, 129.

37.) Watson, P. L., private communication.

38.) Gundersen, G.; Haugen, T.; Haaland, A., J. Organomet. Chem., 1973, 54, 77.

39.) a) Drew, D. A.; Haaland, A.; Weidlein, J., Z. Anorg. Allg. Chem., 1973, 398, 241. b) Haaland, A.; Stokkeland, O., J. Organomet. Chem., 1975, 94, 345.

40.) a) Ouzounis, K.; Riffel, H.; Hess, H.; Kohler, U.; Weidlein, J., Z. Anorg. Allg. Chem., 1983, 504, 67. b) Hess, H.; Hinderer, A.; Steinhauser, S., Z. Anorg. Allg. Chem., 1970, 377, 1.

41.) a) Bottomley, F.; Paez, D. E.; White, P. S., J. Organomet. Chem., 1985, 291, 35. b) Bush, M. A.; Sim, G. A., J. Chem. Soc. (A), 1971, 2225. c) Ryan, R. R.; Penneman, R. A.; Kanellakopulos, B., J. Am. Chem. Soc., 1975, 97, 4258.

42.) a) Allegra, G.; Perego, G., Acta Crystallogr., 1963, 16, 185. b) Schlemper, E. O.; Hamilton, W. C., Inorg. Chem., 1966, 5, 995. c) Clark, H. C.; O'Brien, R. J.; Trotter, J., J. Chem. Soc., 1964, 2332.

43.) Boudreaux, E. A.; Mulay, L. N., "Theory and Applications of Molecular Paramagnetism", Wiley, New York, 1976.

44.) Lifshitz, C.; Tiernan, T. O.; Hughes, B. M., J. Chem. Phys., 1973, 59, 3182.

45.) Smart, B. E., in "The Chemistry of Functional Groups, Supplement

D", S. Patai and Z. Rappoport, eds., John Wiley and Sons, New York, 1983.

46.) Modena, G.; Scorrano, G., in "The Chemistry of the Carbon-Halogen Bond", S. Patai, ed., John Wiley and Sons, New York, 1973.

47.) a) Finke, R. G.; Schiraldi, D. A.; Hirose, Y., J. Am. Chem. Soc., 1981, 103, 1875. b) Finke, R. G.; Keenan, S. R.; Schiraldi, D. A.; Watson, P. L., Organometallics, 1986, 5, 598. c) Finke, R. G.; Keenan. S. R.; Schiraldi, D. A.; Watson, P. L., Organometallics, 1987, 6, 1358.

CHAPTER THREE: Coordination and Inclusion of Polar Molecules

Models for Methane Coordination

The activation of C-H bonds by d-transition metal complexes has been studied extensively in recent years[1]. The wide range of complexes which are capable of activating saturated hydrocarbons includes both nucleophilic and electrophilic species, and high-valent as well as low-valent metal centers. There are a number of requirements which appear to be met in all of these systems, however. The most obvious of these is the need for a sterically uncongested or coordinatively unsaturated ligand set about the metal center. This implies that precoordination of the alkane is required for activation. Complexes containing intramolecular "agostic" C-H···M interactions have been described as plausible models for this coordination step, in which electrons in the C-H bonding pair is donated to the metal in a two-electron, three-center bond[1a,2]. Furthermore, theoretical consideration has been given to the activation of the C-H bonds of by metals and metal surfaces, and it has been suggested that the C-H σ-bonding orbitals can overlap with empty metal d-orbitals[3]. In spite of this, no neutral alkane complexes of d-transition metals have been isolated (although evidence has been presented for the interaction of unsaturated metal fragments with alkane matrixes at low temperature[4]).

Electrophilic complexes of f-transition metals and related early d-transition metals have also been found to activate C-H bonds[5]. As mentioned in the Introduction, $(Me_5C_5)_2LuMe$ has been found to undergo σ-bond metathesis with a number of unsaturated and saturated substrates.

The complex reacts with $^{13}CH_4$, resulting in encorporation of ^{13}C label into the methyl group of the metal complex[5a,e]. Bis(pentamethylcyclopentadienyl)scandium(alkyl) complexes similarly engage in σ-bond methathesis[5b]. These reactions are proposed to proceed in a concerted fashion by way of a four-center, polar intermediate formed by the donation of the σ-bonding electrons of the C-H bond to the acidic metal center. Evidence for prior coordination of the alkane lies in the marked steric selectively of the reactions[5a].

Unlike the d-transition metals, lanthanides are sufficiently electrophilic that an analog of an alkane coordination complex has been isolated. The complex $(Me_5C_5)_2LuMe$ free of coordinating Lewis bases exists in the solid state as an asymmetric dimer[5a]. This dimer is in equilibrium with the monomeric form in solution. The solid state structure reveals that the methyl group of one metal is acting as a donor ligand to the second metal ion, forming a near linear Lu-Me-Lu bridge bond. Unfortunately, there is no report that the hydrogen atoms on the bridging group were located in the room temperature X-ray structure, and so no information may be inferred about the nature of the donor orbital on the methyl group.

The reactivity of trivalent lanthanide alkyls with both saturated and unsaturated C-H bonds in general precludes the isolation of simple alkane coordination compounds. As in the case of olefins and acetylenes, the divalent complex $(Me_5C_5)_2Yb$ provides a likely alternative starting material; it is coordinatively unsaturated, diamagnetic, and contains no M-C σ-bonds capable of metathetical exchange.

As described in Chapter Two, polymerization inhibition experiments suggest that CH_4 does act as a weak Lewis base towards ytterbium, but no simple coordination compound is isolated. It is necessary to employ methane analogs which are activated for coordination, much as was required in the case of the unsaturated hydrocarbons. Theoretical descriptions of alkane coordination[3] suggest that the t_2 bonding orbitals of methane are capable of acting as σ-donor orbitals (see Figure 1). These electrons are quite low in energy, however, as indicated by the first ionization potential of methane of ca. 14 eV[6].

Figure (1) Molecular orbitals of Methane

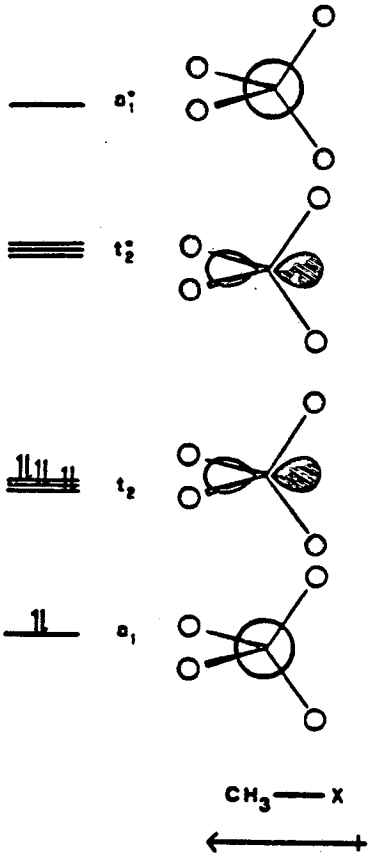

The basicity of methane can be increased by raising the energy of these orbitals; this can be achieved by substituting a hydrogen atom with an element which has a lower electronegativity. In other words, a basic methane analog can be created by choosing the identity of X in the molecule CH_3X so as to create a permanent dipole moment in the direction of the methyl group, in the same way that directional lone pairs induce a dipole moment in traditional Lewis bases.

Electropositive metals appear to be effective substitutents in inducing such a dipole moment. The reaction of $(Me_5C_5)_2Yb$ with triethylaluminum in hydrocarbon solvent results in the formation of a bright green solution from which a green, crystalline, diamagnetic solid precipitates upon standing. The solid is slightly soluble in hot aromatic solvents, and dilute ^{1}HNMR spectra suggest a 2:3 ratio of C_5Me_5 and Et groups, although the exact disposition of the ligands about the metals is unclear. The IR spectrum reveals the presence of low-energy νC-H bands at 2790 and 2695 cm^{-1}; these low energy bands are similar to those found in the spectrum of $(Me_5C_5)_2ScEt$[5b] which have been attributed to β-agostic M···H interactions. This suggests that the alkyl groups are interacting with the ytterbium center in a donor-acceptor fashion. While X-ray quality crystals have not been obtained, preliminary precession photographs indicate that the unit cell is quite large, consistent with a polymeric structure. This formulation is also supported by the low solubility of the complex. The presence of multiple alkyl groups about the electropositive center may allow the coordination by more than one ytterbium molecule, which in turn may then coordinate to other $AlEt_3$ molecules, forming a polymer.

To prevent this type of polymerization, it is necessary to employ a potential ligand which has only one σ-bonded alkyl group. The complex $(Me_5C_5)BeMe$ fulfills this requirement. Although the dipole moment of this complex is not known, values have been reported for similar molecules: 4.26D for $(H_5C_5)BeCl$[7a], and 2.08D for $(H_5C_5)BeH$[7b]. The reaction of $(Me_5C_5)_2Yb$ and $(Me_5C_5)BeMe$ in pentane gives rise to an orange solution from which dark orange prisms can be crystallized in good yield. The IR spectrum of the compound show no new features or bands relative to the spectra of the starting materials. In order to confirn the coordination mode of the $(Me_5C_5)BeMe$ group (in the absence of bands identifiable as lowered C-H stretching modes), the structure of the complex was determined by X-ray crystallography. An ORTEP diagram of the molecule can be found in Figure (2), while intramolecular distances and angles are given in Tables I and II, respectively.

Table I Bond Distances for $(Me_5C_5)_2Yb(\mu\text{-}Me)Be(C_5Me_5)$ (Å)

Yb-C1	2.766(4)	Yb-C11	2.710(3)	Be-C31	1.872(6)
Be-C1	1.705(6)	Yb-C12	2.679(3)	Be-C32	1.881(6)
		Yb-C13	2.657(3)	Be-C33	1.874(5)
C1-H11	0.92(4)	Yb-C14	2.656(3)	Be-C34	1.899(5)
C1-H12	0.90(5)	Yb-C15	2.681(3)	Be-C35	1.879(5)
C1-H13	0.73(6)	Yb-C21	2.696(3)		
		Yb-C22	2.695(3)	Yb-Cp1	2.391
Yb-H11	2.54(4)	Yb-C23	2.677(3)	Yb-Cp2	2.400
Yb-H12	2.51(5)	Yb-C24	2.683(3)	Be-Cp3	1.447
Yb-H13	2.71(6)	Yb-C25	2.668(3)		

Cp1, Cp2, and Cp3 are the centroids of the rings comprised of C11-C15, C21-C25, and C31-C35, respectively.

The structure consists of a $(Me_5C_5)_2Yb$ molecule and a $Be(C_5Me_5)$ unit with a linear, asymmetric methyl bridge. The structural features of the divalent ytterbium unit are comparable to those found in

Table II Intramolecular Angles for $(Me_5C_5)_2Yb(\mu\text{-}Me)Be(C_5Me_5)$ (°)

Yb-C1-Be	177.2(3)	Yb-C1-H11	67(2)
		Yb-C1-H12	64(3)
Be-C1-H11	115(2)	Yb-C1-H13	78(5)
Be-C1-H12	113(3)		
Be-C1-H13	104(5)	C1-Be-Cp3	177.5
H11-C1-H12	105(4)	C1-Yb-Cp1	107.5
H11-C1-H13	100(5)	C1-Yb-Cp2	107.2
H12-C1-H13	121(6)	Cp1-Yb-Cp2	144.6

Figure (2) ORTEP diagram of $(Me_5C_5)_2Yb(\mu\text{-}Me)Be(C_5Me_5)$

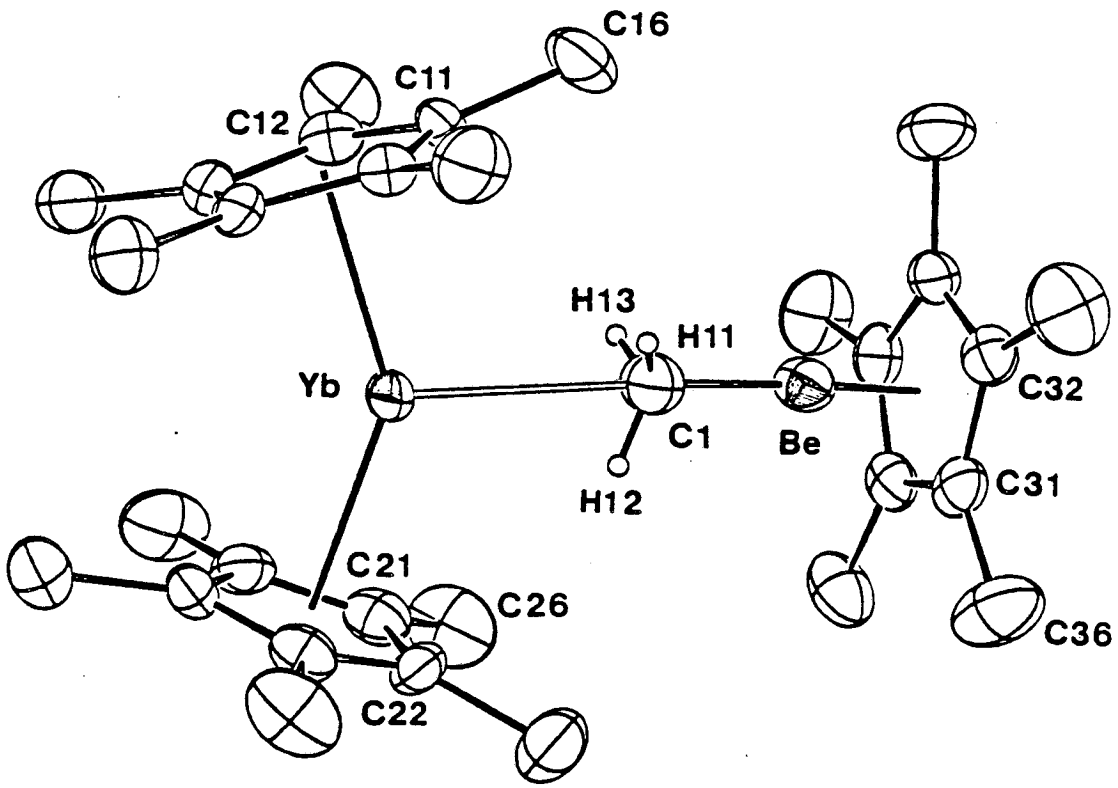

$(Me_5C_5)_5Yb$ and its weak coordination compounds. The average Yb-C (ring) bond distance is 2.680(3) Å, similar to the value of 2.673(3) Å found in $(Me_5C_5)_2Yb(\mu\text{-}C_2H_4)Pt(PPh_3)_2$, and slightly longer than the value of 2.665(3) Å in $(Me_5C_5)_2Yb$. The bend angle of the rings, 144.6°, is very similar to the value of 145.4° determined from the structure of the base-free ytterbium complex, and that of 143.3° found for the 2-butyne

adduct. The rings in are staggered, with a torsional angle of 39.9(2)°.

While the structure of $(Me_5C_5)BeMe$ has not been reported, the structure of the unsubstituted cyclopentadienyl analog has been determined by gas-phase electron diffraction[7b]. The Be-C (ring) distance in $(H_5C_5)BeMe$ is 1.923(3) Å, slightly longer than the average Be-C(ring) distance of 1.881(6) Å found in the ytterbium complex. The Be-C(methyl) distances in the two species are identical: 1.705(6) Å in the ytterbium complex, and 1.706(3) Å in $(H_5C_5)BeMe$.

The most interesting structural feature of the molecule is the bridging interaction. In the vast majority of transition metal complexes containing bridging methyl groups, the M-C-M angle is less than 90°[8]. In $(Me_5C_5)_2Yb(\mu\text{-}Me)Be(C_5Me_5)$, however, Yb-Me-Be angle of 177.2(3)° is very nearly linear, the same as the angle about the bridging methyl group in $(Me_5C_5)_4Lu_2(\mu\text{-}Me)(Me)$[5a], 170(4)°. Few other examples of linear bridging methyl groups have been structurally characterized. In the complex $LiBMe_4$[9], one type of methyl group bridges Li and B in a near linear fashion, with angles about carbon of 176.3(4)° and 178.8(6)° and angles about carbon of 150-160° have been observed in complexes where methyl groups bridge lithium and other electropositive metals[10].

In the complex $(H_5C_5)_4Zr_2(\mu\text{-}Me)[OCH(CH_2CMe_3)]_2AlMe_2$[10a], as well as in the theoretically studied molecule $CH_3Li_2^+$ [11], a model has been used to explain the linear methyl bridge which involves a rehybridization of the methyl carbon so that it is in trigonal bipyramidal coordination, with the metals occupying the axial positions. In this model, the M-C-H angles are 90°, and the H-C-H angles are 120°. In the complex

$(Me_5C_5)_2Yb(\mu\text{-}Me)Be(C_5Me_5)$, while the hydrogen atoms positions are poorly determined, it appears that the Be-C-H angles are significantly larger than 90° (see Table II), indicating that the ytterbium atom interacts with all three hydrogen atoms in a linear tribridged geometry[9]. This type of interaction has been demonstrated in $LiBMe_4$[9], as well as in the tetrameric form of HeLi[10e,f]. The geometry about the methyl group is consistent with the proposal that the orbital serving to donate electron density to the acidic lanthanide is not a C p_z orbital, but rather the HOMO of $(Me_5C_5)BeMe$ (Figure 3). The methyl group does not possess C_{3v} symmetry with respect to the C-Yb axis in the crystal structure, however. The methyl group is tilted so that two of the three hydrogen atoms closely approach the Yb atom (Yb··H11 = 2.54(4) Å, Yb··H12 = 2.51(5) Å), while the third hydrogen atom is significantly farther away (Yb··H13 = 2.71(6) Å).

The hydrogen atom positions located by x-ray diffraction represent centroids of electron density, and do not accurately reflect nuclear positions. A neutron structure would undoubtedly reveal C-H distances of ca. 1.05 Å; this would increase the Yb··H distances slightly.

Figure (3) HOMO of $(Me_5C_5)BeMe$

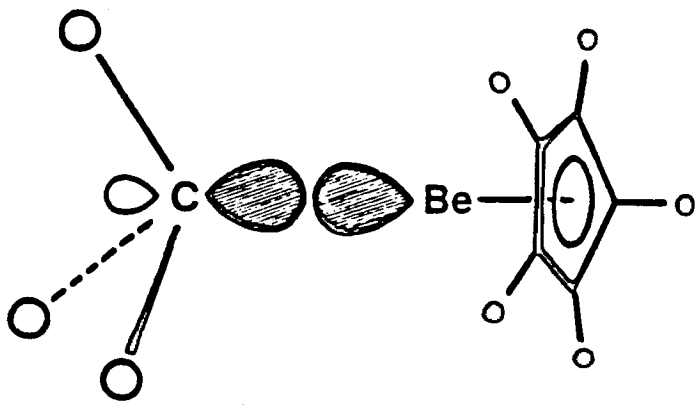

The Yb-C1 bond distance of 2.766(4) Å is comparable to the average Yb-C(ligand) bond distances found in the platinum olefin and 2-butyne coordination complexes described in Chapter One (2.781(3) Å and 2.850(5) Å, respectively). In the dimer of $(Me_5C_5)_2LuMe$, the shared electron pair Lu-C bond distance for the metal in seven-coordination is 2.440(9) Å. Taking into account the differences in the ionic radii of Lu^{3+} and Yb^{2+} [12], the expected ionic Yb(II) to carbon bond length in seven-coordination would be ca. 2.60 Å. The difference between the bond length for a shared electron pair bond vs. a dative bond appears to be 0.15-0.20 Å. This is in agreement with structural results for main group complexes[13], in which it is found that electron pair and dative bond lengths can differ by as much as 0.25 Å. This reflects the difference in the ionic radii of the neutral and anionic carbon atoms.

The lack of significant perturbations in the structures of the component molecules indicates that the interaction between the ytterbium and the methyl group is weak. This is confirmed by variable temperature ^{1}HNMR spectroscopy studies. At room temperature, the spectrum of $(Me_5C_5)BeMe$ displays a singlet at δ 1.76 due to the ring protons, and a methyl singlet at δ -1.27 broadened by quadrupolar coupling to beryllium (I = 3/2). This singlet moves downfield to δ -1.13 in the complex, and the resonance broadens further ($\nu_{1/2}$ = 30 Hz). Addition of approximately one molar equivalent of $(Me_5C_5)BeMe$ yields a single set of resonances for the Be compound, indicating exchange of free and coordinated ligand. At +90°C, the methyl resonance appears as a singlet at δ-1.41 ($\nu_{1/2}$ = 9 Hz). Cooling the sample causes this singlet to broaden and shift downfield. At -25°C, the resonance disappears

entirely, and does not reappear above -70°C. While the intermediate exchange region has been reached, exchange can not be stopped.

The accessibility of the donor orbital appears to be as important as the dipole moment in dictating whether a molecule will coordinate to ytterbium. While the methyl compound of beryllium forms a coordination complex readily, the analogous phenyl compound, $(Me_5C_5)BePh$, does not form an isolable adduct. This is presumably due to the steric emcumbrance encountered in any attempt to bring the carbanionic site on the phenyl ring into the vicinity of the Yb atom.

Other first-row small molecules isoelectronic with methane are known to serve as strong bases towards ytterbium. While H_2O is too acidic to form a kinetically stable coordination compound, ether complexes of $(Me_5C_5)_2Yb$ are well known[14]. Similarly, ammonia has been demonstrated to act as a strong donor molecule towards ytterbium[15]. Moving to the left of carbon in the periodic table, one might wonder whether it might be possible to isolate a coordination complex of the electron-deficient BH_3 molecule.

There are relatively few references in the literature to borane complexes of transition metals. Borane complexes of metal carbonyl anions have been reported[16], in which the borane is proposed to act as an electron-accepting ligand. This suggests that borane may be an unsuitable ligand for a hard Lewis acid such as ytterbium. In order to prepare the BH_3 unit for coordination, it is necessary to incorporate it into a molecule which has a permanent dipole moment in the direction of the borane. One such species, the anion BH_3CN^-, has been used metathetically to prepare lanthanide and actinide complexes of the

formulation Cp_3MX[17]. While the products do show evidence of η^3-BH_3 coordination in the solid state, their solution behavior is complicated by coordination equilibria (equation 1). The Lewis basicity of the

$$(MeC_5H_4)_3UNCBH_3 \rightleftharpoons (MeC_5H_4)_3U(\eta^3\text{-}BH_3CN) \qquad (1)$$

nitrogen is an undesirable side effect of the use of the CN^- group. To effectively study the coordination of the BH_3 unit, it is preferable to use a ligand without other strongly basic sites.

Phosphine-borane adducts may be suitable ligands, because phosphines have been demonstrated to coordinate only weakly to ytterbium. Phosphine adducts of borane are kinetically very stable relative to their amine analogs; they resist hydrolysis even in boiling acid. This stability is attributed to the strength of the B-P bonding. The P→B σ-donation is augmented by π-symmetry back-donation from the filled B-H bonding orbitals to empty phosphorus d orbitals[18]. The molecules also provide the necessary dipole moment; the measured dipole moment of $BH_3 \cdot PMe_3$ is 4.99D, and that of $BH_3 \cdot PPh_3$ is 4.79D. The higher dipole moment of $BCl_3 \cdot PPh_3$ (7.0D) indicates that the moment lies in the direction of the borane.

Reaction of $(Me_5C_5)_2Yb$ with $BH_3 \cdot PMe_3$ results in a rapid precipitation of a light green solid; the analogous $BH_3 \cdot PPh_3$ complex is orange. Both complexes may be recrystallized from toluene (the PMe_3 complex is only soluble in hot toluene), but the $BH_3 \cdot PPh_3$ adduct occludes solvent, which is lost under reduced pressure. The IR spectra reveal the presence of νB-H bands in the expected region; the values are given in Table III.

Table III νB-H for Phosphine-Borane Complexes (cm^{-1})

$BH_3 \cdot PMe_3$	2364s, 2339sh, 2268sh, 2256w
$(Me_5C_5)_2^3Yb(\eta^3\text{-}BH_3 \cdot PMe_3)$	2427m, 2363vw, 2334sh, 2302sh, 2266m
$BH_3 \cdot PPh_3$	2378s, 2344m, 2253vw
$(Me_5C_5)_2^3Yb(\eta^3\text{-}BH_3 \cdot PPh_3)$	2434m, 2380s, 2345m, 2296w, 2265w

Some bands indicate the possible presence of free ligand, suggesting that an equilibrium exists in the mull; this was also noted in the isocyanide complexes discussed in Chapter One. In general, the νB-H bands move to higher energy upon coordination to the acidic lanthanide. This is consistent with reported spectra for $(MeC_5H_4)_3U(\eta^3\text{-}BH_3CN)$[17c]; the values for νB-H are higher than those observed for $[(n\text{-}Bu)_4N][NCBH_3]$.

The ^{1}HNMR spectra of the complexes reveal little about the nature of the coordination; the borane protons are not visible in the spectra of the adducts. The Me resonance in the PMe_3 compound moves upfield upon coordination from δ 0.78 to δ 0.49. The ^{31}P and ^{11}B chemical shifts change little upon coordination, in general moving downfield by less than 1 ppm. In both adducts, however, $J_{B\text{-}P}$ is raised upon coordination of the ligand (the value increases by 18 Hz in the PMe_3 complex, and by 11 Hz in the PPh_3 complex). The coupling constant between two nuclei is believed to be related to the amount of s-orbital character in the bond[19]. It appears that when the ytterbium coordinates to the borane, it inductively increases the P $\rightarrow$ B σ-donation, effectively increasing the bond strength.

In order to make structural comparisons between these complexes and the $(Me_5C_5)BeMe$ complex, the molecular structure of the $BH_3 \cdot PMe_3$ adduct was determined by X-ray crystallography. An ORTEP diagram is presented

in Figure (4), and bond distances and angles can be found in Tables IV and V.

Precession photographs showed thermal diffuse scattering, but attempts to cool crystals of the compound in order to collect a low temperature data set resulted in crystal fracture. The solution obtained from a room temperature data set does show a great deal of thermal motion. Two of the methyl groups on the rings (C11 and C14) and one of the methyl groups on the phosphine (C211) were refined in two half-occupancy positions (see the structural discussion in Appendix I for further details).

The molecule lies on a crystallographic mirror plane defined by the

Figure (4) ORTEP Diagram of $(Me_5C_5)_2Yb(BH_3 \cdot PMe_3)$

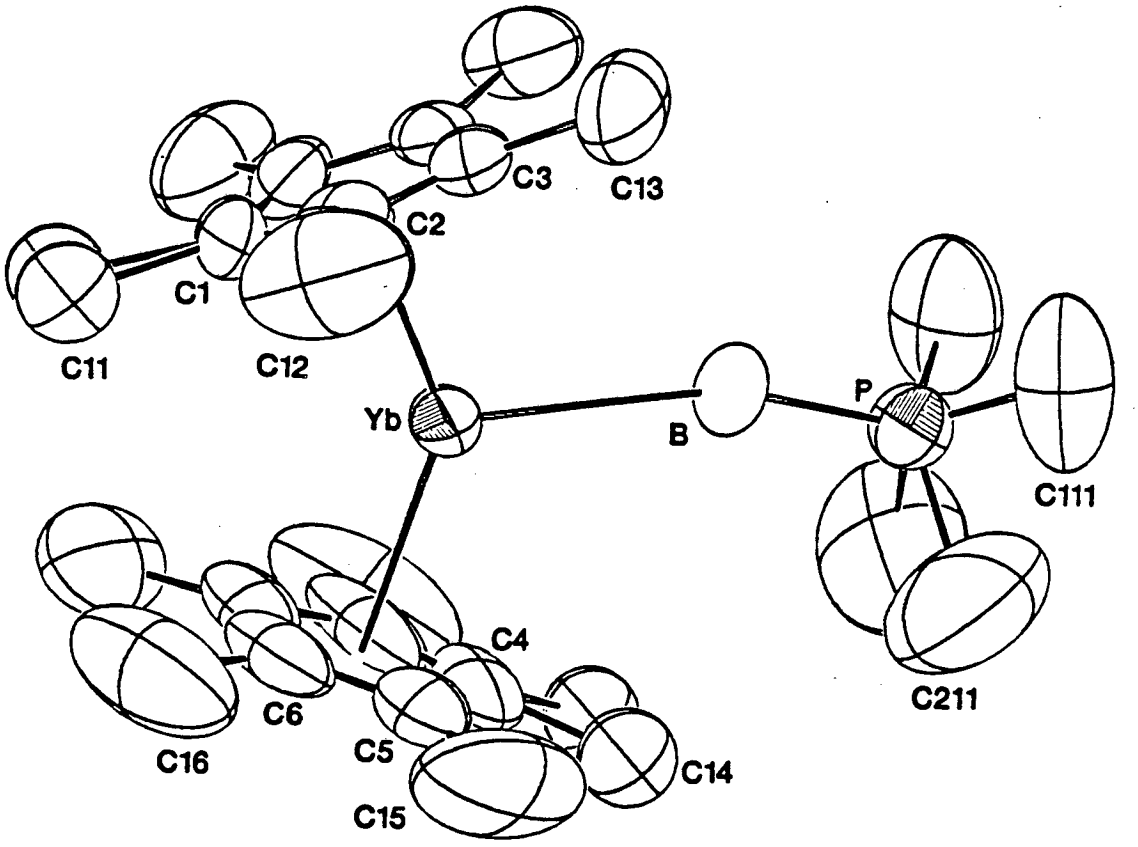

Table IV Bond Distances for $(Me_5C_5)_2Yb(BH_3 \cdot PMe_3)$ (Å)

Yb-B	2.764(8)	Yb-C1	2.699(7)	Yb-C4	2.700(9)
P-B	1.910(8)	Yb-C2	2.705(5)	Yb-C5	2.688(6)
		Yb-C3	2.681(4)	Yb-C6	2.663(5)
P-C111	1.81(1)				
P-C211	1.81(1)	Yb-Cp1	2.420	Yb-Cp2	2.397

Cp1 and Cp2 are the centroids of the rings comprised of C1-C3 and C4-C6 (and their mirror-related counterparts), respectively

Table V Intramolecular Angles for $(Me_5C_5)_2Yb(BH_3 \cdot PMe_3)$ (°)

Yb-B-P	162.3(5)	B-P-C111	112.3(3)
		B-P-C211	111.2(4)
B-Yb-Cp1	108.2	C111-P-C111'	99.0(8)
B-Yb-Cp2	112.4	C111-P-C211	83.6(5)
		C111-P-C211'	131.4(5)
Cp1-Yb-Cp2	139.4	C211-P-C211'	61.0(9)

atoms C1, C4, Yb, B, and P. The $(Me_5C_5)_2Yb$ unit and the trimethylphosphine are bridged in a near-linear fashion by the borane. The structural parameters of the trimethylphosphine-borane unit compare favorably with those determined by microwave spectroscopy for the free complex[20a]; the P-B distance is 1.910(8) Å, compared to 1.901(7) Å in the free ligand, and the average P-C distance (1.81(1) Å) is the same as in $BH_3 \cdot PMe_3$ (1.82(1) Å). The average C-P-C angle calculated from the values of C111-P-C111', C111-P-C211, and C111-P-C211', 104.7(6)°, is similar to the C-P-C value found in the free ligand (105.0(4)°).

The average Yb-C(ring) bond length, 2.687(6) Å, is identical to that found in the beryllium methyl complex (2.680(3) Å), and somewhat longer than in the base-free $(Me_5C_5)_2Yb$ (2.665(3) Å), reflecting the higher coordination number. The centroid-Yb-centroid angle, 139.4°, is somewhat smaller than in most of the Yb(II) compounds crystallographically characterized. This angle is probably compressed somewhat by

steric repulsions between one ring and the trimethylphosphine group (C14···C211 = 3.54(2) Å).

The Yb-B-P bridge is more bent than the Yb-C-Be bridge in the beryllium methyl complex (162.3(5)° vs. 177.2(3)°). The large degree of thermal motion in the structure prevented elucidation of the hydrogen atom positions in the bridging borane, and therefore little can be deduced about the geometry about the borane, but the lack of perturbation in the structure of the ligand upon coordination suggests that the hydrogen atoms are interacting with the Yb in a tribridged linear manner, as in the beryllium structure. Interactions of borane and borate hydrogen atoms with metals have been documented; in the complex $ZnCl_2 \cdot B_2H_4 \cdot 2PMe_3$[20b], the zinc atoms is coordinated to the diborane unit through B-H-M bridge bonds, and Fe-H-B bridges are implied between an iron trimer and a tricapping borate in the complex $(\mu\text{-}H)Fe_3(CO)_9BH_4$[20c].

Electron-Transfer Complexes

During the course of the study of the coordination chemistry of $(Me_5C_5)_2Yb$ with electropositive metal alkyls, the reactions with group 12 alkyl and aryl complexes were conducted. The reaction of $ZnMe_2$ with $(Me_5C_5)_2Yb$ in pentane immediately produces an orange flocculent precipitate, suggestive of a coordination compound, but with continued stirring, the solid redissolves to give a deep purple solution from which zinc metal is precipitated as a mirror. The material can be crystallized at -78°C to give dark purple blocks. The IR spectrum of the compound reveals low energy νC-H bands at 2803, 2771, and 2678 cm^{-1},

indicating "agostic" Yb··H interactions. Such bands would not be expected in a simple compound of the formula $(Me_5C_5)_2YbMe$, however. The IR spectra of the methyl complexes $(Me_5C_5)_4Lu_2(\mu\text{-}Me)(Me)$[5a] and $(Me_5C_5)_2ScMe$[5b] are reported not to show such bands. The analytical data likewise suggested that the compound was not a simple ytterbium alkyl, and yet the ^{1}HNMR spectrum at room temperature showed only one resonance for the C_5Me_5 rings, giving no information about the structure. In order to determine the stoichiometry of the product, the crystal structure of the compound was determined. An ORTEP diagram of the structure is shown in Figure (5), while pertinent bond distances and intramolecular angles are listed in Tables VI and VII.

Figure (5) ORTEP Diagram of $(Me_5C_5)_2Yb(\mu\text{-}Me)_2ZnMe$

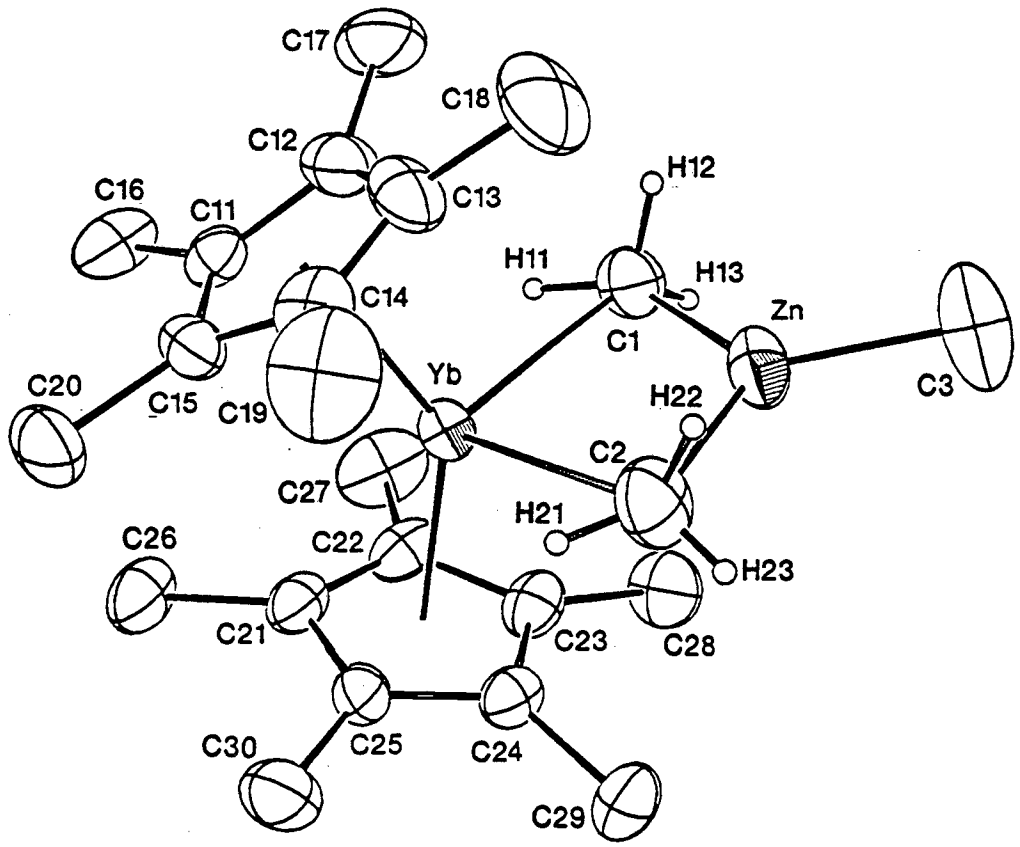

Table VI Bond Distances for $(Me_5C_5)_2Yb(\mu\text{-}Me)_2ZnMe$ (Å)

Yb-C1	2.546(4)	C1-H11	1.02(5)	Yb-C11	2.615(3)
Yb-C2	2.529(5)	C1-H12	1.02(4)	Yb-C12	2.628(4)
		C1-H13	0.91(4)	Yb-C13	2.615(3)
Zn-C1	2.066(4)	C2-H21	0.89(4)	Yb-C14	2.612(3)
Zn-C2	2.075(5)	C2-H22	1.133(5)	Yb-C15	2.612(3)
Zn-C3	1.960(4)	C2-H23	0.840(5)	Yb-C21	2.595(4)
				Yb-C22	2.600(3)
Yb-H11	2.32(5)	Yb-Cp1	2.325	Yb-C23	2.622(3)
Yb-H21	2.25(4)	Yb-Cp2	2.316	Yb-C24	2.639(3)
				Yb-C25	2.591(4)

Cp1 and Cp2 are the centroids of the rings comprised of C11-C15 and C21-C25, respectively.

Table VII Intramolecular Angles for $(Me_5C_5)_2Yb(\mu\text{-}Me)_2ZnMe$ (°)

C1-Yb-C2	89.2(1)	Yb-C1-H11	65.9(3)
C1-Yb-Cp1	103.5	Yb-C1-H12	117.7(2)
C2-Yb-Cp1	103.9	Yb-C1-H13	135.1(3)
C1-Yb-Cp2	105.0	Yb-C2-H21	62.1(3)
C2-Yb-Cp2	105.2	Yb-C2-H22	123.8(4)
Cp1-Yb-Cp2	139.2	Yb-C2-H23	142.2(4)
C1-Zn-C2	118.7(2)	Zn-C1-H11	141.3(3)
C1-Zn-C3	120.9(2)	Zn-C1-H12	91.8(2)
C2-Zn-C3	120.3(2)	Zn-C1-H13	99.9(3)
		Zn-C2-H21	138.2(3)
Yb-C1-Zn	75.9(1)	Zn-C2-H22	94.3(3)
Yb-C2-Zn	76.1(1)	Zn-C2-H23	100.5(4)
H11-C1-H12	110.5(4)	H21-C1-H22	109.8(3)
H11-C1-H13	103.0(4)	H21-C2-H23	111.0(3)
H12-C1-H13	107.0(4)	H22-C2-H23	93.9(4)

The compound is in fact $(Me_5C_5)_2YbMe$ coordinated to another molecule of $ZnMe_2$ to give a zincate complex of Yb(III). Such zincate complexes have precedent in alkali metal chemistry[21], although they have never been structurally characterized. The ytterbium is in pseudo-tetrahedral coordination, with an average Yb-C(ring) bond length (2.613(4) Å) identical to that found for the trivalent Yb in eight-coordination in the complex $(Me_5C_5)_6Yb_4(\mu\text{-}F)_4$. The centroid-Yb-centroid angle, 139.2°, is also comparable to that in the fluoride

complex, as well as in other Yb(III) complexes in eight-coordination[22]. The rings are staggered, with a torsion angle of 33.0(2)°. The zinc atom is in pseudo-trigonal planar coordination. The ZnC_3 unit is not quite planar; C3 lies 0.117(6) Å out of the plane formed by Zn, C1, and C2. The Zn-C(terminal) distance is shorter than the average Zn-C(bridge) distance (1.960(4) Å vs. 2.071(5) Å). This reflects the fact that the two Zn-C(bridge) distances are averages of a single bond and a dative bond, which is likely to be ca. 0.2 Å longer. For comparison, the Zn-C bond length for monomeric $ZnMe_2$ in the gas phase is 1.930(2) Å[23].

The structural parameters relating to the bridging unit are comparable to other known structures of the general formula $Cp_2M(\mu\text{-}Me)_2M'L_n$; these values are given in Table VIII. The acute angle about bridging methyl carbon is very reminiscent of angles about methyl group bridges in main group chemistry (e.g. in Al_2Me_6, the Al-C-Al angle in the gas phase is 75.5(1)°[27]).

Table VIII Structural Parameters for $Cp_2M(\mu\text{-}Me)_2M'L_n$

	M-C (avg, Å)	∠C-M-C (°)	∠M-C-M' (avg,°)	Ref.
$Cp^*_2Yb(\mu\text{-}Me)_2ZnMe$	2.538(5)	89.2(1)	76.0(1)	this work
$Cp_2Y(\mu\text{-}Me)_2YCp_2$	2.54(1)	92.3(3)	87.7(3)	24
$Cp_2Yb(\mu\text{-}Me)_2YbCp_2$	2.51(4)	93.4(4)	86.6(3)	24
$Cp_2Y(\mu\text{-}Me)_2AlMe_2$	2.58(2)	84.5(6)	80.8(5)	25
$Cp_2Yb(\mu\text{-}Me)_2AlMe_2$	2.59(2)	87.1(6)	78.8(5)	26

The $Yb(\mu\text{-}Me)_2Zn$ unit is very nearly planar; the planes represented by Yb-C1-C2 and Zn-C1-C2 meet in a dihedral angle of 5.2(1.5)°. The

methyl bridges are symmetrical within statistical errors. The most interesting feature of the bridging groups is the disposition of the hydrogen atoms. While the hydrogen atoms are poorly located, a pattern emerges which is outside the bounds of statistical error. The bridging methyl groups are eclipsed, and for each methyl group there is one very acute Yb-C-H angle (ca. 64°), bringing a hydrogen atom into close proximity with the ytterbium atom (Yb-H11 = 2.32(5) Å, Yb-H21 = 2.25(4) Å). These distances are far shorter than the closest M···H contacts determined in the structure of $Cp_4Y_2(\mu\text{-}Me)_2$[24], even taking into account the slighter smaller size of Yb. These contacts are undoubtedly the origin of the low energy C-H stretching modes in the IR spectrum.

The lack of an identifiable methyl resonance in the room temperature ^{1}HNMR spectrum suggests that the molecule may be undergoing some form of chemical exchange or fluxionality, with the intermediate exchange region falling at room temperature. Variable temperature NMR studies have been carried out in d^8-toluene. At -10° C, two resonances are visible in the spectrum at δ 3.30 ($\nu_{1/2}$ = 43 Hz) and δ -15.5 ($\nu_{1/2}$ = 160 Hz), in a 10:1 integration. Below this temperature, the resonances shift with temperature as normal paramagnetic resonances. These appear to be the C_5Me_5 and terminal methyl resonances of a stopped-exchange C_{2v} structure. Evidently, the bridging methyl groups are too broad to be observed. At ca. 0° C, the methyl resonances begins to broaden and disappear, so that at 30° C, it is no longer visible. The methyl resonance does not appear below 90° C, indicating that the chemically exchanging methyl resonance is still too broad to be observed.

The question remains whether the exchange process which

equilibrates the bridge and terminal positions is inter- or intramolecular. To answer this question, variable temperature NMR studies have also been carried out with an excess of $ZnMe_2$, to examine the exchange of free and coordinated zinc alkyl. At -10°C in the presence of excess $ZnMe_2$, the resonances for the ring and terminal methyl protons of the complex are visible at nearly the same positions (δ 3.30 and δ -17.3, respectively) as in the spectrum without added zinc alkyl, and a resonance for free $ZnMe_2$ appears at δ -0.14. Above 0°C, the two methyl resonances broaden and move, and the terminal methyl protons disappear entirely above 10° C. As the temperature is raised further, the remaining averaged methyl signal progressively broadens, and it disappears entirely at 70° C. The similarity of the spectra for the experiments with and without added ligand suggests that the mechanism for exchange of bridge and terminal methyl groups is in fact the exchange of free and coordinated $ZnMe_2$:

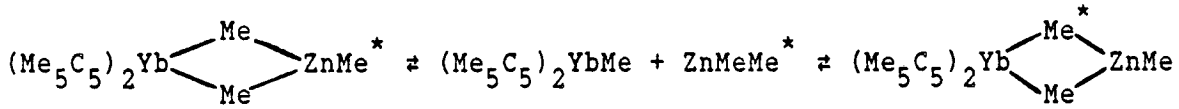

The trimethylzincate complex recrystallizes intact from diethyl ether, but can easily be cleaved with thf to give the previously reported compound $(Me_5C_5)_2YbMe(thf)$[28]. Attempts have been made to obtain the base-free methyl compound by perturbing the above coordinative equilibrium, but heating the compound in toluene and removing the solvent slowly under vacuum merely results in the isolation of a low yield of the divalent species $(Me_5C_5)_2Yb$.

In light of the inability to isolate a coordination compound of

$(Me_5C_5)BePh$ with divalent ytterbium, it was of interest to attempt to prepare the analogous zincate complex with aryl substituents, to examine the steric problems posed by a bridging phenyl group. Either $ZnPh_2$ or $Zn(p\text{-tolyl})_2$ reacts with $(Me_5C_5)_2Yb$ in toluene to give a deep purple solution and a zinc mirror. Removal of the solvent followed by recrystallization from pentane results in the isolation of the triarylzincate complex of ytterbium. The IR spectra of these complexes reveal no unusual νC-H bands, such as were visible in the spectrum of the methyl analog. In the reaction with $Zn(p\text{-tolyl})_2$, a small amount of zinc starting material is always reisolated from the residue of the pentane extract, and a second, very soluble red product can be crystallized from the pentane solution. This species is obtained in very low yield, but NMR and mass spectral evidence suggest that it is the base-free p-tolyl complex of ytterbium. The relative yields of this species and the zincate seem to be insensitive to reaction stoichiometry; a 2:1 reaction of $(Me_5C_5)_2Yb$ and $Zn(p\text{-tolyl})_2$ results in the isolation of a mixture of the ytterbium starting material and the two aryl products. Both of the arylzincates readily lose ZnR_2 in the gas phase, and the highest molecular weight fragments visible in the mass spectrum correspond to $(Me_5C_5)_2YbR$. The complexes are too thermally unstable to sublime on a preparative scale.

The room temperature ^{1}HNMR spectra of these compounds show a single averaged set of resonances for the aryl ligands, indicating that exchange of the bridging and terminal groups is fast on the NMR time scale at room temperature (with respect to the methylzincate). The rate of dissociation of $ZnAr_2$ is undoubtedly enhanced by steric repulsions

between the aryl rings and the C_5Me_5 groups. Variable temperature NMR studies have been undertaken with the intent of studying the barrier to this exchange. As the temperature is lowered to -10° C, the resonances begin to broaden, and by -30°C, the aryl resonances disappear into the baseline. Several paramagnetic peaks start reappearing at -50° C in the spectrum of the phenylzincate, while the spectrum of the p-tolyl analog does not show peaks due to the stopped-exchange limit at temperatures above -60° C. Both complexes have reached the stopped-exchange limit at -75°C. Variable temperature experiments with excess added $ZnAr_2$ show that the barrier to exchange of free and coordinated ligand is the same as that for exchange of bridging and terminal aryl groups.

In the spectra of the stopped exchange limit, there are a bewildering number of peaks (see Figure 6). The peaks and their

Table IX Low Temperature NMR Spectra of Arylzincates

$(Me_5C_5)_2Yb(\mu\text{-}Ph)_2ZnPh$	Integ.	$(Me_5C_5)_2Yb(\mu\text{-}p\text{-}tol)_2Zn(p\text{-}tol)$	Integ.
δ 128.9 ($\nu_{1/2}$ = 1000 Hz)	2	δ 126.9 ($\nu_{1/2}$ = 240 Hz)	2
δ 49.95 ($\nu_{1/2}$ = 95 Hz)	2	δ 32.98 ($\nu_{1/2}$ = 52 Hz)	6
δ 12.52 ($\nu_{1/2}$ = 120 Hz)	1	δ 12.93 ($\nu_{1/2}$ = 180 Hz)	2
δ 3.44 ($\nu_{1/2}$ = 230 Hz)	15	δ 3.60 ($\nu_{1/2}$ = 155 Hz)	15
δ -4.82 ($\nu_{1/2}$ = 85 Hz)	2		
δ -6.01 ($\nu_{1/2}$ = 120 Hz)	2	δ -6.75 ($\nu_{1/2}$ = 55 Hz)	6
δ -20.45 ($\nu_{1/2}$ = 100 Hz)	2	δ -20.62 ($\nu_{1/2}$ = 51 Hz)	2
δ -69.54 ($\nu_{1/2}$ = 900 Hz)	2	δ -69.87 ($\nu_{1/2}$ = 315 Hz)	2

In addition to these resonances, each spectrum shows a very broad feature under other resonances from ca. +10 to -10 ppm.

approximate integrations are given in Table IX (the integrations are approximate owing to the inaccuracy of integration over a very broad sweep width). While there are many similarities between the two spectra, there also appears to be many peaks missing and overlapping. Only one C_5Me_5 ring is visible (the other is probably the broad roll in

Figure (6a) Stopped-Exchange Spectrum of Triphenylzincate

(solvent resonances are off scale)

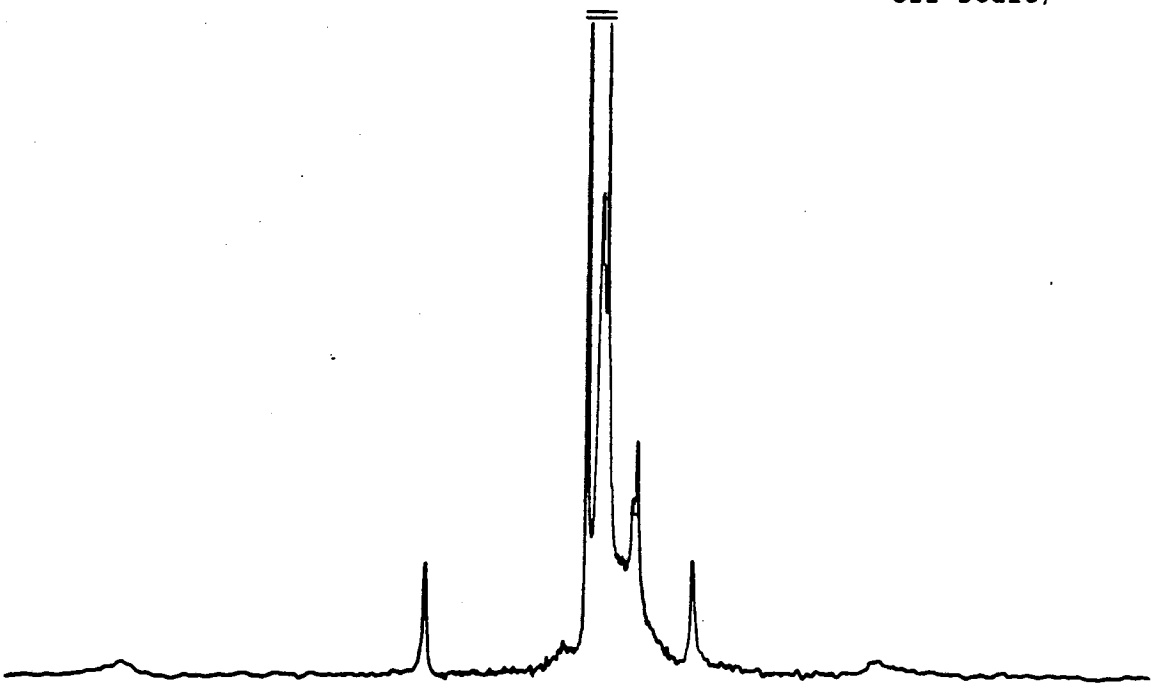

Figure (6b) Stopped-Exchange Spectrum of Tri(p-tolyl)zincate

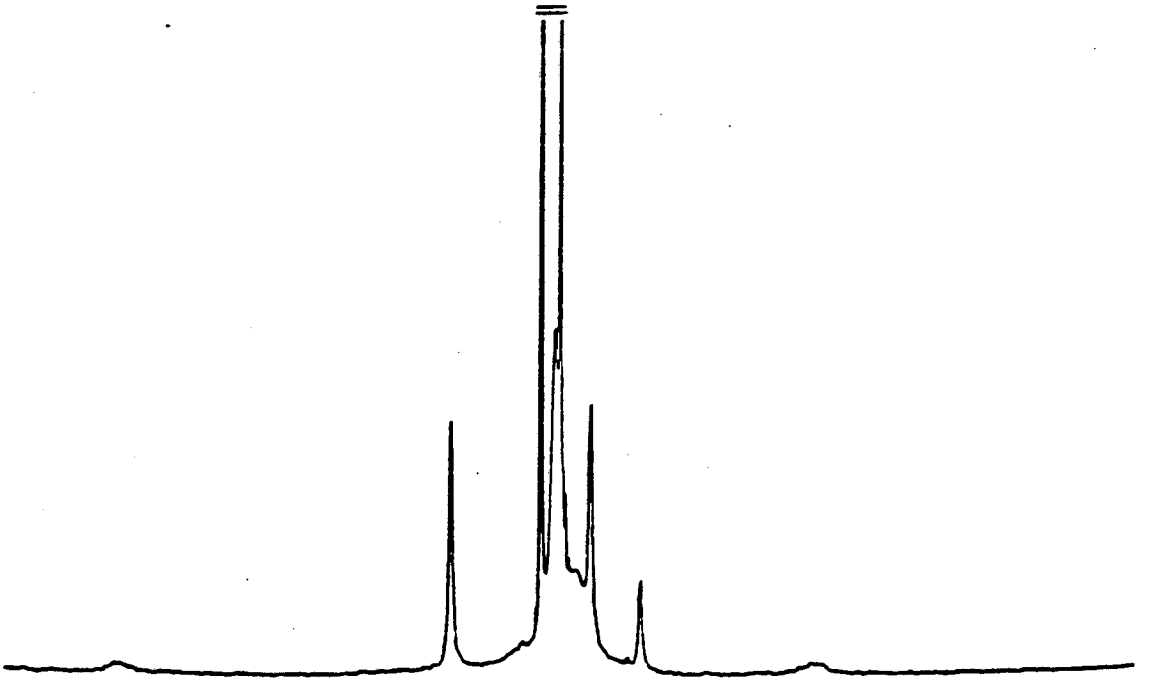

the baseline), and all of the aryl rings appear to be likewise inequivalent, indicating that the low temperature solution structure has far less symmetry than the methylzincate.

The solid state structure of the phenylzincate has been determined by X-ray crystallography in an effort to discover the distortion that could account for such a low symmetry spectrum. An ORTEP diagram of the molecule appears in Figure (7), and bond distances and angles are given in Tables X and XI, respectively.

The solid state structure does show lower symmetry than the analogous methyl complex. The complex consists of a trivalent $(Me_5C_5)_2Yb$ fragment connected by two bridging phenyl groups to a ZnPh moiety, but the bridges are markedly asymmetric, so that the complex more nearly resembles an adduct of $(Me_5C_5)_2YbPh$ and $ZnPh_2$ (see Figure 8). There is also a pronounced bending of the molecule; the dihedral angle between the planes formed fron Yb-C21-C31 and Zn-C21-C31 is 59.3(1)°.

The bridging phenyl groups bend far away from the$(Me_5C_5)_2Yb$ unit. The angles formed with the Yb-C21-C31 plane for C21-C26 and C31-C36 are 36.3(2)° and 47.2(2)°, respectively. In most compounds of electrophilic metals containing bridging phenyl groups, the plane of the phenyl ring is perpendicular to the M-M vector[29]. This is proposed to occur to allow not only overlap between the filled phenyl sp^2 σ-orbital and the bonding combination of the respective metal orbitals, but also overlap between the filled orthogonal p-orbital on the phenyl ring and the anti-bonding combination of the metal orbitals[30]. The bending away of the phenyl groups in this compound is undoubtedly due to severe

Figure (7) ORTEP Diagram of $(Me_5C_5)_2Yb(\mu\text{-}Ph)_2ZnPh$

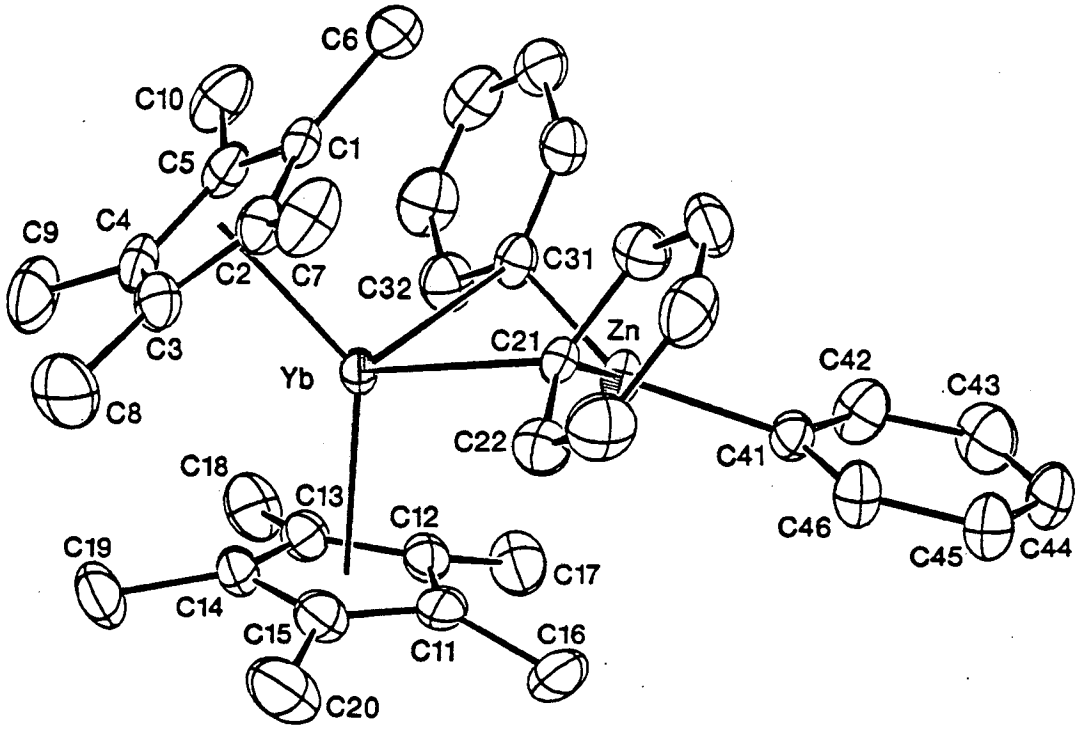

Figure (8) Asymmetric Bridging Phenyl Groups

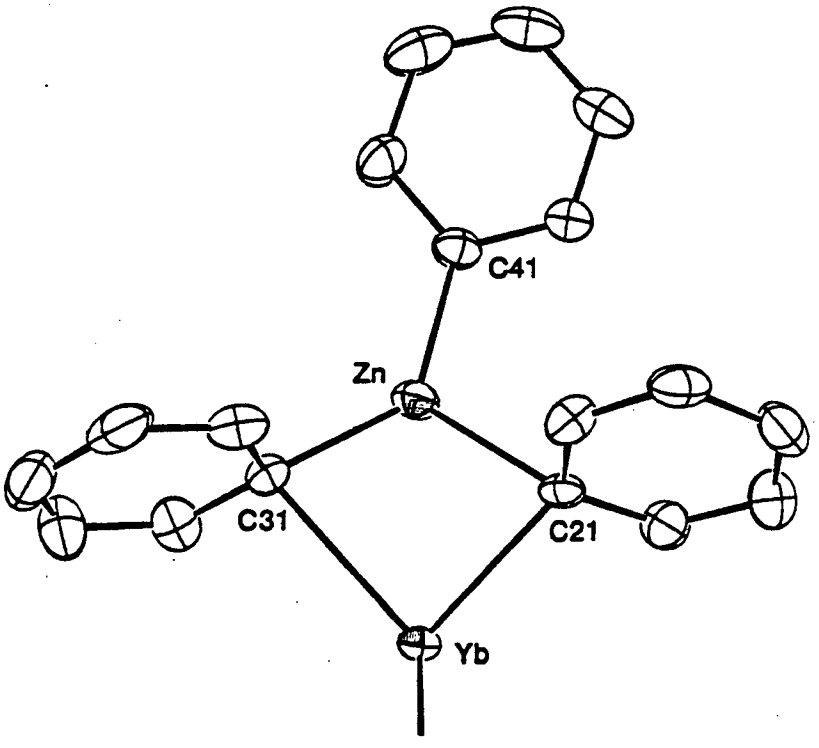

Table X Bond Distances for $(Me_5C_5)_2Yb(\mu\text{-}Ph)_2ZnPh$ (Å)

Yb-C21	2.536(4)	Yb-C1	2.623(4)	C21-C22	1.384(5)
Yb-C31	2.723(4)	Yb-C2	2.623(4)	C21-C26	1.414(5)
		Yb-C3	2.619(4)	C22-C23	1.383(5)
Zn-C21	2.173(3)	Yb-C4	2.627(4)	C23-C24	1.378(6)
Zn-C31	2.065(4)	Yb-C5	2.620(4)	C24-C25	1.370(5)
Zn-C41	1.963(4)	Yb-C11	2.730(4)	C25-C26	1.376(5)
		Yb-C12	2.712(4)		
C41-C42	1.391(5)	Yb-C13	2.649(4)	C31-C32	1.393(5)
C41-C46	1.389(5)	Yb-C14	2.632(4)	C31-C36	1.401(5)
C42-C43	1.402(6)	Yb-C15	2.675(4)	C32-C33	1.400(6)
C43-C44	1.341(7)			C33-C34	1.356(7)
C44-C45	1.368(6)	Yb-Cp1	2.333	C34-C35	1.374(6)
C45-C46	1.392(6)	Yb-Cp2	2.395	C35-C36	1.385(5)

Cp1 and Cp2 are the centroids of the rings comprised of C1-C5 and C11-C15, respectively.

Table XI Intramolecular Angles for $(Me_5C_5)_2Yb(\mu\text{-}Ph)_2ZnPh$ (°)

Yb-C21-Zn	75.0(1)	C21-Zn-C41	111.7(1)
Yb-C31-Zn	72.5(1)	C31-Zn-C41	134.9(2)
C21-Yb-C31	80.1(1)		
C21-Zn-C31	106.1(1)	C22-C21-C26	114.0(3)
		C21-C22-C23	123.3(4)
C21-Yb-Cp1	105.5	C22-C23-C24	120.1(4)
C21-Yb-Cp2	106.2	C23-C24-C25	119.3(4)
C31-Yb-Cp1	108.8	C24-C25-C26	119.6(4)
C31-Yb-Cp2	105.9	C21-C26-C25	123.6(3)
Cp1-Yb-Cp2	136.1		
		C32-C31-C36	114.2(4)
C42-C41-C46	115.4(4)	C31-C32-C33	122.7(4)
C41-C42-C43	121.3(4)	C32-C33-C34	120.8(4)
C42-C43-C44	121.1(4)	C33-C34-C35	118.8(4)
C43-C44-C45	119.8(4)	C34-C35-C36	120.2(4)
C44-C45-C46	119.3(4)	C31-C36-C35	123.3(4)
C41-C46-C45	123.0(4)		

steric repulsions with the C_5Me_5 rings. Several close contacts encourage the tilting of the Ph rings: C6··C26 = 3.471(6) Å, C6··C36 = 3.422(6) Å, C11··C22 = 3.462(6) Å, C12··C32 = 3.390(6) Å, C16··C22 = 3.379 Å, C17··C32 = 3.362(6) Å. The tilting of the rings is eventually stopped by other close contacts: C7··C22 = 3.282(6) Å, C10··C33 =

3.503(6) Å.

The effect of the steric repulsions can be seen in the $(Me_5C_5)_2Yb$ unit as well. The average Yb-C(ring) distance is longer for the ring comprised of C11-C15 (2.680(4) Å for Cp2 vs. 2.622(4) Å for Cp1), and longer than would normally be expected for an Yb(III) complex in eight-coordination. The centroid-Yb-centroid angle is compressed by the steric repulsions in the ligand sphere. Although the rings are staggered (torsion angle of 31.8(3)°), this brings the methyl groups on the back sides of the rings into close proximity (C9··C19 = 3.384(7) Å). The result of all of these close contacts is that the methyl groups on the rings are bent back by an average of 0.230(5) Å in Cp1, and 0.314(5) Å in Cp2.

When the phenyl rings bend away from Yb, the ZnPh moiety appears to move so as to maintain maximum overlap with the orthogonal p-orbitals on the rings; the angles formed by the intersection of the Zn-C21-C31 plane with the planes of the phenyl rings are 84.4(1)° for C21-C26 and 76.2(1)° for C31-C36. The rings themselves exhibit an axial distortion away from hexagonal symmetry. This effect has been noted by others[29,31], but may simply be attributable to crystal packing forces.

The reason for the asymmetric bridge is likewise unknown. The difference in the Yb-C(bridge) bond lengths (2.536(4) Å vs. 2.723(4) Å) nears the proposed distance between a electron pair bond and a dative bond. Likewise, the shorter of the two Zn-C(bridge) bonds, 2.065(4) Å, is closer to the terminal Zn-C bond length (1.963(4) Å) than to the other Zn-C(bridge) distance (2.173(3) Å). The terminal phenyl ring lies substantially off the Yb-Zn axis, reflecting the fact that the Zn is

"halfway between" a coordination number of two and three (C31-Zn-C41 = 134.9(2)°). It is possible that the complex forms an unsymmetric bridge structure because the steric repulsions are not as severe for bringing one phenyl ring close to the Yb ion and moving one farther away as they are in the case where both rings are at an intermediate distance. While it is far from certain that this is the structure at low temperature in solution, the low symmetry is not inconsistent with the NMR spectrum at the stopped-exchange limit.

Attempts have been made to cleave the phenylzincate complex in a manner to the methyl analog, to produce complexes of the type $(Me_5C_5)_2YbPh(L)$. The compound can be recovered intact from diethyl ether, but dissolution in thf gives a red solution. Removal of the solvent and extraction with hexane yields a red solution, from which a small amount of $(Me_5C_5)_2YbPh(thf)$ can be crystallized. Unfortunatly, the hexane extraction does not efficiently remove displaced $ZnPh_2$, and the product is inevitably contaminated with zincate.

The reaction of $(Me_5C_5)_2Yb$ with diarylzinc compounds takes an entirely different course in saturated hydrocarbon solvents. Reaction of $ZnPh_2$ with the ytterbium complex in hexane results in the rapid precipitation of an insoluble black powder, with no formation of zinc metal. Both the phenyl and the p-tolyl products are extremely insoluble in hydrocarbon solvents, and do not react further in toluene with excess $ZnAr_2$ to give the zincate species. The IR spectra reveal that the Yb is probably still divalent (judging from the low energy bands presumed to involve Yb-ring stretching modes), and that aryl groups are present. The ^{1}HNMR spectra of samples hydrolyzed with H_2O show benzene (or

toluene) and C_5Me_5H in an approximate 3:1 area ratio, suggesting that the compounds may arise from a ligand-swapping reaction between $(Me_5C_5)_2Yb$ and $ZnAr_2$, and may have the empirical formula $[(Me_5C_5)YbAr][ZnAr_2]$. No crystals of sufficient quality for X-ray analysis have been obtained.

A verified case of ligand exchange between Yb and Zn can be found in the reaction of $(Me_5C_5)_2Yb$ with $(H_5C_5)ZnMe$. Reaction of these two compounds in hexane rapidly produces a light green powder which is insoluble in hydrocarbon solvents. The IR spectrum of the powder and the ^{1}HNMR spectrum of the hydrolysate show that it contains both C_5H_5 and C_5Me_5 groups (this product will be discussed further in a later section). Removal of the solvent from the filtrate yields a light-colored residue from which colorless crystals can be sublimed. This compound is identified by IR and NMR spectra and from analytical data as $(Me_5C_5)ZnMe$, clearly showing that C_5H_5/C_5Me_5 ring exchange has occured.

Although trialkylzincate complexes have been previously reported, there have been no reports in the literature of trialkyl- or arylmercurates. The reason for this is likely due to the high barrier to rehybridization of the mercury. Electron transfer reaction should therfore not yield mercurates, but base-free alkyl species. Unfortunately, $(Me_5C_5)_2Yb$ does not react with $HgPh_2$, despite the relative ease of reduction of Hg^{2+} (E^o = +0.85 V in aqueous solution, compared to -0.76 V for Zn^{2+})[32], and the weakness of Hg-C bonds when compared to Zn-C bonds[33]. The reason probably again lies in the high reorganization energy required to bring the phenyl group into a bridging position between the metal atoms.

One way to circumvent this difficulty would be to use a mercury reagent with a potentially reducible alkyl or aryl group, such as a fluoroaryl compound. The reaction of $(Me_5C_5)_2Yb$ with $Hg(C_6F_5)_2$ in pentane gives a purple solution and mercury metal, indicating that electron transfer has taken place. Cooling the solution to -78°C produces purple crystalline solid, which can be identified by IR, ^1H and ^{19}FNMR spectroscopy, as well as analytical data, as the base-free aryl species $(Me_5C_5)_2Yb(C_6F_5)$. There is no evidence of mercurate formation. The complex shows a molecular ion in the mass spectrum, and is readily soluble in hydrocarbon solvents. The paramagnetic species can be observed directly by ^{19}FNMR spectroscopy. Three signals are observed at δ 47.0 ($\nu_{1/2}$ = 1400 Hz, 2F, ortho F), δ 1.79 ($\nu_{1/2}$ = 29 Hz, 1F, para F), and δ -7.30 ($\nu_{1/2}$ = 73 Hz, 2F, meta F).

Diethylmercury is similarly reduced by divalent Yb; the reaction in pentane precipitates mercury metal within hours. The solution remains orange, however, and only $(Me_5C_5)_2Yb$ is recovered. Evidently, a base-free ethyl complex is produced, which readily undergoes β-H elimination to give ethylene and $(Me_5C_5)_2YbH$. This can then return to the divalent oxidation state by eliminating H_2, as described in Chapter Two.

Inclusion Compounds

It might be proposed that any molecule that possesses a permanent dipole moment could conceivably coordinate to ytterbium. The olefin, acetylene, and alkyl compounds previously described, however, are all sterically relatively undemanding. If a molecule is too large to "fit" in the space between the bulky C_5Me_5 rings, a weak coordination compound

would not be expected to form. In order to explore this question, the reactions have been conducted between $(Me_5C_5)_2Yb$ and bulky polar molecules, dicarbadodecaboranes (these will be referred to simply as carboranes in this discussion).

The dipole moment of ortho-carborane (4.31D[34]) is comparable to that of the phosphine-borane adducts, and is proposed to be directed so that the carbon atoms lie at the positive end of the dipole. This assignment is supported by the lower dipole moment of meta-carborane, 2.78D. The reaction of $o\text{-}H_2C_2B_{10}H_{10}$ with $(Me_5C_5)_2Yb$ in hexane produces an immediate precipitation of green solid. This solid can be recrystallized from hot toluene to give dark green needles in good yield. The analogous complexes with meta-carborane and 1,2-dimethyl-ortho-carborane are somewhat more soluble, but can be crystallized from hexane at -25°C. Analytical data reveal that the complexes all have a carborane to Yb ratio of 1:1, and the NMR spectra reveal no solution perturbation of the ligand chemical shifts.

The IR spectra do show some notable differences, however. In the spectra of the carboranes, individual stretching frequencies can be discerned which correspond to νC-H and νB-H modes. In the spectra of the complexes, the bands corresponding to C-H stretching modes are lowered substantially, while the B-H bands remain unperturbed (Table XII). This would suggest that the ytterbium is interacting with the hydrogen atoms at the positive end of the molecular dipole.

Another interesting phenomenon is the observed thermochroism of the meta-carborane and 1,2-dimethyl-ortho-carborane complexes. Both are green when isolated at low temperature. When the $o\text{-}Me_2C_2B_{10}H_{10}$ complex

Table XII IR Spectra of Carborane Complexes

Complex	ν C-H (cm^{-1})	ν B-H (cm^{-1})
$o\text{-}H_2C_2B_{10}H_{10}$	3070vs	2604vs, 2578vs
$[Yb][o\text{-}H_2C_2B_{10}H_{10}]$	3074m, 3010vs	2610vs, 2575vs, 2563s
$m\text{-}H_2C_2B_{10}H_{10}$	3064s	2603vs
$[Yb][m\text{-}H_2C_2B_{10}H_{10}]$	3066w, 3024vs	2601vs
$o\text{-}Me_2C_2B_{10}H_{10}$	-	2586vs
$[Yb][o\text{-}Me_2C_2B_{10}H_{10}]$	-	2591vs

is allowed to warm, it is found to consist of two crystalline forms: one that remains green at all temperatures, and one that turns orange above ca. 5°C. The color change in the orange form is reversible. The $m\text{-}H_2C_2B_{10}H_{10}$ complex is green at room temperature, but reversibly turns orange above 95°C. The $o\text{-}H_2C_2B_{10}H_{10}$ compound remains green at all temperatures. The thermochroism of these compounds is reminiscent of the thermochroism of $(Me_5C_5)_2Yb$ itself, which reversibly turns dark orange above ca. 130°C.

In hopes of elucidating the nature of the metal-carborane interaction, as well as the structural source of the thermochroism, the structures of two of the compounds have been determined by X-ray crystallography: green $[(Me_5C_5)_2Yb][o\text{-}H_2C_2B_{10}H_{10}]$, and the orange form of $[(Me_5C_5)_2Yb][o\text{-}Me_2C_2B_{10}H_{10}]$. The results are startling, in that it is apparent that the two individual molecules in the asymmetric unit are entirely non-interacting. Packing diagrams of the two structures are presented in Figures (9) and (10). The labeling schemes for each structure are given in Figures (11) and (12).

The closest contact between Yb and any atom in the carborane unit in the ortho-carborane structure is a Yb···C distance of 5.762(6) Å, while in the 1,2-dimethyl-ortho-carborane structure there is a Yb···B

Figure (9) ORTEP Packing Diagram for $[(Me_5C_5)_2Yb][o\text{-}H_2C_2B_{10}H_{10}]$

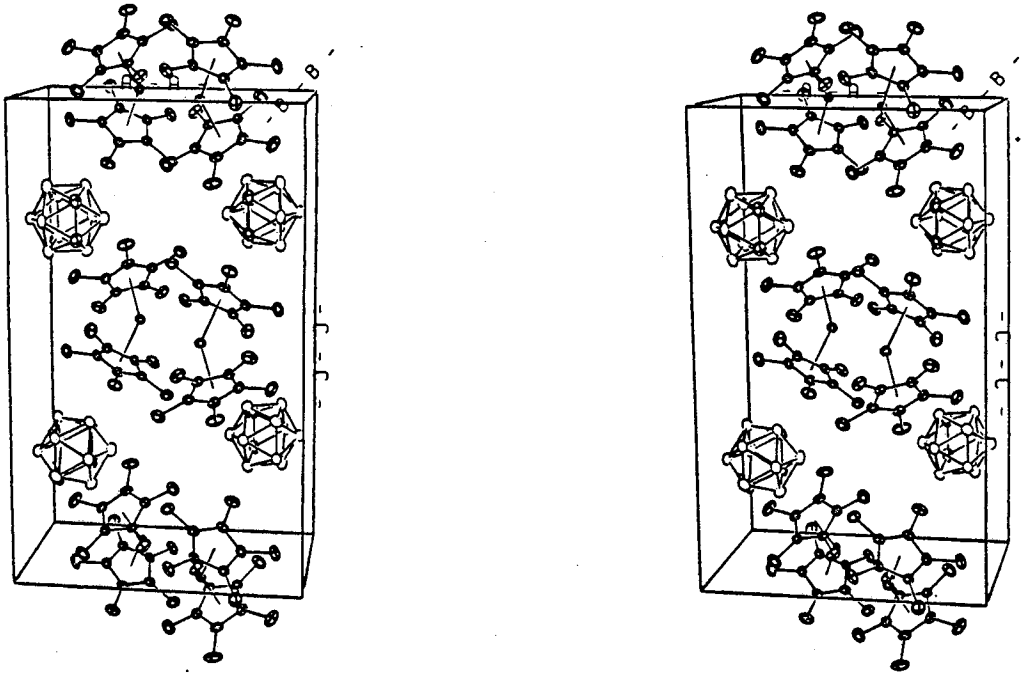

Figure (10) ORTEP Packing Diagram for $[(Me_5C_5)_2Yb][o\text{-}Me_2C_2B_{10}H_{10}]$

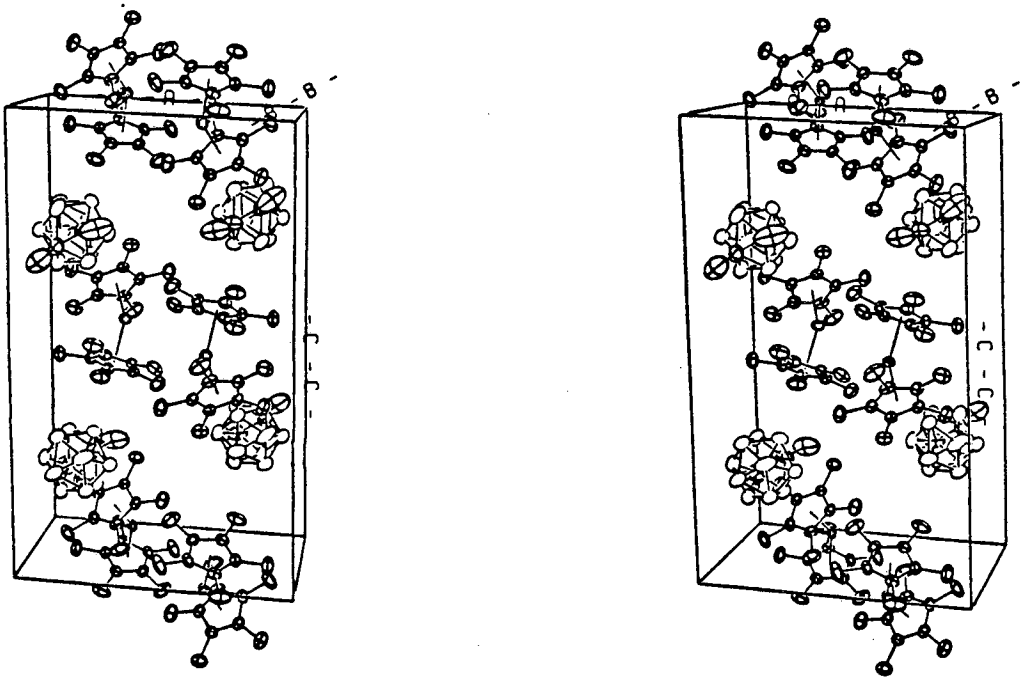

Figure (11) Atom Labeling Scheme for $[(Me_5C_5)_2Yb][o\text{-}H_2C_2B_{10}H_{10}]$

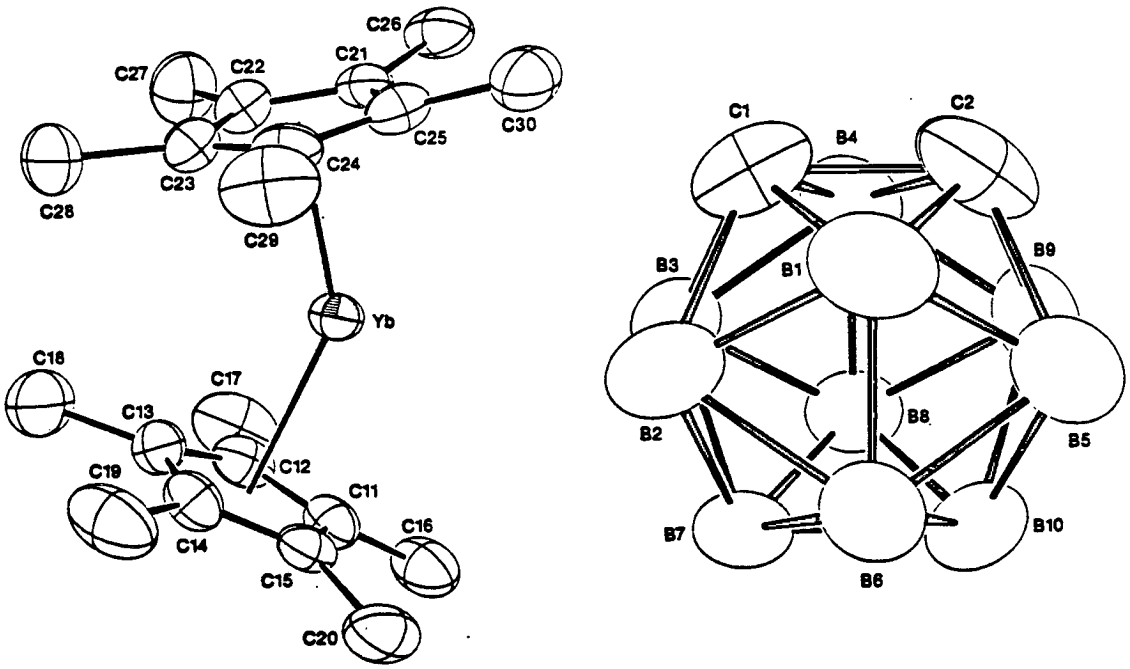

Figure (12) Atom Labeling Scheme for $[(Me_5C_5)_2Yb][o\text{-}Me_2C_2B_{10}H_{10}]$

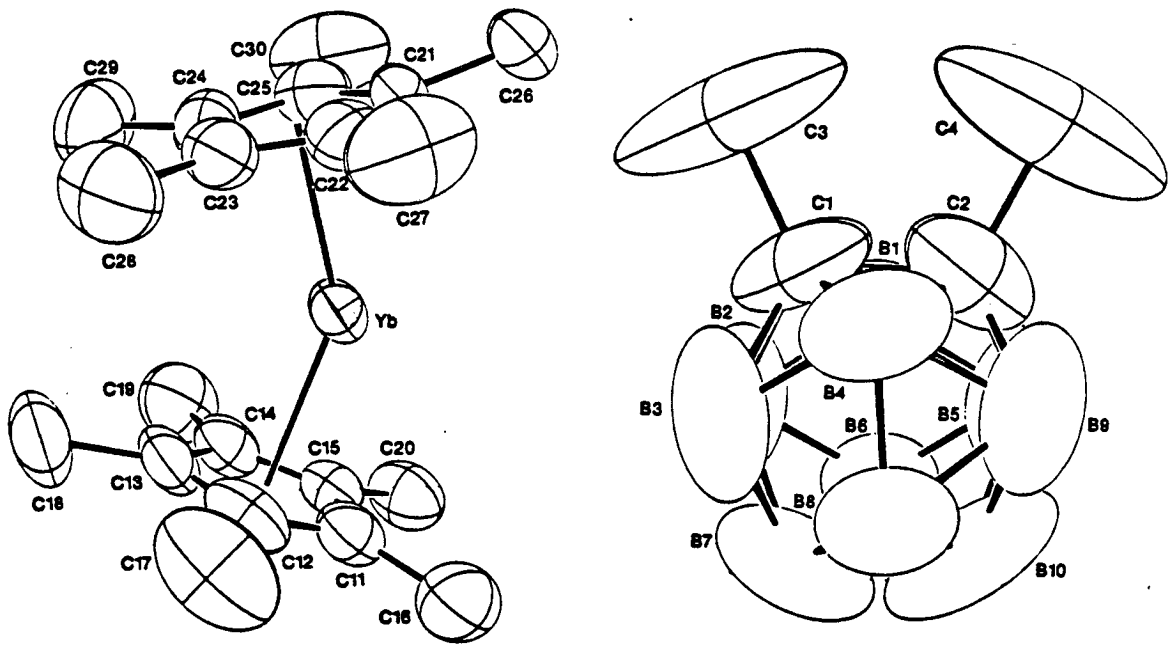

distance of 5.25(1) Å. These distances are far outside the range of any possible van der Waals contact. Even in complexes of the supposedly very weakly coordinating anion $B_{11}CH_{12}^-$, M··H-B interaction are observed which bring the B atoms to within ca. 2.5-3.0 Å of the metal[35]. The complexes reported here are best classed as inclusion or clathrate compounds.

Inclusion compounds are those species whose solid state structures possess vacant spaces, channels, or layers which are occupies by one or more non-interacting "guest" molecules, and whose characteristic properties (e.g. crystalline form) different from those of its components. The first clathrates prepared were complexes of quinol and hydrogen sulfide[36a] or sulfur dioxide[36b]. Since then, the class has grown to include a wide variety of host and guest molecules, and the definition has even expanded outside the realm of solid state structures to include "liquid clathrates"[37].

Many inclusion compounds have guest molecules effectively encapsulated in a hydrogen-bonded cage, such as the hydrate clathrates of inert gases and small molecules[38], but the channels in zeolites and the spaces between layers in intercalation compounds can serve equally well to trap guest molecules. There are also classes of compounds in which the guest molecule is merely held in place between individual molecules in the structure, without any evident polymeric nature to the lattice. The degree to which the trapped molecule is prevented from escaping varies, but some inclusion compounds can be reconstituted once the guest molecule has been removed.

The enthalpy of clathration is often likened to the enthalpy of

monolayer adsorption. This quantity is often of interest, because it can be related directly to the strength of the guest-host interaction, assuming that guest-guest interactions are negligible. Clathration enthalpies have been measured for certain types of inclusion compounds; the values in general lie between -20 and -30 kJ/mol[39], although values as high as -70 kJ/mol have been observed for some clathrate hydrates. The negative enthalpies are sufficient to overcome the unfavorable entropy contribution. There have been no reported examples of inclusion compounds of carboranes, but reports are beginning to appear indicating the successful clathration of metallocenes[40].

In both complexes, the $(Me_5C_5)_2Yb$ unit has an average Yb-C bond length and a centroid-Yb-centroid angle which are reasonble for divalent ytterbium (the corresponding values in the structure of polymeric $(Me_5C_5)_2Yb$ are 2.665(3) Å and 145.4°). The 1,2-dimethyl-ortho-carborane

Table XIII Geometry of $(Me_5C_5)_2Yb$ Units

Lengths (Å)	$[(Me_5C_5)_2Yb][o\text{-}H_2C_2B_{10}H_{10}]$	$[(Me_5C_5)_2Yb][o\text{-}Me_2C_2B_{10}H_{10}]$
Yb-C11	2.683(5)	2.637(5)
Yb-C12	2.657(5)	2.641(4)
Yb-C13	2.647(5)	2.651(4)
Yb-C14	2.667(5)	2.623(4)
Yb-C15	2.675(5)	2.621(4)
Yb-C21	2.681(4)	2.650(4)
Yb-C22	2.675(5)	2.632(4)
Yb-C23	2.661(4)	2.628(5)
Yb-C24	2.663(5)	2.619(5)
Yb-C25	2.685(4)	2.630(4)
Yb-C(avg)	2.669(5)	2.633(4)
Yb-Cp1	2.382	2.350
Yb-Cp2	2.387	2.352
Cp1-Yb-Cp2	142.9°	146.8°

Cp1 and Cp2 are the centroids of the rings comprised of C11-C15 and C21-C25, respectively.

structure shows slightly shorter Yb-C bond lengths and a larger Cp-Yb-Cp angle; this will be discussed later in the context of the intermolecular interactions.

The carborane units also resemble the reported structures of their halogen-substituted analogs[41] (Table XIV). A common problem in the structural determination of carboranes is disorder between carbon and

Table XIV Bond Lengths for Carboranes (Å)

	o-$H_2C_2B_{10}H_{10}$	o-$H_2C_2B_{10}H_8Br_2$ [a]	o-$Me_2C_2B_{10}H_{10}$	o-$Me_2C_2B_{10}H_6Br_4$ [b]
C1-C2	1.67(1)	1.63(3)	1.57(1)	1.65(3)
C1-C3	-	-	1.57(1)	1.48(4)
C2-C4	-	-	1.57(1)	1.54(3)
C1-B1	1.69(1)	1.74(3)	1.65(1)	1.73(3)
C1-B2	1.69(1)	1.70(3)	1.73(2)	1.73(4)
C1-B3	1.69(1)	1.73(3)	1.70(2)	1.75(4)
C1-B4	1.69(1)	1.66(4)	1.67(1)	1.77(4)
C2-B1	1.72(1)	1.75(3)	1.67(1)	1.67(4)
C2-B4	1.71(1)	1.70(3)	1.77(1)	1.75(3)
C2-B5	1.69(1)	1.72(3)	1.58(2)	1.70(4)
C2-B9	1.67(1)	1.76(3)	1.59(1)	1.65(5)
B1-B2	1.72(1)	1.68(3)	1.69(1)	1.83(3)
B1-B5	1.71(1)	1.82(3)	1.71(1)	1.75(4)
B1-B6	1.69(1)	1.71(3)	1.71(1)	1.73(4)
B2-B3	1.79(1)	1.80(3)	1.73(1)	1.79(4)
B2-B6	1.76(1)	1.74(3)	1.71(1)	1.79(4)
B2-B7	1.77(1)	1.79(3)	1.79(2)	1.78(4)
B3-B4	1.75(1)	1.73(4)	1.71(1)	1.73(4)
B3-B7	1.76(1)	1.69(3)	1.80(2)	1.76(4)
B3-B8	1.77(1)	1.78(3)	1.81(1)	1.82(5)
B4-B8	1.75(1)	1.75(3)	1.68(1)	1.81(4)
B4-B9	1.76(1)	1.79(3)	1.68(1)	1.81(5)
B5-B6	1.72(1)	1.75(3)	1.68(1)	1.71(4)
B5-B9	1.78(1)	1.80(3)	1.77(1)	1.77(4)
B5-B10	1.74(1)	1.79(2)	1.73(2)	1.77(4)
B6-B7	1.76(1)	1.77(3)	1.75(1)	1.85(4)
B6-B10	1.75(1)	1.75(3)	1.73(1)	1.79(4)
B7-B8	1.79(1)	1.81(3)	1.76(1)	1.74(4)
B7-B10	1.76(1)	1.73(3)	1.64(2)	1.78(4)
B8-B9	1.76(1)	1.69(3)	1.67(1)	1.84(4)
B8-B10	1.76(1)	1.78(3)	1.73(1)	1.76(4)
B9-B10	1.77(1)	1.75(3)	1.85(4)	1.73(4)

[a] Ref. 41a. [b] Ref. 41b.

boron sites. Some indication of disorder in a structure can be given by examining the average bond length about a certain position in the cage, as well as the distance to the atom *para* to the position in the cage (see Table XV). Assuming bonding radii for B and C of 0.88 Å and 0.82 Å[38a], the expected bond distances are 1.76 Å for B-B, 1.70 Å for B-C, and 1.64 Å for C-C. Therefore, the expected average bond length about a C in a carborane is 1.69 Å. The averages about the B atoms should be 1.73 Å, 1.75 Å, and 1.76 Å depending on whether the B atom is adjacent to two, one, or no C atoms. Likewise, *para*-icosahedral distances can be calculated on the basis of an ideal carborane geometry. In the structure of 1,2-dimethyl-*ortho*-carborane, the random variations about the idealized bond lengths make it difficult to discern any pattern, but

Table XV Comparison of Carborane Sites

avg. bond length (Å)	*o*-$H_2C_2B_{10}H_{10}$	*o*-$Me_2C_2B_{10}H_{10}$	Idealized
C1	1.69(1)	1.66(1)	1.69
C2	1.69(1)	1.64(1)	1.69
B1	1.71(1)	1.68(1)	1.73
B2	1.75(1)	1.73(1)	1.75
B3	1.75(1)	1.75(1)	1.75
B4	1.73(1)	1.70(1)	1.73
B5	1.73(1)	1.69(1)	1.75
B6	1.74(1)	1.72(1)	1.76
B7	1.77(1)	1.75(2)	1.76
B8	1.77(1)	1.73(1)	1.76
B9	1.75(1)	1.69(1)	1.75
B10	1.76(1)	1.71(2)	1.76
para-distances (Å)			
C1-B10	3.20(1)	3.12(1)	3.23
C2-B7	3.24(1)	3.14(1)	3.23
B1-B8	3.31(1)	3.34(1)	3.34
B2-B9	3.37(1)	3.23(1)	3.34
B3-B5	3.34(1)	3.28(1)	3.34
B4-B6	3.33(1)	3.32(1)	3.34

it is clear that the average bond lengths about C1 and C2 are somewhat shorter than those around the proposed B sites, and the para-icosahedral distances for these atoms are much shorter that for the other sites. Considering also the observation that there is no significant residual electron density associated with B atoms suggesting alternate methyl group placements, the structure may be said to be fairly well ordered. The pattern in the ortho-carborane structure may be seen even more clearly. Evidently, the carboranes have a strong orientation preference when included into the lattice.

The two compounds are nearly isostructural, but an important difference can be detected when the intermolecular interactions of the $(Me_5C_5)_2Yb$ units are studied. In the structure of $[(Me_5C_5)_2Yb]$-$[H_2C_2B_{10}H_{10}]$, each ytterbium atom is within close contact distance of two methyl groups on different adjacent molecules (Yb··C26 = 3.076(5) Å, Yb··C20 = 3.284(5) Å), forming a coordination polymer. In the structure of $[(Me_5C_5)_2Yb][Me_2C_2B_{10}H_{10}]$, each ytterbium shows only one close contact with a molecule related by a crystallographic inversion center (Yb··C26 = 2.987(5) Å), forming coordination dimers. The intermolecular interactions are shown in Figures (13) and (14). This situation is very reminiscent of the difference between the two different morphologies of $(Me_5C_5)_2Yb$ discussed in Chapter One.

These intermolecular interactions are responsible for the small but significant differences in the structures of the individual $(Me_5C_5)_2Yb$ units. In the ortho-carborane structure, the Yb cation is in a higher effective coordination number, and this is reflected in the longer Yb-C distances and the smaller centroid-Yb-centroid angle.

Figure (13) Intermolecular Interactions in $[(Me_5C_5)_2Yb][o\text{-}H_2C_2B_{10}H_{10}]$

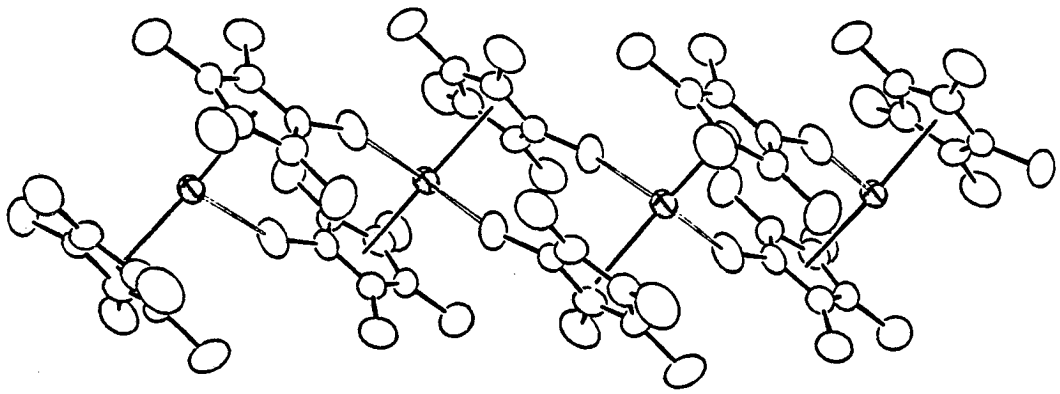

Figure (14) Intermolecular Interactions in $[(Me_5C_5)_2Yb][o\text{-}H_2C_2B_{10}H_{10}]$

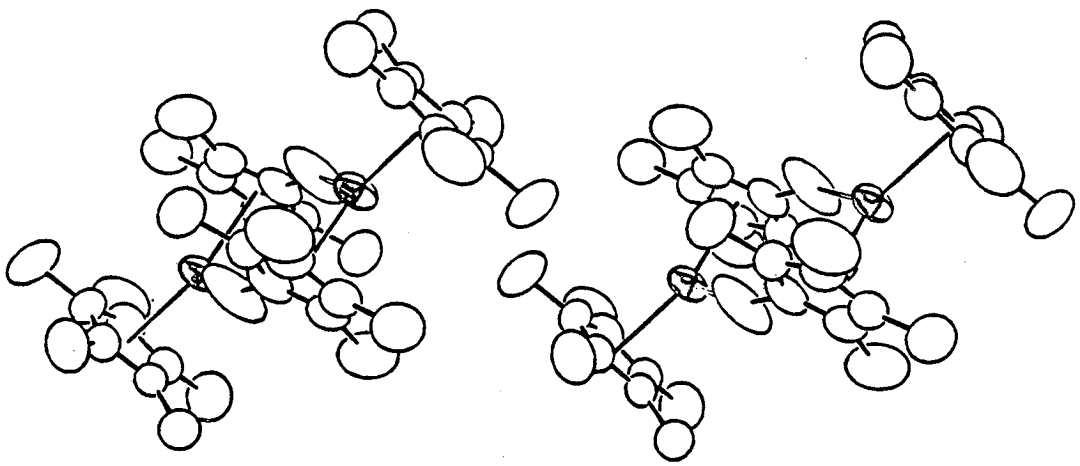

The difference in the orientation of the Yb units in the lattice also changes the unit cell constants slightly (see Table XVI). The coordination polymer chains in the structure of the ortho-carborane complex are parallel to the b axis, and breaking these chains up to form dimeric units lengthens the b axis. In an attempt to discern whether the thermochroism observed in the 1,2-dimethyl-ortho-carborane complex is due to a structural phase change, the unit cell constants of the complex were determined at -80°C, while it was in the green form

(although damage to the crystal induced in the phase change made data collection at this temperature impossible). These cell constants are also given in Table XVI. In the green form of the compound, the b axis suffers a slight compression. This suggests that the intermolecular interactions between Yb units begin to resemble those found in the ortho-carborane structure. This further implies that the phase change which induces thermochroism is related to the alteration in the inter-

Table XVI Unit Cell Constants

Complex	a (Å)	b (Å)	c (Å)	β (°)
$[(Me_5C_5)_2Yb][H_2C_2B_{10}H_{10}]$	12.780(1)	10.047(1)	21.175(3)	91.18(1)
$[(Me_5C_5)_2Yb][Me_2C_2B_{10}H_{10}]$ orange phase	13.061(1)	10.822(1)	21.814(2)	93.211(9)
$[(Me_5C_5)_2Yb][Me_2C_2B_{10}H_{10}]$ green phase	13.109(1)	10.655(2)	21.117(4)	93.04(1)

molecular interactions. Evidently, even these very weak intermolecular forces are capable of altering the ligand-to-metal charge transfer bands thought to be primarily responsible for the colors of f-metal organometallic compounds[42].

The utility of $(Me_5C_5)_2Yb$ as a clathrating agent explains the ready inclusion of solvents during crystallization. As mentioned in Chapter One, all aliphatic and aromatic hydrocarbon solvents used to crystallize the compound are occluded; the solvents are subsequently lost from the lattice under reduced pressure.

The perturbation of the νC-H bands in the IR spectra of these species cannot directly be explained, but similar perturbations in the IR spectra of guest molecules in other types of inclusion compounds[43]. In general, it is assumed that the perturbation is a reflection of the

host-guest interaction; the larger the perturbation, the greater the magnitude of this interaction. Another useful aspect of the host-guest interactions is the immobilization of the guest molecule for crystallographic study. In the carborane complexes, the ytterbium not only provides a heavy atom to facilitate structural solution, it also interacts with the dipole moment of the carborane, creating a preferred direction of orientation, minimizing disorder problems which often plague the crystallography of these molecules.

Metallocene Adducts

Another class of molecules which can suffer from disorder in the solid phase are transition metal metallocenes. Ferrocene was first believed to exist in a D_{5d} staggered conformation in the solid state, but it was later discovered by X-ray and neutron diffraction studies that the room temperature structure is an averaged one, comprised of a superposition of eclipsed molecules in different rotational orientations[44], giving rise to a statistical center of symmetry. The disorder is not entirely static, however. The increase in the vibrational amplitudes of the atoms with temperature suggests a component of librational motion of the ring about the C_5 axis in the disorder. Other first-row metallocenes show similar librational motion[45]. It may be possible to immobilize a metallocene in a lattice of $(Me_5C_5)_2Yb$, facilitating structural studies, provided that such an inclusion compound could be prepared.

The reaction of $(Me_5C_5)_2Yb$ with $(H_5C_5)_2Fe$ in toluene results in the isolation of orange-red crystals of the empirical formula $[(Me_5C_5)_2Yb]_2$-

$[(H_5C_5)_2Fe]$. The analogous brown cobalt complex can be prepared from cobaltocene, provided that the product is isolated within 24 h. Both the IR and ^{1}HNMR spectra of these species appear to be superpositions of the spectra of the respective starting materials. In order to determine the reason for the 2:1 stoichiometry of the complexes, the structure of the cobalt compound has been determined at low temperature by X-ray crystallography. An ORTEP diagram of the adduct is presented in Figure (15), and bond distances and angles are given in Tables XVII and XVIII.

The complex is found not to be an inclusion compound, but rather a 2:1 coordination compound, with the two ytterbium cations coordinated by way of very long Yb-C distances to different rings of a single cobaltocene molecule. The molecule lies on a crystallographic inversion

Figure (15) ORTEP Diagram of $[(Me_5C_5)_2Yb]_2[(H_5C_5)_2Co]$

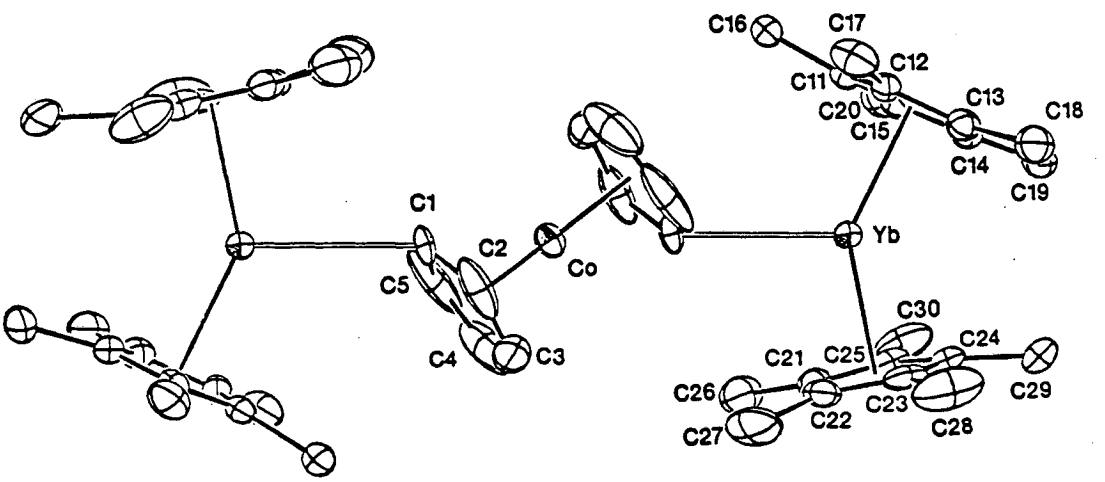

Table XVII Bond Distances for $[(Me_5C_5)_2Yb]_2[(H_5C_5)_2Co]$ (Å)

Yb··C1	2.907(5)	Co-C1	2.102(5)	Yb-C11	2.645(3)
Yb··C5	3.385(9)	Co-C2	2.039(4)	Yb-C12	2.641(4)
		Co-C3	2.096(5)	Yb-C13	2.636(4)
C1-C2	1.369(7)	Co-C4	2.075(5)	Yb-C14	2.657(4)
C2-C3	1.367(8)	Co-C5	2.062(5)	Yb-C15	2.645(4)
C3-C4	1.319(9)			Yb-C21	2.681(4)
C4-C5	1.393(9)	Co-Cp1	1.719	Yb-C22	2.716(4)
C5-C1	1.384(9)			Yb-C23	2.682(4)
		Yb-Cp2	2.354	Yb-C24	2.659(4)
		Yb-Cp3	2.394	Yb-C25	2.634(4)

Cp1, Cp2, and Cp3 are the centroids of the rings comprised of C1-C5, C11-C15, and C21-C25, respectively.

Table XVIII Intramolecular Angles for $[(Me_5C_5)_2Yb]_2[(H_5C_5)_2Co]$ (°)

Yb-C1-C2	126.1(4)	C2-C1-C5	106.8(5)
Yb-C1-Co	164.0(3)	C1-C2-C3	108.4(5)
		C2-C3-C4	108.8(5)
Cp1-Co-Cp1'	180.0	C3-C4-C5	107.5(5)
Cp2-Yb-Cp3	142.6	C1-C5-C4	106.7(5)

center, and so there is only one independent $(Me_5C_5)_2Yb$ unit, and one independent C_5H_5 ring.

The cobaltocene unit has a staggered configuration, as required by the crystallographic inversion center. The average Co-C bond length is 2.071(5) Å, compared to the values for free $(H_5C_5)_2Co$ of 2.096(8) Å in the solid state[46], and 2.119(3) Å in the gas phase[47]. The structure of the free metallocene was found to be staggered in the solid state; gas phase measurements cannot conclusively distinguish between the D_{5d} and D_{5h} conformations. It has been suggested that the barrier to internal rotation of the Cp rings is low enough to permit large-amplitude torsional motion, and that the gas phase structure may be best approximated by assuming free rotation of the cyclopentadienyl groups[47b]. This torsional motion is evidently not completely supressed by coordination to ytterbium; the carbon atoms in the ring are quite

anisotropic, with maximum r.m.s. amplitudes of thermal vibration as high as 0.443 Å.

Although there are significant differences in the C-C bond lengths within the cyclopentadienyl ring, there seems to be no pattern identifiable as a static Jahn-Teller distortion. In the gas phase structural studies of cobaltocene, it is suggested that the Jahn-Teller distortion in the molecule may in fact be dynamic[47a]. There are deviations in the planarity of the ring, however. The maximum displacement from the least-squares plane through C1-C5 is 0.034(6) Å.

The $(Me_5C_5)_2Yb$ unit in the structure has an average Yb-C(ring) bond length of 2.660(4) Å, identical within statistical errors to the value of 2.669(5) Å in the complex of ortho-carborane, but somewhat longer than the value of 2.633(4) Å determined from the structure of the 1,2-dimethyl-ortho-carborane inclusion compound. The centroid-Yb-centroid angle, 142.6°, again resembles that in the coordination polymer form of $(Me_5C_5)_2Yb$ (142.9°), rather than that in the coordination dimer (146.8°). This suggests that the coordination of the metallocene may involve more than one sterically significant Yb··C interaction. The pentamethylcyclopentadienyl rings are staggered (the torsion angle is 24.3(5)°), and the methyl groups are bent out of the planes of the rings by an average of 0.120(6) Å away from the Yb atom.

The closest contacts between the Yb and any carbons on the cyclopentadienyl rings of the cobaltocene are Yb··C1 (2.907(5) Å), and Yb··C5 (3.385(9) Å). These distances are longer than the coordination distances of other weak unsaturated ligands (2.850(5) Å in the 2-butyne adduct of ytterbium), and yet are on the order of the intermolecular

interactions in the various solid-state forms of $(Me_5C_5)_2Yb$. All other Yb··C contacts are greater than 3.8 Å. It may be argued whether this constitutes an η^1- or an η^2-coordination mode.

There are many examples in the literature of cyclopentadienyl rings which are η^1- or η^2-coordinated to lanthanides or alkaline earths. The complex $Nd(MeC_5H_4)_3$ exists as a coordination tetramer in the solid state[48], in which each Nd is coordinated to 3 η^5-rings, and one η^1-ring. The average Nd-C (η^5) distance is 2.79(5) Å, and the intermolecular Nd-C distances range from 2.990(7) Å to 2.978(7) Å. The compound $La(C_5H_5)_3$, however, has a solid state structure in which each metal ion interacts with two carbons in a ring on an adjacent molecule[49]. The La-C intermolecular distances are 3.034(6) Å and 3.032(6) Å. The mixed-valence complex $(Me_5C_5)_2Sm(\mu\text{-}C_5H_5)Sm(C_5Me_5)_2$ is claimed to have an η^5/η^2-bridging cyclopentadienyl group, and yet the two Sm(II)-C (cyclopentadienyl) distances are very different (2.986(8) Å and 3.180(9) Å)[50]. In the solid state structure of $(H_5C_5)_2Ca$, each Ca is said to have a coordination sphere of two η^5-rings, one η^3-ring, and one η^1-ring, and yet the "non-coordinating" distances in the η^3-ring (2.951(2) Å and 2.943(2) Å), are shorter than the Ca-C distance for the proposed η^1-ring (3.100(2) Å)[51]. Clearly, there is no consensus on what constitutes a coordinating distance. This problem, taken with the confusion over the definition of η^1 vs. η^2, suggests that the designation of one label or the other is somewhat arbitrary. In the complex $[(Me_5C_5)_2Yb]_2[(H_5C_5)_2Co]$, the coordination mode is probably somewhere between the two extremes.

The magnetic susceptibility of the compound has been studied as a

function of temperature, in order to determine if coordination of ytterbium affects the magnetic behavior of cobaltocene. The plots of $1/\chi_M$ vs. T for cobaltocene and the ytterbium complex are shown in Figures (16) and (17), respectively. The two plots are virtually identical, indicating that the ligand field of the Co is not perturbed by the weakly coordinating $(Me_5C_5)_2Yb$ unit. The two compounds show Curie-Weiss behavior, with μ = 1.84 B.M. and θ = -8 K for $(H_5C_5)_2Co$, and μ = 1.94 with θ = -4 K for $[(Me_5C_5)_2Yb]_2[(H_5C_5)_2Co]$. These moments are very close to the spin-only value for one unpaired spin.

If cobaltocene and $(Me_5C_5)_2Yb$ are allowed to react for more than 24 h., an insoluble green precipitate begins to appear in the solution. As in the case of the $(H_5C_5)ZnMe$ reaction, this precipitate gives indication of both the substituted and unsubstituted rings in the IR spectrum. Evidently, ring exchange can occur between Co and Yb. This can be accounted for when one considers that Co(II) is a d^7-ion, with one electron in the formally metal-ring antibonding e_{1g} orbital. This makes the complex kinetically labile.

In order to study the products of the ring exchange more completely, the reaction has been carried out with an even more labile metallocene, $(H_5C_5)_2Mn$ (d^5, high spin). The reaction proceeds as expected, yielding an immediate precipitate of green powder. The complex $(Me_5C_5)_2Mn$ can be isolated from the supernatent solution. The green powder dissolves readily in thf, yielding a purple solution. Two products can be isolated from this material; they are separable based on their solubility in toluene. The compound $(H_5C_5)_2Yb(thf)_n$ is isolated as purple crystals from thf, but loses solvent under reduced pressure to

Figure (16) Plot of $1/\chi_M$ vs. T for $(H_5C_5)_2Co$

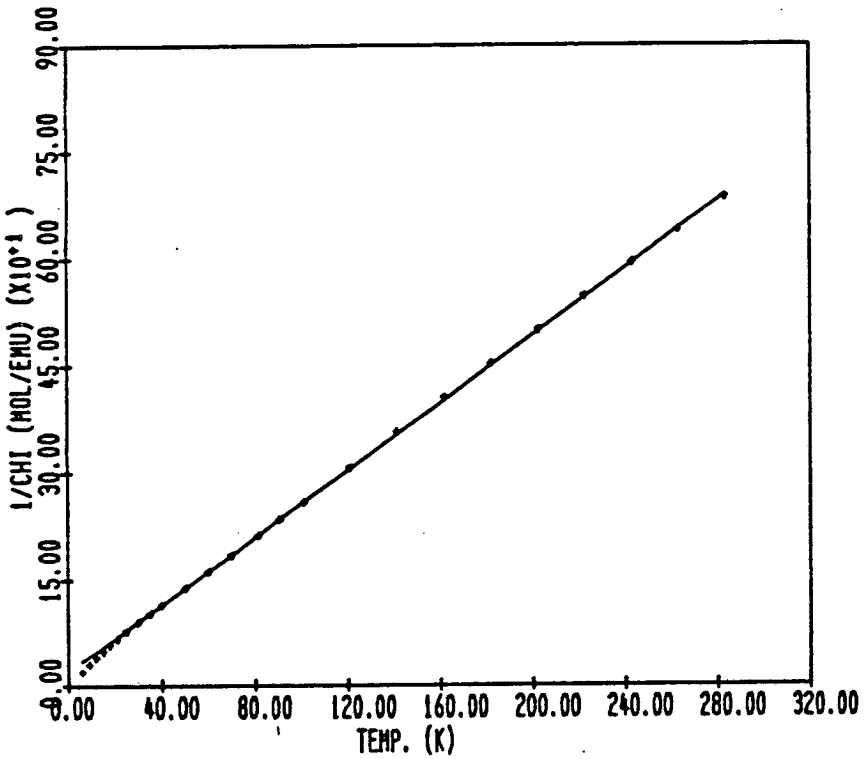

Figure (17) Plot of $1/\chi_M$ vs. T for $[(Me_5C_5)_2Yb]_2[(H_5C_5)_2Co]$

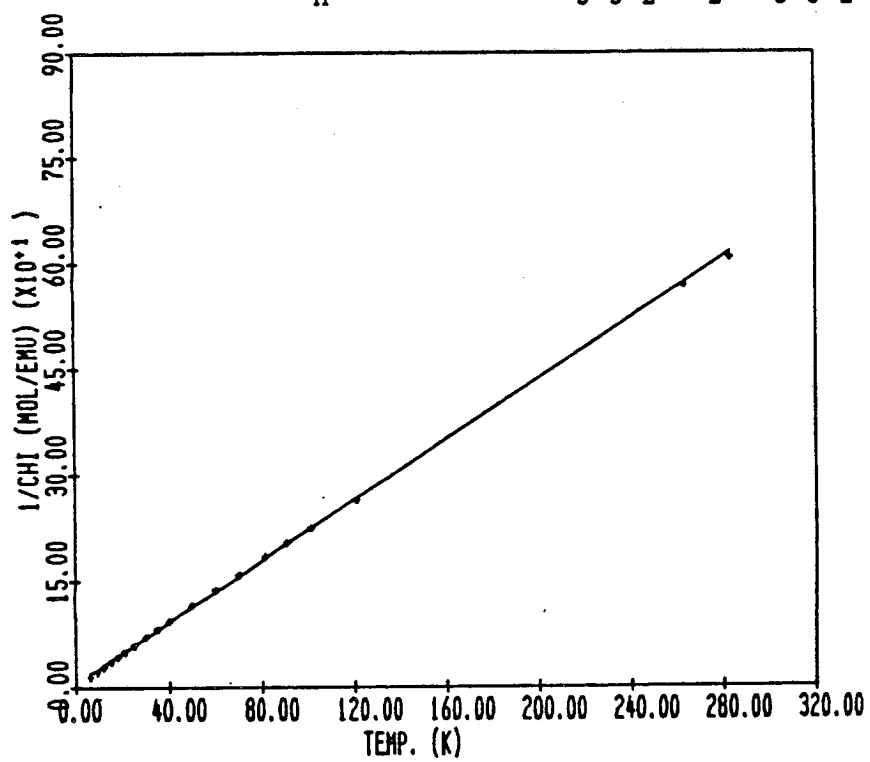

pressure, but they irreversibly turn green and crumble when heated in toluene or heated above 120°C. The red crystals are identified spectroscopically as $(Me_5C_5)(H_5C_5)Yb(thf)_2$. Due to the kinetic lability of ionic complexes of the lanthanides, few methods are available for the synthesis of such mixed-ring species. The yield of the mixed-ring species is ca. 50% of the total ytterbium-containing material isolated. Although this method may not provide a high yield of the mixed-ring compound, it can be readily separated from bis(cyclopentadienyl)-ytterbium, and so the procedure may prove to be of some synthetic utility.

In this Chapter, it has been demonstrated that ytterbium can coordinate to a diverse array of molecules. It would seem that a new definition must be constructed for basic ligands in the $(Me_5C_5)_2Yb$ system: any molecule is potentially a base towards ytterbium if it has a dipole moment, either permanent or induced. Whether or not the molecule then coordinates is determined primarily by steric factors. Even in cases where direct coordination is not possible, molecules may be included in the lattice of $(Me_5C_5)_2Yb$, and evidence can be discerned for host-guest interactions.

References

1.) a) Crabtree, R. H., Chem. Rev., 1985, 85, 245, and references therein. b) Halpern, J., Inorg. Chim. Acta, 1985, 100, 41.

2.) Brookhart, M.; Green, M. L. H., J. Organomet. Chem., 1983, 250, 395.

3.) a) Albright, T. A.; Burdett, J. K.; Whangbo, M. H., "Orbital Interactions in Chemistry", Wiley, New York, 1985. b) Saillard, J.-Y.; Hoffmann, R., J. Am. Chem. Soc., 1984, 106, 2006.

4.) Turner, J. J.; Burdett, J. K.; Perutz, R. N.; Poliakoff, M., Pure, Appl. Chem., 1977, 49, 271.

5.) a) Watson, P. L.; Parshall, G. W., Acc. Chem. Res., 1983, 18, 51. b) Thompson, M. E.; Baxter, S. M.; Bulls, A. R.; Burger, B. J.; Nolan, M. C.; Santarsiero, B. D.; Schaefer, W. P.; Bercaw, J. E., J. Am. Chem. Soc., 1987, 109, 203. c) Fendrick, C. M.; Marks, T. J., J. Am. Chem. Soc., 1984, 106, 2214. d) Bruno, J. W.; Duttera, M. R.; Fendrick, C. M.; Smith, G. M.; Marks, T. J., Inorg. Chim. Acta, 1984, 94, 271. e) Watson, P. L., J. Am. Chem. Soc., 1983, 103, 6491.

6.) DeKock, R. L.; Gray, H. B., "Chemical Structure and Bonding", Benjamin/Cummings Publishing Co., Menlo Park, 1980.

7.) a) Bjorseth, A.; Drew, D. A.; Marstokk, K. M.; Mollendal, H., J. Mol. Str., 1972, 13, 233. b) Drew, D. A.; Haaland, A., Acta Chem. Scand., 1972, 26, 3079.

8.) Holton, J.; Lappert, M. F.; Pearce, R.; Yarrow, P. I. W., Chem. Rev., 1983, 83, 135.

9.) Rhine, W. E.; Stucky, G. D.; Peterson, S. W., J. Am. Chem. Soc., 1975, 97, 6401.

10.) a) Waymouth, R. M.; Santarsiero, B. D.; Coots, R. J.; Bronikowski, M. J.; Grubbs, R. H., J. Am. Chem. Soc., 1986, 108, 1427. b) Kaminsky, W.; Kopf, J.; Sinn, H,; Vollmer, H. J., Angew. Chem. Int. Ed. Engl., 1976, 15, 629. c) Engelhardt, L. M.; Leung, W.; Raston, C. L.; Twiss, P.; White, A. H., J. Chem. Soc., Dalton Trans., 1984, 321. d) Atwood, J. L.; Fjeldberg, T.; Lappert, M. F.; Luong-Thi, N. T.; Shakir, R.; Thorne, A. J., J. Chem. Soc. Chem. Comm., 1984, 1163. e) Weiss, E.; Lucken, A. C., J. Organomet. Chem., 1964, 2, 197. f) Weiss, E.; Hencken, G., J. Organomet. Chem., 1970, 21, 265.

11.) a) Jemmis, E. D.; Chandrasekhar, J.; Schleyer, P. v. R., J. Am. Chem. Soc., 1979, 101, 527. b) Schleyer, P. v. R.; Tidor, B.; Jemmis, E. D.; Chandrasekhar, J.; Wurthwein, E. U.; Kos, A. J.; Luke, B. T.; Pople, J. A., J. Am. Chem. Soc., 1983, 105, 484.

12.) Shannon, R. D., Acta Cryst., 1976, 32A, 751.

13.) a) Anderson, G.; Forgaard, F. R.; Haaland, A., Acta Chem. Scand., 1972, 26, 1947. b) Turova, N. Ya.; Kozunov, V. A., J. Inorg. Nucl. Chem., 1979, 41, 5. c) McDonald, T. R. R.; McDonald, W. S., Acta Cryst., 1972, 28B, 1619. d) Dekker, J.; Boersma, J.; Fernholt, L.; Haaland, A.; Spek, A. L., Organometallics, 1987, 6, 1202.

14.) a) Tilley, T. D.; Andersen, R. A.; Spencer, B.; Ruben, H.; Zalkin, A.; Templeton, D. H., Inorg. Chem., 1980, 19, 2999. b) Tilley, T. D., Ph.D. Thesis, University of California, Berkeley, California, U.S.A., 1982.

15.) a) Calderazzo, F.; Pappalardo, R.; Losi, S., J. Inorg, Nucl. Chem., 1966, 28, 987. b) Fischer, E. O.; Fischer, H., Angew. Chem., 1964, 76, 52. c)Fischer, E. O.; Fischer, H., J. Organomet. Chem., 1966, 6, 141.

16.) Parshall, G. W., J. Am. Chem. Soc., 1964, 86, 361.

17.) a) Marks, T. J.; Kolb, J. R., J. Am. Chem. Soc., 1975, 97, 27. b) Jahn, W.; Yunlu, K.; Oroschin, W.; Amberger, H.-D.; Fischer, R. D., Inorg. Chim. Acta, 1984, 95, 85. c) Fischer, R. D.; Yunlu, K., Z. Naturforsch., 1983, 38b, 1368. d) Fischer, R. D. in "Fundamental and Technological Aspects of Organo-f-Element Chemistry", T. J. Marks, I. L. Fragala, eds., D. Reidel, Amsterdam, 1985.

18.) a) Frisch, M. A.; Heal, H. G.; Mackle, H.; Madden, I. O., J. Chem. Soc., 1965, 899. b) Becke-Goehring, M.; Thielemann, H., Z. Anorg. Allg. Chem., 1961, 308, 33.

19.) Becker, E. D., "High Resolution NMR", Academic Press, London, 1980.

20.) a) Bryan, P. S.; Kuczkowski, R. L., Inorg. Chem., 1972, 11, 553. b) Snow, S. A.; Shimoi, M.; Ostler, C. D.; Thompson, B. K.; Kodama, G.; Parry, R. W., Inorg. Chem., 1984, 5, 511. c) Vites, J.; Housecroft, C. E.; Eigenbrot, C.; Buhl, M. L.; Long, G. J. Fehlner, T. P., J. Am. Chem. Soc., 1986, 108, 3302.

21.) a) Hurd, D. T., J. Org. Chem., 1948, 13, 711. b) Wanklyn, J. A., Annalen, 1858, 108, 67; 1859, 111, 234; 1866, 140, 211. c) Nast, R.; Muller, R., Chem. Ber., 1958, 91, 2861. d) Wittig, G.; Meyer, F. J.; Lange, G., Annalen, 1951, 571, 167. e) Wittig, G.; Hornberger, P., Annalen, 1952, 577, 11.

22.) Boncella, J. M., Ph.D. Thesis, University of California, Berkeley, California, U.S.A., 1984.

23.) a) Rao, R. S.; Stoicheff, B. P.; Turner, R., Can. J. Phys., 1960, 38, 1516. b) Almenningen, A.; Helgaker, T. H.; Haaland, A.; Samdal, S., Acta Chem. Scand., 1982, 36A, 159.

24.) Holton, J.; Lappert, M. F.; Ballard, D. G. H.; Pearce, R.; Atwood, J. L.; Hunter, W. E., J. Chem. Soc., Dalton Trans., 1979, 54.

25.) Holton, J.; Lappert, M. F.; Ballard, D. G. H.; Pearce, R.; Atwood, J. L.; Hunter, W. E., J. Chem. Soc., Dalton, Trans., 1979, 45.

26.) Scollary, G. R., Aust. J. Chem., 1978, 31, 411.

27.) Almenningen, A.; Halvorsen, S.; Haaland, A., Acta Chem. Scand., 1971, 25, 1937.

28.) Watson, P. L.; Herskovitz, T., in "Initiation of Polymerization", F. E. Bailey, ed., ACS Symposium Series, 1983.

29.) a) Malone, J. F.; McDonald, W. S., J. Chem. Soc., Dalton Trans., 1972, 2646. b) Malone, J. F.; McDonald, W. S., J. Chem. Soc., Dalton Trans., 1972, 2649. c) Barber, M.; Liptak, D.; Oliver, J. P., Organometallics, 1982, 1, 1307.

30.) Mason, R.; Mingos, D. M. P., J. Organomet. Chem., 1973, 50, 53.

31.) Malone, J. F.; McDonald, W. S., J. Chem. Soc. (A), 1970, 3362.

32.) Johnson, D. A., "Some Thermodynamic Aspects of Inorganic Chemistry", 2nd ed., Cambridge University Press, Cambridge, 1982.

33.) Pilcher, G.; Skinner, H. A., in "The Chemistry of the Metal-Carbon Bond", F. R. Hartley and S. Patai, eds., John Wiley and Sons, New York, 1982.

34.) Beall, H., in "Boron Hydride Chemistry", E. L. Muetterties, ed., Academic Press, London, 1975.

35.) a) Shelly, K.; Finster, D. C.; Lee, Y. J.; Scheidt, W.R.; Reed, C. A., J. Am. Chem. Soc., 1985, 107, 5955. b) Shelly, K.; Reed, C. A.; Lee, Y. J.; Scheidt, W. R., J. Am. Chem. Soc., 1986, 108, 3117.

36.) a) Wohler, F., Justus Liebigs Ann. Chem., 1849, 69, 297. b) Clemm, A., Justus Liebigs Ann. Chem., 1859, 110, 357.

37.) Atwood, J. L., in "Inclusion Compounds", J. L. Atwood, J. E. D. Davies, D. D. MacNicol, eds., Academic Press, London, 1984.

38.) a) Pauling, L., "The Nature of the Chemical Bond", 3rd ed., Cornell University Press, Ithaca, 1960, p. 464. b) Jeffrey, G. A., in "Inclusion Compounds", J. L. Atwood, J. E. D. Davies, D. D. MacNicol, eds., Academic Press, London, 1984.

39.) Parsonage, N. G.; Stavelely, L. A. K., in "Inclusion Compounds", J. L. Atwood, J. E. D. Davies, D. D. MacNicol, eds., Academic Press, London, 1984.

40.) a) Miki, K.; Kasai, N.; Tsutsumi, H.; Miyata, M.; Takemoto, K., J. Chem. Soc. Chem. Comm., 1987, 545. b) Hough, E.; Nicholson, D. G., J. Chem. Soc., Dalton Trans., 1978, 15. c) Lecomte, J. P.; Lehn, J. M.; Parker, D.; Guilhem, J.; Pascard, C., J. Chem. Soc. Chem. Comm., 1983, 296. d) Harada, A.; Takahashi, S., J. Chem. Soc. Chem. Comm., 1984, 645. e) Alston, D. R.; Slawin, A. M. Z.; Stoddart, J. F.; Williams, D. J., Angew. Chem., 1985, 97, 771.

41.) a) Potenza, J. A.; Lipscomb, W. N., Inorg. Chem., 1966, 5, 1472. b) Potenza, J. A.; Lipscomb, W. N., Inorg. Chem., 1966, 5, 1483. c) Potenza, J. A.; Lipscomb, W. N., Inorg. Chem., 1966, 5, 1478. d) Potenza, J. A.; Lipscomb, W. N., Inorg. Chem., 1964, 3, 1673. e) Pawley, G. S., Acta Cryst., 1966, 20, 631. f) Kirillova, N. I.;

Antipin, M. Yu.; Gol'tyapin, Yu. V.; Struchkov, Yu. T.; Stanko, V. I., Izv. Akad. Nauk SSSR, Ser. Khim., 1978, 4, 859.

42.) Marks, T. J.; Ernst, R. D., in "Comprehensive Organometallic Chemistry", Vol. 3, G. Wilkinson, F. G. A. Stone, and E. W. Abel, eds., Chap. 21, Pergamon Press, Oxford, 1982.

43.) a) Cleaver, K. D.; and Davies, J. E. D., J. Mol. Struct., 1977, 36, 61. b) Akyuz, S.; Dempster, A. B.; Morehouse, R. L., Spectrochim. Acta, 1974, 30A, 1989. c) Davies, J. E. D., in "Inclusion Compounds", J. L. Atwood, J. E. D. Davies, D. D. MacNicol, eds., Academic Press, London, 1984.

44.) a) Seiler, P.; Dunitz, J. D., Acta Cryst., 1979, B35, 1068. b) Takusagawa, F.; Koetzle, T. F., Acta Cryst., 1979, B35, 1074. c) Seiler, P.; Dunitz, J. D., Acta Cryst., 1979, B35, 2020.

45.) Seiler, P.; Dunitz, J. D., Acta Cryst., 1980, B36, 2255.

46.) Bunder, W.; Weiss, E., J. Organomet. Chem., 1975, 92, 65.

47.) a) Almenningen, A.; Gard, E.; Haaland, A.; Brunvoll, J., J. Organomet. Chem., 1976, 107, 273. b) Hedber, A. K.; Hedberg, L.; Hedberg, K., J. Chem. Phys., 1975, 63, 1262.

48.) Burns, J. H.; Baldwin, W. H.; Fink, F. H., Inorg. Chem., 1974, 13, 1916.

49.) Eggers, S.; Kopf, J.; Fischer, R. D., Organometallics, 1986, 5, 383.

50.) Evans, W. J.; Ulibarri, T. A., J. Am. Chem. Soc., 1987, 109, 4292.

51.) Zerger, R.; Stucky, G., J. Organomet. Chem., 1974, 80, 7.

Experimental Section

General

All of the compounds synthesized were oxygen and water sensitive. All operations were carried out under nitrogen utilizing standard Schlenk techniques or in a Vacuum Atmospheres inert atmosphere dry box. All reactions requiring elevated pressures were carried out in Fischer-Porter thick-walled glass pressure bottles. Hydrocarbon and ethereal solvents were distilled under nitrogen from sodium benzophenone ketyl prior to use. Dichloromethane was distilled from calcium hydride. Acetonitrile was distilled from P_2O_5, and and stored over 3Å molecular sieves. Triethylphosphine was dried over KOH. Deuterated solvents for NMR studies were distilled from potassium under nitrogen and stored over sodium. Other chemicals were of reagent grade, unless otherwise specified.

Pentamethylcyclopentadiene and tetramethylethylcyclopentadiene were prepared by published procedures[1]. The compounds $[(C_6H_5)_3P]_2Pt(C_2H_4)$[2], $[(C_6H_5)_3P]_2Ni(C_2H_4)$[3], and $Hg(C_6F_5)_2$[4] were prepared by literature procedures. The compound $[(C_6H_5)_3P]_2Pt(C_4H_6)$[3] was prepared by a reported method, substituting dimethylacetylene for methylphenylacetylene. $(C_5H_5)Zn(CH_3)$[5] was prepared by a procedure previously used to make the ethyl analog, substituting MeMgBr for EtMgBr. $Zn(C_6H_5)_2$ and $Zn(p\text{-}CH_3C_6H_4)_2$[6] were prepared, using a modification of the literature procedure, by the reaction of $ZnCl_2$ with PhMgBr and (p-$CH_3C_6H_4$)Li, respectively.

Infrared spectra were recorded on a Nicolet 5DX FTIR as Nujol mulls

between CsI plates, or as solutions in KBr cells. Melting points were measured on a Thomas-Hoover melting point apparatus in capillaries sealed under N_2, and are uncorrected. ^{1}HNMR spectra were recorded either at 90 MHz on a JEOL FX-90Q spectrometer, or at 200 MHz on a departmental machine at the University of California, Berkelely and referenced to $(CH_3)_4Si$ at $\delta = 0$. ^{13}CNMR spectra were recorded either at 22.5 MHz on the JEOL spectrometer or at 50.8 MHz on the departmental spectrometer and referenced to $(CH_3)_4Si$ at $\delta = 0$. ^{31}PNMR spectra were recorded either at 36.2 MHz on the JEOL spectrometer or at 81.8 MHz on the departmental machine and referenced to 85% H_3PO_4 at $\delta = 0$, with the convention that chemical shifts at higher frequency are positive. ^{19}FNMR spectra were recorded on the JEOL spectrometer at 84.26 MHz and referenced to C_6F_6 at $\delta = 0$. ^{11}BNMR spectra were recorded on the JEOL spectrometer at 28.7 MHz and referenced to $BF_3 \cdot OEt_2$ at $\delta = 0$. Elemental analyses were performed by the analytical laboratories at the University of California, Berkeley. E.I. mass spectra were recorded on a AEI-MS-9 mass spectrometer in the mass spectroscopy laboratories at the University of California, Berkeley. X-ray powder patterns were recorded using a Debye-Scherrer camera and Cu-k_α radiation (λ = 0.1.5418 Å) with a Ni filter, and were indexed manually. Magnetic susceptibility measurements were conducted by Mr. David J. Berg using a S.H.E. Corporation Model 905 SQUID Magnetometer, using reported procedures[7].

Chapter One

MI_2 (M = Sm, Eu)

The thf solvates of EuI_2 and SmI_2 were prepared by the method of Girard, Kagan, and Namy[8]. The thf was removed from these solvates by heating the powders under vacuum (Eu: 180°C, 15h; Sm: 160°C, 16h). During desolvation, the EuI_2 changed color from pale yellow to white, and the SmI_2 changed from blue-gray to deep green. Complete removal of the thf was verified by examination of the infrared spectra (Nujol mulls).

Ytterbium Diiodide

Ammonium iodide was dried by heating to 120°C under vacuum for 12-14 hr. After being cooled to room temperature, it was washed with diethyl ether (100 mL) to remove any iodine formed during heating. Ammonium iodide (12.7 g, 0.0875 mol) was transferred to a large Schlenk-type flask equipped with a magnetic stir bar and a dry ice-ethanol condenser which was vented to a nitrogen manifold. The flask was cooled to -78°C with a dry ice-ethanol bath. Anhydrous ammonia (250-300 mL) was condensed onto the ammonium iodide, and the mixture was stirred to dissolve the solid. Ytterbium chips (7.95 g, 0.0459 mol; a 5% excess of ytterbium was used to ensure complete conversion of ammonium iodide) were added a few chips at a time to the stirring solution of ammonium iodide in ammonia. When all ytterbium had been added, the solution was allowed to stir at -78°C for 1 h. The cold bath was then removed, and the ammonia was allowed to boil away. The

resulting orange-yellow residue was crushed to a powder and dried under vacuum, then heated to 200°C under vacuum for 16-20 h to remove the ammonia of solvation. This resulted in a light yellow powder. It was essential to remove all of the ammonia at this stage to prevent the formation of ammonia complexes in later procedures.

$\underline{MI_2}$ (M = Ca, Sr, and Ba)

The alkaline earth diiodides were prepared as pyridine solvates by the method of Taylor and Grant[9], by the reaction of the metal dihydrides with ammonium iodide in pyridine. The coordinated pyridine was removed by heating the white powders under vacuum (Ca, 210°C, 16h; Sr, 180°C, 16h; Ba, 180°C, 22h). Complete removal of the pyridine was verified by examination of the infrared spectra as Nujol mulls. It was necessary to remove all of the coordinated pyridine at this stage to prevent formation of pyridine complexes in later procedures.

Sodium Pentamethylcyclopentadienide

A 1-L round-bottomed flask was fitted with a dry ice-ethanol condenser and a large magnetic stir bar. The flask was attached to a nitrogen manifold in a fume hood, and the manifold was vented through a oil bubbler. The flask was cooled to -78°C with a dry ice-ethanol bath. A cylinder of anhydrous ammonia was fitted with a short (ca. 3") spout of Tygon tubing. Under nitrogen flush, 500 mL of liquid ammonia was poured into the flask. Approximately 0.5-1 g of sodium metal (cut into small pieces) was dissolved in the ammonia with stirring, and a few crystals of ferric nitrate were added to initiate electron transfer and

production of sodium amide. This produced a color change from blue to brown or tan (this color change could occur instantaneously or could take up to 1 hr to occur, depending on how much sodium was initially added). The rest of the sodium (total amount 8.61g, 0.375 mol) was then added, and the mixture was allowed to stir at -78°C until all of the metal was converted to sodium amide, and the solution had turned gray (ca. 1 hr). At this time the cold bath was removed, and the ammonia was allowed to boil away. The gray-black residue was crushed to a powder and dried under reduced pressure. The sodium amide was suspended in 300 mL of thf. Pentamethylcyclopentadiene (42.55g, 48.91mL, 0.3123 mol) was dissolved in an additional 300 mL of thf, and added by cannula to the suspension of sodium amide. This resulted in the evolution of ammonia, and the solution became warm. The mixture was stirred (vented to a nitrogen manifold) for 8 hr. Stirring was then stopped, and the excess amide was allowed to settle for 1-2 days. The resulting orange-yellow solution was filtered through cannula filters fitted with oven-dried glass microfiber filters affixed with teflon tape (the filters clogged approximately every 20 min. of filtration and had to be replaced). If the filtrate exhibited any cloudiness, it was refiltered in the same manner. The thf was removed under reduced pressure to give an off-white sticky precipitate. The precipitate was washed with 3 x 200 mL of diethyl ether, and the washes were discarded. The remaining white powder was dried under reduced pressure. The total yield of sodium pentamethylcyclopentadienide was 39.33g (79.67%).

$(Me_5C_5)_2Sm(OEt_2)$

Samarium diiodide (4.34g, 0.0107 mol) was slurried with sodium pentamethylcyclopentadienide (3.17g, 0.0200 mol) in 250 mL of diethyl ether, and stirred for 17 h. The resulting deep green-brown solution was filtered and the volume was reduced to 125 mL. Cooling the solution to -15°C produced large deep green needles. Two subsequent batches of crystals were isolated from the mother liquor by reducing the volume and cooling. The total yield was 3.63g (73.2%), MP 190-192°C. Anal. Calcd for $C_{24}H_{40}OSm$: C, 58.2; H, 8.15. Found: C, 58.0; H, 8.20. IR (Nujol): 2723m, 1468m, 1164m, 1145s, 1080vs, 1038s, 1018m, 929m, 837s, 818vw, 799w, 774vw, 731wbr, 635w, 611m, 589w, 443vwbr, 364mbr, 307m, 268sbr cm^{-1}. ^{1}HNMR (C_7D_8, 31°C): ∂ 20.7 (broad triplet, J=6 Hz, 6H), ∂ 2.77 ($\nu_{1/2}$ = 4 Hz, 30H), ∂ -4.50 (broad quartet, 4H). The identity of the ligand as Et_2O was verified by hydrolyzing a sample of the compound in C_6D_6 and examining the ^{1}HNMR spectrum of the hydrolysate. ^{13}CNMR (C_7D_8, 31°C): ∂ 93.01 ($\underline{Me}_5C_5$, q, $^1J_{CH}$= 124 Hz), ∂ 73.21 ($OCH_2\underline{C}H_3$, q, $^1J_{CH}$= 130 Hz), ∂-89.74 ($\underline{C}_5Me_5$, s). The methylene carbon of OEt_2 was not observed at room temperature. Upon cooling the sample to -30°C, however, ^{13}CNMR{^{1}H}NMR spectra showed the following resonances: ∂ 102.6 ($C_5\underline{Me}_5$), ∂ 94.94 ($OCH_2\underline{C}H_3$), ∂ -137.9 ($\underline{C}_5Me_5$). An additional resonance emerged from the region of the toluene aryl carbons at ∂ 135.9, which was attributed to $O\underline{C}H_2CH_3$.

$(Me_5C_5)_2Sm$

Bis(pentamethylcyclopentadienyl)samarium(diethylether) (3.88g, 0.00784 mol) was dissolved in toluene (200 mL) to give a deep green

solution. The solution was heated to 100°C, and the solvent was removed slowly under reduced pressure. The residue was dissolved in an additional 200 mL of toluene, and the process was repeated. The green solid was extracted with 200 mL of toluene, and the solution was filtered. The volume was reduced to 120 mL, and the solution was cooled to -25°C, producing large brown-green blocks. Additional batches of crystals were obtained from the mother liquor by concentrating and cooling. The combined yield was 2.65g (80.3%), MP 214-217°C. The compound sublimed at 125°C/10^{-4} torr. To confirm that all diethyl ether had been removed, a sample was hydrolyzed in C_6D_6, and the hydrolysate was examined by ^{1}HNMR spectroscopy; no diethyl ether was observed. The identity of the compound was confirmed by comparing the IR and ^{1}HNMR spectra with reported values[12]. IR (Nujol): 2712w, 1649vwbr, 1577vw, 1497w, 1436s, 1162w, 1146w, 1058w, 1018w, 950w, 721w, 656w, 628w, 602w, 557vw, 477w, 372sh, 359m, 299sh, 268s cm^{-1}. ^{1}HNMR (C_6D_6, 30°C): ∂ 1.16 (s, $\nu_{1/2}$= 25 Hz). The lower M/e portion of the EI mass spectrum showed a strong M^+ isotopic cluster at 422, which simulated well (all percentages relative to 422 as 100%):

M/e	Simulated %	Experimental %
414	11.6	11.5
415	2.58	2.52
416	0.27	-
417	56.4	61.7
418	54.7	55.1
419	62.6	60.4
420	40.3	37.3
421	7.44	8.81
422	100	100
423	22.2	26.1
424	86.7	79.3
425	19.0	16.2
426	1.99	1.44
427	0.13	-

Ring loss and fragmentation is evident. Without heating, higher weight molecular fragments are observed, corresponding to $(Me_5C_5)_2Sm_2$ and $(Me_5C_5)_3Sm_2$. These fragments also may be simulated (for $(Me_5C_5)_3Sm_2$, all percentages relative to 706 as 100%):

M/e	Simulated %	Experimental %
693	0.57	2.11
694	0.19	-
695	0.03	2.13
696	5.51	7.08
697	5.97	8.75
698	6.75	9.85
699	18.1	22.8
700	25.8	32.4
701	49.6	54.6
702	46.8	50.0
703	42.4	48.4
704	71.2	75.8
705	60.2	65.5
706	100	100
707	83.7	83.8
708	59.6	57.9
709	77.1	74.1
710	22.8	23.3
711	74.3	66.3
712	24.0	22.0
713	33.9	29.1
714	10.5	8.69
715	1.65	-
716	0.17	-
717	0.01	3.93

$(Me_5C_5)_2Eu(OEt_2)(thf)$

$EuI_2(thf)_2$ (0.73g, 0.0012 mol) was slurried in 100 mL of diethyl ether with sodium pentamethylcyclopentadienide (0.40g, 0.0025 mol) and stirred at room temperature for 16 h. The ether solution was filtered, and the volume of the filtrate was reduced to 40 mL; cooling the solution to -25°C produced red-orange prisms. A further batch of crystals was isolated from the mother liquor by concentrating and cooling. The total yield was 0.50g (70%), MP 181-182°C. The identity

of the compound was verified by comparison of the infrared and melting point with previously reported values[10]. IR (Nujol): 2720w, 1640w, 1291w, 1248w, 1208w, 1185vw, 1164sh, 1147m, 1123vw, 1089w, 1055m, 1029vs, 926w, 892vs, 834m, 790m, 773w, 638wbr, 581w, 349m, 276sh, 247sbr cm^{-1}. To confirm the ratio of the coordinating bases, a sample of the compounds was hydrolyzed in C_6D_6, and the hyrolysate was examined by ^{1}HNMR spectroscopy. Diethyl ether, thf, and Me_5C_5H were observed in a 1:1:2 ratio.

$(Me_5C_5)_2Eu(thf)$

$(Me_5C_5)_2Eu(OEt_2)(thf)$ (0.50g, 0.88 mmol) was dissolved in 70 mL of toluene to give a red solution. This solution was heated to 100°C, and the solvent was removed slowly under reduced pressure. The process was then repeated with an additional 70 mL of toluene. The residues were extracted with 100 mL of pentane. The pentane solution was filtered, concentrated to 60 mL, and cooled to -25°C, producing red needles. An additional batch of crystals was isolated from the mother liquors by concentrating and cooling. The total yield was 0.35g (80%), MP 178-181°C. The identity of the compound was confirmed by comparison of the IR and MP with reported values[10]. IR (Nujol): 2720w, 1640wbr, 1293w, 1281w, 1223w, 1210m, 1160w, 1024s, 956sh, 940w, 927m, 870s, 718m, 686w, 664m, 627w, 583m, 395w, 354mbr, 256s cm^{-1}.

$(Me_5C_5)_2Eu$

Bis(pentamethylcyclopentadienyl)europium(diethylether)[11] (2.18g, 0.00439 mol) was dissolved in toluene (200 mL) to give an orange-red

solution. The solution was heated to 100°C, and the solvent was removed slowly under reduced pressure. The residue was dissolved in an additional 200 mL of toluene, and the solvent was removed as before. The orange solid was dissolved in 250 mL of hexane, filtered, reduced to 180 mL in volume, and cooled to -25°C, producing large red prisms. Two more batches of crystals were isolated from the mother liquors by concentrating and cooling. The total yield was 1.62g, 87.4%, MP 219-222°C. The compound sublimes at 125°C/10^{-4} torr. Anal. Calcd for $C_{20}H_{30}Eu$: C, 56.9; H,7.17. Found: C, 55.1; H, 7.18. IR (Nujol): 2725w, 1647wbr, 1494m, 1434vs, 1160w, 1149sh, 1017s, 948w, 720w, 628w, 602w, 584w, 569sh, 547w, 478vwbr, 398brsh, 364sh, 351m, 263vsbr cm^{-1}. To confirm that all diethyl ether had been removed, a sample was hydrolyzed in C_6D_6, and the hydrolysate was examined by ^{1}HNMR spectroscopy: only C_5Me_5H was observed. The mass spectrum shows M^+, successive ring loss, and fragmentation of the rings. The parent molecular ion isotopic cluster may be simulated (intensities relative to 423 as 100%):

M/e	Simulated %	Experimental %
421	89.63	90.53
422	19.98	10.61
423	100	100
424	21.95	11.78
425	2.31	-

$(Me_5C_5)_2Eu(CNR)_2$ (R = 2,6-dimethylphenyl)

Bis(pentamethylcyclopentadienyl)europium (0.23g, 0.54 mmol) was dissolved in 30 mL of toluene, and added with stirring to a toluene solution (10 mL) of 2,6-dimethylphenylisocyanide (0.14g, 1.1 mmol), producing a dark brown solution. The volume of the solution was reduced to 25 mL, and the mixture was cooled to -25°C, yielding dark brown

crystals. A second crop of crystals was isolated from the mother liquors by concentrating and cooling. The combined yield was 0.31g (84%), MP 229-231°C. IR (Nujol): 3071w, 2717m, 2144s, 2115w, 1944vw, 1932vw, 1869vw, 1869vw, 1790vw, 1662vw, 1590w, 1443s, 1299w, 1171m, 1152sh, 1082m, 1036m, 1019w, 993vw, 974vw, 950vwbr, 923w, 897w, 776sh, 769s, 721m, 694vw, 658vw, 639w, 589vw, 574vw, 543vw, 497w, 475wbr, 418vw, 374m, 357w, 316vw, 302sh, 263vs cm^{-1}. Anal. Calcd for $C_{38}H_{48}N_2Eu$: C, 66.6; H, 7.08; N, 4.09. Found: C, 66.1; H, 7.05; N, 4.03. A sample of the compound was hydrolyzed in C_6D_6, and the hydrolysate was examined by ^{1}HNMR spectroscopy: 2,6-dimethylphenylisocyanide and C_5Me_5H were observed in a 1:1 ratio.

$(Me_5C_5)_2Yb$

Method A

Bis(pentamethylcyclopentadienyl)(hexamethyldisilylamine)ytterbium[11] (0.49g, 0.81 mmol) was heated under one atmosphere N_2. The compound melted at ca. 120°C. The resulting red liquid was heated to 200°C, and green-brown crystals began to sublime up the walls of the flask. After heating for 1h, the material was extracted with pentane (50 mL), yielding an orange solution. This solution was reduced in volume and cooled to -25°C. The green needles isolated lost solvent under reduced pressure and turned greenish-tan. A second crop of crystals could be isolated from the mother liquors. The combined yield was 0.29g, 80%.

Method B

Bis(pentamethylcyclopentadienyl)(hexamethyldisilylamine)ytterbium

was sublimed slowly at 90°C at 10^{-4} mm Hg pressure to give dark brown-green crystals. The yield from this method was nearly quantitative.

Method C

Pentamethylcyclopentadiene (1.60 mL, 1.40g, 0.0103 mol) in toluene (20 mL) was added to a solution of bis(hexamethyldisilylamido)ytterbium (2.53g, 0.00512 mol) in toluene (40 mL). This solution was stirred 15h. After filtering the solution, the toluene was removed slowly under reduced pressure. The residue was extracted with pentane (60 mL), filtered, and the volume of the filtrate was reduced to ca. 40 mL. Cooling thd solution to -25°C produced green needles, which lost solvent under vacuum. A second crop of crystals was obtained by concentrating and cooling the mother liquors. The total yield was 1.42g, 62.5%.

Method D

Bis(pentamethylcyclopentadienyl)ytterbium(diethylether)[10] (2.96g, 0.00572 mol) was dissolved in 200 mL of toluene to give a deep green solution. This solution was heated to 100°C, and the solvent removed very slowly under reduced pressure (over 3-4 h.). As the diethyl ether was removed with the toluene, the solution turned deep brown-orange. The residue was dissolved in an additional 200 mL of toluene, and the process was repeated. The solid residue was extracted with 250-300 mL pentane. The pentane solution was reduced in volume to 150 mL and cooled to -25°C. This produced very fine green needles which turned tan upon exposure to vacuum. A second batch of crystals was isolated from the filtrate by concentrating and cooling. The total yield was 2.20g, 86.7%.

The compound reversibly turns orange-red at 130°C, and melts at

189-191°C. Anal. Calcd for $C_{20}H_{30}Yb$: C, 54.2; H, 6.82. Found: C, 53.8; H, 6.96. IR (Nujol): 2725w, 1653vwbr, 1160w, 1148w, 1017m, 792vw, 720w, 623vw, 584w, 403shbr, 352m, 274s cm^{-1}. ^{1}HNMR (C_6D_6, 30°C): δ 1.92 (s). $^{13}C\{^1H\}$NMR (C_6D_6, 30°C): δ 10.61 ($\underline{Me}_5C_5$); δ 113.4 ($\underline{C}_5Me_5$). The mass spectrum shows sequential loss of pentamethylcyclopentadienyl rings, as well as fragmentation of the rings. The parent molecular ion isotopic envelope may be simulated (intensities relative to 444 as 100%):

M/e	Simulated %	Experimental %
438	0.28	-
439	0.06	-
440	8.65	6.21
441	41.82	47.62
442	70.17	70.97
443	59.76	59.11
444	100	100
445	20.87	15.22
446	37.58	36.15
447	8.04	-
448	0.84	-
449	0.05	-

$\underline{(EtMe_4C_5)_2Yb[HN(SiMe_3)_2]}$

Ethyltetramethylcyclopentadiene (1.56 mL, 1.31g, 8.72 mmol) in pentane (20 mL) was added to a stirred solution of bis(hexamethyldisilylamido)ytterbium (2.16g, 4.37 mmol) in pentane (30 mL). The mixture was stirred for 20 h, resulting in a deep orange-brown solution. This solution was filtered, reduced in volume to 15 mL, and cooled to -78°C. The resulting deep green crystals were isolated at low temperature, but melted slightly to a sticky orange-brown solid at room temprature. This color change was reversible. The isolated yield was 0.63g, 23%. The infrared spectrum revealed the presence of both free and coordinated hexa-methyldisilylamine, indicating partial dissociation of the

coordinated ligand. IR (Nujol): 3379w, 3205w, 2726m, 1603w, 1309w, 1248vs, 1217wsh, 1177s, 1044sbr, 986m, 930vs, 868sbr, 837vsbr, 770sh, 752wsh, 686sh, 680m, 658m, 614w, 600w, 583w, 550vw, 431w, 361m, 302s, 277m cm^{-1}. It proved very difficult to remove all solvent from the oily solid; therefore, the compound was not characterized completely, but converted directly to the base-free species.

$(EtMe_4C_5)_2Yb$

Method A

Bis(ethyltetramethylcyclopentadienyl)(hexamethyldisilylamine)ytterbium (0.63g, 0.0010 mol) was heated under one atmosphere N_2. The compound was heated to 170°C for 45 min., during which time red-orange crystalline solid sublimed up the sides of the flask. This solid darkened to brown-orange upon cooling. The sublimed material was collected; the total yield was 0.33g, 70%.

Method B

Bis(ethyltetramethylcyclopentadienyl)(hexamethyldisilylamine)ytterbium (0.70g, 0.0011 mol) was sublimed at 90°C at 10^{-4} mm Hg to give dark brown-orange crystalline material. The total yield was 0.41g, 79%.

The compound turned orange at 120°C, and melted at 158-165°C. Anal. Calcd for $C_{22}H_{34}Yb$: C, 56.0; H, 7.28. Found: C, 56.2; H, 7.34. IR (Nujol): 2722m, 1605w, 1308w, 1158w, 1146wsh, 1037w, 1017m, 866w, 747w, 716w, 549vw, 438w, 360w, 301s, 277m cm^{-1}. ^{1}HNMR (C_6D_6, 30°C): δ 1.98 (s, 12H); δ 1.90 (s, 12H); δ 2.40 (q, 4H); δ 0.97 (t, 6H, $^3J_{HH}$ = 7.2 Hz). The mass spectrum shows successive ring loss, as well as fragmentation of the rings. The parent molecular ion isotopic envelope

may be simulated (all percentages relative to 472 as 100%):

M/e	Simulated %	Experimental %
466	0.28	-
467	0.07	0.18
468	8.53	10.13
469	41.45	44.13
470	70.18	73.20
471	60.52	62.00
472	100	100
473	22.81	22.53
474	37.55	36.47
475	8.76	7.54
476	1.01	0.40
477	0.07	-

$(Me_5C_5)_2Yb(CNR)_2$ (R = 2,6-dimethylphenyl)

Bis(pentamethylcyclopentadienyl)ytterbium (0.14g, 0.32 mmol) was dissolved in toluene (10mL) and added with stirring to a toluene solution (5 mL) of 2,6-dimethylphenylisocyanide (0.080g, 0.61 mmol), giving a green solution. The volume was reduced to 4 mL, and the solution was cooled to -25°C, yielding green-brown blocks. A second batch of crystals was isolated from the mother liquors by concentrating and cooling. The combined yield was 0.18g (84%), MP 199-202°C. IR (Nujol): 2716vw, 2131vs, 2116sh, 2095m, 1975vw, 1928vw, 1852vw, 1653vw, 1603vw, 1591vw, 1466s, 1447sh, 1377s, 1295vw, 1260w, 1172m, 1126sh, 1090m, 1078sh, 1034w, 1017w, 989w, 965vw, 920w, 891brsh, 877wbr, 822wbrsh, 804wbr, 765vs, 726sh, 718m, 700w, 641vw, 618vw, 590vw, 473vw, 382m, 360sh, 308m, 266sbr cm^{-1}. Anal. Calcd for $C_{38}H_{48}N_2Yb$: C, 64.7; H, 6.87; N, 3.97. Found: C, 65.0; H, 6.71; N, 3.98. ^{1}HNMR (C_6D_6, 30°C): δ 6.80 (m, 6H), δ 2.34 (s, $\nu_{1/2}$ = 1.7 Hz, 30H), δ 2.13 (s, $\nu_{1/2}$ = 6.8 Hz, 12H).

$(Me_5C_5)_2Yb(PEt_3)$

Bis(pentamethylcyclopentadienyl)ytterbium (0.30g, 0.68 mmol) was dissolved in pentane (20 mL) and added to a pentane solution (5 mL) of triethylphosphine (0.10 mL, 0.080g, 0.68 mmol), resulting in an immediate color change from orange to deep blue-green. The volume of the solution was reduced to 10 mL, and the solution was cooled to -25°C. Dark green needles were isolated from solution. A second crop of crystals was obtained from the mother liquors by concentrating and cooling. The total yield was 0.30g (77%), MP 128-132°C. IR (Nujol): 2718w, 1144m, 1122s, 1052sh, 1011s, 947m, 935sh, 900sh, 849w, 713w, 693sh, 684m, 677sh, 650m, 629w, 611s, 583m, 561sh, 512w, 474sh, 443sh, 396mbr, 347sh, 281sbr, 263sh cm^{-1}. Anal. Calcd for $C_{26}H_{45}PYb$: C, 55.6; H, 8.09. Found: C, 54.7; H, 8.05. ^{1}HNMR (C_7D_8, 30°C): δ 2.05 (s, 30H), δ 1.24 (t, $^3J_{HH}$ = 7 Hz, 9H, broadened due to unresolved coupling to P), δ 0.93 (q, 6H, broadened due to unresolved coupling to P). $^{31}P\{^1H\}$NMR (C_7D_8, 30°C): δ -20.1 (s).

$(Me_5C_5)_2Ca(OEt_2)$

Calcium diiodide (3.24g, 11.0 mmol) was slurried with Me_5C_5Na (3.35g, 21.2 mmol) in 200 mL of diethyl ether, and the suspension was stirred for 24 h. The ether solution was filtered, and the volume of the filtrate was reduced to 80 mL. The solution was cooled to -25°C, producing large white needles. A second batch of crystals was isolated from the mother liquor by concentrating and cooling. The total yield was 2.82g (69.2%), MP 186-191°C. Anal. Calcd for $C_{24}H_{40}OCa$: C, 74.9; H, 10.5. Found: C, 74.6; H, 10.4. IR (Nujol): 2722m, 1650wbr, 1440s,

1417m, 1301vw, 1286w, 1177sh, 1162sh, 1146s, 1068vs, 1040s, 1017m, 971sh, 924m, 912sh, 837s, 815w, 738sh, 720w, 625w, 613w, 588m, 545wbr, 526sh, 512w, 438m, 409sh, 354wsh, 333vsbr, 279s cm^{-1}. ^{1}H NMR (C_6D_6, 30°C): ∂ 2.92 (q, 4H, $^{3}J_{HH}$= 7 Hz), ∂ 2.05 (s, 30H), ∂ 0.80 (t, 6H, $^{3}J_{HH}$= 7 Hz). ^{13}C NMR (C_6D_6, 30°C): ∂ 113.1 (s, $\underline{C}_5Me_5$), ∂ 66.20 (t, $^{1}J_{CH}$= 143 Hz, $O\underline{C}H_2$), ∂ 13.35 (q, $^{1}J_{CH}$= 126 Hz, $OCH_2\underline{C}H_3$), ∂ 11.38 (q, $^{1}J_{CH}$= 124 Hz, $C_5(\underline{C}H_3)_5$).

$\underline{(Me_5C_5)_2Ca}$

The compound $(Me_5C_5)_2Ca(OEt_2)$ (2.50g, 6.50 mmol) was dissolved in 200 mL of toluene. The solution was heated to 100°C, and the solvent was removed slowly under vacuum. An additional 200 mL of toluene was added, and the process was repeated. The light yellow residue was extracted with 180 mL of hexane. The hexane solution was concentrated to a volume of 50 mL, and cooled to -25°C, producing large colorless blocks. Further batches of crystals were isolated by concentrating and cooling the mother liquor. The total yield was 1.83g (90.6%), MP 207-210°C. The compound sublimed at 75°C/10^{-4} mm. Anal. Calcd for $C_{20}H_{30}Ca$: C, 77.3; H, 9.76. Found: C, 77.1; H, 9.65. IR (Nujol): 2721m, 1653wbr, 1441s, 1418sh, 1162w, 1058w, 1019s, 950vw, 891vw, 723m, 665w, 628w, 594w, 539wbr, 462shbr, 399wsh, 367vs, 291s, 276sh cm^{-1}. ^{1}H NMR (C_6D_6, 31°C): ∂ 1.90 (s). ^{13}C NMR (C_6D_6, 31°C): ∂ 114.3 (s, $\underline{C}_5Me_5$), ∂ 10.27 (q, $^{1}J_{CH}$= 124 Hz, $C_5(\underline{C}H_3)_5$). The EI mass spectrum at the lowest possible temperatures showed M^+ (310) as well as sequential ring loss and fragmentation of the rings (base peak = 136, C_5Me_5H). At higher temperatures, higher cluster fragments were visible, corresponding to

$Ca_2(C_5Me_5)_2$, $Ca_2(C_5Me_5)_3$, $Ca_2(C_5Me_5)_4$, and even $Ca_3(C_5Me_5)_4$ (base peak = 175, Me_5C_5Ca).

$(Me_5C_5)_2Ca(bipy)$

Bis(pentamethylcyclopentadienyl)calcium (0.31g, 0.0010 mol) was dissolved in hexane (30 mL), and added with stirring to a hexane solution (10 mL) of bipyridine (0.16g, 0.0010 mol). The color of the solution immediately turned deep red-purple, and an orange-red microcrystalline precipitate began to appear. The solution was stirred for 12 h. The precipitate was collected, and a second batch of product was isolated by concentrating and cooling the mother liquors. The total yield of product collected was 0.42g (90%). The compound was recrystallized from hot toluene to give large red blades; it was only sparingly soluble in cold toluene. The crystals did not melt below 330°C. IR (Nujol): 3059m, 2721m, 1598s, 1592s, 1575m, 1568m, 1490m, 1475s, 1436vs, 1312m, 1245w, 1224vw, 1175w, 1156m, 1114w, 1103w, 1061w, 1043m, 1021sh, 1012s, 1000sh, 966w, 960sh, 892w, 881w, 813w, 759vs, 742m, 696vw, 668vw, 653vw, 643m, 625m, 588w, 555w, 417wbr, 375sh, 350sh, 327vsbr, 288m cm^{-1}. Anal. Calcd for $C_{40}H_{38}N_2Ca$: C, 77.2; H, 8.21; N, 6.00. Found: C, 76.9; H, 8.27; N, 5.82. ^1H NMR (C_6D_6, 31°C): ∂ 1.91 ($C_5\underline{Me}_5$); ∂ 8.59, ∂ 8.13, ∂ 6.75, ∂ 6.21 (all multiplets assigned to aryl resonances, no coupling resolvable). The insolubility of the compound made it impossible to obtain a high quality spectrum.

$(Me_5C_5)_2Ca(CNR)_2$ (R = 2,6-dimethylphenyl)

Bis(pentamethylcyclopentadienyl)calcium (0.13g, 0.42 mmol) was

dissolved in 10 mL toluene and added with agitation to a toluene solution (20 mL) of 2,6-dimethylphenylisocyanide (0.11g, 0.84 mmol). The volume was reduced to 15 mL, and the yellow solution was cooled to -25°C, producing yellow blocks. A second batch of crystals was isolated from the mother liquors by concentrating the solution further and cooling. The combined yield was 0.18g (75%). The compound darkened slowly above 165°C, and melted irreversibly to an orange oil at 213-215°C. IR (Nujol): 3066w, 2718m, 2145vs, 2115m, 1946w, 1870w, 1790w, 1671w, 1653sh, 1604sh, 1591w, 1552vw, 1488shbr, 1443s, 1300w, 1273w, 1170s, 1150sh, 1098sh, 1085m, 1060vw, 1036m, 1020m, 991vw, 976w, 924w, 897m, 882shbr, 803m, 777vs, 719s, 638w, 589w, 573w, 548w, 511w, 379s, 363s, 334vs, 283sbr cm^{-1}. Anal. Calcd for $C_{38}H_{48}N_2Ca$: C, 79.7; H, 8.45; N, 4.89. Found: C, 78.9; H, 8.54; N, 4.81. ^{1}HNMR (C_6D_6, 30°C): ∂ 6.65 (m, 6H), ∂ 2.35 (s, 30H), ∂ 2.17 (s, 12H). ^{1}HNMR of 2,6-dimethylphenylisocyanide (C_6D_6, 30°C): ∂ 6.62 (m, 3H), ∂ 2.05 (s, 6H).

$(Me_5C_5)_2Ca(PEt_3)$

Bis(pentamethylcyclopentadienyl)calcium (0.14g, 0.45 mmol) was dissolved in 15 mL pentane and added to a degassed solution of triethylphosphine (0.070mL, 0.056g, 0.47 mmol) in pentane (5 mL). The solution was filtered, and the volume was reduced to 5 mL. When cooled to 25°C, the solution produced white needles. A second crop of crystals was obtained from the mother liquors by concentrating the filtrate and cooling. The combined yield was 0.17g (88%), MP 111-113°C. IR (Nujol): 2719m, 1653wbr, 1418m, 1311vw, 1288sh, 1265w, 1250w, 1236sh,

1154m, 1085m, 1062w, 1036s, 1022s, 989sh, 977w, 963w, 937w, 892vw, 800w, 752w, 767sh, 756s, 723m, 701m, 671w, 624wbr, 588w, 551vw, 515vw, 445wbr, 365sh, 343vsbr, 306w, 287sbr cm^{-1}. Anal. Calcd for $C_{26}H_{45}PCa$: C, 72.8; H, 10.6; P, 7.22. Found: C, 73.0; H, 10.7; P, 6.97. ^{1}HNMR (C_6D_6, 30°C): ∂ 1.98 (s, 30H), ∂ 1.21 and ∂ 0.87 (both multiplets, combined integration 15H). ^{31}PNMR{^{1}H} (C_6D_6, 30°C): δ -20.3 ppm (s).

$(Me_5C_5)_2Sr(OEt_2)$

Strontium diiodide (2.30g, 6.74 mmol) and Me_5C_5Na (2.02g, 12.8 mmol) were slurried together in 200 mL of diethyl ether, and the suspension was stirred for 36 h. The solution was then filtered, concentrated to a volume of 120 mL, and cooled to -25°C, producing white needles. Two subsequent batches of crystals were obtained by concentrating and cooling the mother liquors. The combined yield was 1.87g (67.7%), MP 210-215°C. Anal. Calcd for $C_{24}H_{40}OSr$: C, 66.7; H, 9.35. Found: C, 64.6; H, 9.42. IR (Nujol): 2722m, 1650wbr, 1488m, 1419m, 1159m, 1146s, 1079vs, 1038s, 1013m, 927m, 838s, 818w, 797w, 724wbr, 668vw, 620wbr, 588m, 545wbr, 513w, 442vw, 416w, 397w, 355mbr, 282vsbr cm^{-1}. ^{1}H NMR (C_6D_6, 30°C): ∂ 2.82 (q, 4H, $^{3}J_{HH}$= 7 Hz), ∂ 2.07 (s, 30H), ∂ 0.74 (t, 6H, $^{3}J_{HH}$= 7 Hz). ^{13}C NMR (C_6D_6, 31°C): ∂ 112.5 (s, $\underline{C}_5Me_5$), ∂ 66.34 (t, $^{1}J_{CH}$= 143 Hz, $O\underline{C}H_2$), ∂ 13.25 (q, $^{1}J_{CH}$= 127 Hz, $OCH_2\underline{C}H_3$), ∂ 11.09 (q, $^{1}J_{CH}$= 125 Hz, $C_5(\underline{C}H_3)_5$).

$(Me_5C_5)_2Sr$

The compound $(Me_5C_5)_2Sr(OEt_2)$ (1.50g, 3.47 mmol) was dissolved in 200 mL of toluene, and the solution was heated to 100°C. The solvent

was removed slowly under reduced pressure. The process was then repeated with another 200 mL of toluene. The residue was extracted with 150 mL of hexane. This solution was filtered, concentrated to a volume of 80 mL, and cooled to -25°C; white blocks were isolated by filtration. A second batch of crystals was obtained from the mother liquors by concentrating and cooling. The total yield was 1.10g (88.5%), MP 216-218°C. The compound sublimed at 105°C/10^{-4} torr. Anal. Calcd for $C_{20}H_{30}Sr$: C, 67.1; H, 8.45. Found: C, 65.6; H, 8.41. IR (Nujol): 2725w, 1650wbr, 1244w, 1162w, 1148m, 1038m, 1020m, 956w, 721mbr, 737sh, 699sh, 668vw, 631w, 620vw, 589w, 546vw, 516w, 430w, 396vw, 366w, 354m, 308sh, 289vsbr cm^{-1}. ^1H NMR (C_6D_6, 31°C): ∂ 1.95 (s). ^{13}C NMR (C_6D_6, 31°C): ∂ 113.6 (s, $\underline{C}_5Me_5$), ∂ 10.83 (q, $^1J_{CH}$= 125 Hz, $C_5(\underline{C}H_3)_5$). The mass spectrum showed M^+ (358) as well as sequential ring loss and ring fragmentation. The molecular ion isotopic cluster, though small, could be satisfactorily simulated (all percentages relative to 358 as 100%):

M/e	Simulated %	Experimental %
356	11.74	12.05
357	10.91	11.41
358	100	100
359	22.02	21.41

$\underline{(Me_5C_5)_2Sr(bipy)}$

Bis(pentamethylcyclopentadienyl)strontium (0.19g, 0.53 mmol) was dissolved in 15 mL of toluene and added with stirring to a toluene solution (15 mL) of bipyridine (0.08g, 0.51 mmol). The resulting bright red solution was filtered and cooled to -25°C, yielding orange-red needles. A second crop of needles was obtained by concentrating and cooling the mother liquors. The total yield was 0.20g (75%). The

compound did not melt below 330°C. IR (Nujol): 3058m, 2751vw, 2723m, 1660vwbr, 1592s, 1575m, 1568m, 1560w, 1489m, 1477m, 1457s, 1438vs, 1314m, 1282vw, 1244w, 1220vw, 1175m, 1160sh, 1156m, 1105w, 1090w, 1062w, 1043m, 1018w, 1007s, 970vw, 962vw, 928wbr, 902w, 893vw, 763vs, 757sh, 742m, 731sh, 723w, 700vw, 667w, 652w, 641w, 622w, 588vw, 526vw, 415m, 353vw, 342vw, 274vsbr cm^{-1}. Anal. Calcd for $C_{30}H_{38}N_2Sr$: C, 70.0; H, 7.46; N, 5.45. Found: C, 69.4; H, 7.51; N, 5.38. The insolubility of the compound precluded the possibility of obtaining the NMR spectrum.

$(Me_5C_5)_2Sr(CNR)_2$ (R = 2,6-dimethylphenyl)

Bis(pentamethylcyclopentadienyl)strontium (0.18g, 0.50 mmol) was dissolved in 20 mL of warm toluene and added to a toluene solution (15 mL) of 2,6-dimethylphenylisocyanide (0.13g, 0.99 mmol), yielding a pale yellow solution. The volume was reduced to 15 mL, and the solution was cooled to -25°C, producing pale yellow prisms which seemed to lose solvent under vacuum. A second crop of crystals was isolated from the mother liquors by concentrating and cooling the solution. The total yield of product was 0.24g (77%). The compound darkened slowly above 215°C, and melted irreversibly to an orange oil at 230-233°C. IR (Nujol): 2719m, 2150s, 2115m, 1946w, 1931w, 1868w, 1792w, 1671w, 1605sh, 1590m, 1443s, 1297m, 11171s, 1150sh, 1079m, 1062sh, 1037m, 1016w, 991wbr, 973wbr, 923w, 897w, 822vw, 802m, 774vs, 721m, 640w, 612vw, 587w, 572vw, 544vw, 514vw, 496w, 471w, 375m, 360w, 327sh, 309sh, 279vsbr cm^{-1}. Anal. Calcd for $C_{38}H_{48}N_2Sr$: C, 73.6; H, 7.80; N, 4.52. Found: C, 73.3; H, 7.91; N, 4.49. ^{1}HNMR (C_6D_6, -31°C): ∂ 6.58 (m, 6H), ∂ 2.38 (s, 30H), ∂ 2.12 (s, 12H).

$(Me_5C_5)_2Sr(PEt_3)$

Bis(pentamethylcyclopentadienyl)strontium (0.20g, 0.56 mmol) was dissolved in 35 mL hexane, and added to a degassed solution of triethylphosphine (0.082mL, 0.066g, 0.56 mmol) in pentane (5 mL). This solution was filtered, the volume was reduced to 10 mL, and the solution was cooled to -25°C. The resulting small white crystals appeared to lose solvent under vacuum. A second batch of product was isolated from the mother liquors by concentrating and cooling the filtrate. The combined yield was 0.19g (71%), MP 140-142°C. IR (Nujol): 2720m, 1655wbr, 1415w, 1347w, 1309vw, 1239vw, 1210vw, 1149m, 1109vw, 1036s, 1022s, 982sh, 963vw, 932w, 888sh, 873mbr, 767sh, 756m, 720w, 704m, 671w, 624w, 591vw, 515w, 475w, 452vw, 428w, 409sh, 398w, 355w, 325vw, 285vsbr cm^{-1}. Anal. Calcd for $C_{26}H_{45}PSr$: C, 65.6; H, 9.54; P, 6.50. Found: C, 58.6; H, 9.17; P, 2.09. ^{1}HNMR (C_6D_6, 31°C): ∂ 2.03 (s, 30H), ∂ 1.21 and ∂ 0.85 (both multiplets, combined integration 15H). $^{31}P\{^1H\}$NMR (C_6D_6, 31°C): δ -20.1 ppm (s).

$(Me_5C_5)_2Ba(thf)_2$

Barium diiodide (2.60g, 6.65 mmol) and Me_5C_5Na (2.10g, 13.3 mmol) were dissolved in 150-200 mL of thf, and the solution was stirred for 48 h. The solvent was removed under reduced pressure, and the resulting residue was extracted with 150 mL of hot toluene. The volume of the toluene extract was reduced to 100 mL, and the solution was cooled to -25°C, producing white needles. Further batches of crystals were isolated by concentrating and cooling the mother liquor. The combined yield was 2.76g (75.2%), MP 187-191°C. Anal. Calcd for $C_{28}H_{46}O_2Ba$: C,

60.9; H, 8.40. Found: C, 60.9; H, 8.54. IR (Nujol): 2723m, 1651wbr, 1496m, 1294w, 1285w, 1246m, 1212m, 1146w, 1129w, 1080m, 1037vs, 957w, 930w, 899vs, 859sh, 797mbr, 729m, 646w, 642vw, 611mbr, 587sh, 466vw, 419w, 404wbr, 362wbr, 308m, 282sh, 258vsbr cm^{-1}. ^{1}H NMR (C_6D_6, 30°C): ∂ 3.33 (m, 8H, $O\underline{C}H_2CH_2$), ∂ 2.12 (s, 30H), ∂ 1.33 (m, 8H, $OCH_2\underline{C}H_2$). ^{13}C NMR (C_6D_6, 30°C): ∂ 112.7 (s, $\underline{C}_5Me_5$), ∂ 68.02 (t, $^{1}J_{CH}$= 146 Hz, $O\underline{C}H_2CH_2$, additional coupling unresolved), ∂ 25.44 (t, $^{1}J_{CH}$= 134 Hz, $OCH_2\underline{C}H_2$, additional coupling unresolved), ∂ 11.21 (q, $^{1}J_{CH}$= 123 Hz, $C_5(\underline{C}H_3)_5$).

No reaction was observed to occur between BaI_2 and Me_5C_5Na in Et_2O.

$\underline{(Me_5C_5)_2Ba}$

The compound $(Me_5C_5)_2Ba(thf)_2$ (2.50g, 4.53 mmol) was dissolved in 200 mL of toluene, and heated to 100°C. The solvent was removed slowly under reduced pressure. This process was repeated with an additional 200 mL of toluene. The off-white residue was extracted with 180 mL of warm toluene. The volume of the extract was reduced to 90 mL, and the solution was cooled to -25°C, yielding white needles. Further batches of crystals were isolated from the mother liquors by concentrating and cooling. The total yield was 1.60g (86.5%), MP 265-268°C. The compound sublimed very slowly at 10^{-4} torr at temperatures above 135°C. Anal. Calcd for $C_{20}H_{30}Ba$: C, 58.9; H, 7.43. Found: C, 52.0; H, 7.39. IR (Nujol): 2723m, 1653wbr, 1497sh, 1342wsh, 1309vw, 1290vw, 1148w, 1030m, 1019m, 1004sh, 941w, 929w, 860wbr, 775vw, 728m, 719sh, 695w, 668vw, 636w, 626w, 611w, 589w, 464w, 408wbr, 259vs cm^{-1}. ^{1}H NMR (C_6D_6, 31°C): ∂ 1.97 (s). ^{13}C NMR (C_6D_6, 31°C): ∂ 114.0 (s, $\underline{C}_5Me_5$), ∂ 11.10 (q, $^{1}J_{CH}$= 124 Hz, $C_5(\underline{C}H_3)_5$). The mass spectrum showed M^+ (358), as well as

sequential ring loss (the base peak was 273, $(Me_5C_5)Ba$), and ring fragmentation. The molecular ion isotopic cluster could be simulated (all percentages relative to 408 as 100%):

M/e	Simulated %	Experimental %
404	3.23	2.90
405	9.59	10.99
406	12.67	15.29
407	17.62	16.97
408	100	100
409	21.85	27.17
410	2.30	2.26

$(Me_5C_5)_2Ba(bipy)$

Bis(pentamethylcyclopentadienyl)barium (0.21g, 0.51 mmol) was dissolved in 30 mL of toluene and added with stirring to a toluene solution (10 mL) of bipyridine (0.080 g, 0.51 mmol). The resulting bright red solution was reduced in volume to 15 mL and cooled to -25°C, producing orange-red needles. A second crop of needles was isolated from the mother liquors by concentrating further and cooling. The total yield from both crops was 0.21g (71%), MP 317-319°C. IR (Nujol): 3045m, 2721m, 1590m, 1571w, 1488s, 1437vs, 1379s, 1341sh, 1312m, 1244w, 1216vw, 1174w, 1155m, 1043w, 1020w, 1001m, 962vwbr, 937vwbr, 902w, 892sh, 764vs, 738w, 726w, 655w, 639w, 620w, 412w, 306m, 258vsbr cm^{-1}. Anal. Calcd for $C_{30}H_{38}N_2Ba$: C, 63.9; H, 6.80; N, 4.97. Found: C, 63.0; H, 6.92; N, 4.96. The insolubility of the compound precluded the possibility of obtaining the NMR spectrum.

$(Me_5C_5)_2Ba(CNR)_2$ (R = 2,6-dimethylphenyl)

Bis(pentamethylcyclopentadienyl)barium (0.18g, 0.44 mmol) was dissolved in 15 mL of warm toluene and added to a toluene solution (15

mL) of 2,6-dimethylphenylisocyanide (0.12g, 0.91 mmol), yielding a pale yellow solution. The volume was reduced to 5 mL, and the solution was cooled to -25°C, producing yellow prisms which seemed to lose solvent under vacuum. A second crop of crystals was isolated from the mother liquors by concentrating and cooling the solution. The combined yield was 0.24g (80%). The compound darkened slowly above 175°C, and melted irreversibly to a red-orange oil at 211-212°C. IR (Nujol): 2716m, 2138vs, 2115m, 1939w, 1865w, 1789vw, 1739vw, 1664wbr, 1603sh, 1590w, 1544vw, 1485m, 1443s, 1296w, 1167m, 1151w, 1095sh, 1082m, 1034m, 1019w, 988vw, 973vw, 922w, 896vw, 801m, 773vs, 721m, 637w, 498vw, 465vw, 373m, 357w, 258vsbr cm^{-1}. Anal. Calcd for $C_{38}H_{48}N_2Ba$: C, 68.1; H, 7.23; N, 4.18. Found: C, 65.8; H, 7.13; N, 4.20. ^{1}HNMR (C_6D_6, 31°C): ∂ 6.60 (m, 6H), ∂ 2.29 (s, 30H), ∂ 2.11 (s, 12H). A sample of the compound with approximately two excess equivalents of ligand was prepared in d^8-toluene, and the ^{1}HNMR observed as a function of temperature. At room temperature, the methyl resonance of the pentamethylcyclopentadienyl ligands was at ∂ 2.30, and a single methyl resonance was observed for the isocyanide at ∂ 2.11, indicating exchange of free and coordinated ligand. at -80°C, the methyl resonance due to the isocyanide had broadened slightly (∂ 2.09, $\nu_{1/2}$= 10 Hz), but separate signals were not observed for free and coordinated ligand.

$(Me_5C_5)_2Ba(PEt_3)$

Bis(pentamethylcyclopentadienyl)barium (0.20g, 0.49 mmol) was dissolved in 30 mL of warm toluene, and added to a degassed solution of triethylphosphine (0.14 mL, 0.12g, 1.0 mmol) in pentane (10 mL). This

solution was filtered, and the solvent was removed to give a pale yellow oil. The oil was stored at -25°C for several days, during which time it crystallized to give white feathery crystals. These were washed at -25°C with precooled pentane, and dried under vacuum. The yield was 0.15g (58%), MP 250-255°C. IR (Nujol): 2723m, 1660wbr, 1441m, 1342w, 1314vw, 1288w, 1288w, 1140s, 1078vs, 1041s, 1017sh, 979sh, 944m, 928sh, 869wbr, 784w, 770s, 751sh, 725m, 699m, 673w, 663sh, 643sh, 626w, 612w, 591vw, 546vw, 520w, 478vw, 466vw, 449w, 407mbr, 374w, 355w, 320sh, 258vsbr cm^{-1}. Anal. Calcd for $C_{26}H_{45}PBa$: C, 59.4; H, 8.61; P, 5.89. Found: C, 54.2; H, 8.41; P, 2.09. ^{1}HNMR (C_6D_6, 30°C): ∂ 1.96 (s, 30H), ∂ 1.17 and ∂ 0.89 (both multiplets, combined integration 15H). $^{31}P\{^{1}H\}$NMR (C_6D_6, 30°C): δ -20.3 ppm (s).

Chapter Two

$(Me_5C_5)_2Yb(\mu\text{-}C_2H_4)Pt(PPh_3)_2$

Bis(pentamethylcyclopentadienyl)ytterbium(II) (0.18g, 0.41 mmol) was dissolved in 20 mL of toluene and added to a toluene solution (30 mL) of (η2-ethylene)bis(triphenylphosphine)platinum(0) (0.30g, 0.40 mmol). The resulting deep red solution was stirred for 4 h. The solution was concentrated to a volume of ca. 10 mL, and cooled to -25°C. The product was isolated as deep red needles. A second crop was obtained from the mother liquor by concentrating and cooling. The combined yield was 0.27g, 56%, MP 178-180°C (dec). Anal. Calcd for $C_{58}H_{64}P_2PtYb$: C, 58.5; H, 5.43; P, 5.20. Found: C, 58.1; H, 5.31; P, 4.61. IR (Nujol): 3050w, 2723w, 1958vw, 1888vw, 1814vw, 1665vw, 1590w, 1571w, 1477s, 1435vs, 1330vw, 1308w, 1181m, 1159m, 1123sh, 1092vs, 1070sh, 1026m, 998m, 968w, 932vw, 918vw, 902vw, 846w, 799m, 774vs, 694vs br, 620vw, 587vw, 540s, 509vs br, 493sh, 448sh, 437m, 421m, 374w, 274s cm^{-1}. ^1H NMR (C_6D_6, 30°C, 90 MHz): δ 7.47 (m), δ 6.93 (m, total integration of phenyl region: 30H), δ 2.18 (t, 4H, $^2J_{PtH}$ = 56 Hz, broadened due to unresolved ^{31}P coupling), δ 2.08 (s, 30H). $^{31}P\{^1H\}$NMR (C_6D_6, 30°C, 90 MHz): δ 33.0 (t, $^1J_{PtP}$ = 3807 Hz).

$(Me_5C_5)_2Yb(\mu\text{-}C_2H_4)Ni(PPh_3)_2$

Bis(pentamethylcyclopentadienyl)ytterbium (0.26g, 0.59 mmol) was dissolved in pentane (30 mL) and added with stirring to a toluene solution (5 mL) of (η^2-ethylene)bis(triphenylphosphine)nickel (0.36g, 0.59 mmol). The deep green solution was filtered and cooled to -78°C,

resulting in the formation of dark green blocks (0.46g, 74%). Any attempt to concentrate the mother liquors resulted in the decomposition of the solution. Higher yields of microcrystalline material were obtained when the reaction was conducted entirely in hexane, but attempts to recrystallize the material failed (the dissociated ligand in solution decomposed with loss of ethylene under reduced pressure). The compound melted and decomposed at 165-169°C. Anal. Calcd for $C_{58}H_{64}P_2NiYb$: C, 66.0; H, 6.13; P, 5.87. Found: C, 65.2; H, 6.15; P, 4.84. IR (Nujol): 2724w, 1955vw, 1971vw, 1893vwbr, 1815vw, 1662wbr, 1588w, 1576w, 1479s, 1433vs, 1307w, 1181m, 1170m, 1160m, 1142s, 1119s, 1092vs, 1071m, 1026s, 998m, 975vw, 968vw, 929vw, 918vw, 872vwbr, 849vwbr, 831w, 778vw, 757m, 749m, 744s, 741s, 737m, 722sbr, 704sh, 696vsbr, 685sh, 619w, 586vw, 543s, 532s, 519vs, 509s, 505sh, 487m, 452w, 436m, 418w, 274m cm^{-1}. ^{1}HNMR (C_6D_6, 30°C, 90 MHz): δ 7.48 (m), δ 6.94 (m, total integration of phenyl region: 30H), δ 2.03 (s, $\nu_{1/2}$ = 7.5 Hz, 30H), δ 2.34 (s, $\nu_{1/2}$ = 10 Hz, 4H). $^{31}P\{^1H\}$NMR (C_6D_6, 30°C, 36.2 MHz): δ 34.4 ppm (the value for $(C_2H_4)Ni(PPh_3)_2$ is reported as δ 31 ppm[14]).

Reaction of $(Me_5C_5)_2Yb$ with $(MeC{\equiv}CMe)Pt(PPh_3)_2$

Bis(pentamethylcyclopentadienyl)ytterbium (0.20g, 0.45 mmol) was dissolved in 20 mL of hexane and added with stirring to a solution of $(MeC{\equiv}CMe)Pt(PPh_3)_2$ in a minimum volume of toluene (2-3 mL). No color change was detected. The solution was filtered and cooled to -78°C, producing a white precipitate. This precipitate was isolated, and was identified by IR spectroscopy and MP as the platinum starting material.

$(Me_5C_5)_2Yb(\eta^2\text{-}MeC{\equiv}CMe)$

Bis(pentamethylcyclopentadienyl)ytterbium (0.22g, 0.50 mmol) dissolved in pentane (15 mL) was added to a degassed solution of 2-butyne (0.50 mL, 0.35g, 6.5 mmol) in pentane (5 mL). The solution color changed immediately from orange to deep red. The volume of this solution was reduced to 5 mL, and the solution was cooled to -78°C for 12h, resulting in the formation of dark purple-red needles. When isolated and exposed to vacuum, the needles seemed to lose solvent, but did not crumble or change color. The yield was 0.18g (73%), MP 170-173°C. IR (Nujol): 2722m, 1653vwbr, 1492s, 1444vs, 1152m, 1132vw, 1093m, 1063w, 1036sh, 1019s, 997w, 956wbr, 937wbr, 904vw, 876vw, 724w, 705mbr, 676sh, 668m, 622w, 588vw, 549vw, 528vw, 440brsh, 373mbr, 306sbr, 275vsbr cm^{-1}. Anal. Calcd for $C_{24}H_{36}Yb$: C, 57.9; H, 7.31. Found: C, 54.6; H, 7.33. ^{1}HNMR (C_6D_6, 30°C): δ 1.99 (s, 30H), δ 1.27 (s, 6H). ^{13}CNMR{^{1}H} (C_6D_6, 30°C): δ 113.4 ($\underline{C}_5Me_5$), δ 76.86 ($\underline{C}Me$), δ 10.88 ($C_5(\underline{C}H_3)_5$), δ 3.73 ($C(\underline{C}H_3)$). ^{1}HNMR of 2-butyne (C_6D_6, 30°C): δ 1.52 (s). ^{13}CNMR of 2-butyne (C_6D_6, 30°C): δ 74.60 (s, $\underline{C}Me$), δ 3.08 (q, $^1J_{CH}$ = 124.7 Hz, $C(\underline{C}H_3)$).

$(Me_5C_5)_2Ca(\eta^2\text{-}MeC{\equiv}CMe)$

Bis(pentamethylcyclopentadienyl)calcium (0.18g, 0.58 mmol) was dissolved in pentane (15 mL) was added to a degassed solution of 2-butyne (0.5 mL, 0.35g, 6.5 mmol) in pentane (5 mL). The solution remained colorless. The volume of this solution was reduced to 5 mL, and the solution was cooled to -78°C for 12h, resulting in the formation of white crystals. The yield was 0.14g (66%), MP 192-195°C. IR

(Nujol): 2726m, 1665wbr, 1613vw, 1492s, 1443vs, 1347m, 1318vw, 1290w, 1237m, 1146m, 1090sh, 1093m, 1080vs, 1035sh, 1019s, 1006s 973vw, 955wbr, 935s, 748sh, 735sh, 722w, 691vw, 642w, 628m, 619m, 599vw, 586vw, 553sh, 544w, 517w, 455s, 404shbr, 349vsbr, 327sh, 313shbr, 289mbr cm^{-1}. Anal. Calcd for $C_{24}H_{36}Ca$: C, 79.0; H, 9.97. Found: C, 77.7; H, 9.75. ^{1}HNMR (C_6D_6, 25°C): ∂ 1.99 (s, 30H), ∂ 1.26 (s, 6H). ^{13}CNMR{^{1}H} (C_6D_6, 30°C): ∂ 113.4 ($\underline{C}_5Me_5$), ∂ 76.86 ($\underline{C}Me$), ∂ 10.88 ($C_5(\underline{C}H_3)_5$), ∂ 3.73 ($C(\underline{C}H_3)$). ^{1}HNMR of 2-butyne (C_6D_6, 30°C): ∂ 1.52 (s). ^{13}CNMR of 2-butyne (C_6D_6, 30°C): ∂ 74.60 (s, $\underline{C}Me$), ∂ 3.08 (q, ^{1}J = 124.7 Hz, $C(\underline{C}H_3)$).

$\underline{(Me_5C_5)_2Yb(\eta^2\text{-}PhC{\equiv}CPh)}$

Bis(pentamethylcyclopentadienyl)ytterbium (0.29g, 0.65 mmol) was dissolved in 20 mL of hexane and added to a hexane solution (10 mL) of diphenylacetylene (0.12g, 0.67 mmol), yielding a dark orange solution. The volume of the solution was reduced to 10 mL, and the solution was cooled to -25°C, producing black blocks. A second crop of blocks was obtained from the mother liquors by concentrating and cooling. The combined yield was 0.37g (91%), MP 121-123°C. IR (Nujol): 3102w, 3085w, 3054m, 3035m, 3022m, 2725w, 1958vw, 1885vw, 1809vw, 1750vw, 1664wbr, 1605m, 1573w, 1500s, 1444vs, 1310vw, 1179w, 1160sh, 1152w, 1071m, 1028m, 1018sh, 999w, 912w, 844w, 753vs, 690vs, 622w, 590vw, 537m, 510w, 498vw, 488vw, 376mbr, 276s cm^{-1}. Anal. Calcd for $C_{34}H_{40}Yb$: C, 65.7; H, 6.50. Found: C, 64.9; H, 6.62. ^{1}HNMR (C_6D_6, 30°C): δ 1.95 (s, 30H), δ 6.95 (m), δ 7.47 (m, combined integration of phenyl region 10H). $^{13}C\{^{1}H\}$NMR (C_6D_6, 30°C): δ 10.69 ($C_5\underline{Me}_5$), δ 114.0 ($\underline{C}_5Me_5$), δ 123.6 ($\underline{C}Ph$), δ 128.7, δ 131.8 (Ph resonances). Other phenyl resonances were obscured by

solvent peak. ^{1}HNMR of PhC≡CPh (C_6D_6, 30°C): δ 7.48 (m), δ 6.98 (m). $^{13}C\{^{1}H\}$NMR of PhC≡CPh (C_6D_6, 30°C): δ 124.0 (C≡Ph), δ 128.4, δ 128.6, δ 131.9 (Ph resonances).

$(Me_5C_5)_2Yb(\eta^2$-t-BuC≡CMe)

Bis(pentamethylcyclopentadienyl)ytterbium (0.25g, 0.56 mmol) was dissolved in 15 mL of hexane and added to a degassed solution of 4,4-dimethyl-2-pentyne (0.15 mL, 0.11g, 1.1 mmol) in hexane (5 mL), resulting in a darkening of the orange color of the solution of the ytterbium complex. The solution was reduced to 5 mL in volume, and was cooled to -25°C, producing dark green-black feathers. The yield was 0.25g (83%), MP 147-150°C. IR (Nujol): 2727m, 2034vwbr, 1654wbr, 1445s, 1303vw, 1204w, 1151m, 1020m, 955w, 934w, 905vw, 725sh, 707m, 624w, 589w, 544w, 511vw, 477vw, 375mbr, 273vs cm^{-1}. Anal. Calcd for $C_{27}H_{42}Yb$: C, 60.1; H, 7.86. Found: C, 59.1; H, 7.90. ^{1}HNMR (C_6D_6, 20°C): δ 2.00 (s, 30H), δ 1.41 (s, 3H), δ 1.13 (s, 9H). $^{13}C\{^{1}H\}$NMR (C_6D_6, 20°C): δ 113.7 (C_5Me_5), δ 88.82 (C≡C), δ 74.80 (C≡C), δ 30.42 (Me_3CC≡C), δ 27.65 (Me_3CC≡C), δ 11.09 (C_5Me_5), δ 3.77 (C≡CMe). ^{1}HNMR of t-BuC≡CMe (C_6D_6, 20°C): δ 1.54 (s, 3H), δ 1.14 (s, 9H). $^{13}C\{^{1}H\}$NMR of t-BuC≡CMe (C_6D_6, 20°C): δ 87.84 (C≡C), δ 74.03 (C≡C), δ 31.56 (Me_3CC≡C), δ 27.58 (Me_3CC≡C), δ 3.38 (C≡CMe).

$(Me_5C_5)_2Yb(\eta^2$-PhC≡CMe)

Bis(pentamethylcyclopentadienyl)ytterbium (0.28g, 0.63 mmol) was dissolved in 20 mL of hexane and added to a degassed solution of 1-phenyl-1-propyne (0.16 mL, 0.15g, 1.3 mmol) in hexane (5 mL), resulting

in a darkening of the orange color of the solution of the ytterbium complex. The volume of the solution was reduced to 5 mL, and it was cooled to -25°C, producing dark brown-black needles. The yield of the adduct was 0.30g (85%), MP 126-129°C. IR (Nujol): 3096vw, 3081w, 3060w, 3051m, 2723m, 1987vw, 1935vw, 1887vw, 1815vw, 1766vw, 1663wbr, 1597m, 1570m, 1487s, 1440vs, 1315vw, 1284vw, 1180w, 1161w, 1151w, 1074w, 1061sh, 1028sh, 1017m, 996w, 973vw, 964vw, 918w, 848vw, 755vs, 723w, 698s, 668w, 624w, 590vw, 528m, 516vw, 367wbr, 308sh, 280vs cm^{-1}. Anal. Calcd for $C_{29}H_{38}Yb$: C, 62.2; H, 6.86. Found: C, 61.8; H, 6.98. ^{1}HNMR (C_6D_6, 20°C): δ 7.27 (m), δ 6.93 (m, total integration of phenyl region 5H), δ 1.99 (s, 30H), δ 1.48 (s, 3H). $^{13}\{^{1}H\}$NMR (C_6D_6, 20°C): δ 130.6, δ 129.3, δ 129.2, δ 122.4 (phenyl resonances), δ 113.7 ($\underline{C}_5Me_5$), δ 87.14 ($\underline{C}\equiv C$), δ 80.85 ($C\equiv\underline{C}$), δ 11.01 ($C_5\underline{Me}_5$), δ 4.57 ($C\equiv C\underline{Me}$). ^{1}HNMR of PhC≡CMe (C_6D_6, 20°C): δ 7.42 (m), δ 7.01 (m, total integration of phenyl region 5H), δ 1.67 (s, 3H). $^{13}C\{^{1}H\}$NMR of PhC≡CMe (C_6D_6, 20°C): δ 131.8, δ 128.5, δ 127.7, δ 124.8 (phenyl resonances), δ 86.14 ($\underline{C}\equiv C$), δ 80.46 ($C\equiv\underline{C}$), δ 4.00 ($C\equiv C\underline{Me}$).

Polymerization of Ethylene by $(Me_5C_5)_2Yb$

In a representative reaction, bis(pentamethylcyclopentadienyl)-ytterbium (0.10g, 0.23 mmol) was dissolved in ca. 25 mL of hexane (or toluene) and transferred to a thick-walled pressure bottle. Ethylene was admitted to the bottle, and the pressure released three times to flush the air space above the solution. Finally, ethylene was admitted to a pressure of 12 atm., producing an immediate color change from orange (or red) to green, and the formation of cloudiness due to

suspended polyethylene; the solution was stirred for 2 - 4 h. The pressure was then released, whereupon the color reverted to orange (or red), and the bottle was opened to air. The solution was hydrolyzed with dilute HCl, and the polymer formed was washed with acid, water, and acetone, and dried in the air. In polymerization inhibition experiments, the inhibiting gas (CO, H_2, D_2, Xe, or CH_4) was first admitted to a pressure of 7 atm., and then ethylene was added to bring the total pressure above the solution to 14 atm. Any color changes were noted. In all cases, the ytterbium complex could be recovered by removing the solvent under reduced pressure. In polymerization termination experiments, ethylene was first admitted to a pressure of 7 atm., and the polymerization allowed to proceed for ca. 5 min. The inhibiting gas was then admitted to bring the total pressure above the solution to 14 atm. The reaction was then stirred for 6 - 8h. After the pressure was released, the polymer was isolated as before.

Reaction of $(Me_5C_5)_2Yb$ with Propylene

Bis(pentamethylcyclopentadienyl)ytterbium (0.080g, 0.18 mmol) was dissolved in 20 mL of pentane and transferred to a thick-walled glass pressure bottle. The solution was pressurized to 5 atm. with propylene, producing a color change from orange to green. The solution was allowed to stir for 2 days, but no polymer was formed, and the pressure of propylene did not decline significantly. The solution was then heated to 100°C for 3 days with stirring. No reaction was apparent, either in the formation of polymer, or in a reduction of the pressure within the vessel. When the pressure was released, the color reverted to orange.

The ytterbium complex was recovered by removing the solvent under reduced pressure.

Reaction of $(Me_5C_5)_2Yb$ with Gases (CO, H_2, D_2, N_2, Xe, and CH_4)

In a typical reaction, bis(pentamethylcyclopentadienyl)ytterbium (0.30g, 0.68 mmol) was dissolved in 25 mL of pentane, and the orange solution was transferred by stainless steel cannula to a thick-walled pressure bottle equipped with a magnetic stir bar. The gas was admitted and then the pressure released three times to flush the air space above the solution. The gas was then admitted a final time to a pressure of 150 psig (approximately 10 atm.), or to the condensation pressure of the gas. The solution was stirred for 1-12 h (depending on the gas), and any color changes noted. In the case of CO, IR studies were carried out by releasing the gas pressure after 4h, and immediately transferring a portion of the solution to a 0.5 mm KBr solution cell by cannula. In all cases, $(Me_5C_5)_2Yb$ was recovered by removing the solvent under reduced pressure; the identity of the ytterbium complex was verified by IR and MP.

Reaction of $(Me_5C_5)_2M$ with C_2H_4 (M = Ca, Eu, and Sm)

In each case, 0.030-0.050g of compound was dissolved in 30 mL of hexane and transferred to a thick-walled pressure bottle. The solutions were pressurized to 10 atm. with ethylene. When M = Ca or Eu, there was no apparent change in the color of the solution, and after 1 day stirring under ethylene, there was no appreciable formation of polyethylene. When M = Sm, polyethylene formed rapidly, but within

minutes the solution changed color from green to yellow, and polymerization slowed. The polymer formed was isolated in the same manner as in the ytterbium reaction.

$\underline{[(Me_5C_5)_2Yb]_2(\mu\text{-}O)}$

From $\underline{(Me_5C_5)_2Yb}$

Bis(pentamethylcyclopentadienyl)ytterbium (0.41g, 0.92 mmol) was dissolved in 40 mL of pentane, and the solution was transferred to a thick-walled pressure bottle. The bottle was pressurized to 3 atm. with N_2O. Within 10 minutes, the color of the solution had lightened, and orange precipitate had begun to appear. The solution was stirred for 4 h. After the pressure was released, the solution (along with the precipitate) was transferred to a Schlenk flask, and the volume was reduced to 5 mL. The solution was cooled to -25°C to complete precipitation of the solid. The supernatent solution was removed, and the orange solid was recrystallized from a minimum of hot toluene. The yield was 0.23g (55%).

From $\underline{(Me_5C_5)_2Yb(OEt_2)}$

Bis(pentamethylcyclopentadienyl)ytterbium(diethylether) (0.26g, 0.50 mmol) was dissolved in 20 mL of toluene and transferred to a thick-walled pressure bottle. The solution was pressurized to 3 atm. with N_2O. The solution rapidly changed color from green to orange. The reaction mixture was allowed to stir for 4 h. The solution was transferred back into a Schlenk flask and the toluene was removed under reduced pressure, leaving an orange oil. The oil was dissolved in 2 mL

of pentane, and this solution was cooled to -78°C. The yield was 0.040g (18%).

The compound melted at 334-337°C. Anal. Calcd for $C_{40}H_{60}OYb_2$: C, 53.2; H, 6.70. Found: C, 52.7; H, 6.78. IR (Nujol): 2728w, 1650vwbr, 1497m, 1302vw, 1168sh, 1154w, 1133sh, 1024m, 957vw, 895sh, 863wbr, 756vw, 735sh, 724w, 695m, 673vs, 641w, 625m, 593wbr, 566vw, 478vwbr, 432brsh, 384mbr, 309sh, 301vsbr, 283sh cm^{-1}. ^1H NMR (C_6D_6, 31°C): δ 24.40 (s, $\nu_{1/2}$ = 980 Hz). The EI mass spectrum revealed M^+ (904) as well as fragments corresponding to $(Me_5C_5)_3Yb_2O$ (767), $(Me_5C_5)_2Yb_2O$ (635), $(Me_5C_5)Yb_2O$ (497), $(Me_5C_5)_2Yb$ (444), Yb_2O (364), and products of ring fragmentation. The molecular ion isotopic cluster profile compared well with that calculated for $C_{40}H_{60}OYb_2$ (all percentages relative to 902 as 100%):

M/e	Simulated %	Experimental %
897	3.82	11.9
898	15.1	20.2
899	34.6	44.0
900	58.3	45.2
901	85.5	61.3
902	100	100
903	90.9	78.6
904	92.4	87.5
905	49.5	46.4
906	45.3	25.0
907	16.5	19.0
908	9.70	11.3
909	3.27	-

$[(Me_5C_5)_2Sm]_2(\mu\text{-}O)$

From $(Me_5C_5)_2Sm$

Bis(pentamethylcyclopentadienyl)samarium (0.31g, 0.74 mmol) was dissolved in 30 mL of toluene, and the solution was transferred to a thick-walled pressure bottle. The vessel was pressurized to 3 atm. with

N_2O, producing a color change in the reaction mixture from green to yellow. The reaction was stirred for 6 h. The solution was transferred to a Schlenk flask, and the volume was reduce to ca. 10 mL. The solution was cooled to -25°C, producing yellow flakes. A second batch of crystals were obtained from the mother liquor by concentrating and cooling. The total yield was 0.19g (60%).

From $(Me_5C_5)_2Sm(OEt_2)$

Bis(pentamethylcyclopentadienyl)samarium(diethylether) (0.51g, 1.0 mmol) was dissolved in 50 mL of toluene and transferred to a Fischer-Porter pressure apparatus. The solution was pressurized to 3 atm. with N_2O, whereupon the color changed from green to yellow within 10 min. The reaction was allowed to stir for 4 h. The solution was then transferred back to a Schlenk flask, and the volume was reduced to 20 mL. When cooled to -25°C, the solution produced very thin yellow plates. A second crop of product was isolated from the mother liquor by concentrating and cooling. The combined yield of both crops was 0.19g (43%).

The compound gradually darkened irreversibly when heated above 265°C. IR (Nujol): 2727w, 1670vwbr, 1603vwbr, 1317vw, 1295vw, 1187vw, 1149m, 1091s, 1066sh, 1036w, 1022sh, 1011m, 973shbr, 950mbr, 937shbr, 876vwbr, 798w, 729m, 695vw, 681vw, 658m, 634s, 605vs, 589s, 549vw, 516vw, 488vw, 464vw, 451vw, 401wbr, 374wbr, 350vw, 303vsbr, 279sh cm^{-1}. ^{1}HNMR (C_6D_6, 30°C): δ 0.06 (s, $\upsilon_{1/2}$ = 9.5 Hz; reported value δ 0.06 in C_6D_6)[13]. The EI mass spectrum did not show a molecular ion; the highest visible fragment was $M^+ - (C_5Me_5)$ (722). Other fragments present were

$(Me_5C_5)_2Sm_2O$ (586), $(Me_5C_5)Sm_2O$ (453), $(Me_5C_5)_2Sm$ (422), Sm_2O (318), $(Me_5C_5)Sm$ (287), and those due to ring fragmentation.

Reaction of $[(Me_5C_5)_2Yb]_2(\mu\text{-}O)$ with C_2H_4

$[(Me_5C_5)_2Yb]_2(\mu\text{-}O)$ (0.080g, 0.089 mmol) was dissolved in 20 mL of toluene and transferred to a thick-walled glass pressure bottle. The solution was pressurized to 10 atm. with ethylene, and allowed to stir for 24 h. No polymer formed during this time, and no change in color was observed.

$(Me_5C_5)_2Yb[CH(SiMe_3)_2]$

The compound was prepared by an adaptation of a literature method used to prepare other lanthanide bis(trimethylsilyl)methyl complexes[15]. $(Me_5C_5)_2Yb(Cl)_2Li(OEt_2)_2$ (1.23g, 1.84 mmol) and $(Me_3Si)_2CHLi$ (0.32g, 1.9 mmol) were suspended in 50 mL of toluene at 0°C and stirred for 12 h. The solvent was then removed under reduced pressure. The purple residue was extracted with 35 mL of pentane, filtered, concentrated to 15 mL in volume, and cooled to -25°C, producing large purple blocks. A second crop of crystals was isolated from the mother liquors by concentrating and cooling. The combined yield of both crops was 0.85g (77%), MP 187-190°C. IR (Nujol): 2729m, 2046vwbr, 1904vw, 1841vw, 1779vw, 1678vw, 1447s, 1314vw, 1256s, 1248sh, 1239vs, 1189vw, 1154w, 1100m, 1061sh, 1032s, 1023sh, 977wbr, 956wbr, 860vsbr, 835vsbr, 816sh, 806sh, 763s, 736w, 723w, 702m, 674sh, 666s, 607w, 588s, 551vw, 389sbr, 304vsbr cm^{-1}. Anal. Calcd for $C_{27}H_{49}Si_2Yb$: C, 53.8; H, 8.21. Found: C, 53.7; H, 8.19. ^{1}HNMR (C_6D_6, 20°C): δ 72.5 (s, $\nu_{1/2}$ = 1000 Hz, 18H), δ 6.76 (s, $\nu_{1/2}$ =

445 Hz, 30H). The molecular ion (M/e = 603) was visible in the EI mass spectrum, as were fragments corresponding to $(Me_5C_5)_2Yb$, $(Me_5C_5)Yb[CH(SiMe_3)_2]$, $(Me_5C_5)Yb$, $Yb[CH(SiMe_3)_2]$, and ligand fragmentation.

Reaction of $(Me_5C_5)_2Yb[CH(SiMe_3)_2]$ with H_2

Bis(pentamethylcyclopentadienyl)[bis(trimethylsilyl)methyl]ytterbium (0.44g, 0.73 mmol) was dissolved in 30 mL and transferred to a thick-walled glass pressure bottle. The solution was pressurized to 10 atm. with H_2 with stirring. After 2 h stirring, the solution color had lightened to pale red, and purple powder had precipitated from solution. The solution was allowed to stir for 12 h, and then the pressure was released, and the purple powder was collected by filtration. The yield of this product was 0.18g (56%), MP 196-197°C (dec.). IR (Nujol): 2724w, 1653wbr, 1486sh, 1445s, 1395m, 1315vw, 1299vw, 1152m, 1021m, 974vw, 956w, 940shbr, 722w, 675vw, 638sh, 620m, 591w, 550vw, 516vw, 486mbr, 382mbr, 324s, 289mbr, 264mbr cm^{-1}. Anal. Calcd for $C_{40}H_{61}Yb_2$: C, 54.1; H, 6.94. Found: C, 51.9; H, 7.07. The compound was sparingly soluble in hydrocarbon solvents, but a NMR sample was prepared by heating the compound in C_6D_6 in a closed system. ^{1}HNMR (C_6D_6, 30°C): δ 7.80 ($\nu_{1/2}$ = 98 Hz). A sample of the compound was hydrolyzed in C_6D_6, and the hyrolysate was examined by ^{1}HNMR spectroscopy. Only C_5Me_5H was observed. A sample of the compound (0.14g, 0.16 mmol) was slurried in 10 mL of toluene, heated to 90°C, and the solvent was removed slowly under vacuum, leaving a brown residue. This residue was extracted with hexane (15 mL) and filtered. The filtrate was reduced to 3 mL in volume

and cooled to -25°C; ca. 0.10g of $(Me_5C_5)_2Yb$ was isolated as green needles which lost solvent and turned brown under vacuum.

The analogous hydrogenolysis was carried out with D_2, and the IR spectrum of the product was recorded. IR of purple powder (Nujol): 2724m, 2041vwbr, 1653vwbr, 1491m, 1443s, 1311vw, 1208vw, 1166w, 1151w, 1023s, 975sh, 929mbr, 872sh, 741sh, 724w, 695vw, 624vw, 590w, 550vw, 444m, 384m, 359w, 322s, 262s cm^{-1}.

The IR spectra of the H_2 and D_2 products are not superimposable; there appears to be a broad feature underneath the region of the H_2 product spectrum from 1300-1400 cm^{-1} which moves to 900-1000 cm^{-1} in the D_2 product, but no single sharp band can be identified as ν Yb-H/D.

Reaction of $(Me_5C_5)_2Yb$ with vinyltrimethylsilane

Bis(pentamethylcyclopentadienyl)ytterbium (0.26g, 0.59 mmol) was dissolved in 20 mL of hexane, and added to a solution of vinyltrimethylsilane (0.43 mL, 0.29g, 2.9 mmol) in hexane (5 mL), resulting in a green solution. The volume was reduced to ca. 5 mL, and the solution was cooled to -25°C, producing large green plates. When the plates were exposed to vacuum, however, they turned brown and crumbled. The IR spectrum of the resulting material showed no evidence of coordinated ligand.

Reaction of $(Me_5C_5)_2Yb$ with ethylene oxide

Bis(pentamethylcyclopentadienyl)ytterbium (0.31g, 0.70 mmol) was dissolved in 35 mL of toluene, and added with stirring to a solution of ethylene oxide (3 mL) in toluene (15 mL). The solution immediately

changed color from red to orange, and became viscous. The mixture was allowed to stir for 8 h. The solvent was removed under reduced pressure, leaving a sticky polymer. This was extracted with 30 mL of pentane and dried in the air. The pentane extract was concentrated to 5 mL, and cooled, producing a small amount of orange powder. The IR spectrum of this powder showed a strong band at 667 cm^{-1}, matching that in the spectrum of $[(Me_5C_5)_2Yb]_2(\mu\text{-}O)$.

Reaction of $(Me_5C_5)_2Yb$ with cyclopropane

Bis(pentamethylcyclopentadienyl)ytterbium (0.19g, 0.43 mmol) was dissolved in 25 mL of pentane and transferred to a thick-walled pressure bottle. The solution was pressurized with cyclopropane until the volume of the solution had increased noticeably. The solution was allowed to stir for 24h. No reaction was observed. The pressure was released, and the ytterbium compound was recovered by removing the pentane under reduced pressure.

Reaction of $(Me_5C_5)_2Yb$ with styrene

Bis(pentamethylcyclopentadienyl)ytterbium (0.14g, 0.32 mmol) was dissolved 30 mL of pentane, and added to a degassed solution of styrene (3 mL) in pentane (5 mL). The solution immediately turned deep green. The solution was stirred for 12 h, but there was no evidence of polymer formation.

Reaction of $(Me_5C_5)_2Yb$ with allene

Bis(pentamethylcyclopentdienyl)ytterbium (0.35g, 0.79 mmol) was

dissolved in pentane (20 mL) and transferred to a thick-walled glass pressure bottle. Approximately 1 mL of allene was condensed into this solution with stirring. The solution immediately turned dark green-brown. After stirring 20 min., the color of the solution turned red. The mixture was allowed to react for 4 h. The volume of the solution was reduced to 3 mL, and it was cooled to -25°C, producing some brown powder. Attempts to recrystallize this material failed. The solvent was removed from the supernatent under reduced pressure, leaving some red oil. IR (Nujol) of the brown powder: 2725m, 2168m, 2157sh, 1620sh, 1543s, 1511s, 1489sh, 1439s, 1422sh, 1311m, 1210vw, 1163vw, 1154vw, 1037sh, 1021m, 990w, 954vw, 922vw, 864s, 772vs, 722vw, 705sh, 695sh, 682s, 664s, 633s, 624s, 594m, 565w, 554sh, 461w, 425sh, 405sh, 380mbr, 302vsbr cm^{-1}. A ^{1}HNMR spectrum of the material showed ten paramagnetic resonances, with the three largest ones appearing at δ 10.47 ($\nu_{1/2}$ = 250 Hz), δ -4.66 ($\nu_{1/2}$ = 250 Hz), and δ -8.68 ($\nu_{1/2}$ = 180 Hz), in a relative integration of 1:2:1.

Reaction of $(Me_5C_5)_2Yb$ with 1,2-butadiene

Bis(pentamethylcyclopentadienyl)ytterbium (0.31g, 0.70 mmol) was dissolved in 20 mL of pentane. To this was added a pentane solution (5 mL) of 1,2-butadiene (ca. 0.4 mL) with stirring. The orange color of the ytterbium complex in solution changed to dark green-brown. After stirring 1 h, the solution color had changed again to deep red. The mixture was allowed to stir for another 2h. The volume of the solution was then reduced to 5 mL, and the solution was cooled to -78°C, producing red crystals (0.25 g, 72%). The compound was identified as

$(Me_5C_5)_2Yb(\eta^2\text{-MeC}\equiv\text{CMe})$ by examination of its IR spectrum, MP, ^1H and $^{13}C\{^1H\}$NMR spectra.

Reaction of $(Me_5C_5)_2Yb$ with 1,3-butadiene

Bis(pentamethylcyclopentadienyl)ytterbium (0.45g, 1.0 mmol) was dissolved in 30 mL of pentane and was transferred to a thick-walled glass pressure bottle. Approximately 1 mL of butadiene was condensed into the solution. The solution turned dark orange-brown immediately. After stirring for 1 h, the solution had turned orange-red. The mixture was allowed to react for 4 h. The volume of the solution was then reduced to 5 mL, and it was cooled to -25°C. This resulted in the precipitation of ca. 0.20 g of red powder. When the solvent was removed from the filtrate, an orange oil remained. IR (Nujol) of the red powder: 2724w, 1559m, 1310w, 1271w, 1259w, 1237vw, 1198w, 1152w, 1135w, 1023m, 996w, 967w, 913vw, 809s, 797sh, 724m, 699m, 675m, 629vw, 616vw, 590w, 551vw, 517vw, 385wbr, 305vs cm^{-1}. A ^{1}HNMR spectrum of the powder showed four paramagnetic resonances: δ 11.96 ($\nu_{1/2}$ = 50 Hz, relative integration 5), δ 6.00 ($\nu_{1/2}$ = 60 Hz), δ 5.49, and δ 5.16 (overlapping resonances, combined relative integration 3).

$(Me_5C_5)_2Yb$(2,4-hexadiene)

Bis(pentamethylcyclopentadienyl)ytterbium (0.37g, 0.83 mmol) was dissolved in 20 mL of pentane, and was added to a degassed solution of 2,4-hexadiene (mixed isomers, 0.19 mL, 0.14g, 1.7 mmol) in pentane (5 mL). The solution immediately turned dark brown-orange. The volume of the solution was reduced to 5 mL, and it was cooled to -78°C, producing

0.18g (41%) of dark green crystals, MP 90-97°C (melted and bubbled). IR (Nujol): 2725w, 1651wbr, 1615vw, 1444s, 1152m, 1023s, 999sh, 960w, 933m, 924m, 917m, 860w, 705m, 678w, 666m, 620w, 591vw, 389wbr, 304sh, 274s cm^{-1}. Anal. Calcd for $C_{26}H_{40}Yb$: C, 59.4; H, 7.68. Found: C, 58.8; H, 7.77. ^{1}HNMR (C_6D_6, 30°C): δ 5.94 (m, 4H), δ 1.98 (s, 30H), δ 1.46 (s), δ 1.40 (s, combined integration 6H). ^{1}HNMR of 2,4-hexadiene (C_6D_6, 30°C): δ 6.07 (m), δ 5.37 (m), δ 1.63 (s), δ 1.56 (s).

Reaction of $(Me_5C_5)_2Yb$ with AgF

Bis(pentamethylcyclopentadienyl)ytterbium (0.30g, 0.68 mmol) was dissolved in 40 mL of toluene, added to silver fluoride (0.29g, 2.3 mmol), and stirred for 14 h, resulting in the precipitation of silver metal and some dark brown solid from a red solution. The solution was warmed to dissolve precipitated product, and filtered warm. The volume of the filtrate was reduced to 10 mL, and the solution was heated to dissolve all solid. Slow cooling yielded a product which appeared to consist of two different kinds of crystals: green-brown blocks and a few red blades. A second batch of crystals was isolated by reducing the volume of the mother liquor to 3 mL, heating the solution to dissolve precipitate, and cooling it slowly to room temperature. This second batch of crystals consisted primarily of the red product. The total amount of solid isolated was 0.14g; individual yields could not be accurately assessed. Repeated recrystallization from hot toluene increase the amount of the red product in the product mixture. If the reaction mixture was heated in toluene to 90°C for 6-8 h with stirring, only the red product was isolated (0.08g, 27% based on Yb).

Characterization of the two compounds was effected by manual separation of the crystals.

$[(Me_5C_5)_2Yb](\mu\text{-}F)$ - Green-Brown Blocks

The compound melted with decomposition at 290°C. Anal. Calcd for $C_{40}H_{60}Yb_2F$: C, 53.0; H, 6.69. Found: C, 51.5; H, 6.57. IR (Nujol): 2723m, 1652vwbr, 1491m, 1442vs, 1190sh, 1154m, 1100s, 1065m, 1022s, 958w, 934sh, 890vw, 819vw, 730w, 718sh, 696vw, 667w, 625w, 592vw, 568vw, 552vw, 516vw, 501vw, 452sh, 434vs, 398w, 377vw, 363vw, 326vs, 303s, 282sh, 267vs cm^{-1}. The compound was completely insoluble in non-coordinating solvents. The ^{1}HNMR in CD_3CN (30°C) showed no resonances. The highest fragment in the EI mass spectrum was M^+ (906). The rest of the mass spectrum showed the same fragments as that of the tetranuclear complex.

Powder Pattern Data for $[(Me_5C_5)_2Yb]_2(\mu\text{-}F)$

Index	d_{hkl} (meas)	d_{hkl} (calc)	d(calc)/d(meas)	I
1 0 1	9.7445	10.136	1.0402	s
0 0 2	8.1728	8.1171	0.9932	s+
2 0 0	7.8824	7.9033	1.0027	m
0 2 0	7.2104	7.1569	0.9926	m+
2 1 0	6.9024	6.9187	1.0024	m
0 2 1	6.5467	6.5488	1.0003	m
1 1 2	6.0464	5.9831	0.9895	m-
1 2 1	5.7816	5.8464	1.0112	m-
2 2 0	5.3243	5.3050	0.9964	m-
2 0 2	5.0748	5.0679	0.9986	m
3 1 0	4.9279	4.9445	1.0034	w-
1 1 3	4.5177	4.5248	1.0029	s-
0 2 3	4.3164	4.3164	1.0000	m
2 0 3	4.0311	4.0232	0.9980	m+
3 2 1	3.9257	3.9178	0.9980	w+
1 1 4	3.5934	3.5958	1.0007	m+
2 2 3	3.5030	3.5071	1.0012	w
0 4 2	3.2725	3.2744	1.0006	s-
4 1 2	3.1699	3.1687	0.9996	m+
0 3 4	3.0919	3.0914	0.9998	t-
5 0 1	2.9737	2.9677	0.9980	w
0 5 2	2.7005	2.6998	0.9997	m+

$[(Me_5C_5)_3Yb_2F_2]_2 \cdot (PhMe)_2$ - Red Blades

The compound did not melt below 350°C. Anal. Calcd for $C_{74}H_{106}F_4Yb_4$: C, 50.4; H, 6.07. Found: C, 45.8; H, 5.69 (the analysis indicated that toluene may have been lost during combustion; Anal. Calcd for $C_{60}H_{90}F_4Yb_4$: C, 45.6; H, 5.75). IR (Nujol): 2725m, 1653vw, 1604w, 1566wbr, 1526w, 1493m, 1444sh, 1306shbr, 1257m, 1208vw, 1154m, 1102s, 1064m, 1022s, 1008sh, 975sh, 958m, 939sh, 892w, 876sh, 772vw, 730s, 694m, 666s, 624m, 591w, 572vw, 553w, 513sh, 449vs, 438shbr, 386sbr, 365sh, 325sh, 313vs, 301sh, 275vs cm^{-1}. The compound was only sparingly soluble in non-coordinating solvents. The ^{1}HNMR in CD_3CN (30°C) revealed only one visible signal for a diamagnetic C_5Me_5 ring at δ 1.87, as well as toluene (integration to establish the relative ratio of the two was precluded by interference from a small amount of C_5Me_5H). In comparison, $(Me_5C_5)_2Yb$ showed a diamagnetic signal in CD_3CN at δ 1.83. The mass spectrum (EI or CI with methane) did not show a molecular ion. The highest observed fragment was M/e = 789 ($(Me_5C_5)_3Yb_2F_2$ = 791). Other observed fragments were M/e = 767 ($(Me_5C_5)_3Yb_2F$ = 772), 751 ($(Me_5C_5)_3Yb_2$ = 753), 654 ($(Me_5C_5)_2Yb_2F_2$ = 656), 635 ($(Me_5C_5)_2Yb_2F$ = 637), 619 ($(Me_5C_5)_2Yb_2$ = 618), 497 ($(Me_5C_5)Yb_2F$ = 502), 463 ($(Me_5C_5)_2YbF$), 444 ($(Me_5C_5)_2Yb$), 327 ($(Me_5C_5)YbF$ = 328), 309 ($(Me_5C_5)Yb$), 193 (YbF), 174 (Yb), and C_5Me_5H fragments.

Powder Pattern Data for $[(Me_5C_5)_3Yb_2F_2]_2 \cdot (PhMe)_2$

s = strong, m = medium, w = weak, t = trace

Index	d_{hkl} (meas)	d_{hkl} (calc)	d(calc)/d(meas)	I
2 0 0	12.951	12.974	1.0018	m
0 0 2	11.906	11.917	1.0009	m

0 1 0	10.252	10.285	1.0032	m
0 1 1	9.2608	9.4432	1.0197	m+
1 1 1	8.6090	8.6032	0.9993	w+
2 0 2	7.8824	7.8497	0.9959	w
1 1 2	7.1524	7.1422	0.9986	s-
4 0 0	6.3938	6.4868	1.0145	w
2 1 3	5.2850	5.2628	0.9958	t
1 2 0	5.0390	5.0444	1.0011	t-
1 2 1	4.8742	4.8870	1.0026	w-
3 2 0	4.4338	4.4202	0.9969	w
0 2 3	4.3164	4.3170	1.0001	m-
3 2 2	3.9689	3.9812	1.0031	t
2 2 4	3.5442	3.5710	1.0076	t
2 3 0	3.3143	3.3145	1.0001	t-
2 3 3	2.9981	2.9916	0.9978	w+
2 3 5	2.6443	2.6430	0.9995	t
2 5 2	1.9862	1.9898	1.0018	s
5 5 5	1.7269	1.7206	0.9964	m+

Reaction of $(Me_5C_5)_2Yb(OEt_2)$ with AgF

Bis(pentamethylcyclopentadienyl)ytterbium(diethylether) (0.45g, 0.87 mmol) and silver fluoride (0.44g, 3.5 mmol) were slurried together in 50 mL of pentane in a flask wrapped with aluminum foil. The suspension was allowed to stir for 2 days. After this time, the supernatent solution was light-colored, and brown precipitate had appeared, along with silver metal. The supernatent was filtered and discarded. The brown precipitate was extracted with 30 mL of hot toluene. This toluene solution was concentrated and cooled to -25°C, producing a mixture of brown blocks and red needles. Examination of the IR spectra of the solid showed that it was a mixture of the dinuclear and tetranuclear fluoride species, with no evidence of diethyl ether coordination.

$(Me_5C_5)_2YbF(thf)$

Bis(pentamethylcyclopentadienyl)ytterbium(tetrahydrofuran) (0.52g;

1.0 mmol) and silver fluoride (0.51g, 4.0 mmol) were slurried in 30 mL of pentane in a Schlenk-type flask wrapped in aluminum foil, and stirred for 20h. The resulting orange solution was filtered away from the precipitated silver metal residue, and the volume of the filtrate was reduced to 10 mL. Cooling the solution to -25°C produced orange crystals. A second crop of crystals was isolated from the mother liquors by concentrating and cooling. The combined yield was 0.30g, 56%. The compound melted with decomposition at 158-162°C. Anal. Calcd for $C_{24}H_{38}OFYb$: C, 53.9; H, 7.18. Found: C, 53.7; H, 7.08. IR (Nujol): 2724w, 2042vw, 1658m, 1573vw, 1489sh, 1422s, 1340m, 1313vw, 1291vw, 1243w, 1210vw, 1172w, 1153w, 1033sh, 1021vs, 953w, 925m, 916sh, 869s, 855m, 843m, 721w, 705m, 676w, 637w, 618w, 591w, 553vw, 509w, 473vs, 379s, 342sh, 307vs cm^{-1}. ^{1}HNMR (C_6D_6, 20°C): δ2.18 (s, $\nu_{1/2}$ = 250 Hz). To verify the presence of thf, a sample of the compound was hydrolyzed in C_6D_6, and the ^{1}HNMR spectrum of the hydrolysate was examined; C_5Me_5H and thf were observed in a 2:1 ratio.

An attempt was made to remove the thf from the complex by the toluene reflux method. The $(Me_5C_5)_2YbF(thf)$ (0.30g, 0.56 mmol) was dissolved in 50 mL of toluene, and the solution was heated to 100°C. The solvent was then removed slowly under reduced pressure. The remaining red-orange residue was extracted with 30 mL of toluene. The filtrate was filtered, concentrated to 10 mL, and cooled to -25°C. No crystalline material could be isolated. Removal of the solvent left a red-orange oil.

$\underline{(Me_5C_5)_2Yb(NCMe)_2}$

Bis(pentamethylcyclopentadienyl)ytterbium(diethylether) (0.66g, 1.3 mmol) was dissolved in toluene (50 mL), and 5 mL acetonitrile was added with stirring, resulting in an immediate darkening of the green color of the solution and the appearance of dark green precipitate. The solution was warmed slightly to drive the precipitate back into solution. The solution was then cooled to -20°C, resulting in the formation of dark green crystals. A second crop of crystals was isolated from the mother liquors by concentrating and cooling. The combined yield of both crops was 0.66g (99%), MP 195-198°C. IR (Nujol): 2719m, 2392vw, 2303w, 2289w, 2269s, 2261s, 2037vw, 1662vw, 1624vw, 1465s, 1447sh, 1367s, 1358s, 1314sh, 1209vw, 1164w, 1155w, 1021m, 975w, 946vw, 928w, 919sh, 892vw, 799w, 770w, 730m, 722sh, 695vw, 639wbr, 587w, 391w, 368wbr, 266vsbr cm^{-1}. Anal. Calcd for $C_{24}H_{36}N_2Yb$: C, 54.8; H, 6.92; N, 5.33. Found: C, 54.9; H, 6.90; N, 5.02. ^{1}HNMR (C_6D_6, 25°C): δ 2.37 (s, 30H), δ 1.27 (s, 6H, $\nu_{1/2}$ = 100 Hz).

An attempt was made to react this compound with AgF, in order to make a species of the type $(Me_5C_5)_2YbF(L)$ from which L could be removed. The acetronitrile complex (0.54 g, 1.0 mmol) was slurried with silver fluoride (0.13 g, 1.0 mmol) in 40 mL of hexane in a flask wrapped with aluminum foil. This solution was allowed to stir for 16 h. The resulting red-orange solution was filtered away from the precipitated silver metal, and the volume was reduced to 8 mL. Cooling the solution to -25°C produced only a small amount (ca. 0.06 g) of red-orange crystalline material, MP 170-175°C. IR (Nujol): 2725m, 2309vw, 2277w, 2200shbr, 2184s, 2171s, 2151s, 1660m, 1563sh, 1615vs, 1578m, 1522vs,

1444s, 1408m, 1367s, 1321w, 1205sh, 1188w, 1165m, 1150sh, 1143w, 1021m, 984w, 937vw, 926w, 891m, 866vw, 764w, 751w, 722w, 662w, 651w, 643sh, 625w, 600w, 591sh, 561vw, 552vw, 538vw, 527w, 518vw, 479m, 461m, 385mbr, 306 vsbr cm^{-1}.

Reaction of $(Me_5C_5)_2Yb$ with $H_2C{=}CHF$, $H_2C{=}CF_2$, or $F_2C{=}CF_2$

In a representative reaction, bis(pentamethylcyclopentadienyl)-ytterbium (0.45g, 1.0 mmol) was dissolved in 35 mL of hexane and transferred to a thick-walled glass pressure bottle. Tetrafluoroethylene was admitted, and the pressure was released three times to flush the air space above the solution. Finally, the solution was pressurized to 2-3 atm. with C_2F_4. After ca. 5 minutes, the solution began to grow cloudy as a precipitate formed. The solution was stirred for 4h, and then the pressure was released. The solution was pale red, and brown powdery precipitate had formed. The precipitate was isolated and dried under reduced pressure. The total yield was 0.38g (84%). The material was identified as $[(Me_5C_5)_2Yb]_2(\mu\text{-}F)$ by comparison of the IR spectrum, MP, and X-ray powder pattern with those of an authentic sample. Reactions conducted in toluene were slower to begin producing precipitate (15 - 30 minutes). In these reactions, the volume of the toluene solution was reduced to 5 mL, and the solution was cooled to -25°C to complete precipitation of the product. The yield of fluoride from toluene was lower, and IR spectra and x-ray powder patterns showed that the precipitate was a mixture of the dinuclear and tetranuclear species.

Reaction of $(Me_5C_5)_2Yb(OEt_2)$ with C_2F_4

Bis(pentamethylcyclopentadienyl)ytterbium(diethylether) (0.33g, 0.64 mmol) was dissolved in 30 mL of toluene and the solution was transferred to a thick-walled glass pressure bottle. The solution was pressurized to 3 atm. with tetrafluoroethylene, and the solution was allowed to stir for 24 h; no color change occured. The pressure was then released, and the volume of the solution was reduced to 5 mL under reduced pressure. A small amount of red precipitate (ca. 0.03 g) was filtered out of solution and examined by IR spectroscopy; it appeared to consist mostly of the tetranuclear fluoride complex. The filtrate was cooled to -25°C, producing green needles. These were identified as the ytterbium diethylether complex by examination of the IR spectrum and MP.

Reaction of $(Me_5C_5)_2Yb$ with C_6H_5F

Bis(pentamethylcyclopentadienyl)ytterbium (0.29g, 0.65 mmol) was dissolved in 20 mL of hexane and added without stirring to a hexane solution (5 mL) of fluorobenzene (0.12 mL, 0.12g, 1.3 mmol). No immediate reaction was observed. The reaction was allowed to stand for 2 weeks. After 1 week, crystals had formed on the walls of the flask. These crystals were filtered, and identified by IR spectroscopy and the MP to be $[(Me_5C_5)_2Yb]_2(\mu\text{-}F)$. After another week, the mother liquors had deposited more crystals, along with a small amount of pale green powder. The crystals were isolated, and identified by IR spectroscopy and the MP to be mostly $[(Me_5C_5)_3Yb_2F_2]_2$, with a small amount of the dinuclear species mixed in. The green powder melted with decomposition at 280°C. IR of the green powder (Nujol): 2726m, 2039vw, 1658vwbr, 1599vwbr,

1446vs, 1315vw, 1208vw, 1155m, 1019m, 956w, 936wbr, 899vw, 860vw, 738sh, 726m, 696m, 641m, 624w, 591w, 569vw, 398sbr, 299m, 267vsbr cm^{-1}. The remaining solution was hydrolyzed and extracted with diethyl ether. The ether was removed from the extract under reduced pressure to give a pale yellow oil. The highes peak in the mass spectrum of this oil was due to Me_5C_5-C_6H_5 (212). C_5Me_5H and C_5Me_5OH were also visible. There was no evidence that biphenyl was a major product in the solution. The ^{1}HNMR (CD_3CN) showed resonances attributable to C_5Me_5H, as well as resonances at δ 1.80, δ 1.76, and δ 1.69; overlap of all these resonances precluded the possibility of accurate integration.

Reaction of $(Me_5C_5)_2Yb$ with $CF_3C_6H_5$

Bis(pentamethylcyclopentadienyl)ytterbium (0.37g, 0.83 mmol) was dissolved in 30 mL of pentane, and added with stirring to a solution of $CF_3C_6H_5$ (0.040 mL, 0.048g, 0.33 mmol) in pentane (5 mL). No immediate reaction was observed. After 14 h, brown powdery precipitate had come out of solution. The solution volume was reduced to ca. 5 mL, and the solution was cooled to -25°C to complete precipitation. The brown powder was isolated, washed with pentane, and dried under reduced pressure. Examination of the IR spectrum and MP revealed the powder to be $[(Me_5C_5)_2Yb]_2(\mu$-F). The yield of the dinuclear fluoride was 0.20g (67% based on $CF_3C_6H_5$). The mother liquor from the reaction was hydrolyzed and extracted with Et_2O; the extracts were dried over $MgSO_4$, and the solvent was removed under reduced pressure to yield a colorless oil which solidified upon standing. The mass spectrum of this material showed fragments corresponding to C_5Me_5H and C_5Me_5OH, as well as a

fragmentation pattern for Me_5C_5-$CF_2C_6H_5$ (the base peak in the spectrum was M/e = 244, corresponding to M^+ - 2F). There was no evidence for the dimerized species, $(C_6H_5CF_2)_2$. The ^{1}HNMR spectrum (C_6D_6) of the oil showed resonances identifiable as C_5Me_5H, plus resonances at δ 7.24 (m), δ 7.11 (m, total integration of phenyl region 5H), δ 2.13 (s, 3H), δ 2.10 (s, 6H), and δ 1.98 (s, 6H).

Reaction of $(Me_5C_5)_2Yb$ with C_6F_6

Bis(pentamethylcyclopentadienyl)ytterbium (0.51g, 1.1 mmol) was dissolved in 25 mL of pentane and added with stirring to a degassed pentane solution (5 mL) of hexafluorobenzene (0.13 mL, 0.21g, 1.1 mmol). The color of the solution immediately turned purple, and brown precipitate was deposited. The solution was allowed to stir for 1h. The brown powder was isolated by filtration, washed with pentane, and dried under reduced pressure. Examination of the MP, IR spectrum, and X-ray powder pattern revealed this solid to be $[(Me_5C_5)_2Yb]_2(\mu$-F) (0.26g, 50% based on Yb). The purple filtrate was reduced in volume to 3 mL, and cooled to -25°C, producing 0.10g of purple powder, MP 276-280°C (dec). IR (Nujol): 2726m, 1653vwbr, 1530m, 1492sh, 1447s, 1403vs, 1387m, 1366w, 1345vw, 1325vw, 1314vw, 1288vs, 1164w, 1151w, 1121s, 1098vs, 1064w, 1023m, 994vwbr, 919vwbr, 833vs, 801w, 724w, 697w, 669m, 620vw, 592vw, 544vw, 445sbr, 387mbr, 326vsbr, 306vs, 278m cm^{-1}. Anal.: Found: C, 42.9; H, 4.88. ^{1}HNMR (C_6D_6, 30°C): δ 52.07 ($\nu_{1/2}$ = 90 Hz), δ 35.49 ($\nu_{1/2}$ = 87 Hz), δ 25.90 ($\nu_{1/2}$ = 16 Hz), relative integrations 2:2:1. In addition to this, an additional resonance was always observed at δ 11.14 ($\nu_{1/2}$ = 115 Hz), but the relative integration varied from 2-

3. In order to determine the nature of the ligands present, a sample of the compound was hydrolyzed in C_6D_6, and the hydrolysate was examined by ^1H and ^{19}FNMR spectroscopy. The ^1HNMR spectrum revealed the presence of C_5Me_5H, but no proton resonance was visible for C_6F_5H. The ^{19}FNMR spectrum, however, demonstrated that C_6F_5H was present in the hydrolysate: δ 24.98 (m, 2F), δ 10.15 (t, 1F), δ 1.87 (m, 2F). The mass spectrum of the compound showed a large number of fragment ions: 496 ($(Me_5C_5)Yb(C_6F_5)F$ = 495), 478 ($(Me_5C_5)Yb(C_6F_5)$ = 476), 461 $((Me_5C_5)_2YbF$ = 463), 444 $((Me_5C_5)_2Yb)$, 380 $((C_6F_5)YbF_2$ = 379), 362 $((C_6F_5)YbF$ = 360), 344 $((C_6F_5)Yb$ = 341), 329 $((Me_5C_5)YbF$ = 328), 309 $((Me_5C_5)Yb)$, as well as ions due to methyl and fluorine loss from these fragments, and ions due to fragmentation of C_5Me_5H and C_6F_5H.

Reaction of $(Me_5C_5)_2Yb$ with H_3CCF_3 and F_3CCF_3

In a typical reaction, bis(pentamethylcyclopentadienyl)ytterbium (0.25g, 0.56 mmol) was dissolved in 20 mL of hexane, and transferred to a thick-walled glass pressure bottle. The solution was pressurized to 3 atm. with 1,1,1-trifluoroethane; no color change was observed. The solution was allowed to stir for 3 days. The pressure was released, and the solvent was removed under reduced pressure. Only $(Me_5C_5)_2Yb$ was reisolated, as confirmed by examination of the IR spectrum.

Reaction of $(Me_5C_5)_2Yb$ with AgCl

Bis(pentamethylcyclopentadienyl)ytterbium (0.40g, 0.90 mmol) and silver chloride (0.26g, 1.8 mmol) were slurried together in 50 mL of pentane in a foil-wrapped flask. A green solid formed rapidly, then

slowly turned purple and dissolved again with accompanying precipitation of silver metal. The solution was allowed to stir for 12 h; it was then filtered, concentrated to 10 mL in volume, and cooled to -25°C, producing some purple powder. This was recrystallized from a minimum volume of toluene to give 0.26g of light blue microcrystals. The compound decomposed at 328°C without melting. IR (Nujol): 2728w, 1682vwbr, 1614vwbr, 1491m, 1311vw, 1208vw, 1170w, 1121vw, 1083w, 1024m, 975vw, 958vw, 924vwbr, 891vw, 876vwbr, 738sh, 723m, 700w, 660vw, 628vw, 592w, 559vw, 529vw, 396m, 326vs, 311s, 288m, 248s, 222vs cm^{-1}. Anal. Found: C, 36.7; H, 5.03; Cl, 7.67. ^{1}HNMR (C_6D_6): at 30°C, only two resonances were apparent, at δ 45.15 ($\nu_{1/2}$ = 38 Hz) and δ 18.99 ($\nu_{1/2}$ = 50 Hz), in a relative integration of 1:2. When the temperature was raised or lowered, however, the upfield resonance resolved itself into two separate paramagnetic resonances. For example, at -10°C, the three resonances appeared at δ 55.19 ($\nu_{1/2}$ = 34 Hz), δ 23.19 ($\nu_{1/2}$ = 59 Hz), and δ 20.72 ($\nu_{1/2}$ = 43 Hz), in a relative integration of 1:1:1. These resonances shifted normally with temperature, but were inequivalent from +90°C to -80°C.

Reaction of $(Me_5C_5)_2Yb$ with $HgCl_2$

Bis(pentamethylcyclopentadienyl)ytterbium (0.21g, 0.47 mmol) and mercuric chloride (0.13g, 0.47 mmol) were slurried together in 30 mL of hexane. A green precipitate formed rapidly, then turned purple, and finally redissolved, depositing mercury metal. The solution was allowed to stir for 14 h, then was filtered, concentrated to 5 mL, and cooled to -25°C, producing 0.10g small blue crystals. Examination of the IR and

^{1}HNMR spectra revealed that this material was the same as that which was produced by the reaction with silver chloride.

Chapter Three

Reaction of $(Me_5C_5)_2Yb$ with $AlEt_3$

Bis(pentamethylcyclopentadienyl)ytterbium (0.29g, 0.65 mmol) was dissolved in pentane (30 mL) and was added to a pentane solution (0.66 mL of a 0.99M solution, 0.65 mmol) of triethylaluminum. If the solution was stirred, the solution rapidly precipitated a bright green powder. If the compounds were mixed without stirring, the solution turned bright green, and upon standing green polycrystalline material formed on the walls of the flask. When the reaction was conducted in toluene, the solution did not precipitate solid. Removing the solvent resulted the formation of a green oil, which solidified upon addition of pentane. The isolated yield of green material was 0.26g, MP 223-226°C. IR (Nujol): 2790w, 2730w, 2695m, 1411m, 1312vw, 1208vw, 1175w, 1150vw, 1092m, 1016w, 982m, 940m, 907w, 793wbr, 848sh, 766sh, 720m, 686sh, 680sh, 663m, 647sh, 618m, 583mbr, 546m, 471shbr, 414mbr, 359wbr, 281sh, 268m, cm^{-1}. Anal. Found: C, 47.3; H, 7.73. ^{1}HNMR (C_7D_8, 30°C): δ 2.01 (s, 30H), δ 1.21 (t, 9H, $^3J_{HH}$ = 7 Hz, broadened), δ -0.09 (q, 6H, broadened). The EI mass spectrum failed to show any fragments containing aluminum. The spectrum consisted entirely of the fragmentation pattern of $(Me_5C_5)_2Yb$ (444). The reaction of $(Me_5C_5)_2Yb(OEt_2)$ with $AlEt_3$ in hexane produced a green oil which solidified upon standing to give a green solid which had the same IR spectrum and MP as the material produced from the base-free ytterbium complex.

$(Me_5C_5)_2Yb(\mu\text{-}Me)Be(C_5Me_5)$

An orange solution of bis(pentamethylcyclopentadienyl)ytterbium (0.26g, 0.59 mmol) dissolved in pentane (20 mL) was added to a pentane solution (10 mL) of methylpentamethylcyclopentadienylberyllium (0.090g, 0.59 mmol) with stirring. No color change was observed. The volume was reduced to 15 mL, and the solution was cooled to -25°C, resulting in the formation of dark orange prisms. The crystals were isolated by filtration and dried under vacuum. The yield was 0.29g (82%), mp 224-227°C. IR (Nujol): 2723m, 2172vwbr, 2035vwbr, 1652wbr, 1539sh, 1494sh, 1444s, 1393sh, 1347sh, 1197w, 1175sh, 1154m, 1122vs, 1019s, 991sh, 958sh, 942s, 920sh, 904sh, 865vwbr, 738vw, 722w, 705w, 628wbr, 590w, 553vwbr, 503vwbr, 466vwbr, 416sh, 363mbr, 274vsbr cm^{-1}. Anal. Calcd for $C_{31}H_{48}BeYb$: C, 61.8; H, 8.04. Found: C, 62.1; H, 8.10. ^{1}HNMR (C_6D_6, 20°C): δ 2.02 (s, 30H), δ 1.76 (s, 15H), δ -1.13 (br s, 3H). ^{13}CNMR (C_6D_6, 20°C): δ 112.8 (s, YbC_5Me_5), δ 108.7 (s, BeC_5Me_5), δ 10.84 (q, $^1J_{CH}$ = 124 Hz, YbC_5Me_5), δ 8.93 (q, $^1J_{CH}$ = 126 Hz, BeC_5Me_5). No signal was visible for the bridging methyl carbon. ^{1}HNMR of $(Me_5C_5)BeMe$ (C_6D_6, 20°C): δ 1.76 (s, 15H), δ -1.27 (br s, 3H). ^{13}CNMR of $(Me_5C_5)BeMe$ (C_6D_6, 20°C): δ 108.7 (s, C_5Me_5). No signal was visible for the methyl carbon. The mass spectrum of the compound showed no molecular ion; the highest weight fragment corresponded to M^+ - Me, m/e 588. Fragmentation patterns for $(Me_5C_5)_2Yb$ and $(Me_5C_5)BeMe$ were observed.

Reaction of $(Me_5C_5)_2Yb$ with $(Me_5C_5)BePh$

Bis(pentamethylcyclopentadienyl)ytterbium (0.24g, 0.54 mmol) was dissolved in hexane (20 mL) and added to a solution of $(Me_5C_5)BePh$

(0.12g, 0.54 mmol) in hexane (10mL), giving a dark orange-brown solution. The volume of the solution was reduced to 3 mL, and the solution was cooled to -25°C. Green crystals were isolated which turned brown under vacuum; only $(Me_5C_5)_2Yb$ was reisolated.

$\underline{[(Me_5C_5)_2Yb][H_3B{\cdot}PMe_3]}$

Bis(pentamethylcyclopentadienyl)ytterbium (0.35g, 0.79 mmol) was dissolved in 20 mL of hexane and added with stirring to a slurry of trimethylphosphineborane (0.070g, 0.78 mmol) in hexane (5 mL). This resulted in an immediate precipitation of light yellow-green solid; the white phosphineborane dissolved slowly. The solution was allowed to stir for 12 h, and the precipitate was collected by filtration. The yield of this powder was 0.32g (77%), MP 250-253°C. IR (Nujol): 2724w, 2427m, 2363vw, 2334sh, 2302sh, 2266m, 1653vwbr, 1595vwbr, 1457vs, 1437sh, 1314w, 1296m, 1175w, 1155w, 1103w, 1019w, 965s, 950m, 886w, 769w, 722m, 695vw, 646vw, 597w, 374wbr, 250vs, 250sh cm^{-1} (IR of trimethylphosphineborane: 2725vw, 2364s, 2339sh, 2268sh, 2256w, 1429w, 1314w, 1294m, 1137w, 1128sh, 1083w, 1070m, 973sbr, 950s, 889w, 759w, 739vw, 722w, 709m, 581vw, 570w, 516wbr cm^{-1}). Anal. Calcd for $C_{23}H_{42}BPYb$: C, 51.8; H, 7.95; P, 5.81. Found: C, 51.8; H, 7.79; P, 5.79. ^{1}HNMR (C_6D_6, 20°C): δ 2.25 (s, 30H), δ 0.49 (d, $^2J_{PH}$ = 10.9 Hz, 9H). $^{31}P\{^1H\}$NMR (C_6D_6, 30°C): δ -1.64 (1:1:1:1 q, $^1J_{BP}$ = 77.7 Hz). $^{11}B\{^1H\}$NMR (C_6D_6, 30°C): δ -35.41 (d, $^1J_{BP}$ = 78.2 Hz). ^{1}HNMR of $H_3B{\cdot}PMe_3$ (C_6D_6, 20°C): δ 0.78 (d, $^2J_{PH}$ = 10.5 Hz, 9H), δ 1.09 (1:1:1:1 quartet of doublets, $^1J_{BH}$ = 95.4 Hz, $^2J_{PH}$ = 15.5 Hz, 3H). $^{31}P\{^1H\}$NMR (C_6D_6, 30°C): δ -1.59 (1:1:1:1 quartet, $^1J_{BP}$ = 59.8 Hz). $^{11}B\{^1H\}$NMR

(C_6D_6, 30°C): δ -36.71 (d, $^1J_{BP}$ = 59.8 Hz).

$(Me_5C_5)_2Yb(H_3B{\cdot}PPh_3)$

Bis(pentamethylcyclopentadienyl)ytterbium (0.33g, 0.74 mmol) was dissolved in 20 mL of hexane and added with stirring to a slurry of triphenylphosphine-borane (0.21g, 0.76 mmol) in 5 mL of hexane. After stirring for 15-20 minutes, the white solid had disappeared, but an orange precipitate had formed. The solution remained orange throughout. The solution was allowed to stir for 12h, and the precipitate was isolated by filtration. Concentrating and cooling the filtrate completed the precipitation of orange solid. The total yield was 0.43g (80%), MP 155-158°C. The solid was recrystallized from toluene to give large red crystals which lost solvent and turned orange under vacuum. IR (Nujol): 3077w, 3058m, 2722w, 2434m, 2380s, 2345m, 2296w, 2265w, 1967vw, 1897vw, 1817vw, 1774vw, 1667vwbr, 1589w, 1573vw, 1483s, 1436vs, 1336vw, 1314w, 1279sh, 1260w, 1183w, 1161vw, 1145w, 1135w, 1107vs, 1090sh, 1070sh, 1058s, 1027m, 1019sh, 998m, 974vw, 927vw, 920vw, 847vw, 799wbr, 766vw, 751sh, 745vs, 738vs, 704s, 693vs, 677sh, 633m, 624sh, 614m, 606m, 591vw, 542vw, 505vs, 494s, 476w, 450w, 440w, 428w, 376wbr, 273sbr cm^{-1} (IR of $H_3B{\cdot}PPh_3$: 3079w, 3057w, 3026w, 2378s, 2344m, 2253vw, 1966vw, 1903vw, 1828vw, 1778vw, 1588w, 1572vw, 1481s, 1434vs, 1337vw, 1310w, 1262vw, 1199vw, 1184w, 1162vw, 1134m, 1106s, 1057s, 1027m, 1002m, 799wbr, 764w, 746s, 737vs, 721w, 705s, 693s, 624m, 605m, 543w, 505s, 496m, 477m, 439w, 427w cm^{-1}). Anal. Calcd for $C_{38}H_{48}BPYb$: C, 63.4; H, 6.74; P, 4.30. Found: C, 63.8; H, 6.71; P, 4.01. ^{1}HNMR (C_6D_6, 20°C): δ 7.51 (m), δ 6.98 (m, combined of phenyl region 15H), δ 2.20 (s, 30H).

$^{31}P\{^{1}H\}$NMR (C_6D_6, 20°C): δ 22.5 (the resonance had a broadened pseudo-doublet appearance, with J = 57Hz). $^{11}B\{^{1}H\}$NMR (C_6D_6, 30°C): δ -36.47 ($\nu_{1/2}$ = 170 Hz). ^{1}HNMR of $H_3B{\cdot}PPh_3$ (C_6D_6, 20°C): δ 7.62 (m), δ 6.98 (m, combined integration of phenyl region 15H). $^{31}P\{^{1}H\}$NMR (C_6D_6, 20°C): δ 21.2 (the resonance had a broadened pseudo-doublet appearance, with J = 65 Hz). $^{11}B\{^{1}H\}$NMR (C_6D_6, 30°C): δ -37.28 (the resonance had a broadened pseudo-doublet appearance with J = 46 Hz).

$\underline{(Me_5C_5)_2Yb(\mu\text{-}Me)_2ZnMe}$

From $\underline{(Me_5C_5)_2Yb}$:

Bis(pentamethylcyclopentadienyl)ytterbium (0.25g, 0.56 mmol) was dissolved in 25 mL of pentane and added to a solution of $ZnMe_2$ (0.060 mL, 0.094g, 0.98 mmol) in pentane (5 mL) with stirring. An orange flocculent precipitate formed rapidly. The solution was allowed to stir for 14h. After several hours, the orange precipitate had redissolved, and the solution had turned purple; the color change was accompanied by the formation of a zinc mirror on the walls of the flask. The solution was filtered, concentrated to 3 mL in volume, and cooled to -78°C. Dark purple prisms were isolated and dried under reduced pressure. The yield was 0.25g (81%). This was the only product isolated, even when the reagents were combined in different stoichiometries.

From $\underline{(Me_5C_5)_2Yb(OEt_2)}$:

Bis(pentamethylcyclopentadienyl)ytterbium(diethylether) (2.82g, 5.45 mmol) was slurried in 45 mL of hexane, and a solution of $ZnMe_2$ (0.49 mL, 0.78g, 8.16 mmol) in pentane (5 mL) was added to this with stirring. The ytterbium etherate dissolved over a period of hours,

giving a small amount of orange precipitate which rapidly redissolved to give a purple solution and zinc metal. The solution was allowed to stir for 16h, then the metal was allowed to settle, and the solution was filtered. The filtrate was concentrated to 30 mL and cooled to -78°C, producing large purple blocks. A second crop was isolated from the mother liquors by concentrating and cooling. The combined yield was 2.75g (91.1%).

The compound melted at 216-218°C. IR (Nujol): 2803m, 2771m, 2728m, 2678sh, 2041vwbr, 1654vwbr, 1490m, 1440s, 1312vw, 1220w, 1163vw, 1152w, 1060w, 1024m, 739sh, 725w, 689w, 643vs, 618sh, 590m, 529s, 403m, 387w, 312vs, 284sh cm^{-1}. Anal. Calcd for $C_{23}H_{39}YbZn$: C, 50.2; H, 7.17. Found: C, 49.9; H,, 7.11. ^{1}HNMR (C_6D_6, 20°C): δ 2.90 ($\nu_{1/2}$ = 27 Hz); the methyl groups were not visible at this temperature. The EI mass spectrum did not show a molecular ion; the highest observable fragment was $(Me_5C_5)_2YbMe_2$ (475), followed by $(Me_5C_5)_2YbMe$ (459), $(Me_5C_5)_2Yb$ (444), $(Me_5C_5)Yb$ (309), Yb (174), and ions due to ring fragmentation.

$(Me_5C_5)_2YbMe(thf)$

Bis(pentamethylcyclopentadienyl)ytterbium(trimethylzincate) (0.23g, 0.42 mmol) was dissolved in 20 mL of tetrahydrofuran, yielding an orange solution. The solvent was removed under reduced pressure, and the residue was recrystallized from warm hexane to give 0.19g of orange crystals (86%). The compound melted and bubbled at 162-163°C. IR (Nujol): 2806w, 2779w, 2721w, 2041vwbr, 1607vwbr, 1494sh, 1440vs, 1407sh, 1344w, 1314vw, 1296vw, 1257w, 1177sh, 1153m, 1102s, 1063m, 1039sh, 1021vs, 959w, 923w, 869s, 842sh, 737sh, 725w, 695w, 675m, 624w,

594w, 567vw, 531w, 489vw, 429wbr, 397s, 301vsbr cm^{-1}. Anal. Calcd for $C_{25}H_{41}OYb$: C, 56.6; H, 7.80. Found: C, 55.2; H, 7.68. ^{1}HNMR (C_6D_6, 20°C): δ 1.16 ($\nu_{1/2}$ = 185 Hz). To confirm the presence of thf, a sample of the compound was hydrolyzed in C_6D_6, and the hydrolysate was examined by ^{1}HNMR spectroscopy. Both thf and C_5Me_5H were observed in the spectrum in a 1:2 ratio. The EI mass spectrum did not show a molecular ion at M/e = 531; the highest weight fragment was $(Me_5C_5)_2YbMe$ (459), followed by $(Me_5C_5)_2Yb$ (444), $(Me_5C_5)Yb$ (309), Yb (174), and ions due to ring fragmentation.

Attempt to Remove $ZnMe_2$ from $(Me_5C_5)_2Yb(\mu\text{-}Me)_2ZnMe$

Bis(pentamethylcyclopentadienyl)ytterbium(trimethylzincate) (2.52g, 4.55 mmol) was dissolved in 50 mL of toluene to give a dark purple solution. This solution was heated to 100°C, and the solvent was removed very slowly (over a period of 2-3 h) under reduced pressure, leaving a dark red-brown residue. This process was then repeated with an additional 50 mL of toluene. The residue was extracted with 100 mL of pentane, leaving behind a small amount of red-brown powder. The extract was concentrated to 30 mL in volume, and cooled to -25°C. Green crystals were isolated from this solution which lost solvent and turned brown under vacuum. Examination of the IR spectrum and MP confirmed that this material was $(Me_5C_5)_2Yb$. An additional crop of crystals was isolated from the mother liquors by concentrating and cooling. The total amount of the base-free ytterbium complex isolated from solution was 0.52g (26%).

$\underline{(Me_5C_5)_2Yb(\mu\text{-}Ph)_2ZnPh}$

From $\underline{(Me_5C_5)_2Yb}$:

Bis(pentamethylcyclopentadienyl)ytterbium (0.28g, 0.63 mmol) was dissolved in 20 mL of toluene and added with stirring to a slurry of $ZnPh_2$ in 15 mL of toluene. The color of the solution became dark, but no precipitate formed immediately. The solution was allowed to stir for 24 h, at which time the color had changed to purple, accompanied by the formation of a zinc mirror on the walls of the flask. The solution was filtered, and the toluene was removed under reduced pressure. The purple residue was extracted with 35 mL of pentane, filtered, concentrated to a volume of 5 mL, and cooled to -78°C, producing purple blocks. The isolated yield was 0.32g (68%).

From $\underline{(Me_5C_5)_2Yb(OEt_2)}$:

Bis(pentamethylcyclopentadienyl)ytterbium (0.73g, 1.4 mmol) and $ZnPh_2$ (0.46g, 2.1 mmol) were dissolved in 20 mL of toluene, the solution was stirred for 14 h, producing a dark purple solution and a zinc mirror on the walls of the flask. The solution was filtered, and the toluene was removed under reduced pressure. The purple residue was extracted with 40 mL of pentane; the extract was filtered, concentrated to 10 mL, and cooled to -78°C, producing purple crystals. A second crop of crystals was isolated from the mother liquors by concentrating and cooling. The combined yield of the two batches was 0.63g (60%).

The compound melted with decomposition at 111-114°C. IR (Nujol): 3059m, 3037m, 2729w, 2668vw, 1952vw, 1882vw, 1868vw, 1819w, 1772vw, 1757vw, 1671vw, 1628vw, 1593m, 1573vw, 1558vw, 1490s, 1420s, 1297m, 1240m, 1191w, 1171sh, 1153w, 1100m, 1074m, 1048s, 1024m, 1011sh, 993m,

963vw, 938sh, 925vw, 875w, 855sh, 844w, 827vw, 759m, 722vs, 709vs, 701vs, 674w, 654w, 632w, 624w, 619w, 606sh, 599w, 573vw, 496wbr, 442m, 438m, 435m, 383mbr, 339sh, 300sbr cm^{-1}. Anal. Calcd for $C_{38}H_{45}YbZn$: C, 61.7; H, 6.14. Found: C, 61.6; H, 6.24. ^{1}HNMR (C_6D_6, 30°C): δ 12.98 ($\nu_{1/2}$ = 193 Hz, 6H), δ 7.37 ($\nu_{1/2}$ = 380 Hz, 30H), δ 5.78 ($\nu_{1/2}$ = 205 Hz, 3H). The ortho protons were visible only as a very broad resonance ($\nu_{1/2} \approx$ 1500 Hz) at 63 ppm. The EI mass spectrum did not show a molecular ion (740); the highest weight fragment was $(Me_5C_5)_2YbPh$ (521), followed by $(Me_5C_5)_2Yb$ (444), $(Me_5C_5)YbPh$ (385), $(Me_5C_5)Yb$ (309), Yb (174), and ions due to ring fragmentation.

Reaction of $(Me_5C_5)_2Yb(\mu\text{-}Ph)_2ZnPh$ with thf

Bis(pentamethylcyclopentadienyl)ytterbium(triphenylzincate) (0.25g, 0.34 mmol) was dissolved in 15 mL thf to give a red solution. The solvent was then removed under reduced pressure to give a red residue. This was extracted with 30 mL of hexane, giving a purple-red solution. Reducing the volume of the solution to 5 mL and cooling it to -25°C produced a purple film of the zincate on the walls of the flask along with some red crystals. These were separated manually. The yield of red crystals was 0.10g (49%), MP 137-141°C. IR (Nujol): 3041m, 3029m, 2722w, 1931vw, 1856vw, 1806vw, 1734vw, 1634vwbr, 1593w, 1562w, 1490m, 1409m, 1340w, 1306m, 1296m, 1224w, 1171sh, 1149m, 1049s, 1018vs, 993vw, 974vw, 959vw, 934w, 921w, 890sh, 868vs, 852sh, 843sh, 758w, 730sh, 718m, 705vs, 674w, 627w, 618vw, 596w, 449w, 383w, 368sh, 302vsbr cm^{-1}. Anal. Calcd for $C_{30}H_{43}OYb$: C, 60.8; H, 7.33. Found: C, 57.4; H, 7.09. ^{1}HNMR (C_6D_6, 20°C): δ 133.3 ($\nu_{1/2} \simeq$ 1800 Hz), δ 65.0 ($\nu_{1/2}$ = 400 Hz, 2H), δ

0.32 ($\nu_{1/2}$ = 150 Hz, 30H), δ -9.43 ($\nu_{1/2}$ = 100 Hz, 1H). The EI mass spectrum did not show a molecular ion at 593; the highest weight fragment was $(Me_5C_5)_2YbPh$ (521). Tetrahydrofuran was observed at M/e = 72, however, and by examining the time evolution of the mass spectrum, it was observed that the thf came off early in the scan series. Ions were also observed corresponding to $(Me_5C_5)_2Yb$ (444), $(Me_5C_5)YbPh$ (386), $(Me_5C_5)Yb$ (309), Yb (174), and ions due to ligand fragmentation.

Reaction of $(Me_5C_5)_2Yb$ with $Zn(p\text{-tolyl})_2$

From $(Me_5C_5)_2Yb$:

Bis(pentamethylcyclopentadienyl)ytterbium (0.33g, 0.74 mmol) and bis(p-tolyl)zinc (0.28g, 1.1 mmol) were stirred together in 20 mL of toluene for 16 h, resulting in a purple solution and a zinc mirror on the walls of the flask. The solution was filtered, and the solvent was removed under reduced pressure. The residue was extracted with 20 mL of pentane, giving a red solution. Some white solid was left behind by the extraction; this was identified as $Zn(p\text{-tolyl})_2$ by IR and ^{1}HNMR spectroscopy (approximately 0.06g was recovered). The red solution was reduced to 3 mL in volume, and cooled to -78°C, producing a purple woody-looking solid. The yield of this solid was 0.25g (43%), MP 127-132°C. IR (Nujol): 3045m, 3019m, 2727w, 1905vw, 1813vw, 1634vw, 1592m, 1507m, 1490m, 1464s, 1311vw, 1295w, 1241w, 1196w, 1187w, 1151vw, 1066m, 1036sh, 1026s, 1022sh, 1007sh, 965vw, 878vw, 850vw, 821w, 791vs, 729w, 713sh, 696vw, 678w, 649vw, 638vw, 621vw, 595w, 576w, 548w, 482vs, 386wbr, 303sbr cm^{-1}. Anal. Calcd for $C_{41}H_{51}ZnYb$: C, 62.9; H, 6.58. Found: C, 61.3; H, 6.50. ^{1}HNMR (C_7D_8, 30°C): δ 7.10 ($\nu_{1/2}$ = 300 Hz,

30H), δ 11.90 ($\nu_{1/2}$ = 115 Hz, 6H), δ 0.13 ($\nu_{1/2}$ = 36 Hz, 9H). The EI mass spectrum of this solid did not give a molecular ion at 782; the higest weight fragment was $(Me_5C_5)_2Yb(p\text{-tolyl})$, 535. Ions were also visible for $(Me_5C_5)_2Yb$ (444), and $(Me_5C_5)Yb$ (309), as well as those due to ligand fragmentation. The solvent was removed from the filtrate to give a red solid. This solid sublimed at 110°C/10^{-4} torr. The amount of red solid isolated was 0.12g, MP 162-165°C. IR (Nujol): 3030m, 3006sh, 2728m, 2035vw, 1889vwbr, 1794vwbr, 1654vwbr, 1613vw, 1585w, 1509m, 1421m, 1349w, 1308w, 1246m, 1228w, 1213vw, 1187vw, 1165w, 1150m, 1034s, 1021sh, 1010sh, 958w, 928wbr, 852vwbr, 820w, 792m, 777s, 727w, 677m, 636vw, 625vw, 619vw, 589w, 554m, 480s, 386mbr, 325vsbr, 281m cm^{-1}. Anal. Calcd for $C_{27}H_{37}Yb$: C, 60.6; H, 6.99. Found: C, 56.4; H, 7.13. ^{1}HNMR (C_6D_6, 20°C): δ 11.40 ($\nu_{1/2}$ = 585 Hz, 30H), δ -9.54 ($\nu_{1/2}$ = 33 Hz, 3H). The highest molecular weight fragment in the EI mass spectrum of the red material was $(Me_5C_5)_2Yb(p\text{-tolyl})$ (535). There were also fragments corresponding to $(Me_5C_5)_2YbMe$ (459), $(Me_5C_5)_2Yb$ (444), $(Me_5C_5)Yb$ (309), and those due to ligand fragmentation.

Attempts made to produce one of these products exclusively by varying the stoichiometry were futile. Reacting an excess of $Zn(p\text{-tolyl})_2$ with the ytterbium complex just resulted in reisolation, while the reaction of $(Me_5C_5)_2Yb$ and $Zn(p\text{-tolyl})_2$ in a 2:1 ratio resulted in a mixture of the purple and red products with the ytterbium starting material.

From $(Me_5C_5)_2Yb(OEt_2)$:

Bis(pentamethylcyclopentadienyl)ytterbium(diethylether) (0.41g, 0.79 mmol) and bis(p-tolyl)zinc (0.29g, 1.2 mmol) were stirred together

in 15 mL of toluene for 14 h, resulting in the formation of a purple solution and a zinc mirror on the sides of the flask. The solution was filtered, and the solvent was removed under reduced pressure. The residue was extracted with 20 mL of pentane, filtered to remove some white solid, and reduced to 3 mL in volume. Cooling to -78°C produced 0.26g (57%) of the purple product. The solvent was removed from the filtrate under reduced pressure to give a red oil, from which 0.08 g of the red product could be sublimed.

Reaction of $(Me_5C_5)_2Yb$ with $ZnAr_2$ in hexane (Ar = Ph, p-tolyl)

In a representative reaction, bis(pentamethylcyclopentadienyl)-ytterbium (0.30g, 0.68 mmol) was dissolved in 25 mL of hexane and added to a slurry of diphenylzinc (0.15g, 0.68 mmol) in 5 mL of hexane. The white solid dissolved during the first 10 minutes of stirring, precipitating in its place a black powder. The solution was allowed to stir for 4 h; the precipitate was then collected by filtration, washed with pentane, and dried under vacuum. The yield of black precipitate was 0.25g. The black precipitate was insoluble in all hydrocarbon solvents. Attempts to dissolve the precipitate in thf yielded a brown oil. When hexane was then added to this oil, the solution turned bright red and precipitated zinc metal. Attempts to isolate a single product from the hexane solution were fruitless.

$ZnPh_2$ product:

The compound melted with decomposition at 196-198°C. IR (Nujol): 3053m, 3035m, 2726w, 1950vw, 1877vw, 1822vw, 1604sh, 1593w, 1559w, 1495w, 1485m, 1417s, 1309w, 1300w, 1261m, 1236sh, 1193w, 1183w, 1158w,

1078m, 1055s, 1030sh, 1021s, 998sh, 991sh, 938wbr, 893vw, 870vw, 847w, 760m, 746m, 737m, 726s, 705vs, 675w, 641w, 467w, 444m, 433w, 395mbr, 270mbr cm^{-1}. Anal. Found: C, 56.2; H, 5.21. A dilute ^{1}HNMR spectrum was obtained by heating a sample of the powder in C_6D_6: δ 7.02 (m), δ 1.59 (s), in an approximate area ratio of 4:5. A small paramagnetic resonance was also visible at δ 7.98 ($\nu_{1/2}$ = 60 Hz). A sample of the compound was then hydrolyzed in CD_3CN and the hydrolysate was examined by ^{1}HNMR spectroscopy. Benzene and C_5Me_5H were visible in approximately a 3:1 ratio.

Zn(p-tolyl)$_2$ product:

The compound melted with decomposition at 168-172°C. IR (Nujol): 3045m, 3022sh, 2994sh, 2725w, 1905vw, 1823vw, 1737vw, 1680vw, 1643vw, 1587m, 1507m, 1487m, 1313vw, 1251m, 1240w, 1233w, 1217vw, 1193s, 1081m, 1038s, 1019sh, 872vw, 856vw, 807m, 799sh, 787s, 727w, 721vw, 714sh, 707vw, 640vw, 594vw, 556w, 485vs, 480vs, 275mbr cm^{-1}. Anal. Found: C, 52.6; H, 5.35. A very dilute ^{1}HNMR spectrum was obtained by heating a sample of the powder in C_6D_6: δ 7.02 (m), δ 2.10 (s), δ 1.64 (s), in an approximate relative integration of 4:3:5. The ^{1}HNMR spectrum also showed two small paramagnetic peaks at δ 7.70 ($\nu_{1/2}$ = 100 Hz) and δ 2.28 ($\nu_{1/2}$ = 60 Hz). A sample of the compound was hydrolyzed in CD_3CN and the hydrolysate was examined by ^{1}HNMR spectroscopy: C_5Me_5H and toluene were visible in approximately a 1:3 ratio.

The diarylzinc compounds were found not to react with $(Me_5C_5)_2Yb(OEt_2)$ in hexane. Attempts were made to react the black powder with excess diarylzinc in hot toluene. In all cases, the black powders did not react further, but were reisolated.

Reaction of $(Me_5C_5)_2Yb$ with $(H_5C_5)ZnMe$

Bis(pentamethylcyclopentadienyl)ytterbium (0.29g, 0.65 mmol) was dissolved in 20 mL of hexane and added with stirring to a solution of $(H_5C_5)ZnMe$ (0.19g, 1.3 mmol) in hexane (5 mL). The solution rapidly precipitated a light green solid. The solution was stirred for 6h, then the green precipitate was collected by filtration. IR (Nujol): 2724w, 1650wbr, 1521w, 1305vw, 1191vw, 1149w, 1040m, 1012s, 905wbr, 874vw, 837w, 796sh, 780sh, 770vs, 723w, 666vwbr, 627w, 567w, 393wbr, 351w, 309w, 270w, 247w cm^{-1}. The green solid melted in a very broad range from 180-280°C. A sample of this precipitate was hydrolyzed in C_6D_6, and the hydrolysate showed both C_5H_6 and C_5Me_5H in the ^{1}HNMR spectrum, in an approximate area ration of 1:2.5. The solvent was removed from the filtrate under reduced pressure, leaving a white residue. The residue was heated under vacuum, and 0.21g of colorless solid sublimed on the sides of the flask. This white solid melted at 92-96°C. IR (Nujol): 2728w, 1658vwbr, 1418s, 1377s, 1308vw, 1206vw, 1166m, 1155m, 1022s, 974shbr, 864wbr, 720m, 701s, 571s, 532w, 465w, 396wbr, 340m cm^{-1}. Anal. Calcd for $C_{11}H_{18}Zn$: C, 61.3; H, 8.43. Found: C, 61.1; H, 8.57. ^{1}HNMR (C_6D_6, 20°C): δ 1.97 (s, 15H), δ -0.65 (s, 3H).

Reaction of $(Me_5C_5)_2Yb$ with $HgEt_2$

Bis(pentamethylcyclopentadienyl)ytterbium (0.25g, 0.56 mmol) was dissolved in 20 mL of pentane and was added slowly with stirring to a solution of diethylmercury (0.090 mL, 0.22g, 0.85 mmol) in pentane (5 mL). At the beginning of the addition, a purple tinge appeared in the formerly clear solution of diethylmercury, along with some turbidity.

As the remainder of the ytterbium complex was added, however, the solution took on the orange color of the ytterbium compound. After stirring for 4h, the solution remained orange, but a precipitate of mercury metal had appeared. The solution was filtered, concentrated, and cooled to -25°C; only $(Me_5C_5)_2Yb$ was reisolated.

Reaction of $(Me_5C_5)_2Yb$ with $HgPh_2$

Bis(pentmethylcyclopentadienyl)ytterbium (0.38g, 0.86 mmol) and diphenylmercury (0.15g, 0.42 mmol) were dissolved together in 35 mL of toluene and stirred for 3 days. There was no precipitation of mercury or color change. The solution was then refluxed for 6h. The solution remained red orange, and no precipitate formed. After cooling, the volume of the solution was reduced to 10 mL, and the mixture was cooled to -25°C, producing white crystals. Examination of the IR of the crystals revealed that they were diphenylmercury. When the reaction was carried out in hexane, the results were the same.

$(Me_5C_5)_2Yb(C_6F_5)$

Bis(pentamethylcyclopentadienyl)ytterbium (0.43g, 0.97 mmol) was dissolved in 20 mL of pentane and was added to a solution of bis(pentafluorophenyl)mercury (0.26g, 0.49 mmol) in pentane (10 mL). The solution was stirred for 14h, which resulted in the precipitation of mercury metal and a color change to purple. The solution was filtered, concentrated to 10 mL in volume, and cooled to -78°C. Purple crystalline solid was isolated by filtration. A second crop of crystals was isolated from the mother liquors by concentrating the solution

further and cooling to -78°C. The combined yield was 0.37g (63%), MP 129-132°C. The material was recrystallized from pentane to remove impurities of $Hg(C_6F_5)_2$. IR (Nujol): 2730w, 1632m, 1603m, 1531m, 1510sh, 1495vs, 1435vs, 1360m, 1309m, 1291w, 1262m, 1247s, 1208vw, 1164m, 1151w, 1099sh, 1084s, 1066s, 1027vs, 964m, 914vsbr, 894sh, 881sh, 865vw, 834sh, 820sh, 803s, 746vw, 725w, 696vw, 672w, 635vw, 621vw, 586w, 573vw, 551vw, 475w, 444vw, 392mbr, 345m, 327vs, 308sh cm^{-1}. Anal. Calcd for $C_{26}H_{30}F_5Yb$: C, 51.1; H, 4.96. Found: C, 50.9; H, 5.21. ^{1}HNMR (C_6D_6, 30°C): δ 12.0 ($\nu_{1/2}$ = 335 Hz). ^{19}FNMR (C_6D_6, 30°C): δ 47.0 ($\nu_{1/2}$ ≃ 1400Hz, 2F), δ 1.79 ($\nu_{1/2}$ = 29 Hz, 1F), δ -7.30 ($\nu_{1/2}$ = 73 Hz, 2F). To verify the presence of the C_6F_5 group, a sample of the compound was hydrolyzed in C_6D_6. While there was no evidence of C_6F_5H in the ^{1}HNMR spectrum of the hydrolysate, it was visible in the ^{19}F spectrum: δ 24.86 (m, 2F), δ 10.01 (t, 1F), δ 1.76 (m, 2F). The EI mass spectrum showed a molecular ion (611), as well as ions corresponding to $(Me_5C_5)Yb(C_6F_5)$ (475), $(Me_5C_5)YbF$ (463), $(Me_5C_5)_2Yb$ (444), $(Me_5C_5)Yb$ (309), Yb (174), and ions corresponding to ligand fragmentation.

[$(Me_5C_5)_2Yb$][o-$H_2C_2B_{10}H_{10}$]

Bis(pentamethylcyclopentadienyl)ytterbium (0.26g, 0.59 mmol) was dissolved in hexane (20 mL) and added with stirring to a slurry of ortho-carborane (0.080g, 0.55 mmol) in hexane (5 mL). A green precipitate rapidly formed as the ortho-carborane dissolved. The solution was allowed to stir for 10 h, and the green precipitate was collected by filtration. The yield of green solid was 0.28g (87%), MP 205-207°C. The solid could be recrystallized from a minimum volume of

hot toluene to give dark green needles. IR (Nujol): 3074m, 3010vs, 2730w, 2657sh, 2610vs, 2575vs, 2563s, 2544sh, 1854vwbr, 1656wbr, 1466m, 1305vw, 1213w, 1154w, 1140m, 1036m, 1018s, 989w, 944wbr, 923w, 794w, 772vw, 723s, 718s, 714s, 699vw, 643wbr, 631vw, 589w, 400shbr, 367w, 283sbr cm^{-1} (IR of o-$H_2C_2B_{10}H_{10}$: 3070s, 2604vs, 2578vs, 1466m, 1214w, 1152m, 1140w, 1048w, 1035m, 1015m, 985m, 943w, 919w, 886vw, 787vw, 717s cm^{-1}). Anal. Calcd for $C_{22}H_{42}B_{10}Yb$: C, 45.0; H, 7.22. Found: C, 44.1; H, 7.38. ^{1}HNMR (C_6D_6, 20°C): δ 1.91 (s, 30H), δ 1.74 (s, $\nu_{1/2}$ = 12 Hz, 2H). ^{1}HNMR of ortho-carborane (C_6D_6, 20°C): δ 2.11 (s, $\nu_{1/2}$ = 16 Hz).

[$(Me_5C_5)_2$Yb][o-$Me_2C_2B_{10}H_{10}$]

Bis(pentamethylcyclopentadienyl)ytterbium (0.28g, 0.63 mmol) was dissolved in 20 mL of hexane and added to a solution of 1,2-dimethyl-ortho-carborane (0.11g, 0.64 mmol) in hexane (10 mL) with stirring; no color change was observed. The solution was filtered, reduced to 10 mL in volume, and cooled to -25°C. The first batch of product was isolated as green crystals which reversibly turned orange above +5°C. The second crop of compound consisted of two kinds of crystals: the thermochroic form, and green crystals which stayed green at room temperature. The two kinds of crystals were identical spectroscopically. The combined yield of material was 0.30g (77%). The orange crystals melted at 170-172°C, while the green crystals melted at 195-197°C. IR (Nujol): 3074w, 3012sh, 2729m, 2591vsbr, 2561sh, 2037vwbr, 1957vwbr, 1939vwbr, 1869vwbr, 1850vwbr, 1655wbr, 1536shbr, 1447s, 1395w, 1217sh, 1195w, 1152m, 1138sh, 1020s, 951w, 938w, 921w, 903sh, 792m, 773w, 739w, 728m, 696w, 678vw, 666w, 646w, 630sh, 591vw, 514w, 482vw, 453vw, 370mbr, 289vs cm^{-1} (IR of

o-$Me_2C_2B_{10}H_{10}$: 3071w, 3048sh, 2586vsbr, 2033vwbr, 1948vwbr, 1856vwbr, 1666vwbr, 1536shbr, 1395s, 1314vw, 1262vw, 1195w, 1151vw, 1142vw, 1089vw, 1072vw, 1022s, 988vw, 949w, 939sh, 920w, 905vw, 788m, 770w, 739m, 729s, 678w, 663w, 644w, 512w, 479w, 454w cm^{-1}). Anal. Calcd for $C_{24}H_{46}B_{10}Yb$: C, 46.8; H, 7.54. Found: C, 47.0; H, 7.71. ^{1}HNMR (C_6D_6, 20°C): δ 1.94 (s, 30H), δ 1.14 (s, 6H). ^{1}HNMR of 1,2-dimethyl-ortho-carborane (C_6D_6, 20°C): δ 1.17 (s).

[$(Me_5C_5)_2$Yb][m-$H_2C_2B_{10}H_{10}$]

Bis(pentamethylcyclopentadienyl)ytterbium (0.29g, 0.65 mmol) was dissolved in 20 mL of hexane and added to meta-carborane (0.09g, 0.62 mmol) with stirring. The carborane dissolved, but there was no visible change in the orange color of the solution. The volume was reduced to 10 mL, and the solution was cooled to -25°C, resulting in the formation of green blades. The crystals were isolated by filtration and dried under reduced pressure. The yield was 0.25g (69%). The compound turned brown at 60°C, then orange at 95°C, and finally melted at 186-188°C. These color changes were all reversible. IR (Nujol): 3066w, 3024vs, 2730w, 2601vs, 1655vwbr, 1562vwbr, 1444s, 1315vw, 1164w, 1153s, 1072m, 1027m, 994w, 959vw, 939vw, 813w, 780vw, 720s, 698vw, 662vw, 627w, 590vw, 406sh, 366mbr, 307sh, 285sbr cm^{-1} (IR of m-$H_2C_2B_{10}H_{10}$: 3064s, 2603vsbr, 2096vw, 1844vw, 1459s, 1307vw, 1160s, 1072s, 1056w, 1024s, 991s, 971vw, 939vw, 927vw, 895vw, 887sh, 811vw, 775vw, 720vs cm^{-1}). Anal. Calcd for $C_{22}H_{42}B_{10}Yb$: C, 45.0; H, 7.22. Found: C, 45.1; H, 7.20. ^{1}HNMR (C_6D_6, 20°C): only one resonance observed at δ 1.93 (s). ^{1}HNMR of meta-carborane (C_6D_6, 20°C): δ 1.97 (s, $\nu_{1/2}$ = 16 Hz).

[$(Me_5C_5)_2Yb]_2[(H_5C_5)_2Fe$]

Bis(pentamethylcyclopentadienyl)ytterbium (0.22g, 0.50 mmol) was dissolved in 10 mL of toluene and was added to a solution of ferrocene (0.09g, 0.48 mmol) in toluene (10 mL). The volume of the solution was reduced to 3 mL, and 5 mL of pentane was added. The mixture was cooled to -25°C, producing orange-red blocks. The yield was 0.15g (58%), MP 199-202°C. IR (Nujol): 3101vw, 3069m, 2723w, 1653vwbr, 1495vs, 1448s, 1418m, 1407m, 1313vw, 1164sh, 1150w, 1103s, 1019vs, 1005s, 908vw, 886sh, 857w, 846sh, 826s, 815s, 752vw, 728w, 693w, 665w, 629vw, 591vw, 496m, 476m, 393brsh, 368mbr, 309sh, 280vs cm^{-1}. Anal. Calcd for $C_{50}H_{70}Yb_2Fe$: C, 56.0; H, 6.59. Found: C, 55.5; H, 6.55. ^{1}HNMR (C_6D_6, 30°C): δ 3.99 (s, 10H), δ 1.93 (s, 60H). ^{1}HNMR of ferrocene (C_6D_6, 20°C): δ 4.00 (s).

[$(Me_5C_5)_2Yb]_2[(H_5C_5)_2Co$]

Bis(pentamethylcyclopentadienyl)ytterbium (0.28g, 0.63 mmol) was dissolved in toluene (20 mL) and added with stirring to a solution of cobaltocene (0.060g, 0.32 mmol) in toluene (10 mL). The solution remained dark red-orange. The volume was reduced to 3 mL, and 5 mL of pentane was added to the solution. The mixture was then cooled to -25°C, producing brown blocks. The yield from this reaction was 0.26g (77%). The crystals gradually turned bright green as they were heated above ca. 150°C, but they did not melt below 300°C. IR (Nujol): 3107sh, 3067m, 2725w, 2035vwbr, 1814vw, 1656wbr, 1448s, 1419sh, 1404w, 1336sh, 1214vw, 1164sh, 1153w, 1103m, 1061sh, 1046m, 1020m, 1007s, 994sh, 911w, 887vw, 832m, 802vs, 780sh, 723w, 695w, 664vw, 633vwbr, 623vwbr, 590w, 568vw, 522vw, 428wbr, 367mbr, 326sh, 308sh, 282vs cm^{-1}. Anal. Calcd for

$C_{50}H_{70}CoYb$: C, 55.8; H, 6.57. Found: C, 55.5; H, 6.59. ^{1}HNMR (C_6D_6, 30°C): δ 1.93 (s, 60H), δ -49.84 ($\nu_{1/2}$ = 130 Hz, 10H). ^{1}HNMR of $(H_5C_5)_2Co$ (C_6D_6, 30°C): δ -50.1 ($\nu_{1/2}$ = 145 Hz). The product was independent of the reaction stoichiometry; a 1:1 reaction gave the same species upon crystallization. It was found that if the solution was stirred for more than 10-12h, a green precipitate began to appear, indicating slow ring exchange between the Yb and Co centers.

Reaction of $(Me_5C_5)_2Yb$ with $(H_5C_5)_2Mn$

Bis(pentamethylcyclopentadienyl)ytterbium (0.29g, 0.65 mmol) was dissolved in toluene (15 mL) and added to a solution of manganocene (0.12g, 0.65 mmol) in toluene (10 mL) with stirring. The solution immediately precipitated bright green powder. The mixture was allowed to stir for 24h. The green powder was isolated by filtration. The solvent was removed from the filtrate under reduced pressure, and the resulting orange residue was heated to 100°C under vacuum. Some dark orange crystals (ca. 0.08g) sublimed out of the residue, followed more slowly by some yellow-orange crystalline solid (ca. 0.05g). The dark orange crystals melted at 82-84°C. IR (Nujol): 3090m, 2730m, 2680w, 2671vw, 2058vw, 1733w, 1671w, 1618m, 1602sh, 1522m, 1424w, 1414w, 1309vw, 1167vw, 1156vw, 1110m, 1106m, 1067w, 1025m, 1005vs, 895vw, 850vw, 801s, 774vs, 723sh, 710sh, 666vw, 629vw, 586vw, 540s, 483s, 442w, 414w, 278m cm^{-1}. Anal. Calcd for $C_{20}H_{30}Mn$: C, 73.8; H, 9.31. Found: C, 73.7; H, 9.21. The EI mass spectrum showed $(Me_5C_5)_2Mn$ at 325, as well as a small ion for $(Me_5C_5)(H_5C_5)Mn$ at 255. The mass spectrum of the yellow-orange material showed only the fragmentation pattern for

$(Me_5C_5)_2Mn$.

The green solid from the reaction was dissolved in thf, giving a purple solution. The solution was filtered, and the solvent was removed under reduced pressure, leaving a red-purple residue. The residue was extracted with toluene, leaving behind an orange solid (ca. 0.10g). The red toluene solution was reduced in volume to 3 mL, and cooled to -25°C. Green solid precipitated out of the solution (ca. 0.13g). Both solids were then recrystallized from thf. The orange solid recrystallized from thf as purple blocks which lost solvent and turned orange under reduced pressure. These orange blocks did not melt below 320°C. IR (Nujol): 3088m, 3072m, 2707vw, 1739vwbr, 1700vwbr, 1639wbr, 1573wbr, 1465s, 1367w, 1340w, 1312vw, 1294vw, 1177w, 1033vs, 1008vs, 928w, 878s, 844sh, 789s, 770vs, 748vsbr, 670w, 485wbr, 396mbr cm^{-1}. Anal. Calcd for $C_{14}H_{18}OYb$: C, 44.8; H, 4.84. Found: C, 43.8; H, 4.74. ^{1}HNMR (d^8-thf, 20°C): δ 5.68 (s, 10H), δ 3.58 (m, 4H), δ 1.73 (m, 4H). The green material recrystallized from thf as red crystals. These crystals did not lose solvent at room temperature under vacuum, but turned green when heated in toluene or when heated above 120°C (did not melt below 320°C). IR (Nujol): 3087w, 3072w, 3056w, 2720w, 1581vw, 1449s, 1340w, 1311vw, 1294vw, 1173w, 1034vs, 1009s, 917m, 880s, 820sh, 799w, 774mbr, 742vs, 723sh, 670w, 589vw, 266m cm^{-1}. Anal. Calcd for $C_{23}H_{36}O_2Yb$: C, 53.4; H, 7.02. Found: C, 51.9; H, 6.84. ^{1}HNMR (C_7D_8, 20°C): δ 6.02 (s, 5H), δ 3.44 (m, 8H), δ 2.15 (s, 15H), δ 1.40 (m, 8H).

Reaction of $(Me_5C_5)_2Yb$ with $(Me_5C_5)_2Mn$

Bis(pentamethylcyclopentadienyl)ytterbium (0.27g, 0.61 mol) was

dissolved in 20 mL of hexane and added to a solution of bis(pentamethyl-cyclopentadienyl)manganese (0.20g, 0.61 mmol) in hexane (15 mL), and the mixture was allowed to stir for 14 h. No reaction was apparent. The solution was then filtered, concentrated to 10 mL in volume, and cooled to -25°C; the two starting materials crystallized out separately.

X-Ray Crystallographic Studies

$(Me_5C_5)_2Yb$ - polymeric form

Brown-black crystals of the compound were grown by extremely slow cooling of a hexane solution to -15°C over several days. Bis(pentamethylcyclopentadienyl)ytterbium has a strong tendency to occlude hydrocarbon solvents, but very slow cooling of the solution allowed the formation of solvent-free crystals. A crystal was cleaved to give a fragment of approximate dimensions 0.32 mm x 0.44 mm x 0.60 mm, which was lodged into a thin-walled 0.5 mm quartz capillary in a nitrogen-filled drybox. The capillary was flame sealed.

Preliminary precession photographs indicated monoclinic Laue symmetry, and yielded preliminary cell dimensions. The crystal was transferred to an Enraf-Nonius automated diffractometer[16] and centered in the beam. Automatic peak indexing procedures yielded the same unit cell as the precession photographs and confirmed the Laue symmetry. Examination of the 0 k 0 and h 0 l zones showed the following systematic absences: 0 k 0, k = 2n + 1; h 0 l, h + l = 2n + 1, consistent only with the space group $P2_1/n$. Accurate cell parameters and the orientation matrix were determined by a least-squares fit to the setting angles of the unresolved MoKα components of 24 symmetry related reflections with 2θ between 27 and 29°. The results are given in Table (I) along with the parameters used for data collection.

The 5577 raw data were converted to structure factor amplitudes and their esd's by correcting for scan speed, background, and Lorentz-

polarization effects[17-19]. Analysis of the azimuthal scan data[20] showed a variation of I_{min}/I_{max} of 0.563 in the average relative intensity curve. An empirical absorption correction was applied using the average relative intensity curve of the azimuthal scan data[18].

The unique set of 4933 data were used to solve and refine the structure. The ytterbium atoms were located through the use of a three-dimensional Patterson map. The remaining non-hydrogen atoms were located through the use of standard Fourier techniques. All non-hydrogen atoms were refined anisotropically. All of the hydrogen atoms were located in a difference Fourier map. The hydrogen atoms were placed in calculated positions, and were included in the structure factor calculation, but were not refined.

The final residuals for 380 variables refined against the 4190 data for which $F_o^2 > 3\sigma(F_o^2)$ were R = 0.0206, R_w = 0.0289, and GOF = 1.491. The R value for all 4933 data was 0.0379.

The quantity minimized by the least-squares program was $\Sigma w(|F_o|-|F_c|)^2$, where w is the weight of a given observation. The p-factor[21], used to reduce the weight of intense reflections, was set to 0.03 throughout the refinement. The analytical forms for the scattering factor tables for the neutral atoms[22] were used and all non-hydrogen scattering factors were corrected for both the real and imaginary components of anomalous dispersion[23].

Inspection of the residuals ordered in ranges of $\sin\theta/\lambda$, $|F_o|$, and parity and value of the individual indexes showed no unusual features or trends. There was evidence of secondary extinction in the low-angle, high-intensity data, and a secondary extinction correction was applied

to the data[24]. The secondary extinction coefficient was refined in the least-squares calculations to a value of $1.45(2) \times 10^{-7}$ e^{-2}.

The highest and lowest peaks in the final difference Fourier map had electron densities of 0.456 and -0.686 $e/Å^3$, respectively, and were associated with Yb(2).

Table (I). Crystal Data for $(Me_5C_5)_2Yb$ (25°C)

Space Group	$P2_1/n$
a, Å	31.013(3)
b, Å	12.466(2)
c, Å	9.836(1)
β, deg	95.960(9)
V, $Å^3$	3782(2)
Z	4
fw	887.00
d (calc.), g/cm^3	1.56
μ (calc.), 1/cm	49.25
size, mm	0.32 x 0.44 x 0.60
radiation	MoKα (λ = 0.71073Å)
monochromator	highly oriented graphite
scan range, type	$3° \leq 2\theta \leq 45°$, ω
scan speed, deg/min	0.694 - 6.71, variable
scan width, deg	$\Delta\theta = 0.55 + 0.35 \tan\theta$
reflections collected	5577; ±h, +k, +l
unique reflections	4933
reflections, $F_o^2 > 3\sigma(F_o^2)$	4190
variables	380
R, %	0.0206
R_w, %	0.0289
R_{all}, %	0.0379
GOF	1.491
g, e^{-2}	$1.45(2) \times 10^{-7}$
largest Δ/σ in the last least-squares cycle	0.11

Intensity Standards: 2, 7, -4; 8, 4, 5; 20, 2, 1; measured every two hours of x-ray exposure time. Over the period of data collection no decay in intensity was observed.

Orientation Standards: 3 reflections were checked after every 250 measurements. Crystal orientation was redetermined if any of the reflections were offset from their predicted positions by more than 0.1°. Reorientation was required 5 times during data collection.

$(Me_5C_5)_2Yb(\mu\text{-}C_2H_4)Pt(PPh_3)_2$

Deep red needles of the compound were grown by slow cooling of a warm toluene solution to room temperature. A large needle was cleaved to yield a crystal of approximate dimensions 0.15 mm x 0.30 mm x 0.40 mm. This was lodged into a thin walled 0.3 mm quartz capillary in a nitrogen filled drybox. The capillary was then flame sealed.

Preliminary precession photographs indicated triclinic Laue symmetry. The crystal was transferred to an Enraf-Nonius automated diffractometer[16], cooled to -80°C, and centered in the beam. Automatic peak indexing procedures yielded cell parameters and confirmed the Laue symmetry.

Accurate cell parameters and the orientation matrix were determined by a least-squares fit to the setting angles of the unresolved MoKα components of 24 symmetry related reflections with 2θ between 26 and 29°. The results are given in Table (II) along with the parameters used for data collection.

The 6568 raw data were converted to structure factor amplitudes and their esd's by correcting for scan speed, background, and Lorentz-polarization effects[17-19]. Analysis of the azimuthal scan data[20] showed a variation of I_{min}/I_{max} of 0.601 in the average relative intensity curve. An analytical absorption correction was applied to the data using the sizes of the indexed faces of the crystal and a 16 x 6 x 10 Gaussian grid of internal points[18]. The maximum and minimum transmission factors were 0.548 and 0.294, respectively.

The unique set of 6568 data were used to solve and refine the

structure. The heavy atoms were located through the use of a three-dimensional Patterson map. The remaining atoms were located through the use of standard Fourier and difference Fourier techniques. The non-hydrogen atoms were refined anisotropically. The hydrogen atoms on the ethylene carbons were located in a difference Fourier map, and they were refined isotropically. The hydrogen atoms on the phenyl carbons and on the methyl carbons were located in a difference Fourier map, then placed in calculated positions with fixed thermal parameters; they were included in structure factor calculations, but were not refined.

The final residuals for 576 variables refined against the 5929 data for which $F_o^2 > 3\sigma(F_o^2)$ were R = 0.0200, R_w = 0.0314, and GOF = 1.70. The R value for all 6568 data was 0.0256.

The quantity minimized by the least-squares program was $\Sigma w(|F_o| - |F_c|)^2$, where w is the weight of a given observation. The p-factor[21], used to reduce the weight of intense reflections, was set to 0.03 throughout the refinement. The analytical forms for the scattering factor tables for the neutral atoms[22] were used and all non-hydrogen scattering factors were corrected for both the real and imaginary components of anomalous dispersion.[23]

Inspection of the residuals ordered in ranges of $\sin\theta/\lambda$, $|F_o|$, and parity and value of the individual indexes showed no unusual features or trends. There was evidence of secondary extinction in the low-angle, high-intensity data, and a secondary extinction correction was applied to the data[24]. The secondary extinction coefficient was refined in the least-squares calculations to a value of 6.2(7) x 10^{-8} e^{-2}. Three

reflections showed anomalously large values of $w \times \Delta^2$. These were rejected as "bad" data, and were not included in the least-squares refinement.

The largest peak in the final difference Fourier map had an electron density of 0.919 e/Å3. and was associated with the Pt atom.

Table (II). Crystal Data for $(Me_5C_5)_2Yb(\mu\text{-}C_2H_4)Pt(PPh_3)_2$ (-80°C)

Space Group	$P\bar{1}$
a, Å	9.577(2)
b, Å	14.797(2)
c, Å	18.429(2)
α, deg	96.90(1)
β, deg	92.56(1)
γ, deg	102.77(1)
V, Å3	2522(1)
Z	2
fw	1191.23
d (calc.), g/cm^3	1.57
μ (calc.), 1/cm	47.35
size, mm	0.15 x 0.20 x 0.40
radiation	MoKα (λ = 0.71073Å)
monochromator	highly oriented graphite
scan range, type	$3° \leq 2\theta \leq 45°$, θ-2θ
scan speed, deg/min	0.838 - 6.71, variable
scan width, deg	$\Delta\theta = 0.65 + 0.35 \tan\theta$
reflections collected	6568; +h, ±k, ±l
unique reflections	6568
reflections, $F_o^2 > 3\theta(F_o^2)$	5933
variables	576
R, %	0.0200
R_w, %	0.0314
R_{all}, %	0.0256
GOF	1.70
g, e^{-2}	$6.2(7) \times 10^{-8}$
Largest Δ/θ in final least-squares cycle	0.12

Intensity Standards: -1, 5, -12; -4, 9, -3; -6, 1, 3: measured every two hours of x-ray exposure time. Over the period of data collection no decay in intensity was observed.

Orientation Standards: 3 reflections were checked after every 250 measurements. Crystal orientation was redetermined if any of the reflections were offset from their predicted positions by more than 0.1°. Reorientation was required 5 times during data collection. The cell constants and errors were taken to be the average of the initial and final values.

$(Me_5C_5)_2Yb(\eta^2\text{-}MeC{\equiv}CMe)$

Crystals were grown by slow cooling of a saturated solution of the compound in a 4:1 mixture of octane/2-butyne. A large crystal was cleaved to yield a small fragment of approximate dimensions 0.18 mm x 0.33 mm x 0.40 mm suitable for data collection. The fragment was lodged in a 0.3 mm quartz capillary in a nitrogen-filled drybox, and the capillary was flame sealed.

Precession photographs indicated monoclinic Laue symmetry, and yielded preliminary cell dimensions. The crystal was transferred to an Enraf-Nonius automated diffractometer[16], cooled to -80°C, and centered in the beam. Automatic peak indexing procedures yielded the same unit cell as the precession photographs and confirmed the Laue symmetry. Examination of the 0 k 0 and h 0 l zones showed the following systematic absences: 0 k 0, k = 2n + 1; h 0 l, h + l = 2n + 1, consistent only with the space group $P2_1/n$. Accurate cell parameters and the orientation matrix were determined by a least-squares fit to the setting angles of the unresolved MoKα components of 24 symmetry related reflections with 2θ between 28 and 30°. The results are given in Table (III) along with the parameters used for data collection.

The 3324 raw data were converted to structure factor amplitudes and their esd's by correcting for scan speed, background, and Lorentz-polarization effects[17-19]. Analysis of the azimuthal scan data[20] showed a variation of I_{min}/I_{max} of 0.567 in the average relative intensity curve. An empirical absorption correction was applied using the average relative intensity curve of the azimuthal scan data[18].

The unique set of 2971 data were used to solve and refine the structure. The ytterbium atom was located through the use of a three-dimensional Patterson map. The carbon atoms were located through the use of standard Fourier techniques. All non-hydrogen atoms were refined with anisotropic thermal parameters. The hydrogen atoms on the 2-butyne ligand were located in a difference map, and were refined with isotropic thermal parameters. The hydrogen atoms on the pentamethylcyclopentadienyl rings were located in a difference Fourier map, then placed in calculated positions. They were included in the structure factor calculation, but were not refined.

The final residuals for 251 variables refined against the 2449 data for which $F_0^2 > 3\sigma(F_0^2)$ were R = 0.022, R_w = 0.029, and GOF = 1.505. The R value for all 2971 data was 0.044.

The quantity minimized by the least-squares program was $\Sigma w(|F_0| - |F_c|)^2$, where w is the weight of a given observation. The p-factor[21], used to reduce the weight of intense reflections, was set to 0.03 throughout the refinement. The analytical forms for the scattering factor tables for the neutral atoms[22] were used and all non-hydrogen scattering factors were corrected for both the real and imaginary components of anomalous dispersion[23].

Inspection of the residuals ordered in ranges of $\sin\theta/\lambda$, $|F_0|$ and parity and value of the individual indexes showed no unusual features or trends. There was evidence of secondary extinction in the low-angle, high-intensity data, and a secondary extinction correction was applied to the data[24]. The secondary extinction coefficient was refined in the

least-squares calculations to a value of 3.1(8) x 10^{-8} e^{-2}. Two reflections showed anomalously high values of w x Δ^2. They were rejected as "bad" data, and were not included in the refinement.

The highest and lowest peaks in the final difference Fourier map had electron densities of 0.709 and -0.438 e/$Å^3$, respectively, and both were associated with the ytterbium atom.

Table (III). Crystal Data for $(Me_5C_5)_2Yb(\eta^2\text{-}MeC{\equiv}CMe)$ (-80°C)

Space Group	$P2_1/n$
a, Å	15.738(2)
b, Å	15.299(1)
c, Å	9.724(1)
β, deg	103.90(1)
V, Å^3	2272.6(8)
Z	4
fw	497.59
d (calc.), g/cm^3	1.45
μ (calc.), 1/cm	41.06
size, mm	0.18 x 0.33 x 0.40
radiation	MoKα (λ = 0.71073Å)
monochromator	highly oriented graphite
scan range, type	$3° \leq 2\theta \leq 45$Å, θ-2θ
scan speed, deg/min in θ	0.838 - 6.71, variable
scan width, deg	$\Delta\theta = 0.65 + 0.35 \tan\theta$
reflections collected	3324, ±h, +k, +l
unique reflections	2971
reflections, $F_0^2 > 3\sigma(F_0^2)$	2441
variables	251
R, %	0.022
R_w, %	0.029
R_{all}, %	0.044
GOF	1.505
g, e^{-2}	3.1(8) x 10^{-8}
largest Δ/σ in final least-squares cycle	0.03

Intensity Standards: 10 2 2, 1 10 2, 2 1 6; measured every two hours of x-ray exposure time. Over the period of data collection 3.5% decay in intensity was observed. A linear decay correction was applied to the raw data.

Orientation Standards: 3 reflections were checked after every 250 measurements. Crystal orientation was redetermined if any of the reflections were offset from their predicted positions by more than 0.1°. Reorientation was required 2 times during data collection.

$[(Me_5C_5)_2Yb]_2(\mu\text{-}F)$

Brown blocks of the compound were grown by slow cooling of a warm saturated toluene solution to room temperature, and were separated from the accompanying crystals of the tetranuclear species manually. A crystal of approximate dimensions 0.17 mm x 0.23 mm x 0.42 mm was selected and lodged in a thin-walled 0.3 mm quartz capillary in a nitrogen-filled drybox. The capillary was then flame-sealed.

Preliminary precession photographs indicated monoclinic Laue symmetry, and yielded preliminary cell dimensions. The crystal was then transferred to an Enraf-Nonius automated diffractometer[16] and centered in the beam. Automatic peak indexing procedures yielded the same unit cell as the precession photographs and confirmed the Laue symmetry. Examination of the h 0 l and h 1 l zones showed the following systematic absences: h 0 l; l = 2n + 1; h k l; h + k = 2n + 1, consistent with both space groups Cc and C2/c. Selection of the space group C2/c for data refinement was proven correct by the successful convergence of the solution. Accurate cell parameters and the orientation matrix were determined by a least-squares fit to the setting angles of the unresolved MoKα components of 24 symmetry related reflections with 2θ between 26 and 32°. The results are given in Table (IV) along with the parameters used for data collection.

The 2695 raw data were converted to structure factor amplitudes and their esd's by correcting for scan speed, background, and Lorentz-polarization effects[17-19]. Analysis of the azimuthal scan data[20] showed a variation of I_{min}/I_{max} of 0.766 in the average relative intensity

curve. An analytical absorption correction was applied to the data using the sizes of the indexed faces of the crystal and a 10 x 8 x 8 Gaussian grid of internal points[18]. The maximum and minimum transmission factors were 0.495 and 0.353, respectively.

The unique set of 2483 data were used to solve and refine the structure. The ytterbium atoms were located through the use of a three-dimensional Patterson map. The remaining non-hydrogen atoms were located through the use of standard Fourier techniques. All non-hydrogen atoms were refined anisotropically. The hydrogen atoms on the methyl groups were located in a difference Fourier map, then placed in idealized positions and given isotropic thermal parameters 1.20 times those of the carbons to which they were attached. They were included in the structure factor calculation, but were not refined.

The final residuals for 197 variables refined against the 2256 data for which $F_o^2 > 3\sigma(F_o^2)$ were R = 0.0173, R_w = 0.0248, and GOF = 1.75.

The quantity minimized by the least-squares program was $\Sigma w(|F_o|-|F_c|)^2$, where w is the weight of a given observation. The p-factor[21], used to reduce the weight of intense reflections, was set to 0.02 throughout the refinement. The analytical forms for the scattering factor tables for the neutral atoms[22] were used and all non-hydrogen scattering factors were corrected for both the real and imaginary components of anomalous dispersion[23].

Inspection of the residuals ordered in ranges of $\sin\theta/\lambda$, $|F_o|$, an parity and value of the individual indexes showed no unusual features or trends. There was evidence of secondary extinction in the low-angle, high-intensity data, and a secondary extinction correction was applied

to the data[24]. The secondary extinction coefficient was refined in the least-squares calculations to a value of 1.44(7) x 10^{-7} e^{-2}.

The largest peak in the final difference Fourier map had an electron density of 0.667 e/$Å^3$, and was associated with Yb(2).

Table (IV). Crystal Data for $[(Me_5C_5)_2Yb]_2(\mu\text{-}F)$ (25°C)

Space Group	C2/c
a, Å	16.319(2)
b, Å	14.314(1)
c, Å	16.760(2)
β, deg	104.39(1)
V, Å^3	3792(2)
Z	4
fw	906.00
d (calc.), g/cm^3	1.597
μ (calc.), 1/cm	49.17
size, mm	0.17 x 0.23 x 0.42
radiation	MoKα (λ = 0.71073Å)
monochromator	highly oriented graphite
scan range, type	$3° \leq 2\theta \leq 45°$, θ-2θ
scan speed, deg/min	0.745 - 6.71, variable
scan width, deg	$\Delta\theta = 0.60 + 0.35 \tan\theta$
reflections collected	2695, +h, +k, ±l
unique reflections	2483
reflections, $F_o^2 > 3\sigma(F_o^2)$	2256
variables	197
R, %	0.0173
R_w, %	0.0248
GOF	1.745
g, e^{-2}	1.44(7) x 10^{-7}
largest Δ/σ in the last least-squares cycle	0.00

Intensity Standards: 11, 1, 3; 2, 10, 1; 3, 1, -11; measured every two hours of x-ray exposure time. Over the period of data collection 0.9% decay in intensity was observed. No decay correction was applied.

Orientation Standards: 3 reflections were checked after every 250 measurements. Crystal orientation was redetermined if any of the reflections were offset from their predicted positions by more than 0.1°. Reorientation was not required during data collection.

$[(Me_5C_5)_3Yb_2F_2]_2 \cdot (PhMe)_2$

Red needles of the compound were grown by slow cooling of a hot toluene solution to room temperature. A large needle was cleaved, yielding a fragment of approximate dimensions 0.12 mm x 0.24 mm x 0.30 mm suitable for diffraction. This fragment was lodged in a 0.3 mm thin walled quartz capillary in a nitrogen-filled drybox, and the capillary was flame sealed. Precession photographs indicated monoclinic Laue symmetry, and yielded preliminary cell dimensions.

The crystal was transferred to an Enraf-Nonius automated diffractometer[16] and centered in the beam. Automatic peak indexing procedures yielded the same unit cell as the precession photographs and confirmed the Laue symmetry. Examination of the h 0 l and h 1 l zones showed the following systematic absences: h 0 l; l = 2n + 1, h k l; h + k = 2n + 1, consistent with both space groups Cc and C2/c. Selection of the space group C2/c for data refinement was proven correct by successful convergence of the solution. Accurate cell parameters and the orientation matrix were determined by a least-squares fit to the setting angles of the unresolved MoKα components of 24 symmetry related reflections with 2θ between 28 and 29°. The results are given in Table (V) along with the parameters used for data collection.

The 4690 raw data were converted to structure factor amplitudes and their esd's by correcting for scan speed, background, and Lorentz-polarization effects[17-19]. Analysis of the azimuthal scan data[20] showed a variation of I_{min}/I_{max} of 0.559 in the average relative intensity curve. An analytical absorption correction was applied to the data

using the dimensions of the indexed faces of the crystal and a 12 x 12 x 6 Gaussian grid of internal points[18]. The maximum and minimum transmission factors were 0.549 and 0.268, respectively.

The unique set of 4287 data was used to solve and refine the structure. The ytterbium atoms were located through the use of a three-dimensional Patterson map. The remaining non-hydrogen atoms were located through the use of standard Fourier techniques.

During the course of the refinement, the difference Fourier map indicated the presence of one disordered molecule of toluene per asymmetric unit. The toluene was placed and refined isotropically as two half-occupancy molecules related by the two-fold axis. The C-C-C angles were constrained to be 120°, the C(Ph)-C(Ph) bond lengths to be 1.40Å, and the C(Ph)-C(Me) length to be 1.50Å during least-squares refinement. The ring carbons were furthermore all constrained to have the same isotropic thermal parameter. The three largest peaks in the final difference Fourier map were all around the disordered ring, indicating that there may have been another disordered position, but no other ring model could be fitted successfully.

The hydrogen atoms on the pentamethylcyclopentadienyl rings on Yb(1) were located. These atoms were placed and included in the structure factor calculations with isotropic thermal parameters, but were not refined.

The final residuals for 329 variables refined against the 3305 data for which $F_o^2 > 3\sigma(F_o)^2$ were R = 0.0272, R_w = 0.0356, and GOF = 1.58. The R value for all 4287 data was 0.0508. The quantity minimized by the least-squares program was $\Sigma w(|F_o| - |F_c|)2$, where w is the weight of a

given observation. The p-factor[21], used to reduce the weight of intense reflections, was set to 0.03 throughout the refinement. The analytical forms for the scattering factor tables for the neutral atoms[22] were used and all non-hydrogen scattering factors were corrected for both the real and imaginary components of anomalous dispersion[23].

Inspection of the residuals ordered in ranges of $\sin\theta/\lambda$, $|F_o|$, and parity and value of the individual indexes showed no unusual features or trends. There was evidence of secondary extinction in the low-angle, high-intensity data, and a secondary extinction correction was applied to the data[24]. The secondary extinction coefficient was refined in the least-squares calculations to a value of $3.1(4) \times 10^{-8}\ e^{-2}$.

The largest peak in the final difference Fourier map had an electron density of 0.837 e/Å3, and was associated with the disordered toluene molecule.

Table (V). Crystal Data for $[(Me_5C_5)_3Yb_2F_2]_2 \cdot (PhMe)_2$ (25°C)

Space Group	C2/c
a, Å	26.805(3)
b, Å	10.285(1)
c, Å	24.621(2)
β, deg	104.530(9)
V, Å^3	6570(2)
Z	4
fw	1763.96
d (calc.), g/cm^3	1.78
μ (calc.), 1/cm	56.80
size, mm	0.12 x 0.24 x 0.30
radiation	MoKα (λ = 0.71073Å)
monochromator	highly oriented graphite
scan range, type	$3° \leq 2\theta \leq 45°$, θ-2θ
scan speed, deg/min	0.694 - 6.71, variable
scan width, deg	$\Delta\theta = 0.55 + 0.35 \tan\theta$
reflections collected	4690; ±h, +k, +l
unique reflections	4287
reflections, $F_o^2 > 3\sigma(F_o^2)$	3305
variables	329
R, %	0.0272
R_w, %	0.0356
R_{all}, %	0.0508
GOF	1.58
g, e^{-2}	3.1(4) x 10^{-8}
largest Δ/θ in final least squares cycle	9.71

Intensity Standards: 3, 7, -3; 0, 0, 12; 12, 0, 2: measured every two hours of x-ray exposure time. Over the period of data collection, 2.4 % decay in intensity was observed. A linear decay correction was applied to the raw data.

Orientation Standards: 3 reflections were checked after every 250 measurements. Crystal orientation was redetermined if any of the reflections were offset from their predicted positions by more than 0.1°. No reorientation was required during data collection.

$\underline{(Me_5C_5)_2Yb(\mu\text{-}Me)Be(C_5Me_5)}$

Crystals were grown by slow cooling of a saturated pentane solution. A dark orange prism of approximate dimensions 0.14 mm x 0.35mm x 0.31mm was selected, loaded into a 0.3mm quartz capillary in a nitrogen-filled dry box, and flame sealed.

Preliminary precession photographs indicated monoclinic Laue symmetry, and yielded preliminary cell dimensions. The crystal was transferred to an Enraf-Nonius automated diffractometer[16], cooled to -80°C, and centered in the beam. Automatic peak indexing procedures yielded the same unit cell as the precession photographs and confirmed the Laue symmetry. Examination of the 0 k 0 and h 0 l zones showed the following systematic absences: 0 k 0, k = 2n + 1; h 0 l, h + l = 2n + 1; consistent only with the space group $P2_1/n$. Accurate cell parameters and the orientation matrix were determined by a least-squares fit to the setting angles of the unresolved MoKα components of 24 symmetry related reflections with 2θ between 27 and 29°. The results are given in Table (VI) along with the parameters used for data collection.

The 4383 raw data were converted to structure factor amplitudes and their esd's by correcting for scan speed, background, and Lorentz-polarization effects[17-19]. Analysis of the azimuthal scan data[20] showed a variation of I_{min}/I_{max} of 0.613 in the average relative intensity curve. An analytical absorption correction was applied to the data using the sizes of the indexed faces of the crystal and a 12 x 12 x 6 Gaussian grid of internal points[18]. The maximum and minimum transmission factors were 0.7719 and 0.4408, respectively.

The unique set of 3887 data were used to solve and refine the structure. The Yb atom was located through the use of a three-dimensional Patterson map. The remaining non-hydrogen atoms were located through the use of standard Fourier techniques.

Examination of the difference Fourier map revealed the presence of all hydrogen atoms. The hydrogen atoms on the pentamethylcyclopentadienyl rings were placed in idealized positions and given isotropic thermal parameters 1.30 times those of the carbons to which they were attached. They were included in the structure factor calculation, but were not refined. Difference Fourier maps subsequently revealed an alternate placement of the hydrogen atoms attached to C19. These hydrogen atoms were replaced in idealized positions rationalized to reflect this geometry. The hydrogen atoms on the bridging methyl group were placed and refined with isotropic thermal parameters.

During data collection, the low temperature apparatus malfunctioned three times, causing the temperature to drop rapidly. The data collected during these intervals exhibited extremely large negative values of Δ. Three separate ranges of data were rejected in the refinement; a total of 62 data were affected.

The quantity minimized by the least-squares program was $\Sigma w(|F_o|-|F_c|)^2$, where w is the weight of a given observation. The p-factor[21], used to reduce the weight of intense reflections, was set to 0.02 throughout the refinement. The analytical forms for the scattering factor tables for the neutral atoms[22] were used and all non-hydrogen scattering factors were corrected for both the real and imaginary components of anomalous dispersion[23].

The final residuals for 311 variables refined against the 3176 data for which $F_o^2 > 3\sigma(F_o^2)$ were R = 0.0226, R_w = 0.0278, and GOF = 1.741. The R value for all 3887 data was 0.0436.

Inspection of the residuals ordered in ranges of $\sin\theta/\lambda$, $|F_o|$, and parity and value of the individual indexes showed no unusual features or trends. There was evidence of secondary extinction in the low-angle, high-intensity data, and a secondary extinction correction was applied to the data[24]. The secondary extinction coefficient was refined in the least-squares calculations to a value of $1.8(8) \times 10^{-8}\ e^{-2}$.

The highest and lowest peaks in the final difference Fourier map had electron densities of 0.625 and -0.670 $e/Å^3$, respectively, and were associated with the Yb atom.

Table (VI). Crystal Data for $(Me_5C_5)_2Yb(\mu\text{-}Me)Be(C_5Me_5)$ (-80°C)

Space Group	$P2_1/n$
a, Å	11.265(1)
b, Å	11.102(1)
c, Å	24.125(3)
β, deg	82.904(9)
V, $Å^3$	2994(1)
Z	4
fw	602.78
d (calc.), g/cm^3	1.34
μ (calc.), 1/cm	31.28
size, mm	0.14 x 0.35 x 0.31
radiation	MoKα (λ = 0.71073Å)
monochromator	highly oriented graphite
scan range, type	$3° \leq 2\theta \leq 45°$, θ-2θ
scan speed, deg/min	0.838 - 6.71, variable
scan width, deg	$\Delta\theta = 0.65 + 0.35 \tan\theta$
reflections collected	4383, +h, +k, ±l
unique reflections	3887
reflections, $F_o^2 > 3\sigma(F_o^2)$	3176 (after rejection of 62 "bad" data - see discussion)
variables	311
R, %	0.0226
R_w, %	0.0278
R_{all}, %	0.0436
GOF	1.741
g, e^{-2}	$1.8(8) \times 10^{-8}$
largest Δ/σ in the last least-squares cycle	0.05

Intensity Standards: -7, 2, 3; -1, 2, 15; -4, 6, 5; measured every two hours of x-ray exposure time. Over the period of data collections 3.2% decay in intensity was observed. A linear decay correction was applied to the raw data.

Orientation Standards: 3 reflections were checked after every 250 measurements. Crystal orientation was redetermined if any of the reflections were offset from their predicted positions by more than 0.1°. No reorientation was required during data collection.

$(Me_5C_5)_2Yb(BH_3 \cdot PMe_3)$

Bright green crystals of the compound were grown by slow cooling of a hot toluene solution to room temperature. A large block was cleaved to yield a fragment of approximate dimensions 0.26 mm x 0.43 mm x 0.63 mm, which was lodged into a thin-walled 0.3 mm quartz capillary in a nitrogen-filled drybox. The capillary was then flame sealed.

Preliminary precession photographs indicated orthorhombic Laue symmetry, and yielded preliminary cell dimensions. The crystal was transferred to an Enraf-Nonius automated diffractometer[16] and centered in the beam. Automatic peak indexing procedures yielded the same unit cell as the precession photographs and confirmed the Laue symmetry. Examination of the 0 k 1 and h k 0 zones showed the following systematic absences: 0 k 1, k + 1 = 2n + 1; and h k 0, h = 2n + 1, consistent with the space groups $Pna2_1$ and Pnma. Selection of the space group Pnma for data refinement was proven correct by successful convergence of the solution. Accurate cell parameters and the orientation matrix were determined by a least-squares fit to the setting angles of the unresolved MoKα components of 24 symmetry related reflections with 2θ between 28.6 and 29.0°. The results are given in Table (VII) along with the parameters used for data collection.

The 3793 raw data were converted to structure factor amplitudes and their esd's by correcting for scan speed, background, and Lorentz-polarization effects[17-19]. Analysis of the azimuthal scan data[20] showed a variation of I_{min}/I_{max} of 0.733 in the average relative intensity curve. An analytical absorption correction was applied to the data

using the sizes of the indexed faces of the crystal and a 16 x 6 x 16 Gaussian grid of internal points[18]. The maximum and minimum transmission factors were 0.449 and 0.285, respectively.

After rejection of the systematically absent data, the 3421 remaining reflections were averaged. The agreement factors for the averaging (based on F_{obs}) were 0.011 for the observed data, and 0.033 for all data. The unique set of 1799 data were used to solve and refine the structure. The ytterbium atom was located through the use of a three-dimensional Patterson map. The remaining non-hydrogen atoms were located through the use of standard Fourier techniques.

The large and highly anisotropic thermal parameters for the methyl groups on the cyclopentadienyl ring indicated that the rings were probably undergoing librational motion about the pseudo-C_5 axis. The methyl groups on the crystallographic mirror plane were most severely affected, and were best refined as two half-occupancy carbon positions lying off of the mirror plane. The half-occupancy carbons were refined isotropically, as including anisotropic thermal parameters did not improve the refinement. Attempts to refine the other methyl groups on the ring in the same manner led to unreasonable values for the C(ring)-C(Me) bond lengths, and so C12, C13, C15, and C16 were refined anisotropically in single positions. Examination of difference Fourier maps did not unambiguously reveal the hydrogen atom positions, and so they were not included in the structure.

The final residuals for 130 variables refined against the 1160 data for which $F_o^2 > 3\sigma(F_o^2)$ were R = 0.0295, R_w = 0.0488, and GOF = 2.378. The R value for all 1799 data was 0.0598.

The quantity minimized by the least-squares program was $\Sigma w(|F_o|-|F_c|)^2$, where w is the weight of a given observation. The p-factor[21], used to reduce the weight of intense reflections, was set to 0.03 throughout the refinement. The analytical forms for the scattering factor tables for the neutral atoms[22] were used and all non-hydrogen scattering factors were corrected for both the real and imaginary components of anomalous dispersion[23].

Inspection of the residuals ordered in ranges of $\sin\theta/\lambda$, $|F_o|$, an parity and value of the individual indexes showed no unusual features or trends. There was evidence of secondary extinction in the low-angle, high-intensity data, and a secondary extinction correction was applied to the data[24]. The secondary extinction coefficient was refined in the least-squares calculations to a value of $8(2) \times 10^{-8}$ e^{-2}.

The highest and lowest peaks in the final difference Fourier map had electron densities of 0.463 and -0.460 $e/Å^3$, and were associated with C14 and Yb, respectively.

Table (VII). Crystal Data for $(Me_5C_5)_2Yb(BH_3 \cdot PMe_3)$ (25°C)

Space Group	Pnma
a, Å	19.778(2)
b, Å	13.266(2)
c, Å	9.801(1)
V, $Å^3$	2630(1)
Z	4
fw	533.42
d (calc.), g/cm^3	1.35
μ (calc.), 1/cm	36.10
size, mm	0.26 x 0.43 x 0.63
radiation	MoKα (λ = 0.71073Å)
monochromator	highly oriented graphite
scan range, type	$3° \leq 2\theta \leq 45°$, θ-2θ
scan speed, deg/min	0.805 - 6.71, variable
scan width, deg	$\Delta\theta = 0.60 + 0.35 \tan\theta$
reflections collected	3793; +h, ±k, +l
unique reflections	1799
reflections, $F_o^2 > 3\sigma(F_o^2)$	1160
variables	130
R, %	0.0295
R_w, %	0.0488
R_{all}, %	0.0598
GOF	2.378
g, e^{-2}	$8(2) \times 10^{-8}$
largest Δ/σ in the last least-squares cycle	0.19

Intensity Standards: 6, 2, -6; 9, 7, -1; 12, 4,-2; measured every two hours of x-ray exposure time. Over the period of data collection 4.5 % decay in intensity was observed. A linear decay correction was applied to the raw data.

Orientation Standards: 3 reflections were checked after every 250 measurements. Crystal orientation was redetermined if any of the reflections were offset from their predicted positions by more than 0.1°. Reorientation was not required during data collection.

$\underline{(Me_5C_5)_2Yb(\mu\text{-}Me)_2ZnMe}$

Purple crystals of the compound were grown by cooling a saturated pentane solution to -78°C. A purple prism of approximate dimensions 0.30 mm x 0.30 mm x 0.38 mm was chosen and wedged into a thin-walled 0.3 mm quartz capillary in a nitrogen-filled drybox. The capillary was then flame sealed.

Preliminary precession photographs indicated orthogonal Laue symmetry, and yielded preliminary cell dimensions. The crystal was transferred to an Enraf-Nonius automated diffractometer[16], cooled to -80°C, and centered in the beam. Automatic peak indexing procedures yielded the same unit cell as the precession photographs and confirmed the Laue symmetry. Examination of the 0 k 1, h 0 1, and h k 0 zones showed the following systematic absences: 0 k 1, k = 2n + 1; h 0 1, l = 2n + 1, and h k 0; h = 2n + 1, consistent with the space group Pbca. Accurate cell parameters and the orientation matrix were determined by a least-squares fit to the setting angles of the unresolved MoKα components of 24 symmetry related reflections with 2θ between 26 and 29°. The results are given in Table (VIII) along with the parameters used for data collection.

The 3368 raw data were converted to structure factor amplitudes and their esd's by correcting for scan speed, background, and Lorentz-polarization effects[17-19]. Analysis of the azimuthal scan data[20] showed a variation of I_{min}/I_{max} of 0.724 in the average relative intensity curve. An empirical absorption correction was applied to the data using the average relative intensity curve ot the azimuthal scan data[18].

The unique set of 2980 data was used to solve and refine the structure. The ytterbium atom was located through the use of a three-dimensional Patterson map. The remaining non-hydrogen atoms were located through the use of standard Fourier techniques. All non-hydrogen atoms were refined anisotropically.

Examination of a difference Fourier map revealed the presence of all of the hydrogen atoms. The hydrogen atoms on the pentamethyl-cyclopentadienyl rings were placed in idealized positions. The hydrogen atoms on C(3) were placed in located positions, and then these positions were rationalized to reflect idealized methyl group geometry. All of these hydrogen atoms were given isotropic thermal parameters 1.30 times those of the carbons to which they were attached. They were included in the structure factor calculation, but were not refined. Subsequent difference Fourier maps revealed alternate orientations of the hydrogen atoms about C(16) and C(30). These hydrogen atoms were placed in the located positions, and then the positions were rationalized to reflect idealized methyl group geometry. The hydrogen atoms on the bridging methyl groups (C(1) and C(2)) were located and refined isotropicallly.

The final residuals for 251 variables refined against the 2322 data for which $F_o^2 > 3\sigma(F_o^2)$ were R = 0.0185, R_w = 0.0246, and GOF = 1.573. The R value for all 2980 data was 0.0468.

The quantity minimized by the least-squares program was $\Sigma w(|F_o|-|F_c|)^2$, where w is the weight of a given observation. The p-factor[21], used to reduce the weight of intense reflections, was set to 0.02 throughout the refinement. The analytical forms for the scattering factor tables for the neutral atoms[22] were used and all non-hydrogen

scattering factors were corrected for both the real and imaginary components of anomalous dispersion[23].

Inspection of the residuals ordered in ranges of $\sin\theta/\lambda$, $|F_o|$, an parity and value of the individual indexes showed no unusual features or trends. There was evidence of secondary extinction in the low-angle, high-intensity data, and a secondary extinction correction was applied to the data[24]. The secondary extinction coefficient was refined in the least-squares calculations to a value of $2.3(2) \times 10^{-8}\ e^{-2}$. Several reflections showed anomalously high values of $w \times \Delta^2$, possibly due to multiple reflection. Twelve reflections were rejected prior to the final refinement as "bad" data.

The highest and lowest peaks in the final difference Fourier map had electron densities of 0.600 and -0.455 $e/Å^3$, respectively, and were associated with the ytterbium atom.

Table (VIII). Crystal Data for $(Me_5C_5)_2Yb(\mu\text{-}Me)_2ZnMe$ (-80°C)

Space Group	Pbca
a, Å	19.472(2)
b, Å	15.595(1)
c, Å	15.063(2)
V, $Å^3$	4574(1)
Z	8
fw	553.98
d (calc.), g/cm^3	1.73
μ (calc.), 1/cm	51.38
size, mm	0.30 x 0.30 x 0.38
radiation	MoKα (λ = 0.71073Å)
monochromator	highly oriented graphite
scan range, type	$3° \leq 2\theta \leq 45°$, θ-2θ
scan speed, deg/min	0.838 - 6.71, variable
scan width, deg	$\Delta\theta = 0.65 + 0.35 \tan\theta$
reflections collected	3368, +h, +k, +l
unique reflections	2980
reflections, $F_o^2 > 3\sigma(F_o^2)$	2322
variables	251
R, %	0.0185
R_w, %	0.0246
R_{all}, %	0.0468
GOF	1.573
g, e^{-2}	$2.3(2) \times 10^{-8}$
largest Δ/σ in the last least-squares cycle	0.03

Intensity Standards: 3, 10, 4; 2, 4, 12; 9, 3, 2; measured every two hours of x-ray exposure time. Over the period of data collection 1.7% decay in intensity was observed. A linear decay correction was applied to the raw data.

Orientation Standards: 3 reflections were checked after every 250 measurements. Crystal orientation was redetermined if any of the reflections were offset from their predicted positions by more than 0.1°. Reorientation was not required during data collection.

$\underline{(Me_5C_5)_2Yb(\mu\text{-}Ph)_2ZnPh}$

Crystals of the compound were grown by slowly cooling a saturated pentane solution to -78°C. A purple block of approximate dimensions 0.24 mm x 0.26 mm x 0.40 mm was selected and loaded into a thin-salled 0.3 mm quartz capillary in a nitrogen-filled drybox. The capillary was then flame sealed.

Preliminary precession photographs indicated tetragonal Laue symmetry, and yielded preliminary cell dimensions. The crystal was transferred to an Enraf-Nonius automated diffractometer[16], cooled to -80°C, and centered in the beam. Automatic peak indexing procedures yielded the same unit cell as the precession photographs and confirmed the Laue symmetry. Examination of the 0 0 1 and h k 0 zones showed the following systematic absences: 0 0 1, 1 = 2n + 1; h k 0, h + k = 2n + 1, consistent only with the space group $P4_2/n$. Accurate cell parameters and the orientation matrix were determined by a least-squares fit to the setting angles of the unresolved MoKα components of 24 symmetry related reflections with 2θ between 28 and 29°. The results are given in Table (IX) along with the parameters used for data collection.

The 4654 raw data were converted to structure factor amplitudes and their esd's by correcting for scan speed, background, and Lorentz-polarization effects[17-19]. Analysis of the azimuthal scan data[20] showed a variation of I_{min}/I_{max} of 0.897 in the average relative intensity curve. An analytical absorption correction was applied to the data using the sizes of the indexed faces of the crystal and a 12 x 10 x 12

Gaussian grid of internal points[18]. The maximum and minimum transmission factors were 0.462 and 0.400, respectively.

The unique set of 4166 data were used to solve and refine the structure. The ytterbium atom was located through the use of a three-dimensional Patterson map. The remaining non-hydrogen atoms were located through the use of standard Fourier techniques. All non-hydrogen atoms were refined anisotropically.

Examination of a difference Fourier map revealed the presence of all the hydrogen atoms. All hydrogen atoms were placed in calculated positions, and were given isotropic thermal parameters 1.30 times those of the carbons to which they were attached. They were included in the structure factor calculation, but were not refined. Subsequent difference Fourier maps revealed an alternate orientation of the methyl hydrogens about C(19). These hydrogen atoms were placed in the located positions, and the positions were rationalized to reflect idealized methyl geometry.

The final residuals for 362 variables refined against the 3338 data for which $F_o^2 > 3\sigma(F_o^2)$ were R = 0.0250, R_w = 0.0312, and GOF = 1.538. The R value for all 4166 data was 0.0494.

The quantity minimized by the least-squares program was $\Sigma w(|F_o|-|F_c|)^2$, where w is the weight of a given observation. The p-factor[21], used to reduce the weight of intense reflections, was set to 0.03 throughout the refinement. The analytical forms for the scattering factor tables for the neutral atoms[22] were used and all non-hydrogen scattering factors were corrected for both the real and imaginary components of anomalous dispersion[23].

Inspection of the residuals ordered in ranges of $\sin\theta/\lambda$, $|F_o|$, and parity and value of the individual indexes showed no unusual features or trends. Two reflections had intensities that were an order of magnitude higher than any other reflection, and were strongly affected by secondary extinction. As such, they interfered with the calculation of an extinction coefficient for the rest of the data. They were rejected as "bad" data, and were not included in the final refinements. Even after this rejection, there was evidence of secondary extinction in the low-angle, high-intensity data, and a secondary extinction correction was applied to the data[24]. The secondary extinction coefficient was refined in the least-squares calculations to a value of $3.7(4) \times 10^{-8}$ e^{-2}.

The highest and lowest peaks in the final difference Fourier map had electron densities of 1.256 and -0.544 $e/Å^3$, respectively, and were associated with the ytterbium atom.

Table (IX). Crystal Data for $(Me_5C_5)_2Yb(\mu\text{-}Ph)_2ZnPh$ (-80°C)

Space Group	$P4_2/n$
a, Å	21.263(3)
c, Å	14.089(2)
V, $Å^3$	6370(2)
Z	8
fw	740.19
d (calc.), g/cm^3	1.54
μ (calc.), 1/cm	37.05
size, mm	0.24 x 0.26 x 0.40
radiation	MoKα (λ = 0.71073Å)
monochromator	highly oriented graphite
scan range, type	$3° \leq 2\theta \leq 45°$, θ-2θ
scan speed, deg/min	0.805 - 6.71, variable
scan width, deg	$\Delta\theta = 0.65 + 0.35 \tan\theta$
reflections collected	4654; +h, +k, +l
unique reflections	4166
reflections, $F_o^2 > 3\sigma(F_o^2)$	3338
variables	362
R, %	0.0250
R_w, %	0.0312
R_{all}, %	0.0494
GOF	1.538
g, e^{-2}	$3.7(4) \times 10^{-8}$
largest Δ/σ in the last least-squares cycle	0.00

Intensity Standards: 4, 2, 9; 2, 14, 2; 11, 8, 4; measured every two hours of x-ray exposure time. Over the period of data collection 1.5% decay in intensity was observed. A linear decay correction was applied to the raw data.

Orientation Standards: 3 reflections were checked after every 250 measurements. Crystal orientation was redetermined if any of the reflections were offset from their predicted positions by more than 0.1°. Reorientation was not required during data collection.

$(Me_5C_5)_2Yb(o\text{-}H_2C_2B_{10}H_{10})$

Dark green needles of the compound were grown by slowly cooling a saturated toluene solution to -15°C. A needle was cleaved to yield a piece of approximate dimensions 0.12 mm x 0.16 mm x 0.27 mm. This fragment was wedged into a thin-walled 0.3 mm quartz capillary in a nitrogen-filled drybox. The capillary was flame sealed.

Preliminary precession photographs indicated monoclinic Laue symmetry, and yielded preliminary cell dimensions. The crystal was transferred to an Enraf-Nonius automated diffractometer[16] and centered in the beam. Automatic peak indexing procedures yielded the same unit cell as the precession photographs and confirmed the Laue symmetry. Examination of the 0 k 0 and h 0 l zones showed the following systematic absences: 0 k 0, k = 2n + 1; h 0 l, l = 2n + 1, consistent only with the space group $P2_1/c$. Accurate cell parameters and the orientation matrix were determined by a least-squares fit to the setting angles of the unresolved MoKα components of 24 symmetry related reflections with 2θ between 28 and 29°. The results are given in Table (X) along with the parameters used for data collection.

The 3988 raw data were converted to structure factor amplitudes and their esd's by correcting for scan speed, background, and Lorentz-polarization effects[17-19]. Analysis of the azimuthal scan data[20] showed a variation of I_{min}/I_{max} of 0.877 in the average relative intensity curve. An analytical absorption correction was applied to the data using the sizes of the indexed faces of the crystal and a 10 x 16 x 8

Gaussian grid of internal points[18]. The maximum and minimum transmission factors were 0.685 and 0.624, respectively.

The unique set of 3543 data were used to solve and refine the structure. The ytterbium atom was located through the use of a three-dimensional Patterson map. The remaining non-hydrogen atoms were located through the use of standard Fourier techniques. All non-hydrogen atoms were refined anisotropically. There was evidence of disorder in the carborane comprised of partial carbon occupancy in the B(1) site (see discussion in the text). Due to an insufficient number of data, and to the high correlation that would exist between the thermal parameters and the carbon occupancies of atoms within the carborane, it was deemed unwise to attempt to model this disorder.

All hydrogen atoms were located in a difference Fourier map. They were placed in calculated positions, with r[C(Me)-H] = 0.95Å and r[C(or B)-H] = 1.05Å. These hydrogen atoms were included in the structure factor calculation, but were not refined.

The final residuals for 299 variables refined against the 2117 data for which $F_o^2 > 3\sigma(F_o^2)$ were R = 0.0196, R_w = 0.0239, and GOF = 1.486. The R value for all 3543 data was 0.102.

The quantity minimized by the least-squares program was $\Sigma w(|F_o|-|F_c|)^2$, where w is the weight of a given observation. The p-factor[21], used to reduce the weight of intense reflections, was set to 0.02 throughout the refinement. The analytical forms for the scattering factor tables for the neutral atoms[22] were used and all non-hydrogen scattering factors were corrected for both the real and imaginary components of anomalous dispersion[23].

Inspection of the residuals ordered in ranges of $\sin\theta/\lambda$, $|F_o|$, an parity and value of the individual indexes showed no unusual features or trends. There was evidence of secondary extinction in the low-angle, high-intensity data, and a secondary extinction correction was applied to the data[24]. The secondary extinction coefficient was refined in the least-squares calculations to a value of $2.6(5) \times 10^{-8}\ e^{-2}$.

The highest and lowest peaks in the final difference Fourier map had electron densities of 0.528 and 0.333 $e/Å^3$, respectively; both were associated with the ytterbium atom.

Table (X). Crystal Data for $(Me_5C_5)_2Yb(o\text{-}H_2C_2B_{10}H_{10})$ (25°C)

Space Group	$P2_1/c$
a, Å	12.780(1)
b, Å	10.047(1)
c, Å	21.175(3)
β, deg	91.18(1)
V, Å^3	2718.3(8)
Z	4
fw	587.73
d (calc.), g/cm^3	1.47
μ (calc.), 1/cm	34.39
size, mm	0.12 x 0.16 x 0.27
radiation	MoKα (λ = 0.71073Å)
monochromator	highly oriented graphite
scan range, type	$3° \leq 2\theta \leq 45°$, θ-2θ
scan speed, deg/min	0.805 - 6.71, variable
scan width, deg	$\Delta\theta = 0.65 + 0.35 \tan\theta$
reflections collected	3988; +h, +k, ±l
unique reflections	3543
reflections, $F_o^2 > 3\sigma(F_o^2)$	2117
variables	299
R, %	0.0196
R_w, %	0.0239
R_{all}, %	0.102
GOF	1.486
g, e^{-2}	$2.6(5) \times 10^{-8}$
largest Δ/σ in the last least-squares cycle	0.01

Intensity Standards: 4, 6, 2; 4, 4, -10; 8, 2, 4; measured every two hours of x-ray exposure time. Over the period of data collection 1.5% decay in intensity was observed. A linear decay correction was applied to the raw data.

Orientation Standards: 3 reflections were checked after every 250 measurements. Crystal orientation was redetermined if any of the reflections were offset from their predicted positions by more than 0.1°. Reorientation was not required during data collection.

$(Me_5C_5)_2Yb(o\text{-}Me_2C_2B_{10}H_{10})$

Crystals of the compound were grown by slowly cooling a saturated toluene solution to -25°C. The crystals were green when isolated at low temperature, but turned orange at about +5°C when warmed slowly to room temperature. This color change was reversible. Attempts were made to determine the crystal structure of the green form of the compound at -80°C, but every crystal cooled on the diffractometer suffered irreversible damage in the phase change. Further crystals were studied at +25°C. An orange crystal fragment of approximate dimensions 0.26 mm x 0.27 mm x 0.28 mm was selected and wedged into a thin-walled 0.3 mm quartz capillary in a nitrogen-filled drybox. The capillary was flame sealed.

Preliminary precession photographs indicated monoclinic Laue symmetry, and yielded preliminary cell dimensions. The crystal was transferred to an Enraf-Nonius automated diffractometer[16] and centered in the beam. Automatic peak indexing procedures yielded the same unit cell as the precession photographs and confirmed the Laue symmetry. Examination of the 0 k 0 and h 0 l zones showed the following systematic absences: 0 k 0, k = 2n + 1; h 0 l, l = 2n + 1, consistent only with the space group $P2_1/c$. Accurate cell parameters and the orientation matrix were determined by a least-squares fit to the setting angles of the unresolved MoKα components of 24 symmetry related reflections with 2θ between 27.6 and 28.4°. The results are given in Table (XI) along with the parameters used for data collection. One crystal was centered at

-80°C, and the cell constants of the green phase were determined: a = 13.109(1)Å, b = 10.655(2)Å, c = 21.117(4)Å, β = 93.04(1)°.

The 4502 raw data were converted to structure factor amplitudes and their esd's by correcting for scan speed, background, and Lorentz-polarization effects[17-19]. Analysis of the azimuthal scan data[20] showed a variation of I_{min}/I_{max} of 0.904 in the average relative intensity curve. An analytical absorption correction was applied to the data using the sizes of the indexed faces of the crystal and a 14 x 12 x 10 Gaussian grid of internal points[18]. The maximum and minimum transmission factors were 0.594 and 0.471, respectively.

The unique set of 4016 data were used to solve and refine the structure. The ytterbium atom was located through the use of a three-dimensional Patterson map. The remaining non-hydrogen atoms were located through the use of standard Fourier techniques. There were no indications in final difference Fourier maps of alternate locations for the carborane methyl carbons, suggesting that there was no disorder in the carborane molecule. All non-hydrogen atoms were refined anisotropically.

The hydrogen atoms on the pentamethylcyclopentadienyl rings and those attached to borons in the carborane were located in a difference Fourier map. These hydrogens were placed in calculated positions, with r[C(Me)-H] = 0.95Å and r[B-H] = 1.05Å. They were included in the structure factor calculation, but were not refined. The carborane methyl hydrogens could not be located, and they were not placed.

The final residuals for 317 variables refined against the 3072 data

for which $F_o^2 > 3\sigma(F_o^2)$ were R = 0.0260, R_w = 0.0329, and GOF = 1.516. The R value for all 4016 data was 0.0647.

The quantity minimized by the least-squares program was $\Sigma w(|F_o|-|F_c|)^2$, where w is the weight of a given observation. The p-factor[21], used to reduce the weight of intense reflections, was set to 0.03 throughout the refinement. The analytical forms for the scattering factor tables for the neutral atoms[22] were used and all non-hydrogen scattering factors were corrected for both the real and imaginary components of anomalous dispersion[23].

Inspection of the residuals ordered in ranges of $\sin\theta/\lambda$, $|F_o|$, an parity and value of the individual indexes showed no unusual features or trends. There was some evidence of secondary extinction in the low-angle, high-intensity data, and a secondary extinction correction was applied to the data[24]. The secondary extinction coefficient was refined in the least-squares calculations to a value of $2.7(8) \times 10^{-8}\ e^{-2}$.

The highest peak in the final difference Fourier map had an electron density of 0.585 $e/Å^3$, and was associated with the ytterbium atom. The lowest peak in the final difference Fourier map had an electron density of -0.368 $e/Å^3$, and was close to C(1).

Table (XI). Crystal Data for $(Me_5C_5)_2Yb(o\text{-}Me_2C_2B_{10}H_{10})$ (25°C)

Space Group	$P2_1/c$
a, Å	13.061(1)
b, Å	10.822(1)
c, Å	21.814(2)
β, deg	93.211(9)
V, Å^3	3079(1)
Z	4
fw	615.78
d (calc.), g/cm^3	1.33
μ (calc.), 1/cm	30.40
size, mm	0.26 x 0.27 x 0.28
radiation	MoKα (λ = 0.71073Å)
monochromator	highly oriented graphite
scan range, type	$3° \leq 2\theta \leq 45°$, θ-2θ
scan speed, deg/min	0.805 - 6.71, variable
scan width, deg	$\Delta\theta = 0.65 + 0.35 \tan\theta$
reflections collected	4502; +h, +k, ±l
unique reflections	4016
reflections, $F_o^2 > 3\sigma(F_o^2)$	3072
variables	317
R, %	0.0260
R_w, %	0.0329
R_{all}, %	0.0647
GOF	1.516
g, e^{-2}	$2.7(8) \times 10^{-8}$
largest Δ/σ in the last least-squares cycle	0.01

Intensity Standards: 2, 7, 4; 8, 1, 6; 3, 4, 11; measured every two hours of x-ray exposure time. Over the period of data collection 4.8% decay in intensity was observed. A linear decay correction was applied to the raw data.

Orientation Standards: 3 reflections were checked after every 250 measurements. Crystal orientation was redetermined if any of the reflections were offset from their predicted positions by more than 0.1°. Reorientation was not required during data collection.

$[(Me_5C_5)_2Yb]_2[(H_5C_5)_2Co]$

Crystals of the compound were grown by slow cooling of a 1:1 toluene/pentane solution to -25°C. A crystals of approximate dimensions 0.33 mm x 0.30 mm x 0.42 mm was selected and lodged into a 0.3 mm thin-walled quartz capillary in a nitrogen-filled drybox, and the capillary was flame sealed. Preliminary precession photographs indicated tetragonal Laue symmetry, and yielded preliminary cell dimensions.

The crystal was transferred to an Enraf-Nonius automated diffractometer[16], cooled to -110°C, and centered in the beam. Automatic peak indexing procedures yielded the same unit cell as the precession photographs and confirmed the Laue symmetry. Examination of the data revealed the following systematic conditions: h k l, h + k + l = 2n; 0 0 l, l = 4n; h k 0, h = 2n, consistent only with the space group $I4_1/a$. Accurate cell parameters and the orientation matrix were determined by a least-squares fit to the setting angles of the unresolved MoKα components of 24 symmetry related reflections with 2θ between 27.6 and 27.8°. The results are given in Table (XII) along with the parameters used for data collection.

The 3216 raw data were converted to structure factor amplitudes and their esd's by correcting for scan speed, background, and Lorentz-polarization effects[17-19]. Analysis of the azimuthal scan data[20] showed a variation of I_{min}/I_{max} of 0.776 in the average relative intensity curve. An empirical absorption correction was applied to the data using the average relative intensity curve of the azimuthal scan data[18].

The unique set of 2918 data were used to solve and refine the structure. The ytterbium and cobalt atoms were located through the use of a three-dimensional Patterson map. The remaining non-hydrogen atoms were located through the use of standard Fourier techniques. All non-hydrogen atoms were refined anisotropically.

Examination of a difference Fourier map revealed the presence of all hydrogen atoms. All hydrogen atoms were placed in calculated positions; the hydrogen atoms on the pentamethylcyclopentadienyl rings, were given isotropic thermal parameters 1.20 times those of the carbons to which they were attached, and the hydrogen atoms on the cyclopentadienyl ring were given thermal parameters 1.30 times those of the carbons to which they were attached. The hydrogen atoms were included in the structure factor calculation, but were not refined.

The final residuals for 242 variables refined against the 2200 data for which $F_o^2 > 3\sigma(F_o^2)$ were R = 0.0190, R_w = 0.0255, and GOF = 1.694. The R value for all 2918 data was 0.0524.

The quantity minimized by the least-squares program was $\Sigma w(|F_o| - |F_c|)^2$, where w is the weight of a given observation. The p-factor[21], used to reduce the weight of intense reflections, was set to 0.02 throughout the refinement. The analytical forms for the scattering factor tables for the neutral atoms[22] were used and all non-hydrogen scattering factors were corrected for both the real and imaginary components of anomalous dispersion[23].

Inspection of the residuals ordered in ranges of $\sin\theta/\lambda$, $|F_o|$, and parity and value of the individual indexes showed no unusual features or trends. There was evidence of secondary extinction in the low-angle,

high-intensity data, and a secondary extinction correction was applied to the data[24]. The secondary extinction coefficient was refined in the least-squares calculations to a value of $2.3(2) \times 10^{-8}\ e^{-2}$. There were several reflections of low intensity which displayed large positive values of Δ, indicating that they were affected by multiple reflection. Ten reflections were rejected, and were not included in the final refinement.

The highest and lowest peaks in the final difference Fourier map had electron densities of 0.341 and -0.422 $e/Å^3$, and were associated with C22 and the ytterbium atom, respectively.

Table (XII). Crystal Data for $[(Me_5C_5)_2Yb]_2[(H_5C_5)_2Co]$ (-110°C)

Space Group	$I4_1/a$
a, Å	21.286(2)
c, Å	19.703(3)
V, Å^3	8927(3)
Z	8
fw	1076.13
d (calc.), g/cm^3	1.60
μ (calc.), 1/cm	45.43
size, mm	0.33 x 0.30 x 0.42
radiation	MoKα (λ = 0.71073Å)
monochromator	highly oriented graphite
scan range, type	$3° \leq 2\theta \leq 45°$, θ-2θ
scan speed, deg/min	0.805 - 6.71, variable
scan width, deg	$\Delta\theta = 0.65 + 0.35 \tan\theta$
reflections collected	3216; +h, +k, +l
unique reflections	2918
reflections, $F_o^2 > 3\sigma(F_o^2)$	2200
variables	242
R, %	0.0190
R_w, %	0.0255
R_{all}, %	0.0524
GOF	1.694
g, e^{-2}	2.3(2) x 10^{-8}
largest Δ/σ in the last least-squares cycle	0.01

Intensity Standards: -13 -6 -1, -2 -14 -2, -2 -6 -12; measured every two hours of x-ray exposure time. Over the period of data collection 0.3% decay in intensity was observed. No decay correction was applied.

Orientation Standards: 3 reflections were checked after every 250 measurements. Crystal orientation was redetermined if any of the reflections were offset from their predicted positions by more than 0.1°. Reorientation was not required during data collection.

References

1.) Threlkel, R. S.; Bercaw, J. E. J. Organomet. Chem., 1977, 136, 1.

2.) Nagel, U., Chem. Ber., 1982, 115, 1998.

3.) Greaves, E. O.; Lock, C. J. L.; Maitlis, P. M., Can J. Chem., 1968, 46, 3879.

4.) Chambers, R. D.; Coates, G. E.; Livingstone, J. G.; Musgrave, W. K. R., J. Chem. Soc., 1962, 4367.

5.) Strohmeier, V. H.; Landsfeld, H., Z. Naturforsch., 1968, 15b, 332.

6.) Wittig, G.; Meyer, F. J.; Lange, G., Annal., 1951, 571, 167.

7.) Berg, D. J., Ph.D. Thesis, University of California, Berkeley, California, U.S.A., 1987.

8.) Girard, P.; Namy, J. L.; Kagan, H. B., J. Am. Chem. Soc., 1980, 102(8), 2693.

9.) Taylor, M. D.; Grant, L. R., J. Am. Chem. Soc., 1955, 77, 1507.

10.) Tilley, T. D., Ph.D. Thesis, University of California, Berkeley, California, U.S.A., 1982.

11.) Boncella, J. M., Ph.D. Thesis, University of California, Berkeley, California, U.S.A., 1984.

12.) Evans, W. J.; Hughes, L. A.; Hanusa, T. P., J. Am. Chem. Soc., 1984, 106, 4270.

13.) Evans, W. J.; Grate, J. W.; Bloom, I.; Hunter, W. E.; Atwood, J. L., J. Am. Chem. Soc., 1985, 107, 405.

14.) Tolman, C. A.; Seidel, W. C.; Gerlach, D. H., J. Am. Chem. Soc., 1972, 94, 2669.

15.) Jeske, G.; Lauke, H.; Mauermann, H.; Swepston, P. N.; Schumann, H.; Marks, T. J., J. Am. Chem. Soc., 1985, 107, 8091.

16.) Instrumentation at the University of California Chemistry Department X-ray Crystallographic Facility (CHEXRAY) consists of two Enraf-Nonius CAD-4 diffractometers, one controlled by a DEC PDP 8/a with an RK05 disk and the other by a DEC PDP 8/e with an RL01 disk. Both use Enraf-Nonius software as described in the CAD-4 Operation Manual, Enraf-Nonius, Delft, Nov. 1977, updated Jan. 1980.

17.) All calculations were performed on a DEC Microvax II using locally modified Nonius-SDP[3] software operating under Micro-VMS operating

system.

18.) Structure Determination Package User's Guide, 1985, B.A. Frenz and Associates, Inc., College Station, Texas 77840.

19.) The data reduction formulae are:

$$F_o^2 = \frac{\omega}{Lp}(C - 2B) \qquad \sigma_o(F_o^2) = \frac{\omega}{Lp}(C + 4B)^{1/2}$$

$$F_o = \sqrt{F_o^2} \qquad \sigma_o(F) = \sqrt{F_o^2 + \sigma_o(F_o^2)} - F_o$$

where C is the total count in the scan, B the sum of the two background counts, ω is the scan speed used in deg/min, and

$$\frac{1}{Lp} = \frac{\sin 2\theta\,(1 + \cos^2 2\theta_m)}{1 + \cos^2 2\theta_m - \sin^2 2\theta}$$

is the correction for Lorentz and polarization effects for a reflection with scattering angle 2θ and radiation monochromatized with a 50% perfect single-crystal monochrometer with scattering angle $2\theta_m$.

20.) Reflections used for azimuthal scans were located near $\chi = 90°$ and the intensities were measured at 10° increments of rotation of the crystal about the diffraction vector.

21.)
$$R = \frac{\Sigma\,||F_o| - |F_c||}{\Sigma|F_o|} \qquad R_w = \left\{\frac{\Sigma w(|F_o| - |F_c|)^2}{\Sigma w F_o^2}\right\}^{1/2}$$

$$GOF = \left\{\frac{\Sigma w(|F_o| - |F_c|)^2}{(n_o - n_v)}\right\}^{1/2}$$

where n_o is the number of observations, n_v the number of variable parameters, and the weights w were given by

$$w = \frac{1}{\sigma^2(F_o)} \qquad \sigma(F_o^2) = \sqrt{\sigma_o^2(F_o^2) + (pF^2)^2}$$

where $\sigma^2(F_o)$ is calculated as above from $\sigma(F_o^2)$ and where p is the factor used to lower the weight of intense reflections.

22.) D.T. Cromer, J.T. Waber, "International Tables for X-ray Crystallography," Vol. IV, The Kynoch Press, Birmingham, England, 1974, Table 2.2B.

23.) D.T. Cromer, ibid., Table 2.3.1.

24.) W.H. Zachariesen, Acta Crystallogr., 1963, 16, 1139.

Appendix I. Tables of Positional and Thermal Parameters

$(Me_5C_5)_2Yb$

Table of Positional Parameters and Their Estimated Standard Deviations

Atom	x	y	z	B(A2)
YB1	0.13103(1)	0.10409(1)	0.24370(2)	3.410(4)
YB2	0.12122(1)	0.40485(1)	-0.22348(2)	3.125(4)
C1	0.2006(1)	0.0801(3)	0.4249(4)	4.92(9)
C2	0.1719(1)	-0.0047(3)	0.4499(4)	4.71(9)
C3	0.1692(1)	-0.0749(3)	0.3372(4)	4.44(9)
C4	0.1956(1)	-0.0338(3)	0.2418(4)	4.54(9)
C5	0.2150(1)	0.0617(3)	0.2968(4)	4.89(9)
C6	0.2179(2)	0.1653(4)	0.5247(5)	7.9(1)
C7	0.1510(2)	-0.0209(4)	0.5794(4)	7.7(1)
C8	0.1459(2)	-0.1808(4)	0.3282(5)	7.1(1)
C9	0.2070(2)	-0.0882(4)	0.1123(5)	6.7(1)
C10	0.2493(2)	0.1267(4)	0.2342(6)	8.1(2)
C11	0.0503(1)	0.1438(4)	0.1321(4)	5.5(1)
C12	0.0585(1)	0.0314(3)	0.1048(4)	5.4(1)
C13	0.0899(1)	0.0316(3)	0.0094(4)	4.21(8)
C14	0.1011(1)	0.1386(3)	-0.0164(4)	4.58(9)
C15	0.0767(1)	0.2066(3)	0.0573(4)	5.13(9)
C16	0.0154(2)	0.1825(5)	0.2167(6)	9.6(2)
C17	0.0361(2)	-0.0642(5)	0.1545(6)	8.8(1)
C18	0.1042(2)	-0.0638(3)	-0.0676(5)	6.3(1)
C19	0.1333(2)	0.1740(3)	-0.1153(4)	6.0(1)
C20	0.0743(2)	0.3279(4)	0.0471(5)	7.8(1)
C21	0.1811(1)	0.4465(3)	-0.0130(4)	4.44(9)
C22	0.2049(1)	0.4192(3)	-0.1214(4)	4.71(9)
C23	0.1978(1)	0.5003(3)	-0.2228(4)	4.86(9)
C24	0.1696(1)	0.5774(3)	-0.1753(4)	4.50(9)
C25	0.1593(1)	0.5442(3)	-0.0479(4)	4.49(9)
C26	0.1853(2)	0.3906(3)	0.1229(5)	6.6(1)
C27	0.2369(1)	0.3282(4)	-0.1223(5)	6.8(1)
C28	0.2211(2)	0.5100(4)	-0.3509(5)	7.6(1)
C29	0.1586(2)	0.6852(3)	-0.2393(5)	7.0(1)
C30	0.1307(2)	0.6037(3)	0.0423(5)	6.7(1)
C31	0.0865(1)	0.3433(3)	-0.4711(4)	4.42(9)
C32	0.0896(1)	0.4561(3)	-0.4774(4)	4.54(9)
C33	0.0600(1)	0.4984(3)	-0.3928(4)	5.6(1)

Table of Positional Parameters and Their Estimated Standard Deviations (cont.)

Atom	x	y	z	B(A2)
C34	Ø.ØØ389(1)	Ø.4139(4)	-Ø.3354(4)	6.8(1)
C35	Ø.ØØ55Ø(1)	Ø.3161(4)	-Ø.3831(4)	5.5(1)
C36	Ø.11Ø9(2)	Ø.2668(4)	-Ø.5553(5)	7.2(1)
C37	Ø.1154(2)	Ø.5187(4)	-Ø.57Ø2(4)	7.6(1)
C38	Ø.ØØ475(2)	Ø.6146(4)	-Ø.3789(6)	11.1(2)
C39	Ø.ØØØ5(2)	Ø.4221(7)	-Ø.2515(6)	13.4(3)
C4Ø	Ø.Ø381(2)	Ø.2Ø5Ø(5)	-Ø.36Ø4(6)	1Ø.3(2)

The thermal parameter given for anisotropically refined atoms is the isotropic equivalent thermal parameter defined as:
(4/3) * [a2*B(1,1) + b2*B(2,2) + c2*B(3,3) + ab(cos gamma)*B(1,2) + ac(cos beta)*B(1,3) + bc(cos alpha)*B(2,3)]
where a,b,c are real cell parameters, and B(i,j) are anisotropic betas.

Table of Anisotropic Thermal Parameters - B's

Name	B(1,1)	B(2,2)	B(3,3)	B(1,2)	B(1,3)	B(2,3)	Beqv
YB1	3.651(8)	3.514(8)	2.928(8)	Ø.7Ø9(6)	-Ø.3Ø8(7)	-Ø.643(5)	3.41Ø(4)
YB2	3.151(8)	3.158(7)	2.979(6)	-Ø.Ø64(5)	-Ø.Ø98(6)	Ø.Ø55(5)	3.125(4)
C1	5.4(2)	4.Ø(2)	5.Ø(2)	Ø.7(2)	-1.4(2)	-Ø.3(1)	4.92(9)
C2	5.8(2)	4.8(2)	3.6(2)	1.5(2)	Ø.5(1)	Ø.4(1)	4.71(9)
C3	5.1(2)	3.4(1)	4.8(2)	Ø.5(1)	Ø.6(2)	Ø.Ø(1)	4.44(9)
C4	5.1(2)	4.4(2)	4.2(2)	1.2(1)	Ø.4(2)	Ø.1(1)	4.54(9)
C5	4.1(2)	4.5(2)	6.Ø(2)	Ø.6(2)	Ø.2(2)	Ø.7(2)	4.89(9)
C6	8.2(3)	6.5(2)	8.1(3)	1.6(2)	-3.6(2)	-2.3(2)	7.9(1)
C7	11.3(3)	7.5(3)	4.7(2)	2.3(2)	2.4(2)	Ø.8(2)	7.7(1)
C8	8.2(3)	4.5(2)	8.8(3)	-Ø.6(2)	1.5(2)	-Ø.3(2)	7.1(1)
C9	6.8(2)	8.5(3)	4.9(2)	2.9(2)	Ø.9(2)	-Ø.7(2)	6.7(1)
C1Ø	6.3(3)	5.9(2)	12.1(4)	-Ø.2(2)	1.1(3)	2.2(2)	8.1(2)
C11	3.1(2)	8.1(2)	5.Ø(2)	1.Ø(2)	-Ø.1(2)	-1.5(2)	5.5(1)
C12	4.Ø(2)	6.7(2)	5.3(2)	-1.6(2)	-Ø.Ø(2)	-Ø.5(2)	5.4(1)
C13	4.2(2)	3.9(2)	4.4(2)	-Ø.5(1)	-Ø.4(1)	-Ø.4(1)	4.21(8)
C14	5.1(2)	4.4(2)	4.1(2)	Ø.2(2)	-Ø.4(2)	-Ø.4(1)	4.58(9)
C15	4.8(2)	5.3(2)	5.1(2)	Ø.7(2)	-Ø.5(2)	-Ø.2(2)	5.13(9)
C16	4.8(2)	15.4(4)	8.8(3)	1.2(3)	1.3(2)	-3.Ø(3)	9.6(2)
C17	7.4(3)	11.Ø(3)	8.Ø(3)	-4.4(2)	Ø.6(2)	Ø.8(3)	8.8(1)
C18	7.4(3)	5.3(2)	6.1(2)	-Ø.Ø(2)	-Ø.1(2)	-2.1(2)	6.3(1)
C19	7.7(3)	5.5(2)	4.9(2)	-Ø.3(2)	1.2(2)	Ø.5(2)	6.Ø(1)

Table of Anisotropic Thermal Parameters - B's (Continued)

Name	B(1,1)	B(2,2)	B(3,3)	B(1,2)	B(1,3)	B(2,3)	Beqv
C20	9.7(3)	5.1(2)	8.0(3)	1.9(2)	-0.9(3)	-0.4(2)	7.8(1)
C21	4.8(2)	4.7(2)	3.6(2)	-0.3(2)	-0.4(1)	-0.4(1)	4.44(9)
C22	3.7(2)	4.9(2)	5.3(2)	0.1(1)	-0.4(2)	-1.0(2)	4.71(9)
C23	4.6(2)	5.2(2)	5.0(2)	-1.5(2)	1.0(1)	-0.3(2)	4.86(9)
C24	5.2(2)	3.4(1)	4.8(2)	-0.8(1)	0.3(2)	0.0(1)	4.50(9)
C25	5.2(2)	3.8(2)	4.4(2)	-0.1(2)	0.4(2)	-1.1(1)	4.49(9)
C26	8.4(3)	6.4(2)	4.7(2)	0.4(2)	-0.8(2)	0.0(2)	6.6(1)
C27	4.5(2)	6.4(2)	9.3(3)	1.3(2)	0.1(2)	-2.2(2)	6.8(1)
C28	6.7(2)	9.2(3)	7.3(2)	-1.5(2)	3.2(2)	-0.7(2)	7.6(1)
C29	8.8(3)	4.6(2)	7.5(2)	-0.1(2)	1.0(2)	1.2(2)	7.0(1)
C30	8.2(3)	5.5(2)	6.5(2)	0.4(2)	1.5(2)	-1.6(2)	6.7(1)
C31	4.2(2)	4.9(2)	3.9(2)	0.7(1)	-0.5(1)	-1.0(1)	4.42(9)
C32	5.0(2)	4.8(2)	3.7(2)	0.6(2)	-0.4(1)	-0.0(1)	4.54(9)
C33	5.7(2)	6.2(2)	4.6(2)	2.6(2)	-0.6(2)	-0.8(2)	5.6(1)
C34	3.5(2)	12.7(3)	4.0(2)	1.8(2)	-0.2(2)	-1.0(2)	6.8(1)
C35	3.9(2)	7.2(2)	5.0(2)	-1.5(2)	-0.8(2)	0.5(2)	5.5(1)
C36	7.5(3)	7.8(2)	6.0(2)	2.5(2)	-0.6(2)	-2.7(2)	7.2(1)
C37	9.7(3)	8.1(3)	4.9(2)	-2.0(2)	0.5(2)	1.7(2)	7.6(1)
C38	13.4(4)	9.7(3)	9.2(3)	7.8(2)	-4.0(3)	-4.2(2)	11.1(2)
C39	5.0(3)	29.3(8)	6.2(3)	3.5(4)	1.8(2)	-1.2(4)	13.4(3)
C40	9.3(3)	11.7(3)	9.4(3)	-6.0(2)	-2.1(3)	3.1(3)	10.3(2)

The form of the anisotropic temperature factor is:
exp[-0.25(h2a2B(1,1) + k2b2B(2,2) + l2c2B(3,3) + 2hkabB(1,2) + 2hlacB(1,3) + 2klbcB(2,3))] where a,b, and c are reciprocal lattice constants.

$(Me_5C_5)_2Yb(\mu\text{-}C_2H_4)Pt(PPh_3)_2$

Table of Positional Parameters and Their Estimated Standard Deviations

Atom	x	y	z	B(Å^2)
PT	0.22439(1)	0.34578(1)	0.22261(1)	1.756(3)
YB	0.36512(2)	0.65579(1)	0.32113(1)	1.950(4)
P1	0.3230(1)	0.22866(7)	0.25651(5)	1.97(2)
P2	0.0619(1)	0.28012(7)	0.12718(5)	1.87(2)
C1	0.3206(5)	0.4628(3)	0.2972(2)	2.70(9)
C2	0.2050(4)	0.4824(3)	0.2539(2)	2.64(9)
C11	0.4794(4)	0.6466(3)	0.1903(2)	2.45(9)
C12	0.5963(4)	0.6745(3)	0.2430(2)	2.60(9)
C13	0.5970(4)	0.7660(3)	0.2768(2)	2.51(9)
C14	0.4782(4)	0.7938(3)	0.2445(2)	2.62(9)
C15	0.4065(4)	0.7195(3)	0.1913(2)	2.46(9)
C16	0.4504(5)	0.5601(4)	0.1341(2)	3.8(1)
C17	0.7087(5)	0.6209(4)	0.2567(3)	4.0(1)
C18	0.7148(5)	0.8261(4)	0.3293(3)	4.2(1)
C19	0.4449(5)	0.8892(3)	0.2589(2)	3.5(1)
C20	0.2768(5)	0.7210(4)	0.1423(2)	3.7(1)
C21	0.2144(5)	0.7391(3)	0.4148(2)	2.85(9)

Table of Positional Parameters and Their Estimated Standard Deviations (cont.)

Atom	x	y	z	B(Å^2)
C22	Ø.36Ø9(5)	Ø.7739(3)	Ø.44Ø7(2)	2.9(1)
C23	Ø.4Ø97(5)	Ø.6981(3)	Ø.4645(2)	2.9(1)
C24	Ø.2957(5)	Ø.6194(3)	Ø.4556(2)	2.95(9)
C25	Ø.174Ø(5)	Ø.644Ø(3)	Ø.4245(2)	2.93(9)
C26	Ø.1162(6)	Ø.7933(4)	Ø.384Ø(3)	5.2(1)
C27	Ø.4383(6)	Ø.8748(4)	Ø.4537(3)	4.8(1)
C28	Ø.5577(6)	Ø.7ØØ5(4)	Ø.4965(3)	4.6(1)
C29	Ø.2972(6)	Ø.5279(3)	Ø.4843(3)	4.6(1)
C3Ø	Ø.Ø25Ø(5)	Ø.5831(4)	Ø.41Ø1(3)	4.9(1)
C111	Ø.51Ø5(4)	Ø.2673(3)	Ø.2937(2)	2.24(8)
C112	Ø.5692(5)	Ø.2235(3)	Ø.3466(2)	3.4(1)
C113	Ø.7119(5)	Ø.2562(4)	Ø.372Ø(2)	4.Ø(1)
C114	Ø.7965(5)	Ø.33Ø1(3)	Ø.3451(3)	3.6(1)
C115	Ø.7418(5)	Ø.3725(3)	Ø.2919(3)	3.8(1)
C116	Ø.5974(4)	Ø.34Ø5(3)	Ø.2669(2)	2.96(9)
C121	Ø.3298(4)	Ø.1262(3)	Ø.1912(2)	1.99(8)
C122	Ø.4548(4)	Ø.122Ø(3)	Ø.156Ø(2)	2.68(9)
C123	Ø.4554(5)	Ø.Ø494(3)	Ø.1ØØ8(2)	3.3(1)
C124	Ø.3325(5)	-Ø.Ø2Ø9(3)	Ø.Ø817(2)	3.3(1)
C125	Ø.21Ø6(5)	-Ø.Ø179(3)	Ø.1166(2)	3.Ø(1)
C126	Ø.2Ø79(5)	Ø.Ø562(3)	Ø.1711(2)	2.72(9)
C131	Ø.2259(4)	Ø.1786(3)	Ø.3311(2)	2.29(8)
C132	Ø.1464(4)	Ø.2315(3)	Ø.3714(2)	2.54(9)
C133	Ø.Ø7Ø9(5)	Ø.199Ø(3)	Ø.4297(2)	3.4(1)
C134	Ø.Ø771(6)	Ø.1129(4)	Ø.4472(3)	5.2(1)
C135	Ø.1591(7)	Ø.Ø588(3)	Ø.4Ø89(3)	6.Ø(1)
C136	Ø.2314(6)	Ø.Ø915(3)	Ø.35Ø2(3)	4.2(1)
C211	Ø.1363(4)	Ø.2614(3)	Ø.Ø387(2)	1.96(8)
C212	Ø.Ø569(4)	Ø.2547(3)	-Ø.Ø279(2)	2.55(9)
C213	Ø.1197(5)	Ø.2434(3)	-Ø.Ø935(2)	3.2(1)
C214	Ø.2612(5)	Ø.2397(3)	-Ø.Ø938(2)	3.4(1)
C215	Ø.3412(5)	Ø.2454(3)	-Ø.Ø295(2)	3.5(1)
C216	Ø.2811(4)	Ø.2572(3)	Ø.Ø375(2)	2.88(9)
C221	-Ø.Ø527(4)	Ø.167Ø(3)	Ø.138Ø(2)	1.98(8)
C222	-Ø.Ø841(4)	Ø.Ø9Ø7(3)	Ø.Ø844(2)	2.39(9)
C223	-Ø.166Ø(5)	Ø.ØØ6Ø(3)	Ø.Ø986(2)	3.Ø(1)
C224	-Ø.2166(5)	-Ø.ØØ28(3)	Ø.1665(3)	3.3(1)
C225	-Ø.1885(5)	Ø.Ø732(3)	Ø.221Ø(2)	3.3(1)
C226	-Ø.1Ø56(4)	Ø.1582(3)	Ø.2Ø74(2)	2.7Ø(9)
C231	-Ø.Ø656(4)	Ø.3494(3)	Ø.1Ø5Ø(2)	2.34(8)
C232	-Ø.Ø111(5)	Ø.4421(3)	Ø.Ø952(3)	3.4(1)
C233	-Ø.Ø977(6)	Ø.4983(3)	Ø.Ø759(3)	4.8(1)
C234	-Ø.2413(5)	Ø.4659(4)	Ø.Ø67Ø(3)	4.7(1)
C235	-Ø.3ØØ9(5)	Ø.3753(4)	Ø.Ø766(3)	5.3(1)
C236	-Ø.214Ø(5)	Ø.3165(4)	Ø.Ø955(3)	3.8(1)
H1	Ø.4Ø7(5)	Ø.489(4)	Ø.292(3)	6(1)*
H2	Ø.294(5)	Ø.45Ø(3)	Ø.351(2)	5(1)*
H3	Ø.23Ø(4)	Ø.521(2)	Ø.218(2)	2.1(8)*
H4	Ø.112(4)	Ø.479(3)	Ø.273(2)	2.8(9)*

* -- Atoms refined with isotropic thermal parameters.

Anisotropically refined atoms are given in the form of the isotropic equivalent thermal parameter defined as:

$(4/3) * [a^2*B(1,1) + b^2*B(2,2) + c^2*B(3,3) + ab(\cos \text{gamma})*B(1,2)$

$- ac(\cos \text{beta})*B(1,3) + bc(\cos \text{alpha})*B(2,3)]$

Table of General Temperature Factor Expressions - B's

Name	B(1,1)	B(2,2)	B(3,3)	B(1,2)	B(1,3)	B(2,3)	Beqv
PT	1.8Ø1(6)	1.496(6)	1.838(6)	Ø.2Ø7(5)	Ø.ØØ4(5)	Ø.Ø23(5)	1.756(3)
YB	2.248(7)	1.575(7)	1.916(6)	Ø.2Ø5(6)	Ø.3ØØ(6)	Ø.141(6)	1.95Ø(4)
P1	2.Ø4(4)	1.87(4)	1.92(4)	Ø.35(3)	Ø.1Ø(3)	Ø.Ø7(3)	1.97(2)
P2	1.72(4)	1.86(4)	1.96(4)	Ø.33(3)	Ø.24(3)	Ø.Ø9(3)	1.87(2)
C1	3.1(2)	1.6(2)	3.Ø(2)	Ø.Ø(1)	-Ø.3(2)	-Ø.1(1)	2.7Ø(9)
C2	2.8(2)	1.9(2)	3.1(2)	Ø.3(1)	Ø.5(1)	Ø.2(1)	2.64(9)

Table of General Temperature Factor Expressions - B's (Continued)

Name	B(1,1)	B(2,2)	B(3,3)	B(1,2)	B(1,3)	B(2,3)	Beqv
C11	2.4(2)	2.8(2)	2.3(2)	Ø.7(1)	Ø.8(1)	Ø.7(1)	2.45(9)
C12	2.3(2)	2.8(2)	3.Ø(2)	Ø.8(1)	Ø.8(1)	1.Ø(1)	2.6Ø(9)
C13	1.7(2)	2.8(2)	2.9(2)	-Ø.1(1)	Ø.3(1)	1.2(1)	2.51(9)
C14	2.7(2)	2.5(2)	2.8(2)	Ø.4(1)	Ø.8(1)	1.Ø(1)	2.62(9)
C15	2.5(2)	2.9(2)	2.1(1)	Ø.4(1)	Ø.7(1)	1.Ø(1)	2.46(9)
C16	3.8(2)	4.4(2)	3.Ø(2)	Ø.7(2)	1.2(2)	-Ø.1(2)	3.6(1)
C17	2.7(2)	4.6(2)	5.3(2)	1.4(2)	Ø.7(2)	1.6(2)	4.Ø(1)
C18	3.3(2)	4.5(2)	4.2(2)	-Ø.2(2)	-Ø.3(2)	Ø.7(2)	4.2(1)
C19	4.2(2)	2.8(2)	4.Ø(2)	1.1(2)	1.1(2)	1.2(2)	3.5(1)
C2Ø	2.9(2)	4.9(2)	3.4(2)	Ø.8(2)	Ø.Ø(2)	1.2(2)	3.7(1)
C21	3.2(2)	2.6(2)	2.7(2)	Ø.9(1)	Ø.7(1)	-Ø.1(1)	2.65(9)
C22	4.Ø(2)	2.1(2)	2.2(2)	Ø.1(2)	Ø.7(1)	-Ø.4(1)	2.9(1)
C23	3.3(2)	3.3(2)	2.Ø(2)	Ø.5(2)	Ø.2(1)	Ø.1(1)	2.9(1)
C24	4.3(2)	2.8(2)	2.Ø(1)	1.Ø(2)	1.2(1)	Ø.5(1)	2.95(9)
C25	3.3(2)	2.8(2)	2.5(2)	Ø.4(2)	1.1(1)	Ø.1(1)	2.93(9)
C26	5.6(2)	5.Ø(2)	5.8(3)	3.2(2)	1.1(2)	Ø.7(2)	5.2(1)
C27	6.7(3)	2.8(2)	4.1(2)	-Ø.1(2)	1.2(2)	-Ø.7(2)	4.8(1)
C28	4.6(2)	6.3(3)	3.1(2)	1.8(2)	-Ø.1(2)	Ø.1(2)	4.6(1)
C29	7.7(3)	3.5(2)	3.Ø(2)	1.6(2)	1.4(2)	1.1(2)	4.6(1)
C3Ø	3.5(2)	4.8(3)	5.6(2)	-Ø.2(2)	1.9(2)	-Ø.4(2)	4.9(1)
C111	2.2(2)	2.5(2)	1.9(1)	Ø.6(1)	-Ø.1(1)	-Ø.2(1)	2.24(8)
C112	3.6(2)	4.3(2)	2.6(2)	1.4(2)	Ø.4(2)	Ø.6(2)	3.4(1)
C113	3.5(2)	6.6(2)	2.4(2)	2.6(2)	-Ø.4(2)	Ø.1(2)	4.Ø(1)
C114	2.3(2)	4.2(2)	4.5(2)	1.1(2)	-Ø.5(2)	-1.3(2)	3.8(1)
C115	2.1(2)	3.Ø(2)	6.3(3)	Ø.7(2)	Ø.1(2)	-Ø.Ø(2)	3.8(1)
C116	2.4(2)	2.4(2)	4.1(2)	Ø.9(1)	-Ø.2(2)	Ø.3(2)	2.96(9)
C121	2.Ø(1)	2.Ø(1)	2.Ø(1)	Ø.6(1)	-Ø.Ø(1)	Ø.1(1)	1.99(8)
C122	2.8(2)	2.7(2)	2.4(2)	Ø.4(1)	Ø.4(1)	Ø.1(1)	2.68(9)
C123	4.Ø(2)	3.9(2)	2.4(2)	2.Ø(2)	Ø.8(1)	Ø.3(2)	3.3(1)
C124	4.6(2)	3.1(2)	2.4(2)	1.8(2)	Ø.Ø(2)	-Ø.7(2)	3.3(1)
C125	3.3(2)	2.3(2)	3.2(2)	Ø.4(2)	-Ø.1(2)	-Ø.2(2)	3.Ø(1)
C126	3.1(2)	2.2(2)	2.8(2)	Ø.7(1)	Ø.1(1)	-Ø.3(1)	2.72(9)
C131	2.1(2)	2.3(2)	2.4(2)	Ø.2(1)	Ø.3(1)	Ø.3(1)	2.29(8)
C132	2.9(2)	2.6(2)	2.2(2)	Ø.7(1)	Ø.4(1)	Ø.5(1)	2.54(9)
C133	3.7(2)	3.4(2)	3.3(2)	1.Ø(2)	1.Ø(2)	Ø.4(2)	3.4(1)
C134	7.8(3)	3.7(2)	4.6(2)	1.Ø(2)	3.2(2)	1.6(2)	5.2(1)
C135	1Ø.2(3)	2.5(2)	6.Ø(2)	1.8(2)	5.2(2)	1.6(2)	6.Ø(1)
C136	6.3(2)	2.7(2)	4.3(2)	1.7(2)	2.3(2)	1.Ø(2)	4.2(1)

Table of General Temperature Factor Expressions - B's (Continued)

Name	B(1,1)	B(2,2)	B(3,3)	B(1,2)	B(1,3)	B(2,3)	Beqv
C211	2.3(2)	1.Ø(1)	2.3(1)	-Ø.Ø(1)	Ø.4(1)	-Ø.1(1)	1.96(8)
C212	2.8(2)	2.3(2)	2.5(2)	Ø.6(1)	Ø.1(1)	Ø.2(1)	2.55(9)
C213	5.Ø(2)	2.5(2)	2.1(2)	Ø.8(2)	Ø.5(2)	Ø.2(1)	3.2(1)
C214	5.Ø(2)	2.1(2)	2.9(2)	Ø.3(2)	2.Ø(2)	Ø.1(1)	3.4(1)
C215	2.8(2)	4.1(2)	3.5(2)	Ø.4(2)	1.3(2)	Ø.3(2)	3.5(1)
C216	2.4(2)	3.3(2)	2.9(2)	Ø.2(2)	Ø.6(1)	Ø.6(2)	2.68(9)
C221	1.3(1)	2.3(2)	2.1(1)	Ø.1(1)	Ø.1(1)	Ø.2(1)	1.98(8)
C222	2.4(2)	2.3(2)	2.2(2)	-Ø.Ø(1)	Ø.3(1)	Ø.2(1)	2.39(9)
C223	2.6(2)	2.5(2)	3.4(2)	Ø.1(2)	-Ø.1(2)	Ø.Ø(2)	3.Ø(1)
C224	2.8(2)	2.4(2)	4.4(2)	-Ø.2(2)	Ø.7(2)	1.Ø(2)	3.3(1)
C225	2.9(2)	3.5(2)	3.4(2)	Ø.2(2)	1.3(1)	1.Ø(2)	3.3(1)
C226	2.5(2)	2.7(2)	2.9(2)	Ø.5(1)	Ø.6(1)	Ø.3(1)	2.7Ø(9)
C231	2.1(1)	3.3(2)	1.6(1)	1.Ø(1)	Ø.Ø(1)	-Ø.3(1)	2.34(8)
C232	3.5(2)	2.4(2)	4.3(2)	1.Ø(2)	-Ø.3(2)	Ø.3(2)	3.4(1)
C233	6.6(3)	3.6(2)	4.9(2)	2.6(2)	-Ø.5(2)	Ø.4(2)	4.8(1)
C234	5.4(2)	6.1(2)	3.9(2)	4.Ø(2)	Ø.5(2)	Ø.7(2)	4.7(1)
C235	2.7(2)	9.7(3)	4.4(2)	3.4(2)	Ø.3(2)	Ø.7(2)	5.3(1)
C236	2.4(2)	5.2(2)	3.9(2)	1.Ø(2)	Ø.3(2)	Ø.6(2)	3.8(1)

The form of the anisotropic thermal parameter is:

$\exp[-Ø.25(h^2a^{*2}B(1,1) + k^2b^{*2}B(2,2) + l^2c^{*2}B(3,3) + 2hka^*b^*B(1,2) + 2hla^*c^*B(1,3) + 2klb^*c^*B(2,3))]$, where a*,b*, and c* are reciprocal lattice constants.

$(Me_5C_5)_2Yb(\eta^2\text{-}MeC{\equiv}CMe)$

Table of Positional Parameters and Their Estimated Standard Deviations

Atom	x	y	z	B(A2)
Yb	Ø.3712l(1)	Ø.23167(1)	Ø.1679Ø(2)	2.495(4)
C1	Ø.3473(3)	Ø.1184(3)	Ø.3854(5)	4.1(1)
C2	Ø.2794(3)	Ø.1118(4)	Ø.3878(5)	4.1(1)
C3	Ø.4335(4)	Ø.1285(4)	Ø.4858(7)	5.7(2)
C4	Ø.1916(4)	Ø.1ØØ2(4)	Ø.218Ø(7)	6.Ø(2)
C11	Ø.3Ø91(3)	Ø.3492(3)	Ø.3225(5)	4.2(1)
C12	Ø.3977(4)	Ø.3697(3)	Ø.3412(5)	4.1(1)
C13	Ø.41Ø8(3)	Ø.4Ø12(3)	Ø.2115(5)	3.5(1)
C14	Ø.3292(3)	Ø.3985(3)	Ø.1119(5)	3.3(1)
C15	Ø.2663(3)	Ø.3662(4)	Ø.1777(5)	4.Ø(1)
C16	Ø.2636(5)	Ø.32Ø6(4)	Ø.4359(6)	8.Ø(2)

Table of Positional Parameters and Their Estimated Standard Deviations (cont.)

Atom	x	y	z	B(A2)
C17	0.4667(6)	0.3686(5)	0.4799(7)	7.8(2)
C18	0.4941(4)	0.4489(4)	0.1988(7)	5.3(2)
C19	0.3094(4)	0.4357(4)	-0.0385(6)	5.4(2)
C20	0.1696(4)	0.3577(5)	0.1186(8)	6.5(2)
C21	0.4588(4)	0.0957(4)	0.1814(5)	4.8(1)
C22	0.5057(3)	0.1687(4)	0.0818(5)	4.1(1)
C23	0.4564(3)	0.2154(3)	-0.0353(5)	3.6(1)
C24	0.3774(3)	0.1696(4)	-0.0840(5)	4.0(1)
C25	0.3782(3)	0.0966(4)	0.0002(6)	4.8(1)
C26	0.4892(5)	0.0204(5)	0.2820(7)	10.1(2)
C27	0.5965(4)	0.1941(7)	0.1631(7)	8.3(2)
C28	0.4890(5)	0.2901(5)	-0.1091(7)	7.6(2)
C29	0.3063(5)	0.1948(7)	-0.2153(7)	8.7(2)
C30	0.3114(5)	0.0246(5)	-0.0244(8)	12.2(2)
H31	0.437(4)	0.174(5)	0.564(7)	7(2)*
H32	0.482(4)	0.151(5)	0.453(7)	8(2)*
H33	0.439(5)	0.081(6)	0.526(8)	10(3)*
H41	0.167(3)	0.041(3)	0.207(5)	3(1)*
H42	0.151(4)	0.132(5)	0.248(6)	6(2)*
H43	0.180(3)	0.133(4)	0.121(6)	4(1)*

Starred atoms were refined isotropically.
Anisotropically refined atoms are given in the form of the isotropic equivalent displacement parameter defined as:
(4/3) * [a2*B(1,1) + b2*B(2,2) + c2*B(3,3) + ab(cos gamma)*B(1,2) + ac(cos beta)*B(1,3) + bc(cos alpha)*B(2,3)]

Table of Refined Displacement Parameter Expressions - Beta's

Name	B(1,1)	B(2,2)	B(3,3)	B(1,2)	B(1,3)	B(2,3)
Yb	0.00331(1)	0.00226(1)	0.00728(2)	0.00056(2)	0.00455(2)	0.00088(2)
C1	0.0055(2)	0.0025(3)	0.0163(6)	0.0010(4)	0.0113(6)	0.0009(7)
C2	0.0057(3)	0.0032(3)	0.0122(6)	0.0018(4)	0.0078(6)	0.0022(7)
C3	0.0067(3)	0.0051(4)	0.0165(8)	0.0024(6)	0.0025(9)	0.0006(9)
C4	0.0053(3)	0.0049(3)	0.024(1)	-0.0010(5)	0.0077(9)	-0.000(1)
C11	0.0083(3)	0.0023(2)	0.0110(5)	0.0034(4)	0.0121(6)	0.0017(6)
C12	0.0074(3)	0.0027(3)	0.0071(5)	0.0012(5)	0.0021(7)	-0.0007(6)
C13	0.0054(2)	0.0025(2)	0.0091(5)	0.0002(4)	0.0050(6)	0.0006(6)
C14	0.0047(2)	0.0033(2)	0.0080(5)	0.0014(4)	0.0058(5)	0.0026(6)
C15	0.0046(2)	0.0030(3)	0.0150(7)	0.0032(4)	0.0066(6)	0.0021(7)

Table of Refined Displacement Parameter Expressions - Beta's (Continued)

Name	B(1,1)	B(2,2)	B(3,3)	B(1,2)	B(1,3)	B(2,3)
C16	Ø.Ø157(4)	Ø.ØØ38(4)	Ø.Ø252(7)	Ø.ØØ37(6)	Ø.Ø323(7)	Ø.ØØ35(8)
C17	Ø.Ø142(6)	Ø.ØØ45(4)	Ø.Ø114(8)	-Ø.ØØØ6(8)	-Ø.ØØ5(1)	-Ø.ØØ21(9)
C18	Ø.ØØ56(3)	Ø.ØØ43(3)	Ø.Ø184(8)	-Ø.ØØ25(5)	Ø.ØØ49(8)	-Ø.ØØØ9(9)
C19	Ø.ØØ77(3)	Ø.ØØ52(3)	Ø.Ø113(7)	Ø.ØØ31(6)	Ø.ØØ48(8)	Ø.ØØ58(8)
C2Ø	Ø.ØØ55(3)	Ø.ØØ53(4)	Ø.Ø28(1)	Ø.ØØ27(5)	Ø.Ø1Ø4(9)	Ø.ØØ4(1)
C21	Ø.ØØ85(3)	Ø.ØØ38(3)	Ø.Ø118(6)	Ø.ØØ6Ø(4)	Ø.Ø133(6)	Ø.ØØ27(6)
C22	Ø.ØØ38(2)	Ø.ØØ59(3)	Ø.ØØ96(5)	Ø.ØØ21(4)	Ø.ØØ5Ø(5)	-Ø.ØØ13(7)
C23	Ø.ØØ56(2)	Ø.ØØ26(3)	Ø.Ø1Ø9(5)	Ø.ØØØ6(4)	Ø.ØØ92(5)	Ø.ØØØ8(6)
C24	Ø.ØØ39(2)	Ø.ØØ6Ø(3)	Ø.ØØ71(5)	Ø.ØØØ4(5)	Ø.ØØ27(6)	-Ø.ØØ24(7)
C25	Ø.ØØ74(3)	Ø.ØØ33(3)	Ø.Ø17Ø(6)	-Ø.ØØ35(4)	Ø.Ø165(6)	-Ø.ØØ66(7)
C26	Ø.Ø2Ø5(5)	Ø.ØØ66(4)	Ø.Ø226(8)	Ø.Ø165(7)	Ø.Ø318(9)	Ø.Ø13Ø(9)
C27	Ø.ØØ4Ø(3)	Ø.Ø166(7)	Ø.Ø161(8)	Ø.ØØ35(8)	Ø.ØØ41(8)	-Ø.ØØØ(1)
C28	Ø.Ø128(4)	Ø.ØØ56(4)	Ø.Ø239(8)	-Ø.ØØ2Ø(6)	Ø.Ø276(7)	Ø.ØØ13(9)
C29	Ø.ØØ79(4)	Ø.Ø158(7)	Ø.Ø1Ø2(7)	Ø.ØØ62(9)	Ø.ØØ21(9)	-Ø.ØØ5(1)
C3Ø	Ø.Ø171(5)	Ø.ØØ98(4)	Ø.Ø44(1)	-Ø.Ø181(7)	Ø.Ø42(1)	-Ø.Ø31(1)

The form of the anisotropic displacement parameter is:
exp[-(B(1,1)*h2 + B(2,2)*k2 + B(3,3)*l2 + B(1,2)*hk + B(1,3)*hl + B(2,3)*kl)].

$[(Me_5C_5)_2Yb]_2(\mu\text{-}F)$

Table of Positional Parameters and Their Estimated Standard Deviations

Atom	x	y	z	B(A2)
Yb1	Ø.ØØØ	Ø.ØØØ55(1)	Ø.25Ø	3.686(5)
Yb2	Ø.ØØØ	Ø.38799(1)	Ø.25Ø	3.161(5)
F	Ø.ØØØ	Ø.2424(2)	Ø.25Ø	3.94(7)
C1	-Ø.1621(2)	Ø.1ØØ8(3)	Ø.2535(2)	4.14(9)
C2	-Ø.1629(2)	Ø.Ø368(3)	Ø.1891(2)	4.37(9)
C3	-Ø.1267(2)	-Ø.Ø465(3)	Ø.2247(3)	5.5(1)
C4	-Ø.1Ø19(3)	-Ø.Ø337(3)	Ø.31Ø9(3)	5.6(1)
C5	-Ø.1226(2)	Ø.Ø573(3)	Ø.3283(2)	4.69(9)
C6	-Ø.2ØØ5(3)	Ø.1968(3)	Ø.2429(3)	6.7(1)
C7	-Ø.1999(3)	Ø.Ø518(4)	Ø.Ø988(3)	7.4(1)
C8	-Ø.1272(3)	-Ø.1382(4)	Ø.18Ø3(4)	9.6(2)
C9	-Ø.Ø7ØØ(4)	-Ø.1Ø81(4)	Ø.3746(4)	1Ø.5(2)

Table of Positional Parameters and Their Estimated Standard Deviations (cont.)

Atom	x	y	z	B(A2)
C1Ø	-Ø.1155(4)	Ø.ØØ973(4)	Ø.4119(3)	8.6(2)
C11	-Ø.Ø146(2)	Ø.41ØØ(3)	Ø.3985(2)	3.88(8)
C12	Ø.ØØ47(3)	Ø.3665(3)	Ø.4Ø51(2)	4.14(8)
C13	Ø.1167(2)	Ø.4316(3)	Ø.3773(2)	4.16(9)
C14	Ø.Ø7Ø7(3)	Ø.5144(3)	Ø.3567(2)	4.42(9)
C15	-Ø.Ø1Ø6(3)	Ø.5ØØ7(3)	Ø.3694(2)	4.29(9)
C16	-Ø.ØØ76(3)	Ø.37Ø5(4)	Ø.4288(3)	6.8(1)
C17	Ø.Ø9Ø9(4)	Ø.27Ø3(3)	Ø.4395(3)	6.3(1)
C18	Ø.2Ø7Ø(3)	Ø.4162(4)	Ø.3749(3)	7.Ø(1)
C19	Ø.1Ø75(4)	Ø.6Ø6Ø(3)	Ø.3399(3)	7.7(1)
C2Ø	-Ø.Ø779(3)	Ø.5741(3)	Ø.3675(3)	6.7(1)

Anisotropically refined atoms are given in the form of the isotropic equivalent displacement parameter defined as:
(4/3) * [a2*B(1,1) + b2*B(2,2) + c2*B(3,3) + ab(cos gamma)*B(1,2) + ac(cos beta)*B(1,3) + bc(cos alpha)*B(2,3)]

Table of General Displacement Parameter Expressions - B's

Name	B(1,1)	B(2,2)	B(3,3)	B(1,2)	B(1,3)	B(2,3)	Beqv
Yb1	3.384(9)	3.Ø45(9)	4.78(1)	Ø	1.3Ø4(8)	Ø	3.686(5)
Yb2	3.74(1)	2.915(9)	2.857(8)	Ø	Ø.879(7)	Ø	3.161(5)
F	5.Ø(1)	2.4(1)	4.3(1)	Ø	Ø.9(1)	Ø	3.94(7)
C1	3.5(2)	3.8(1)	5.5(2)	Ø.Ø(1)	1.7(1)	Ø.5(1)	4.14(9)
C2	3.8(2)	5.Ø(2)	4.5(2)	-Ø.6(1)	1.4(1)	-Ø.4(1)	4.37(9)
C3	4.5(2)	3.9(2)	8.9(2)	-Ø.8(2)	3.2(1)	-1.Ø(2)	5.5(1)
C4	3.9(2)	5.4(2)	7.5(2)	-Ø.2(2)	1.4(2)	2.5(2)	5.6(1)
C5	4.2(2)	6.Ø(2)	4.1(2)	-1.2(2)	1.4(1)	Ø.3(2)	4.69(9)
C6	5.9(2)	4.5(2)	1Ø.7(3)	Ø.4(2)	4.1(2)	Ø.8(2)	6.7(1)
C7	6.Ø(2)	11.3(3)	4.9(2)	-2.9(2)	1.2(2)	-Ø.1(2)	7.4(1)
C8	7.2(2)	5.3(2)	18.1(4)	-2.1(2)	6.5(2)	-4.1(3)	9.6(2)
C9	6.Ø(3)	1Ø.4(3)	15.3(4)	1.6(2)	3.2(2)	8.6(2)	1Ø.5(2)
C1Ø	9.4(3)	11.7(4)	4.7(2)	-4.7(3)	2.1(2)	-1.4(2)	8.6(2)
C11	4.5(2)	4.4(2)	3.1(1)	-Ø.8(1)	1.8(1)	-Ø.9(1)	3.88(8)
C12	5.5(2)	4.Ø(1)	2.8(1)	Ø.2(2)	Ø.8(1)	-Ø.1(1)	4.14(8)
C13	4.Ø(2)	5.3(2)	3.1(1)	-Ø.5(1)	Ø.7(1)	-Ø.8(1)	4.16(9)
C14	5.9(2)	4.1(2)	3.5(1)	-1.4(1)	1.5(1)	-1.Ø(1)	4.42(9)
C15	5.Ø(2)	4.2(2)	3.6(1)	Ø.5(1)	1.Ø(1)	-Ø.9(1)	4.29(9)
C16	6.7(2)	8.3(3)	6.7(2)	-2.4(2)	3.9(2)	-1.7(2)	6.8(1)

Table of General Displacement Parameter Expressions - B's (Continued)

Name	B(1,1)	B(2,2)	B(3,3)	B(1,2)	B(1,3)	B(2,3)	Beqv
C17	9.8(3)	4.6(2)	4.2(2)	1.3(2)	1.Ø(2)	Ø.3(2)	6.3(1)
C18	4.4(2)	1Ø.1(3)	6.4(2)	-1.1(2)	1.Ø(2)	-3.Ø(2)	7.Ø(1)
C19	11.5(3)	5.8(2)	6.1(2)	-4.Ø(2)	2.7(2)	-Ø.8(2)	7.7(1)
C2Ø	8.Ø(3)	6.2(2)	5.6(2)	2.3(2)	1.2(2)	-1.6(2)	6.7(1)

The form of the anisotropic displacement parameter is:
exp[-Ø.25(h2a2B(1,1) + k2b2B(2,2) + l2c2B(3,3) + 2hkabB(1,2) + 2hlacB(1,3) + 2klbcB(2,3))] where a,b, and c are reciprocal lattice constants.

$[(Me_5C_5)_3Yb_2F_2]_2 \cdot (PhMe)_2$

Table of Positional Parameters and Their Estimated Standard Deviations

Atom	x	y	z	B(Å^2)
YB1	Ø.19Ø86(1)	Ø.16551(3)	Ø.Ø7565(1)	4.411(8)
YB2	Ø.34782(1)	Ø.1Ø367(3)	Ø.Ø7363(1)	3.932(7)
F1	Ø.2759(1)	Ø.1567(4)	Ø.Ø896(2)	5.4(1)
F2	Ø.1613(2)	Ø.2582(4)	-Ø.ØØ76(2)	5.4(1)
C1	Ø.1741(4)	Ø.11Ø(2)	Ø.1761(4)	14.3(4)
C2	Ø.1376(4)	Ø.2Ø4(1)	Ø.15Ø9(4)	1Ø.5(3)
C3	Ø.1Ø38(3)	Ø.1521(9)	Ø.1Ø81(4)	7.Ø(2)
C4	Ø.1177(3)	Ø.Ø265(9)	Ø.1Ø16(4)	6.6(2)
C5	Ø.16Ø1(3)	Ø.ØØØ(1)	Ø.1442(4)	9.5(3)
C6	Ø.2158(5)	Ø.Ø96(2)	Ø.2277(6)	28.Ø(9)
C7	Ø.1439(7)	Ø.328(1)	Ø.1844(5)	24.9(5)
C8	Ø.Ø548(4)	Ø.219(2)	Ø.Ø737(6)	15.9(4)
C9	Ø.Ø851(5)	-Ø.Ø69(1)	Ø.Ø57Ø(6)	14.5(4)
C1Ø	Ø.1796(5)	-Ø.148(1)	Ø.15Ø7(6)	17.6(4)
C11	Ø.32ØØ(3)	-Ø.1422(7)	Ø.Ø667(3)	5.1(2)
C12	Ø.2855(3)	-Ø.Ø8Ø1(7)	Ø.Ø221(3)	4.4(2)
C13	Ø.3131(3)	-Ø.Ø414(8)	-Ø.Ø159(3)	4.8(2)
C14	Ø.3648(3)	-Ø.Ø791(7)	Ø.ØØ52(4)	5.4(2)
C15	Ø.3684(3)	-Ø.1444(7)	Ø.Ø56Ø(4)	5.3(2)
C16	Ø.3Ø52(4)	-Ø.2Ø59(9)	Ø.1157(4)	7.6(3)
C17	Ø.2278(3)	-Ø.Ø677(8)	Ø.Ø144(4)	5.9(2)
C18	Ø.2912(4)	Ø.Ø244(8)	-Ø.Ø7Ø8(4)	6.6(2)
C19	Ø.4Ø76(4)	-Ø.Ø621(9)	-Ø.Ø235(4)	7.5(3)
C2Ø	Ø.414Ø(4)	-Ø.2247(9)	Ø.Ø865(4)	7.7(3)
C21	Ø.3826(3)	Ø.2866(8)	Ø.1448(4)	6.3(2)
C22	Ø.3798(3)	Ø.1771(9)	Ø.1763(4)	6.2(2)
C23	Ø.416Ø(3)	Ø.Ø883(8)	Ø.1695(4)	5.8(2)
C24	Ø.4421(3)	Ø.1431(8)	Ø.1325(4)	5.8(2)
C25	Ø.4219(3)	Ø.2663(8)	Ø.1172(4)	6.Ø(2)
C26	Ø.3513(5)	Ø.4Ø8(1)	Ø.1453(6)	11.2(4)
C27	Ø.3461(5)	Ø.164(2)	Ø.2172(5)	12.2(4)
C28	Ø.4311(5)	-Ø.Ø35(1)	Ø.2Ø46(5)	1Ø.8(4)
C29	Ø.4897(4)	Ø.Ø88(1)	Ø.12ØØ(5)	11.7(4)
C3Ø	Ø.4388(5)	Ø.363(1)	Ø.Ø828(5)	11.2(4)
C31	Ø.5ØØ	Ø.3688(2)	Ø.25Ø	11.6(3)*
C32	Ø.4635(1)	Ø.4Ø34(2)	Ø.28Ø1(1)	11.6*
C33	Ø.45148(8)	Ø.5366(4)	Ø.2853(1)	11.6*
C34	Ø.4793(2)	Ø.6316(2)	Ø.2656(2)	11.6*
C35	Ø.518ØØ(9)	Ø.595Ø(2)	Ø.2389(1)	11.6*
C36	Ø.52798(6)	Ø.4618(2)	Ø.2315Ø(9)	11.6*
C37	Ø.5684(3)	Ø.4234(3)	Ø.2Ø26(4)	19(1)*

* -- Atoms refined with isotropic thermal parameters.

Anisotropically refined atoms are given in the form of the isotropic equivalent thermal parameter defined as:

$(4/3) * [a^2*B(1,1) + b^2*B(2,2) + c^2*B(3,3) + ab(\cos\ gamma)*B(1,2)$

$+ ac(\cos\ beta)*B(1,3) + bc(\cos\ alpha)*B(2,3)]$

Table of General Temperature Factor Expressions - B's

Name	B(1,1)	B(2,2)	B(3,3)	B(1,2)	B(1,3)	B(2,3)	Beqv
YB1	3.48(1)	5.62(2)	4.38(1)	-Ø.Ø7(1)	1.46(1)	Ø.13(1)	4.411(8)
YB2	3.18(1)	3.81(1)	4.73(1)	Ø.29(1)	Ø.85(1)	-Ø.Ø5(1)	3.932(7)
F1	3.7(2)	5.8(2)	6.9(2)	Ø.3(2)	1.4(2)	-1.6(2)	5.4(1)
F2	6.2(2)	4.7(2)	5.1(2)	-Ø.2(2)	Ø.8(2)	Ø.7(2)	5.4(1)
C1	7.5(4)	32(1)	3.6(4)	-1Ø.(6)	1.7(4)	-Ø.9(7)	14.3(4)
C2	13.4(5)	11.1(6)	1Ø.2(5)	-6.1(5)	8.9(4)	-5.1(5)	1Ø.5(3)
C3	6.2(4)	8.1(5)	8.4(4)	1.2(4)	5.Ø(3)	1.4(4)	7.Ø(2)
C4	7.3(4)	6.5(4)	7.4(4)	-2.2(4)	4.6(3)	-Ø.9(4)	6.6(2)
C5	5.6(3)	14.2(6)	1Ø.4(4)	4.4(4)	5.4(3)	8.4(4)	9.5(3)
C6	11.6(7)	65(3)	6.6(7)	-1(1)	Ø.1(6)	6(1)	28.Ø(9)
C7	5Ø(1)	12.1(7)	23.5(7)	-15.(8)	3Ø.Ø(6)	-11.(6)	24.9(5)
C8	8.2(5)	2Ø(1)	23(1)	7.7(6)	9.1(5)	11.1(8)	15.9(4)
C9	15.8(7)	16.2(8)	14.7(7)	-1Ø.(6)	1Ø.Ø(5)	-6.4(7)	14.5(4)
C1Ø	18.1(7)	16.6(8)	24.2(8)	1Ø.5(6)	16.5(5)	13.8(6)	17.6(4)
C11	5.9(3)	3.2(3)	7.2(4)	Ø.2(3)	3.4(3)	Ø.2(3)	5.1(2)
C12	4.1(3)	3.8(3)	5.4(4)	-Ø.4(3)	1.2(3)	-1.2(3)	4.4(2)
C13	5.5(4)	4.7(3)	4.4(3)	Ø.2(3)	1.5(3)	-Ø.9(3)	4.8(2)
C14	5.Ø(3)	4.2(4)	7.7(4)	Ø.Ø(3)	3.1(3)	-1.Ø(3)	5.4(2)
C15	5.2(4)	4.Ø(3)	6.7(4)	Ø.8(3)	1.8(3)	-Ø.1(3)	5.3(2)
C16	9.2(5)	5.7(4)	8.5(5)	-1.4(4)	3.2(4)	Ø.4(4)	7.6(3)
C17	4.2(3)	5.5(4)	8.1(5)	-Ø.1(3)	1.7(3)	-1.5(4)	5.9(2)
C18	8.1(5)	5.Ø(4)	6.Ø(5)	-Ø.5(4)	Ø.8(4)	-Ø.9(4)	6.6(2)
C19	7.5(4)	6.8(5)	9.3(5)	-Ø.5(4)	4.3(4)	-1.1(4)	7.5(3)
C2Ø	8.Ø(5)	5.4(4)	9.1(6)	2.8(4)	1.Ø(5)	-Ø.4(4)	7.7(3)
C21	5.6(4)	4.2(3)	7.1(5)	Ø.2(3)	-2.Ø(4)	-1.3(4)	6.3(2)
C22	4.3(3)	9.Ø(5)	5.2(4)	-1.1(4)	1.4(3)	-1.6(4)	6.2(2)
C23	5.6(4)	5.5(4)	5.3(4)	-Ø.Ø(3)	-Ø.3(4)	Ø.6(3)	5.8(2)
C24	3.5(3)	7.3(5)	6.6(4)	-Ø.Ø(3)	1.2(3)	-Ø.7(4)	5.8(2)
C25	5.6(4)	5.8(4)	6.Ø(4)	-2.2(3)	Ø.1(4)	1.Ø(4)	6.Ø(2)
C26	9.8(7)	7.8(6)	12.6(8)	2.Ø(5)	-3.9(6)	-3.7(5)	11.2(4)
C27	8.9(7)	2Ø(1)	7.9(6)	-2.2(8)	2.3(5)	-4.3(7)	12.2(4)
C28	13.4(9)	8.6(6)	7.7(6)	-Ø.9(7)	-2.8(6)	2.3(5)	1Ø.8(4)
C29	4.4(4)	19(1)	12.2(8)	Ø.8(6)	2.6(5)	-4.1(7)	11.7(4)
C3Ø	11.Ø(7)	12.2(7)	8.4(6)	-6.1(5)	-1.7(6)	3.4(5)	11.2(4)

The form of the anisotropic thermal parameter is:

$$\exp[-Ø.25(h^2 a^{*2} B(1,1) + k^2 b^{*2} B(2,2) + l^2 c^{*2} B(3,3) + 2hka^*b^*B(1,2) + 2hla^*c^*B(1,3) + 2klb^*c^*B(2,3))]$$

, where a*,b*, and c* are reciprocal lattice constants.

$(Me_5C_5)_2Yb(\mu\text{-}Me)Be(C_5Me_5)$

Table of Positional Parameters and Their Estimated Standard Deviations

Atom	x	y	z	B(A2)
YB	0.05923(2)	0.21077(2)	0.17317(1)	2.469(4)
C1	0.0073(4)	0.2003(4)	0.2881(2)	3.7(1)
C11	0.2163(4)	0.0365(4)	0.1948(2)	2.42(9)
C12	0.1360(4)	-0.0172(4)	0.1609(2)	2.70(9)
C13	0.1531(4)	0.0342(4)	0.1075(2)	2.58(9)
C14	0.2446(3)	0.1225(4)	0.1069(2)	2.27(8)
C15	0.2833(3)	0.1246(4)	0.1601(2)	2.35(8)
C16	0.2376(4)	0.0000(5)	0.2520(2)	4.0(1)
C17	0.0520(4)	-0.1193(5)	0.1791(2)	4.3(1)
C18	0.0948(4)	-0.0069(4)	0.0577(2)	4.0(1)
C19	0.3002(5)	0.1914(4)	0.0569(2)	3.8(1)
C20	0.3852(4)	0.1985(4)	0.1761(2)	3.6(1)
C21	-0.1566(4)	0.3175(4)	0.1771(2)	3.0(1)
C22	-0.0744(4)	0.4128(4)	0.1795(2)	2.64(9)
C23	-0.0012(4)	0.4182(4)	0.1275(2)	2.56(9)
C24	-0.0386(4)	0.3272(4)	0.0925(2)	2.64(9)
C25	-0.1327(4)	0.2642(4)	0.1233(2)	2.83(9)
C26	-0.2588(5)	0.2883(6)	0.2206(3)	5.7(1)
C27	-0.0747(5)	0.5023(5)	0.2261(2)	5.0(1)
C28	0.0906(4)	0.5137(5)	0.1100(2)	4.6(1)
C29	0.0037(5)	0.3127(5)	0.0315(2)	4.4(1)
C30	-0.2086(5)	0.1679(5)	0.1009(3)	5.5(1)
C31	-0.0562(4)	0.3114(4)	0.4172(2)	2.77(9)
C32	0.0372(4)	0.2301(4)	0.4252(2)	2.64(9)
C33	-0.0092(4)	0.1119(4)	0.4234(2)	2.62(9)
C34	-0.1314(4)	0.1204(4)	0.4160(2)	2.83(9)
C35	-0.1593(4)	0.2438(4)	0.4114(2)	2.74(9)
C36	-0.0438(5)	0.4459(5)	0.4140(3)	5.1(1)
C37	0.1636(5)	0.2647(5)	0.4320(3)	5.1(1)
C38	0.0616(5)	-0.0028(4)	0.4275(2)	4.4(1)
C39	-0.2129(5)	0.0156(5)	0.4115(3)	5.4(1)
C40	-0.2781(4)	0.2936(5)	0.3998(2)	4.5(1)

Table of Positional Parameters and Their Estimated Standard Deviations (cont.)

Atom	x	y	z	B(A2)
BE	-0.0294(5)	0.1996(5)	0.3589(3)	2.8(1)
H11	0.088(4)	0.206(4)	0.276(2)	1(1)*
H12	-0.026(4)	0.262(5)	0.271(2)	3(1)*
H13	-0.003(5)	0.139(6)	0.288(2)	5(2)*

Starred atoms were included with isotropic thermal parameters.
The thermal parameter given for anisotropically refined atoms is the isotropic equivalent thermal parameter defined as:
(4/3) * [a2*B(1,1) + b2*B(2,2) + c2*B(3,3) + ab(cos gamma)*B(1,2) + ac(cos beta)*B(1,3) + bc(cos alpha)*B(2,3)]
where a,b,c are real cell parameters, and B(i,j) are anisotropic betas.

Table of Anisotropic Thermal Parameters - B's

Name	B(1,1)	B(2,2)	B(3,3)	B(1,2)	B(1,3)	B(2,3)	Beqv
YB	3.007(7)	2.898(7)	1.444(7)	1.002(8)	-0.037(6)	0.061(7)	2.469(4)
C1	4.3(2)	4.0(2)	2.7(2)	1.2(2)	0.1(2)	0.3(2)	3.7(1)
C11	2.8(2)	2.8(2)	1.7(2)	0.9(2)	-0.3(1)	0.4(1)	2.42(9)
C12	2.6(2)	2.3(2)	3.1(2)	0.1(2)	-0.2(2)	0.0(2)	2.70(9)
C13	2.9(2)	2.6(2)	2.4(2)	0.6(2)	-0.7(1)	-0.5(2)	2.58(9)
C14	2.7(2)	2.4(2)	1.6(2)	0.7(2)	0.3(1)	-0.1(2)	2.27(8)
C15	2.5(2)	2.2(2)	2.3(2)	0.5(2)	-0.4(1)	-0.1(2)	2.35(8)
C16	4.6(2)	4.3(2)	3.2(2)	1.1(2)	-1.0(2)	1.2(2)	4.0(1)
C17	4.1(2)	4.1(2)	4.9(3)	-0.8(2)	-0.7(2)	0.7(2)	4.3(1)
C18	4.7(2)	3.7(2)	4.1(2)	1.1(2)	-2.0(2)	-1.0(2)	4.0(1)
C19	4.6(2)	4.1(2)	2.6(2)	0.4(2)	0.2(2)	0.3(2)	3.8(1)
C20	3.9(2)	3.1(2)	4.2(2)	-0.4(2)	-1.2(2)	-0.5(2)	3.6(1)
C21	2.3(2)	3.3(2)	3.4(2)	0.3(2)	-0.1(2)	0.6(2)	3.0(1)
C22	2.7(2)	2.4(2)	2.8(2)	0.8(2)	-0.8(1)	-1.0(2)	2.64(9)
C23	2.0(2)	2.7(2)	3.0(2)	0.0(2)	-0.4(1)	0.6(2)	2.56(9)
C24	3.0(2)	3.0(2)	1.9(2)	0.8(2)	-0.4(1)	0.3(1)	2.64(9)
C25	3.2(2)	1.9(2)	3.6(2)	0.2(2)	-1.0(2)	-0.1(2)	2.83(9)
C26	3.6(2)	6.9(3)	5.9(3)	-0.0(3)	1.2(2)	1.5(3)	5.7(1)
C27	5.8(3)	4.7(2)	4.8(3)	1.6(2)	-1.7(2)	-2.1(2)	5.0(1)
C28	3.8(2)	4.9(2)	5.3(3)	-1.0(2)	-1.0(2)	1.5(2)	4.6(1)
C29	5.3(2)	5.1(3)	2.9(2)	1.6(2)	-0.8(2)	0.2(2)	4.4(1)
C30	5.8(3)	3.4(2)	7.8(3)	-0.7(2)	-3.2(2)	-0.6(2)	5.5(1)
C31	3.4(2)	2.8(2)	1.9(2)	0.0(2)	0.3(2)	-0.1(2)	2.77(9)
C32	2.3(2)	3.2(2)	2.3(2)	0.1(2)	-0.1(1)	-0.1(2)	2.64(9)
C33	3.3(2)	2.8(2)	1.7(2)	0.4(2)	-0.1(1)	0.3(2)	2.62(9)
C34	2.9(2)	3.5(2)	2.1(2)	-0.7(2)	-0.1(1)	-0.1(2)	2.83(9)

Table of Anisotropic Thermal Parameters - B's (Continued)

Name	B(1,1)	B(2,2)	B(3,3)	B(1,2)	B(1,3)	B(2,3)	Beqv
C35	2.4(2)	4.Ø(2)	1.7(2)	Ø.6(2)	Ø.2(1)	Ø.1(2)	2.74(9)
C36	6.6(3)	3.Ø(2)	5.3(3)	Ø.1(2)	1.Ø(3)	Ø.1(2)	5.1(1)
C37	3.5(2)	6.Ø(3)	5.9(3)	-1.3(2)	-1.4(2)	-Ø.Ø(3)	5.1(1)
C38	5.8(3)	3.4(2)	3.9(2)	1.5(2)	Ø.2(2)	Ø.6(2)	4.4(1)
C39	5.2(2)	4.9(2)	6.2(3)	-2.4(2)	-1.Ø(2)	-Ø.7(2)	5.4(1)
C4Ø	3.1(2)	6.8(3)	3.6(2)	Ø.7(2)	-Ø.5(2)	Ø.5(2)	4.5(1)
BE	2.6(2)	3.1(2)	2.5(2)	Ø.6(2)	Ø.1(2)	Ø.3(2)	2.8(1)

The form of the anisotropic temperature factor is:
exp[-Ø.25(h2a2B(1,1) + k2b2B(2,2) + l2c2B(3,3) + 2hkabB(1,2) + 2hlacB(1,3) + 2klbcB(2,3))] where a,b, and c are reciprocal lattice constants.

$(Me_5C_5)_2Yb(BH_3 \cdot PMe_3)$

Table of Positional Parameters and Their Estimated Standard Deviations

Atom	x	y	z	B(A2)
YB	Ø.ØØ896(2)	Ø.25Ø	Ø.ØØ144(3)	4.71(1)
P	-Ø.Ø768(1)	Ø.25Ø	-Ø.3461(3)	6.92(9)
C1	Ø.2158(5)	Ø.25Ø	Ø.Ø45(1)	6.5(3)
C2	Ø.2Ø37(3)	Ø.3336(7)	-Ø.Ø361(7)	5.7(2)
C3	Ø.1832(3)	Ø.3ØØ7(5)	-Ø.1639(5)	4.7(1)
C4	-Ø.Ø362(5)	Ø.25Ø	Ø.1427(9)	12.2(6)
C5	Ø.ØØ12(4)	Ø.3346(8)	Ø.19Ø1(7)	1Ø.2(3)
C6	Ø.Ø571(4)	Ø.3Ø23(6)	Ø.2588(6)	7.4(2)
C11	Ø.2494(6)	Ø.278(1)	Ø.187(1)	6.4(3)*
C12	Ø.2147(6)	Ø.442(1)	Ø.ØØ63(8)	11.5(3)
C13	Ø.1721(4)	Ø.3671(7)	-Ø.2891(7)	8.8(2)
C14	-Ø.1Ø22(7)	Ø.293(1)	Ø.Ø77(2)	7.1(4)*
C15	-Ø.Ø168(7)	Ø.443(1)	Ø.177(1)	18.3(4)
C16	Ø.1Ø77(6)	Ø.3666(9)	Ø.3451(8)	13.7(4)
C111	-Ø.Ø755(6)	Ø.351(1)	-Ø.466(1)	14.Ø(4)
C211	-Ø.1464(7)	Ø.318(1)	-Ø.271(1)	22.4(7)
B	Ø.ØØØ3(5)	Ø.25Ø	-Ø.229(1)	6.1(3)

Starred atoms were included with isotropic thermal parameters.
The thermal parameter given for anisotropically refined atoms is the isotropic equivalent thermal parameter defined as:
(4/3) * [a2*B(1,1) + b2*B(2,2) + c2*B(3,3) + ab(cos gamma)*B(1,2) + ac(cos beta)*B(1,3) + bc(cos alpha)*B(2,3)]
where a,b,c are real cell parameters, and B(i,j) are anisotropic betas.

Table of Anisotropic Thermal Parameters - B's

Name	B(1,1)	B(2,2)	B(3,3)	B(1,2)	B(1,3)	B(2,3)	Beqv
YB	3.28(2)	7.45(3)	3.39(2)	Ø	Ø.ØØ4(2)	Ø	4.71(1)
P	3.9(1)	11.5(2)	5.4(1)	Ø	-Ø.7(1)	Ø	6.92(9)
C1	3.Ø(4)	12.4(9)	4.Ø(3)	Ø	-Ø.7(4)	Ø	6.5(3)
C2	3.6(3)	7.1(4)	6.4(3)	-1.2(3)	-Ø.1(3)	-1.2(3)	5.7(2)
C3	2.8(2)	6.8(4)	4.5(2)	Ø.1(2)	Ø.6(2)	Ø.8(3)	4.7(1)
C4	3.6(4)	29(2)	3.5(4)	Ø	1.1(4)	Ø	12.2(6)
C5	9.9(5)	16.7(7)	4.Ø(3)	6.2(5)	2.2(3)	2.Ø(4)	1Ø.2(3)
C6	9.Ø(4)	9.7(6)	3.5(3)	-Ø.4(4)	1.8(3)	-1.Ø(3)	7.4(2)
C12	8.7(6)	1Ø.7(7)	14.9(8)	-2.Ø(6)	1.2(4)	-5.9(5)	11.5(3)
C13	5.9(4)	12.Ø(6)	8.5(4)	1.Ø(4)	Ø.1(3)	5.5(4)	8.8(2)
C15	27(1)	14.6(6)	12.8(7)	15.1(6)	8.3(6)	4.9(7)	18.3(4)
C16	15.8(7)	16.5(9)	8.9(5)	-5.5(8)	2.9(5)	-5.Ø(5)	13.7(4)
C111	18(1)	11.3(9)	12.9(6)	Ø.3(8)	-7.Ø(5)	3.Ø(6)	14.Ø(4)
C211	12.6(8)	32(2)	23(1)	8(1)	-2.7(8)	-6(1)	22.4(7)
B	3.7(5)	9.1(8)	5.5(5)	Ø	-1.6(5)	Ø	6.1(3)

The form of the anisotropic temperature factor is:
exp[-Ø.25(h2a2B(1,1) + k2b2B(2,2) + l2c2B(3,3) + 2hkabB(1,2) + 2hlacB(1,3) + 2klbcB(2,3))] where a,b, and c are reciprocal lattice constants.

$(Me_5C_5)_2Yb(\mu\text{-}Me)_2ZnMe$

Table of Positional Parameters and Their Estimated Standard Deviations

Atom	x	y	z	B(A2)
YB	Ø.12695(1)	Ø.12215(1)	Ø.23922(1)	2.127(4)
ZN	Ø.24212(3)	Ø.14Ø5Ø(3)	Ø.12288(3)	3.48(1)
C1	Ø.1596(2)	Ø.2232(3)	Ø.1133(3)	3.6(1)
C2	Ø.2423(2)	Ø.ØØ493(3)	Ø.2232(3)	4.2(1)
C3	Ø.3217(3)	Ø.1523(4)	Ø.ØØ441(3)	6.4(1)
C11	Ø.ØØØ2(2)	Ø.2267(3)	Ø.36Ø8(2)	2.64(9)
C12	Ø.1353(2)	Ø.27Ø1(3)	Ø.3221(3)	3.6(1)
C13	Ø.1965(2)	Ø.2257(3)	Ø.342Ø(3)	3.8(1)
C14	Ø.1787(2)	Ø.1548(3)	Ø.3956(2)	3.5(1)
C15	Ø.1Ø61(2)	Ø.1549(3)	Ø.4Ø72(2)	2.82(9)
C16	Ø.ØØ78(3)	Ø.26Ø2(3)	Ø.3636(3)	4.2(1)
C17	Ø.1311(3)	Ø.3566(3)	Ø.2786(4)	5.7(2)
C18	Ø.2672(3)	Ø.2554(4)	Ø.3193(4)	5.9(1)

Table of Positional Parameters and Their Estimated Standard Deviations (cont.)

Atom	x	y	z	B(A2)
C19	Ø.2266(3)	Ø.ØØ964(4)	Ø.4439(3)	6.3(1)
C2Ø	Ø.Ø682(3)	Ø.1ØØ4(3)	Ø.4734(3)	4.4(1)
C21	Ø.ØØ78(2)	Ø.Ø479(3)	Ø.2337(3)	2.89(9)
C22	Ø.Ø158(2)	Ø.ØØ876(3)	Ø.15Ø4(3)	2.94(9)
C23	Ø.Ø693(2)	Ø.Ø444(3)	Ø.1Ø41(3)	2.99(9)
C24	Ø.Ø934(2)	-Ø.Ø224(3)	Ø.1591(3)	2.63(9)
C25	Ø.Ø567(2)	-Ø.Ø19Ø(3)	Ø.2399(2)	2.56(9)
C26	-Ø.Ø52Ø(2)	Ø.Ø614(3)	Ø.2955(3)	4.2(1)
C27	-Ø.Ø29Ø(2)	Ø.1574(3)	Ø.1138(3)	5.Ø(1)
C28	Ø.Ø892(3)	Ø.Ø578(3)	Ø.ØØ84(3)	4.2(1)
C29	Ø.1425(2)	-Ø.Ø924(3)	Ø.13Ø8(3)	4.1(1)
C3Ø	Ø.Ø641(3)	-Ø.Ø835(3)	Ø.3143(3)	4.Ø(1)
H11	Ø.111(2)	Ø.232(3)	Ø.137(2)	1.3(9)*
H12	Ø.189(3)	Ø.275(3)	Ø.128(3)	7(2)*
H13	Ø.154(2)	Ø.223(3)	Ø.Ø54(3)	2(1)*
H21	Ø.214(2)	Ø.Ø3Ø(3)	Ø.265(2)	2(1)*
H22	Ø.291(2)	Ø.Ø74(3)	Ø.255(3)	3(1)*
H23	Ø.262(2)	Ø.ØØ8(3)	Ø.197(3)	2(1)*

Starred atoms were included with isotropic thermal parameters.
The thermal parameter given for anisotropically refined atoms is the isotropic equivalent thermal parameter defined as:
(4/3) * [a2*B(1,1) + b2*B(2,2) + c2*B(3,3) + ab(cos gamma)*B(1,2) + ac(cos beta)*B(1,3) + bc(cos alpha)*B(2,3)]
where a,b,c are real cell parameters, and B(i,j) are anisotropic betas.

Table of Anisotropic Thermal Parameters - B's

Name	B(1,1)	B(2,2)	B(3,3)	B(1,2)	B(1,3)	B(2,3)	Beqv
YB	1.918(8)	2.461(9)	2.ØØ2(6)	-Ø.Ø12(7)	-Ø.177(6)	Ø.294(6)	2.127(4)
ZN	2.62(2)	4.74(2)	3.Ø8(2)	-Ø.46(2)	Ø.41(2)	-Ø.Ø9(2)	3.48(1)
C1	4.Ø(2)	3.9(2)	2.8(2)	-Ø.Ø(2)	Ø.1(2)	Ø.6(2)	3.6(1)
C2	2.8(2)	4.8(2)	5.Ø(2)	Ø.3(2)	Ø.4(2)	Ø.5(2)	4.2(1)
C3	3.5(2)	1Ø.8(4)	4.8(2)	Ø.4(3)	Ø.9(2)	2.1(3)	6.4(1)
C11	3.1(2)	2.8(2)	2.Ø(2)	Ø.1(2)	Ø.Ø(2)	-Ø.4(1)	2.64(9)
C12	5.1(2)	3.Ø(2)	2.7(2)	-1.2(2)	-Ø.1(2)	-Ø.1(2)	3.6(1)
C13	3.7(2)	4.7(2)	2.9(2)	-2.1(2)	-Ø.2(2)	-Ø.4(2)	3.8(1)
C14	3.2(2)	5.Ø(2)	2.2(2)	Ø.1(2)	-1.1(2)	-Ø.4(2)	3.5(1)
C15	3.4(2)	3.2(2)	1.9(2)	-1.1(2)	-Ø.1(2)	-Ø.Ø(1)	2.82(9)
C16	4.4(2)	3.8(2)	4.5(2)	Ø.5(2)	-Ø.4(2)	-1.4(2)	4.2(1)
C17	1Ø.Ø(4)	2.7(2)	4.5(2)	-1.1(2)	1.2(3)	Ø.2(2)	5.7(2)

Table of Anisotropic Thermal Parameters - B's (Continued)

Name	B(1,1)	B(2,2)	B(3,3)	B(1,2)	B(1,3)	B(2,3)	Beqv
C18	4.Ø(2)	8.6(3)	5.2(3)	-3.2(2)	Ø.1(2)	-Ø.9(2)	5.9(1)
C19	5.8(3)	9.4(4)	3.6(2)	1.3(3)	-2.2(2)	Ø.7(2)	6.3(1)
C2Ø	6.Ø(3)	4.4(2)	2.7(2)	-1.6(2)	Ø.7(2)	Ø.4(2)	4.4(1)
C21	2.3(2)	2.9(2)	3.5(2)	-Ø.1(2)	Ø.1(2)	-1.1(2)	2.89(9)
C22	2.6(2)	3.1(2)	3.2(2)	Ø.6(2)	-Ø.9(2)	-1.Ø(1)	2.94(9)
C23	3.Ø(2)	3.6(2)	2.4(2)	Ø.1(2)	-Ø.3(2)	-Ø.8(2)	2.99(9)
C24	2.1(2)	2.7(2)	3.2(2)	Ø.2(2)	-Ø.2(2)	-Ø.4(2)	2.63(9)
C25	2.4(2)	2.6(2)	2.7(2)	-Ø.3(2)	Ø.2(1)	-Ø.2(1)	2.56(9)
C26	2.2(2)	4.9(2)	5.4(2)	-Ø.6(2)	1.Ø(2)	-2.1(2)	4.2(1)
C27	4.2(2)	4.9(2)	5.9(2)	1.2(2)	-2.2(2)	-Ø.7(2)	5.Ø(1)
C28	5.6(3)	4.8(2)	2.3(2)	-Ø.3(2)	-Ø.2(2)	Ø.1(2)	4.2(1)
C29	3.6(2)	3.8(2)	4.8(2)	Ø.8(2)	Ø.9(2)	-Ø.7(2)	4.1(1)
C3Ø	4.9(3)	3.2(2)	3.8(2)	-Ø.5(2)	Ø.2(2)	Ø.4(2)	4.Ø(1)

The form of the anisotropic temperature factor is:
exp[-Ø.25(h2a2B(1,1) + k2b2B(2,2) + l2c2B(3,3) + 2hkabB(1,2) + 2hlacB(1,3) + 2klbcB(2,3))] where a,b, and c are reciprocal lattice constants.

$(Me_5C_5)_2Yb(\mu\text{-}Ph)_2ZnPh$

Table of Positional Parameters and Their Estimated Standard Deviations

Atom	x	y	z	B(A2)
YB	-Ø.24136(1)	-Ø.Ø1278(1)	Ø.ØØ3716(1)	1.7Ø9(4)
ZN	-Ø.22334(2)	-Ø.ØØ517(2)	-Ø.1652Ø(4)	2.25(1)
C1	-Ø.2983(2)	-Ø.1194(2)	Ø.Ø744(3)	2.11(9)
C2	-Ø.3388(2)	-Ø.Ø718(2)	Ø.1Ø85(3)	2.28(9)
C3	-Ø.3Ø88(2)	-Ø.Ø426(2)	Ø.186Ø(3)	2.5(1)
C4	-Ø.25Ø1(2)	-Ø.Ø722(2)	Ø.2ØØ1(3)	2.5(1)
C5	-Ø.2441(2)	-Ø.1194(2)	Ø.13Ø3(3)	2.4(1)
C6	-Ø.317Ø(2)	-Ø.1686(2)	Ø.ØØ23(4)	3.3(1)
C7	-Ø.4Ø57(2)	-Ø.Ø616(3)	Ø.Ø783(4)	3.5(1)
C8	-Ø.3415(3)	Ø.ØØ29(3)	Ø.2531(4)	4.3(1)
C9	-Ø.2Ø68(3)	-Ø.Ø665(3)	Ø.2841(4)	4.3(1)
C1Ø	-Ø.1927(2)	-Ø.1684(2)	Ø.1299(4)	3.8(1)
C11	-Ø.2158(2)	Ø.1Ø78(2)	-Ø.Ø169(3)	2.7(1)
C12	-Ø.1569(2)	Ø.Ø766(2)	-Ø.Ø14Ø(3)	2.5(1)
C13	-Ø.1445(2)	Ø.Ø6Ø1(2)	Ø.ØØØ7(3)	2.5(1)
C14	-Ø.1954(2)	Ø.ØØ13(2)	Ø.1368(3)	2.6(1)
C15	-Ø.24ØØ(2)	Ø.11Ø3(2)	Ø.Ø768(4)	2.8(1)

Table of Positional Parameters and Their Estimated Standard Deviations (cont.)

Atom	x	y	z	B(A2)
C16	-0.2399(3)	0.1469(2)	-0.0979(4)	4.2(1)
C17	-0.1086(2)	0.0785(3)	-0.0932(4)	4.0(1)
C18	-0.0826(2)	0.0373(3)	0.1200(4)	4.0(1)
C19	-0.1944(3)	0.0899(3)	0.2438(4)	4.0(1)
C20	-0.2951(3)	0.1488(2)	0.1100(4)	4.2(1)
C21	-0.3165(2)	-0.0027(2)	-0.1018(3)	1.80(9)
C22	-0.3597(2)	0.0433(2)	-0.0778(3)	2.6(1)
C23	-0.4215(2)	0.0427(2)	-0.1081(4)	3.2(1)
C24	-0.4423(2)	-0.0040(2)	-0.1684(4)	3.0(1)
C25	-0.4012(2)	-0.0498(2)	-0.1969(3)	2.7(1)
C26	-0.3406(2)	-0.0497(2)	-0.1627(3)	2.6(1)
C31	-0.1754(2)	-0.0767(2)	-0.0975(3)	2.25(9)
C32	-0.1185(2)	-0.0764(2)	-0.0486(4)	3.3(1)
C33	-0.0799(3)	-0.1296(3)	-0.0417(4)	4.1(1)
C34	-0.0964(2)	-0.1844(2)	-0.0841(4)	3.9(1)
C35	-0.1523(2)	-0.1873(2)	-0.1328(4)	3.5(1)
C36	-0.1905(2)	-0.1347(2)	-0.1390(3)	2.9(1)
C41	-0.2236(2)	0.0293(2)	-0.2944(3)	2.15(9)
C42	-0.1799(2)	0.0136(2)	-0.3640(4)	3.2(1)
C43	-0.1880(3)	0.0322(3)	-0.4587(4)	4.0(1)
C44	-0.2369(3)	0.0682(3)	-0.4846(4)	3.9(1)
C45	-0.2807(2)	0.0857(3)	-0.4186(4)	3.6(1)
C46	-0.2742(2)	0.0653(2)	-0.3253(3)	2.8(1)

The thermal parameter given for anisotropically refined atoms is the isotropic equivalent thermal parameter defined as:
(4/3) * [a2*B(1,1) + b2*B(2,2) + c2*B(3,3) + ab(cos gamma)*B(1,2) + ac(cos beta)*B(1,3) + bc(cos alpha)*B(2,3)]
where a,b,c are real cell parameters, and B(i,j) are anisotropic betas.

Table of Anisotropic Thermal Parameters - B's

Name	B(1,1)	B(2,2)	B(3,3)	B(1,2)	B(1,3)	B(2,3)	Beqv
YB	1.957(8)	1.944(8)	1.225(8)	-0.046(6)	-0.042(6)	0.016(7)	1.709(4)
ZN	2.38(2)	2.76(2)	1.61(2)	-0.04(2)	-0.04(2)	0.42(2)	2.25(1)
C1	3.1(2)	1.9(2)	1.4(2)	-0.1(2)	0.4(2)	0.3(2)	2.11(9)
C2	2.0(2)	2.8(2)	2.1(2)	-0.1(2)	0.0(2)	0.4(2)	2.28(9)
C3	3.0(2)	2.8(2)	1.8(2)	0.1(2)	0.8(2)	-0.0(2)	2.5(1)
C4	2.7(2)	3.1(2)	1.5(2)	-0.2(2)	-0.2(2)	0.7(2)	2.5(1)
C5	2.7(2)	2.4(2)	2.1(2)	0.3(2)	0.5(2)	0.8(2)	2.4(1)
C6	4.7(2)	2.7(2)	2.5(2)	-1.0(2)	0.7(2)	0.0(2)	3.3(1)

Table of Anisotropic Thermal Parameters - B's (Continued)

Name	B(1,1)	B(2,2)	B(3,3)	B(1,2)	B(1,3)	B(2,3)	Beqv
C7	2.6(2)	4.5(2)	3.3(2)	Ø.1(2)	Ø.2(2)	1.5(2)	3.5(1)
C8	4.8(3)	4.3(3)	3.6(3)	Ø.1(2)	2.Ø(2)	-Ø.9(2)	4.3(1)
C9	4.7(3)	5.6(3)	2.5(2)	-Ø.6(2)	-1.2(2)	1.1(2)	4.3(1)
C1Ø	3.6(2)	3.7(2)	4.1(3)	1.1(2)	Ø.7(2)	1.6(2)	3.8(1)
C11	3.7(2)	2.Ø(2)	2.5(2)	-1.Ø(2)	-Ø.9(2)	Ø.2(2)	2.7(1)
C12	2.8(2)	2.6(2)	2.1(2)	-1.Ø(2)	Ø.Ø(2)	-Ø.1(2)	2.5(1)
C13	2.6(2)	2.7(2)	2.4(2)	-Ø.3(2)	-Ø.6(2)	-Ø.1(2)	2.5(1)
C14	3.7(2)	2.6(2)	1.7(2)	-Ø.8(2)	-Ø.2(2)	-Ø.2(2)	2.6(1)
C15	3.1(2)	2.6(2)	2.6(2)	-Ø.2(2)	-Ø.1(2)	-Ø.4(2)	2.8(1)
C16	6.4(3)	2.4(2)	3.7(3)	-Ø.5(2)	-2.Ø(2)	1.Ø(2)	4.2(1)
C17	3.9(2)	5.Ø(3)	3.2(2)	-2.Ø(2)	Ø.4(2)	-Ø.Ø(2)	4.Ø(1)
C18	3.Ø(2)	5.3(3)	3.6(3)	-Ø.5(2)	-1.Ø(2)	-Ø.8(2)	4.Ø(1)
C19	5.1(3)	4.6(3)	2.2(2)	-1.Ø(2)	-Ø.1(2)	-1.1(2)	4.Ø(1)
C2Ø	4.7(3)	3.6(2)	4.4(3)	Ø.7(2)	-Ø.7(2)	-1.4(2)	4.2(1)
C21	2.4(2)	1.7(2)	1.3(2)	-Ø.1(1)	Ø.2(2)	Ø.3(2)	1.8Ø(9)
C22	2.8(2)	2.4(2)	2.5(2)	Ø.1(2)	-Ø.1(2)	-Ø.1(2)	2.6(1)
C23	2.9(2)	3.Ø(2)	3.7(2)	Ø.7(2)	-Ø.2(2)	Ø.2(2)	3.2(1)
C24	2.5(2)	3.6(2)	2.8(2)	-Ø.Ø(2)	-Ø.8(2)	Ø.8(2)	3.Ø(1)
C25	3.1(2)	3.4(2)	1.6(2)	-Ø.8(2)	-Ø.1(2)	-Ø.4(2)	2.7(1)
C26	2.5(2)	2.8(2)	2.5(2)	Ø.Ø(2)	Ø.5(2)	-Ø.3(2)	2.6(1)
C31	2.Ø(2)	2.9(2)	1.8(2)	Ø.4(2)	Ø.5(2)	Ø.3(2)	2.25(9)
C32	3.1(2)	3.7(2)	3.1(2)	Ø.6(2)	-Ø.3(2)	Ø.Ø(2)	3.3(1)
C33	3.2(2)	4.7(3)	4.3(3)	1.4(2)	-Ø.2(2)	Ø.7(2)	4.1(1)
C34	4.Ø(2)	3.8(2)	3.7(3)	1.8(2)	1.7(2)	Ø.9(2)	3.9(1)
C35	4.8(2)	3.2(2)	2.6(2)	Ø.4(2)	1.7(2)	-Ø.1(2)	3.5(1)
C36	3.4(2)	3.3(2)	2.Ø(2)	-Ø.2(2)	Ø.5(2)	-Ø.Ø(2)	2.9(1)
C41	2.3(2)	2.3(2)	1.8(2)	-Ø.4(2)	Ø.Ø(2)	Ø.2(2)	2.15(9)
C42	2.7(2)	3.9(2)	2.9(2)	Ø.5(2)	Ø.9(2)	Ø.6(2)	3.2(1)
C43	4.4(3)	5.Ø(3)	2.7(2)	-Ø.6(2)	1.6(2)	-Ø.2(2)	4.Ø(1)
C44	5.7(3)	4.Ø(3)	1.9(2)	-Ø.9(2)	-Ø.1(2)	Ø.8(2)	3.9(1)
C45	4.3(2)	3.9(2)	2.5(2)	-Ø.Ø(2)	-1.Ø(2)	Ø.4(2)	3.6(1)
C46	2.8(2)	3.7(2)	1.9(2)	Ø.4(2)	-Ø.Ø(2)	Ø.1(2)	2.8(1)

The form of the anisotropic temperature factor is:
exp[-Ø.25(h2a2B(1,1) + k2b2B(2,2) + l2c2B(3,3) + 2hkabB(1,2) + 2hlacB(1,3) + 2klbcB(2,3))] where a,b, and c are reciprocal lattice constants.

$(Me_5C_5)_2Yb(o\text{-}H_2C_2B_{10}H_{10})$

Table of Positional Parameters and Their Estimated Standard Deviations

Atom	x	y	z	B(A2)
YB	Ø.36837(1)	Ø.24721(3)	Ø.ØØ276(1)	2.8Ø9(4)
C11	Ø.3971(4)	Ø.3949(6)	Ø.1Ø72(3)	3.5(1)
C12	Ø.3175(5)	Ø.3Ø3Ø(6)	Ø.12Ø9(3)	3.8(1)
C13	Ø.2296(4)	Ø.3361(6)	Ø.ØØ37(3)	3.7(1)
C14	Ø.2544(4)	Ø.4484(6)	Ø.Ø463(2)	3.3(1)
C15	Ø.3584(4)	Ø.4831(5)	Ø.Ø6Ø9(2)	3.Ø(1)
C16	Ø.5ØØ6(5)	Ø.4Ø84(7)	Ø.1431(3)	5.4(2)
C17	Ø.322Ø(7)	Ø.1938(8)	Ø.1696(3)	6.7(2)
C18	Ø.12Ø4(5)	Ø.278Ø(7)	Ø.Ø9Ø8(3)	6.5(2)
C19	Ø.1795(5)	Ø.5274(7)	Ø.ØØ4Ø(3)	5.8(2)
C2Ø	Ø.4134(5)	Ø.6Ø64(6)	Ø.Ø38Ø(3)	5.1(2)
C21	Ø.3725(4)	Ø.Ø284(5)	-Ø.Ø696(2)	2.9(1)
C22	Ø.27Ø5(4)	Ø.Ø326(6)	-Ø.Ø444(2)	3.1(1)
C23	Ø.2192(4)	Ø.1439(6)	-Ø.Ø718(3)	3.4(1)
C24	Ø.2884(4)	Ø.2Ø89(5)	-Ø.1129(3)	3.3(1)
C25	Ø.3832(4)	Ø.1348(6)	-Ø.1117(2)	3.3(1)
C26	Ø.4496(5)	-Ø.Ø843(6)	-Ø.Ø6Ø3(3)	4.6(1)
C27	Ø.2252(5)	-Ø.Ø674(7)	Ø.ØØØ2(3)	5.4(2)
C28	Ø.1Ø34(5)	Ø.1736(7)	-Ø.Ø67Ø(3)	5.2(2)
C29	Ø.2623(6)	Ø.3266(8)	-Ø.1539(3)	5.5(2)
C3Ø	Ø.4744(5)	Ø.1537(7)	-Ø.1549(3)	4.7(2)
C1	Ø.7766(5)	Ø.Ø757(7)	Ø.2Ø62(3)	5.Ø(2)
C2	Ø.7745(5)	Ø.Ø7ØØ(7)	Ø.2848(3)	5.6(2)
B1	Ø.89Ø7(5)	Ø.Ø526(7)	Ø.2465(4)	4.1(2)
B2	Ø.8859(6)	Ø.1521(8)	Ø.18Ø6(4)	4.6(2)
B3	Ø.7617(5)	Ø.2335(8)	Ø.1797(3)	4.1(2)
B4	Ø.6918(5)	Ø.1745(8)	Ø.2442(4)	4.5(2)
B5	Ø.8838(6)	Ø.1445(9)	Ø.3141(4)	4.7(2)
B6	Ø.9518(5)	Ø.2Ø18(8)	Ø.25Ø2(3)	4.Ø(2)
B7	Ø.8736(5)	Ø.3174(8)	Ø.2Ø84(4)	3.8(2)
B8	Ø.7527(6)	Ø.33Ø8(8)	Ø.2491(4)	4.2(2)
B9	Ø.7587(5)	Ø.2223(8)	Ø.3143(3)	4.4(2)
B1Ø	Ø.8715(6)	Ø.31Ø6(8)	Ø.2915(4)	4.6(2)

The thermal parameter given for anisotropically refined atoms is the isotropic equivalent thermal parameter defined as:
(4/3) * [a2*B(1,1) + b2*B(2,2) + c2*B(3,3) + ab(cos gamma)*B(1,2) + ac(cos beta)*B(1,3) + bc(cos alpha)*B(2,3)]
where a,b,c are real cell parameters, and B(i,j) are anisotropic betas.

Table of Anisotropic Thermal Parameters - B's

Name	B(1,1)	B(2,2)	B(3,3)	B(1,2)	B(1,3)	B(2,3)	Beqv
YB	3.Ø13(8)	2.648(8)	2.758(8)	Ø.23(2)	-Ø.125(7)	-Ø.34(2)	2.8Ø9(4)
C11	3.6(2)	3.9(3)	3.Ø(2)	Ø.6(2)	Ø.2(2)	-Ø.5(2)	3.5(1)
C12	5.2(3)	3.Ø(2)	3.1(2)	Ø.3(2)	1.3(2)	Ø.3(2)	3.8(1)
C13	3.4(2)	3.8(3)	3.8(3)	-Ø.5(2)	Ø.9(2)	-Ø.6(3)	3.7(1)
C14	3.7(2)	3.6(3)	2.8(2)	Ø.8(2)	Ø.4(2)	Ø.1(2)	3.3(1)
C15	3.9(2)	2.5(2)	2.7(2)	Ø.3(2)	Ø.9(2)	-Ø.4(2)	3.Ø(1)
C16	5.2(3)	5.9(4)	5.Ø(3)	1.5(3)	-1.3(3)	-1.7(3)	5.4(2)
C17	1Ø.8(5)	5.4(4)	4.1(3)	1.Ø(4)	1.8(3)	1.7(3)	6.7(2)
C18	5.3(3)	6.8(5)	7.4(3)	-2.Ø(3)	2.8(3)	-2.Ø(3)	6.5(2)
C19	6.9(3)	5.6(4)	4.9(3)	2.9(3)	-1.5(3)	-Ø.9(3)	5.8(2)
C2Ø	6.8(3)	2.8(3)	5.7(3)	-Ø.7(3)	2.6(3)	-Ø.1(3)	5.1(2)
C21	3.1(2)	2.3(2)	3.3(2)	Ø.4(2)	-Ø.8(2)	-Ø.7(2)	2.9(1)
C22	3.3(2)	3.Ø(3)	3.1(2)	-Ø.4(2)	-Ø.4(2)	Ø.2(2)	3.1(1)
C23	2.9(2)	3.9(3)	3.5(2)	-Ø.2(2)	-Ø.6(2)	-Ø.8(2)	3.4(1)
C24	4.4(3)	2.4(3)	3.Ø(2)	Ø.4(2)	-Ø.9(2)	-Ø.1(2)	3.3(1)
C25	4.Ø(3)	3.1(3)	2.7(2)	-Ø.7(2)	-Ø.5(2)	-Ø.3(2)	3.3(1)
C26	4.6(3)	3.6(3)	5.5(3)	1.2(3)	-1.9(3)	-1.5(3)	4.6(1)
C27	5.2(3)	4.4(4)	6.6(4)	-Ø.4(3)	Ø.4(3)	1.Ø(3)	5.4(2)
C28	3.3(3)	5.7(4)	6.4(4)	1.3(3)	-1.2(3)	-1.2(3)	5.2(2)
C29	7.4(4)	4.6(3)	4.3(3)	Ø.2(3)	-1.3(3)	Ø.7(3)	5.5(2)
C3Ø	5.3(3)	5.3(4)	3.6(3)	-1.4(3)	Ø.5(3)	-Ø.7(3)	4.7(2)
C1	4.2(3)	4.3(3)	6.4(4)	-Ø.1(3)	-Ø.9(3)	-1.6(3)	5.Ø(2)
C2	4.2(3)	5.4(4)	7.1(4)	-Ø.6(3)	Ø.6(3)	2.8(3)	5.6(2)
B1	2.8(3)	3.2(3)	6.4(4)	1.Ø(3)	Ø.2(3)	Ø.7(3)	4.1(2)
B2	3.5(3)	4.7(4)	5.7(4)	-Ø.5(3)	Ø.Ø(3)	-1.2(3)	4.6(2)
B3	3.5(2)	4.7(4)	4.Ø(3)	-Ø.3(3)	-Ø.8(2)	Ø.1(4)	4.1(2)
B4	3.1(3)	4.7(4)	5.7(4)	Ø.1(3)	Ø.2(3)	Ø.9(4)	4.5(2)
B5	3.2(3)	5.1(4)	5.7(4)	Ø.2(3)	-Ø.7(3)	1.7(3)	4.7(2)
B6	2.8(3)	4.9(4)	4.4(3)	-Ø.2(3)	Ø.2(3)	Ø.5(3)	4.Ø(2)
B7	3.3(3)	3.2(3)	4.8(3)	-Ø.6(3)	-Ø.4(3)	Ø.5(3)	3.8(2)
B8	3.8(3)	3.3(4)	5.3(4)	Ø.1(3)	-Ø.4(3)	Ø.2(3)	4.2(2)
B9	4.3(3)	5.1(5)	4.Ø(3)	Ø.7(3)	Ø.8(2)	Ø.7(3)	4.4(2)
B1Ø	5.1(4)	3.7(3)	4.8(4)	-Ø.8(3)	-Ø.9(3)	-Ø.6(3)	4.6(2)

The form of the anisotropic temperature factor is:
exp[-Ø.25(h2a2B(1,1) + k2b2B(2,2) + l2c2B(3,3) + 2hkabB(1,2) + 2hlacB(1,3) + 2klbcB(2,3))] where a,b, and c are reciprocal lattice constants.

$(Me_5C_5)_2Yb(o\text{-}Me_2C_2B_{10}H_{10})$

Table of Positional Parameters and Their Estimated Standard Deviations

Atom	x	y	z	B(A2)
YB	Ø.33230(2)	Ø.17732(2)	Ø.Ø1364(1)	5.216(5)
C1	Ø.2571(7)	Ø.6340(6)	Ø.2485(4)	10.3(2)
C2	Ø.1531(6)	Ø.6365(7)	Ø.2091(4)	10.5(2)
C3	Ø.312(1)	Ø.5061(8)	Ø.2595(5)	22.6(4)
C4	Ø.111(1)	Ø.508(1)	Ø.1866(6)	23.8(4)
C11	Ø.3670(4)	Ø.3591(5)	Ø.Ø976(3)	5.Ø(1)
C12	Ø.3004(4)	Ø.4085(5)	Ø.Ø512(3)	6.Ø(1)
C13	Ø.2041(4)	Ø.3493(5)	Ø.Ø546(3)	5.6(1)
C14	Ø.2139(4)	Ø.2629(5)	Ø.1021(2)	5.2(1)
C15	Ø.3133(4)	Ø.2693(5)	Ø.1286(2)	4.4(1)
C16	Ø.4759(5)	Ø.4022(6)	Ø.1155(4)	8.4(2)
C17	Ø.3245(6)	Ø.5192(7)	Ø.ØØ99(3)	11.1(2)
C18	Ø.1071(5)	Ø.3863(7)	Ø.Ø189(3)	9.9(2)
C19	Ø.1274(5)	Ø.1846(6)	Ø.1234(4)	8.6(2)
C20	Ø.3537(5)	Ø.1979(5)	Ø.1843(3)	7.1(2)
C21	Ø.3748(4)	Ø.Ø160(5)	-Ø.Ø677(2)	5.7(1)
C22	Ø.3663(4)	Ø.1309(5)	-Ø.Ø969(2)	5.6(1)
C23	Ø.2642(4)	Ø.1665(5)	-Ø.Ø969(2)	5.6(1)
C24	Ø.2107(4)	Ø.Ø773(5)	-Ø.Ø671(2)	5.8(1)
C25	Ø.2781(4)	-Ø.Ø161(5)	-Ø.Ø486(2)	5.6(1)
C26	Ø.4683(5)	-Ø.Ø690(7)	-Ø.Ø660(3)	10.8(2)
C27	Ø.4502(6)	Ø.1995(8)	-Ø.1278(4)	11.2(2)
C28	Ø.2187(7)	Ø.2817(7)	-Ø.1294(3)	10.2(2)
C29	Ø.Ø951(5)	Ø.Ø750(8)	-Ø.Ø613(4)	9.9(2)
C30	Ø.2501(8)	-Ø.1358(7)	-Ø.Ø182(4)	11.3(3)
B1	Ø.2585(7)	Ø.6895(8)	Ø.1781(4)	8.8(2)
B2	Ø.3235(6)	Ø.768(1)	Ø.2345(5)	11.Ø(3)
B3	Ø.2646(7)	Ø.747(1)	Ø.3028(4)	11.Ø(3)
B4	Ø.1556(7)	Ø.6614(7)	Ø.2894(5)	9.6(2)
B5	Ø.1404(7)	Ø.756(1)	Ø.1678(5)	11.1(3)
B6	Ø.2438(7)	Ø.8458(7)	Ø.1831(4)	8.2(2)
B7	Ø.2419(9)	Ø.8878(9)	Ø.2606(4)	11.4(3)
B8	Ø.1379(7)	Ø.8148(8)	Ø.2937(4)	8.5(2)
B9	Ø.Ø780(7)	Ø.734(1)	Ø.2368(5)	11.6(3)
B10	Ø.1328(8)	Ø.875(1)	Ø.2203(5)	13.2(3)

Starred atoms were included with isotropic thermal parameters.
The thermal parameter given for anisotropically refined atoms is the isotropic equivalent thermal parameter defined as:
(4/3) * [a2*B(1,1) + b2*B(2,2) + c2*B(3,3) + ab(cos gamma)*B(1,2) + ac(cos beta)*B(1,3) + bc(cos alpha)*B(2,3)]
where a,b,c are real cell parameters, and B(i,j) are anisotropic betas.

Table of Anisotropic Thermal Parameters - B's

Name	B(1,1)	B(2,2)	B(3,3)	B(1,2)	B(1,3)	B(2,3)	Beqv
YB	4.869(9)	6.Ø7(1)	4.635(9)	2.324(9)	-Ø.338(8)	-1.19(1)	5.216(5)
C1	16.Ø(5)	7.Ø(3)	7.9(4)	5.5(3)	Ø.6(4)	1.3(3)	1Ø.3(2)
C2	9.9(4)	9.7(4)	12.2(5)	-3.3(4)	2.7(4)	-3.9(4)	1Ø.5(2)
C3	4Ø(1)	12.4(5)	16.3(8)	16.Ø(5)	7.7(8)	5.3(6)	22.6(4)
C4	32(1)	15.9(6)	24.9(9)	-14.3(6)	13.7(8)	-12.4(6)	23.8(4)
C11	4.9(2)	4.3(2)	6.Ø(3)	Ø.5(2)	1.4(2)	-Ø.4(2)	5.Ø(1)
C12	8.5(3)	4.1(2)	5.6(3)	1.7(2)	2.3(2)	Ø.9(2)	6.Ø(1)
C13	5.4(2)	5.3(3)	6.2(3)	2.6(2)	Ø.6(2)	-Ø.6(2)	5.6(1)
C14	4.9(2)	4.6(2)	6.1(3)	Ø.7(2)	1.7(2)	-Ø.4(2)	5.2(1)
C15	5.3(2)	3.6(2)	4.3(2)	Ø.8(2)	Ø.5(2)	-Ø.1(2)	4.4(1)
C16	6.8(3)	7.Ø(4)	11.4(5)	-1.1(3)	1.8(3)	-1.5(4)	8.4(2)
C17	15.4(6)	8.2(4)	1Ø.1(4)	2.3(4)	5.1(4)	4.5(3)	11.1(2)
C18	8.8(3)	11.5(4)	8.9(4)	6.5(3)	-1.9(3)	-1.5(4)	9.9(2)
C19	6.5(3)	8.3(4)	11.1(5)	-Ø.7(3)	2.5(3)	-Ø.4(4)	8.6(2)
C2Ø	9.5(4)	5.8(3)	6.1(3)	1.4(3)	Ø.3(3)	Ø.4(3)	7.1(2)
C21	5.Ø(2)	6.6(3)	5.2(2)	2.3(2)	-Ø.9(2)	-2.2(2)	5.7(1)
C22	5.4(2)	6.7(3)	4.8(2)	-Ø.4(2)	1.1(2)	-1.1(2)	5.6(1)
C23	6.8(3)	5.4(3)	4.5(2)	1.2(2)	-Ø.4(2)	-Ø.1(2)	5.6(1)
C24	4.6(2)	7.4(3)	5.4(3)	Ø.4(2)	Ø.1(2)	-Ø.4(3)	5.8(1)
C25	7.2(3)	4.7(3)	4.9(2)	Ø.1(2)	-Ø.5(2)	Ø.1(2)	5.6(1)
C26	8.4(3)	13.1(4)	1Ø.4(4)	6.2(3)	-3.5(3)	-6.7(3)	1Ø.8(2)
C27	1Ø.8(4)	14.1(6)	9.Ø(4)	-4.9(4)	3.6(4)	-1.5(4)	11.2(2)
C28	14.9(5)	8.7(4)	6.6(4)	4.1(4)	-1.6(4)	1.2(3)	1Ø.2(2)
C29	4.9(3)	14.7(6)	1Ø.2(4)	-Ø.Ø(4)	Ø.5(3)	-2.7(4)	9.9(2)
C3Ø	16.6(7)	7.6(4)	7.6(4)	-2.6(5)	-Ø.3(5)	1.3(4)	11.3(3)
B1	9.5(5)	7.9(5)	9.1(5)	Ø.6(4)	2.4(4)	-Ø.Ø(4)	8.8(2)
B2	6.3(4)	18.2(8)	8.5(5)	-1.3(5)	1.2(4)	3.Ø(6)	11.Ø(3)
B3	8.4(5)	18.6(8)	5.7(4)	-3.9(5)	-1.Ø(4)	2.6(5)	11.Ø(3)
B4	1Ø.2(5)	6.9(4)	12.1(5)	Ø.3(4)	4.7(4)	3.Ø(4)	9.6(2)
B5	7.4(5)	15.6(8)	1Ø.4(6)	Ø.6(5)	1.3(4)	3.Ø(6)	11.1(3)
B6	1Ø.Ø(5)	6.5(4)	8.2(4)	Ø.1(4)	2.5(4)	Ø.9(4)	8.2(2)
B7	17.8(7)	8.2(5)	8.7(5)	-5.4(5)	4.3(5)	-1.5(4)	11.4(3)
B8	1Ø.9(5)	7.1(4)	7.8(4)	Ø.8(4)	3.2(4)	Ø.2(4)	8.5(2)
B9	5.1(4)	2Ø.5(9)	8.2(5)	2.3(5)	1.1(4)	-1.3(6)	11.6(3)
B1Ø	15.6(6)	12.8(5)	12.Ø(5)	8.7(4)	7.8(4)	6.Ø(5)	13.2(3)

The form of the anisotropic temperature factor is:
exp[-Ø.25(h2a2B(1,1) + k2b2B(2,2) + l2c2B(3,3) + 2hkabB(1,2) + 2hlacB(1,3) + 2klbcB(2,3))] where a,b, and c are reciprocal lattice constants.

$[(Me_5C_5)_2Yb]_2[(H_5C_5)_2Co]$

Table of Positional Parameters and Their Estimated Standard Deviations

Atom	x	y	z	B(A2)
YB	Ø.24356(1)	Ø.22256(1)	-Ø.ØØØØ6(1)	1.793(4)
CO	Ø.25Ø	Ø.25Ø	-Ø.25Ø	2.1Ø(2)
C1	Ø.2354(3)	Ø.228Ø(3)	-Ø.1472(3)	4.9(2)
C2	Ø.1826(3)	Ø.2176(3)	-Ø.1853(3)	4.5(1)
C3	Ø.162Ø(3)	Ø.274Ø(4)	-Ø.2Ø99(3)	5.4(2)
C4	Ø.2Ø32(4)	Ø.3178(3)	-Ø.1938(3)	6.8(2)
C5	Ø.25Ø8(3)	Ø.29Ø8(3)	-Ø.1551(3)	6.4(2)
C11	Ø.14Ø5(2)	Ø.2916(2)	Ø.ØØ91(2)	2.1(1)
C12	Ø.1911(2)	Ø.3315(2)	Ø.Ø3Ø1(2)	2.Ø(1)
C13	Ø.2141(2)	Ø.3Ø72(2)	Ø.Ø923(2)	2.2(1)
C14	Ø.1782(2)	Ø.2534(2)	Ø.1Ø99(2)	2.1(1)
C15	Ø.1335(2)	Ø.2439(2)	Ø.Ø578(2)	1.87(9)
C16	Ø.Ø977(2)	Ø.3Ø31(3)	-Ø.Ø5Ø7(3)	3.Ø(1)
C17	Ø.2121(2)	Ø.39Ø4(2)	-Ø.ØØ41(3)	3.3(1)
C18	Ø.2643(3)	Ø.3377(3)	Ø.1363(3)	3.4(1)
C19	Ø.18ØØ(3)	Ø.2184(3)	Ø.1755(3)	3.2(1)
C2Ø	Ø.Ø831(2)	Ø.1946(3)	Ø.Ø582(3)	3.1(1)
C21	Ø.3ØØØ(2)	Ø.118Ø(2)	-Ø.Ø3Ø5(3)	2.5(1)
C22	Ø.3529(2)	Ø.1652(2)	-Ø.Ø347(3)	2.7(1)
C23	Ø.3624(2)	Ø.19Ø7(2)	Ø.Ø294(3)	2.7(1)
C24	Ø.3235(2)	Ø.1573(2)	Ø.Ø759(2)	2.6(1)
C25	Ø.2895(2)	Ø.113Ø(2)	Ø.Ø372(3)	2.6(1)
C26	Ø.2841(3)	Ø.Ø755(3)	-Ø.Ø865(3)	5.Ø(2)
C27	Ø.3911(3)	Ø.1816(3)	-Ø.Ø98Ø(3)	5.5(2)
C28	Ø.4111(3)	Ø.2388(3)	Ø.Ø492(4)	5.7(2)
C29	Ø.3292(3)	Ø.16Ø8(3)	Ø.1521(3)	5.2(2)
C3Ø	Ø.2388(3)	Ø.Ø688(3)	Ø.Ø632(4)	4.9(2)

Starred atoms were included with isotropic thermal parameters.
The thermal parameter given for anisotropically refined atoms is the isotropic equivalent thermal parameter defined as:
(4/3) * [a2*B(1,1) + b2*B(2,2) + c2*B(3,3) + ab(cos gamma)*B(1,2) + ac(cos beta)*B(1,3) + bc(cos alpha)*B(2,3)]
where a,b,c are real cell parameters, and B(i,j) are anisotropic betas.

Table of Anisotropic Thermal Parameters - B's

Name	B(1,1)	B(2,2)	B(3,3)	B(1,2)	B(1,3)	B(2,3)	Beqv
YB	1.737(7)	2.Ø15(8)	1.629(8)	Ø.391(6)	Ø.Ø1Ø(8)	Ø.Ø21(8)	1.793(4)
CO	2.13(3)	2.36(3)	1.82(3)	-Ø.13(3)	Ø.48(4)	-Ø.Ø4(4)	2.1Ø(2)
C1	5.7(3)	8.2(4)	Ø.8(2)	3.6(3)	1.Ø(2)	Ø.6(2)	4.9(2)
C2	4.6(3)	6.1(3)	2.8(2)	-2.7(2)	2.3(2)	-1.6(2)	4.5(1)
C3	3.8(3)	9.7(4)	2.8(3)	3.2(3)	Ø.7(2)	1.1(3)	5.4(2)
C4	11.4(5)	3.3(3)	5.6(3)	1.5(3)	5.5(3)	Ø.9(3)	6.8(2)
C5	4.5(3)	9.3(4)	5.5(3)	-3.6(3)	2.5(2)	-6.Ø(2)	6.4(2)
C11	1.9(2)	2.7(2)	1.8(2)	Ø.6(2)	Ø.1(2)	-Ø.5(2)	2.1(1)
C12	2.6(2)	1.7(2)	1.8(2)	Ø.4(2)	Ø.Ø(2)	-Ø.Ø(2)	2.Ø(1)
C13	2.2(2)	1.9(2)	2.5(2)	Ø.1(2)	-Ø.1(2)	-Ø.4(2)	2.2(1)
C14	2.Ø(2)	2.4(2)	1.8(2)	Ø.7(2)	Ø.1(2)	Ø.1(2)	2.1(1)
C15	2.Ø(2)	1.8(2)	1.8(2)	Ø.1(2)	Ø.6(2)	-Ø.1(2)	1.87(9)
C16	2.9(2)	3.8(2)	2.1(2)	1.3(2)	-Ø.3(2)	-Ø.6(2)	3.Ø(1)
C17	3.8(2)	2.3(2)	3.9(2)	Ø.1(2)	1.4(2)	Ø.2(2)	3.3(1)
C18	3.Ø(2)	3.5(2)	3.6(2)	Ø.5(2)	-Ø.8(2)	-1.3(2)	3.4(1)
C19	4.1(3)	3.5(2)	2.1(2)	1.3(2)	Ø.8(2)	Ø.6(2)	3.2(1)
C2Ø	2.6(2)	3.7(2)	3.1(2)	-Ø.1(2)	Ø.7(2)	-Ø.4(2)	3.1(1)
C21	2.5(2)	2.3(2)	2.8(2)	Ø.6(2)	-Ø.9(2)	-Ø.7(2)	2.5(1)
C22	2.4(2)	2.8(2)	2.8(2)	1.Ø(2)	Ø.6(2)	Ø.5(2)	2.7(1)
C23	1.4(2)	2.1(2)	4.7(3)	Ø.4(2)	-Ø.9(2)	-Ø.6(2)	2.7(1)
C24	2.1(2)	3.1(2)	2.6(2)	1.3(2)	-Ø.5(2)	-Ø.Ø(2)	2.6(1)
C25	2.Ø(2)	2.1(2)	3.7(2)	Ø.3(2)	-Ø.7(2)	Ø.2(2)	2.6(1)
C26	5.3(3)	4.6(3)	5.1(3)	1.8(3)	-2.3(3)	-2.4(3)	5.Ø(2)
C27	3.4(3)	7.6(4)	5.4(3)	2.Ø(3)	2.5(2)	2.6(3)	5.5(2)
C28	3.1(3)	3.1(3)	1Ø.9(5)	-Ø.5(2)	-2.1(3)	-Ø.7(3)	5.7(2)
C29	5.2(3)	7.4(4)	3.1(3)	3.6(3)	-1.8(2)	-Ø.9(3)	5.2(2)
C3Ø	3.2(3)	3.8(3)	7.7(4)	-Ø.4(2)	-Ø.7(3)	2.7(3)	4.9(2)

The form of the anisotropic temperature factor is:
exp[-Ø.25(h2a2B(1,1) + k2b2B(2,2) + l2c2B(3,3) + 2hkabB(1,2) + 2hlacB(1,3) + 2klbcB(2,3))] where a,b, and c are reciprocal lattice constants.

LAWRENCE BERKELEY LABORATORY
TECHNICAL INFORMATION DEPARTMENT
UNIVERSITY OF CALIFORNIA
BERKELEY, CALIFORNIA 94720